STRUCTURAL STUDIES

OF

'SOFT' FERROELECTRICS

RICHARD JOHN NELMES

Ph.D.

University of Edinburgh

August, 1969.

Acknowledgements

Throughout my candidature for this degree I have been fortunate in the very generous measure of personal and financial assistance I have received.

I would like to thank the Science Research Council and the University of Edinburgh for the award of Research Studentships, St. John's College, Cambridge, for a Strathcona Research Studentship, and the Whitgift Foundation for an O.W. Memorial Exhibition.

I am very grateful to Professor N. Feather for extending to me the facilities of the Department of Natural Philosophy, Edinburgh University, and to the Science Research Council for granting me access to the facilities of A.E.R.E., Harwell.

I happily extend my warm personal thanks to my supervisor, Professor W. Cochran, for his unstinted guidance, encouragement and assistance; to Dr. G.S. Pawley, Mr. P. Bradfield and Dr. J.G. Burns for frequent and highly valued assistance with various aspects of the work; to Mr. T.J. Renouf for patient guidance in the early part of the experimental work; to Mr. J. Polson, without whose very considerable help the task of data reduction would have been formidable; to the staff of A.E.R.E., Harwell, for their kindness and assistance; to many other friends in Edinburgh, to my parents and to my sister for enlightenment and solace; and to Mrs. A. Coyle for her patient and painstaking part in preparing this thesis.

Abstract

The work described in this thesis comprises an X-ray and neutron diffraction study of the structure of the monoclinic, room-temperature, non-ferroelectric phase of the 'soft' ferroelectric, ammonium hydrogen sulphate (AHS). A major experimental problem encountered at the outset was the extreme deliquescence of this compound. A method of enclosing specimens was devised which preserved them reliably for several months while introducing only negligible errors into the intensity data. Preliminary measurements revealed a systematic intensity distribution indicating that the actual structure of AHS arose from small displacements of the constituent atoms from a structure of higher symmetry. This feature made careful and accurate intensity measurements of the systematically weak reflections important, and presented considerable difficulties in structure analysis. Three-dimensional X-ray intensity data was collected on a four-circle diffractometer out to $\sin\theta/\lambda = 0.81\text{Å}^{-1}$, with all reasonable care and precautions. Neutron data was collected only in the ($h0\ell$) layer, primarily to locate the hydrogen atoms. A total of 15,000 intensities were measured in the X-ray experiment. They were recorded as digitised profiles punched on paper tape. A versatile data reduction program was written to extract integrated intensities from such reflection profiles. Certain problems relating to the correct removal of white radiation background were successfully tackled. The final refined structure can be described as being composed of distorted sulphate tetrahedral ions linked into chains along the monoclinic b-axis by short hydrogen bonds in which the protons are in ordered acentric

positions, these chains alternating in both the a and c directions with rows, along b, of ammonium ions. The latter appear to be in free rotation. This non-ferroelectric structure displays unusual features in being pseudo-symmetric and in having protons already ordered in bonds which are expected to play a rôle in the transition to the ferroelectric phase. Some brief comments are made on the significance of these features with regard to possible and proposed further experiments on this particular transition.

Contents

Contents (Contd.)

Contents (Contd.)

Contents (Contd.)

Contents (Contd.)

Note

To supplement and clarify allusions made in several parts of the text to particular features of the AHS structure, a drawing of an asymmetric unit of the refined structure is presented in appendix 5.

CHAPTER 1

INTRODUCTION

1.1. Objectives

This work is concerned with the application of the methods of crystal structure analysis to the study of phase transitions in the solid state. In particular it is concerned with structural studies of transitions between non-ferroelectric and ferroelectric phases in 'soft' ferroelectric crystals. The thesis comprises an account of the determination of the structure of ammonium hydrogen sulphate in its room-temperature, non-ferroelectric phase, using the techniques of X-ray and neutron diffraction. Ammonium hydrogen sulphate is a 'soft' ferroelectric crystal which passes through a transition to its ferroelectric phase at -3°C. The ultimate aim of the project is to relate the structural changes associated with this transition to a general microscopic theory of ferroelectric transitions.

1.2. Ferroelectricity

A ferroelectric crystal (hereafter, a ferroelectric) may be defined as one possessing a spontaneous electric polarisation which is reversible by an externally applied electric field*. The appearance of a spontaneous polarisation implies that the unit cell is polar and hence that a ferroelectric must belong to one of the ten polar crystal classes. However, a crystal may be polar and yet non-ferroelectric. To constitute a ferroelectric the forces within a polar crystal must be so delicately balanced as to permit the required polarisation reversal – from which it follows that the free energy of the polar state is comparable to that of the non-ferroelectric state (Jona and Shirane, 1962, p.11 and p.25).

In general a ferroelectric has a non-ferroelectric phase. The temperature, T_c, at which the transition to this phase occurs is known as the Curie temperature or the Curie point. Usually the static dielectric constant of the crystal, when measured in the direction of the spontaneous polarisation, shows an anomaly at T_c (fig. 1.2.1.).

The transition may be first- or second-order (Pippard, 1964, p.135). In a first-order transition the spontaneous polarisation appears discontinuously at T_c; in a second-order transition the

---

*The term 'ferroelectric' will sometimes be used in the wider sense of meaning a crystal which has a ferroelectric phase. This is an established usage (e.g. Jona and Shirane, 1962, p.13).

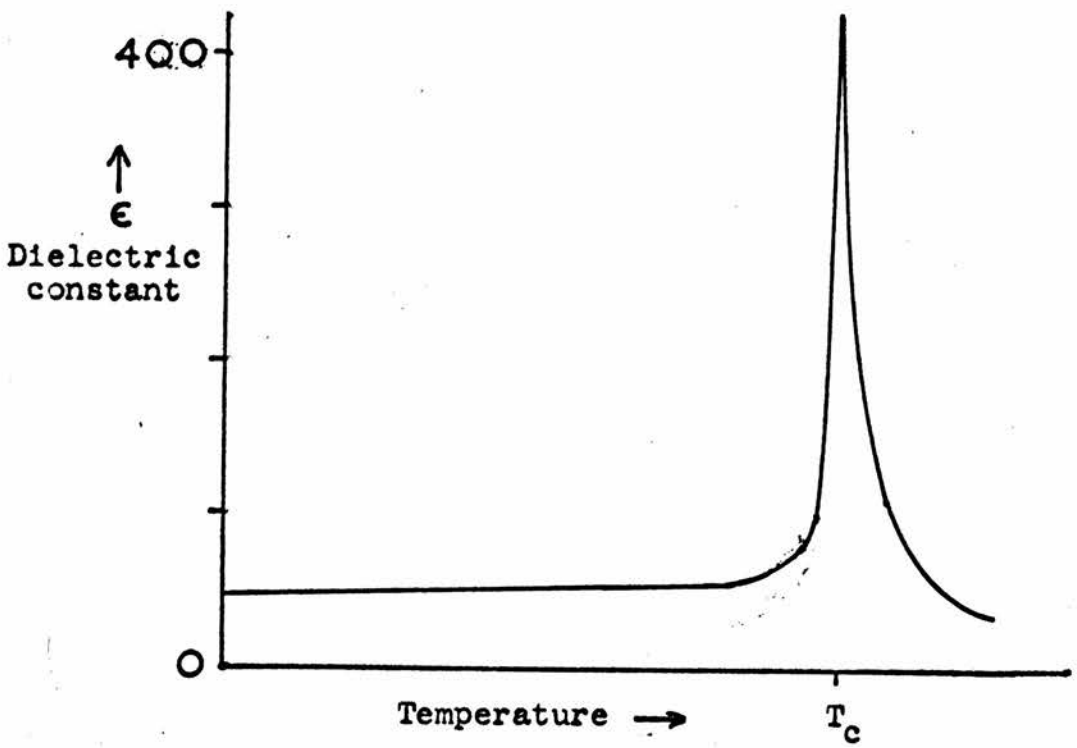

Typical dielectric constant anomaly

Fig. 1.2.1.

spontaneous polarisation increases continuously from T_c (fig. 1.2.2.).

The classification of ferroelectrics into 'hard' and 'soft' is due to Merz, 1952. 'Soft' ferroelectrics are mechanically soft; they usually melt at relatively low temperatures and are water-soluble and hydrogen bonded. 'Hard' ferroelectrics are mechanically hard; they are usually ionic and melt at relatively high temperatures.

1.3. Theories of ferroelectricity

The theoretical approaches to the appearance of ferroelectricity in certain crystals may be divided into phenomenological theories and model theories. The former treat the crystal as a thermodynamic system and establish relationships between its macroscopic properties (see, for example, Megaw, 1957, ch.8 and Devonshire, 1954). Model theories attempt to derive the macroscopic behaviour of a crystal quantitatively from a microscopic model of its structure and interatomic forces. At least a qualitative model of the transition mechanism is often invoked or implied.

The phenomenological approach is quite general, and it has been successful in deriving useful relationships between the various properties of the substances to which it has been applied. However, being independent of any assumed microscopic model for those substances, it affords no direct insight into the mechanism of their transitions.

Until recently model theories have generally been restricted in their application. In the absence of complete or accurate

structural information, older theories have sometimes assumed certain features of the structure in the ferroelectric phase and, although often successful, have applied to only the one material. For example, Slater's theory of KH_2PO_4 (KDP) (Slater, 1941) postulates a structure for the ferroelectric phase, and does not explicitly contain any features which explain why the isomorphous $NH_4H_2PO_4$ (ADP) is not also a ferroelectric, nor why the substitution of deuterium for hydrogen in KDP has such a large effect on the Curie point (Megaw, 1957, p.185).

A more general microscopic model theory has now been proposed (Cochran, 1960). Its main thesis is that a ferroelectric transition in certain crystals is "the result of an instability of the crystal for a certain normal mode of vibration, and can be treated as a problem in lattice dynamics". The displacements of the atoms which occur at the transition to the ferroelectric phase may be interpreted as the 'freezing-in' of one of the normal modes of vibration of the non-ferroelectric phase. The frequency of this mode is thus expected to drop towards zero as the temperature approaches T_c.

Lyddane et al., 1941, showed that for a diagonally cubic crystal with two atoms in the unit cell

$$\frac{\epsilon_o}{\epsilon_\infty} = \left(\frac{\omega_L}{\omega_T}\right)^2. \qquad (1.3.1)$$

ϵ_o is the static clamped dielectric constant and ϵ_∞ is the high frequency dielectric constant – strictly the dielectric constant at zero frequency when the contribution from the displacements of the atoms is suppressed. The frequencies ω_L and ω_T are

those at $\underline{q} = 0$ for longitudinal and transverse optical modes.

It has been shown by Cochran and Cowley, 1962, that a more general version of (1.3.1.) applies to any crystal for which the adiabatic and harmonic approximations are valid. The conclusion remains the same as that deduced from (1.3.1.): if the frequency of one of the transverse optical modes of vibration tends to zero then the static dielectric constant tends to infinity. This is the basic connection between the dielectric behaviour associated with a ferroelectric transition and the dynamics of the crystal lattice.

The structural approach to the problem is essentially static: it attempts to identify the displacements of the atoms, in passing from the non-ferroelectric phase to the ferroelectric phase, with a 'frozen-in' normal mode of vibration.

1.4. Historical summary

The phenomenon of ferroelectricity was first reported in Rochelle salt (sodium potassium tartrate tetrahydrate) by Valasek in 1921. Some time elapsed before the discovery of another ferroelectric – KDP (Busch and Scherrer, 1935). Ten years later the phenomenon was found in the perovskite, barium titanate (von Hippel et al., 1946; Wul and Goldman, 1945) – the first 'hard' ferroelectric – and in several other perovskites soon after. In 1952 the double oxide $CdNb_2O_7$ was shown to be ferroelectric by Cook and Jaffe. This compound is not a perovskite, but it contains a similar structural element in its oxygen octahedra.

At this time ferroelectricity was known only in double

oxides, dihydrogen phosphates and arsenates, and some tartrates; it was believed to be a rather rare phenomenon. Then in 1955 it was discovered in guanidinium aluminium sulphate hexahydrate (GASH) (Holden et al., 1955), and soon after in a number of alums (Pepinsky et al., 1956). This stimulated a re-examination of numerous compounds known to undergo phase transitions associated with dielectric anomalies, and led to a rapid expansion of the list of known ferroelectrics. The significance of ions such as NH_4^+, SO_4^{2-}, BeF_4^{2-}, SeO_4^{2-} and SeO_3^{2-} became apparent.

Early successes of this vigorous research were the discovery in 1956 of ferroelectricity in ammonium sulphate (Matthias and Remeika, 1956) and in the subsequently much-investigated triglycine sulphate (TGS) (Matthias et al., 1956). Two years later ferroelectricity was discovered in ammonium hydrogen sulphate (Pepinsky et al., 1958), and then in the isomorphous rubidium hydrogen sulphate (Pepinsky and Vedam, 1960).

The number of known ferroelectric compounds is now large: Jona and Shirane, 1962, list seventy-six — excluding many solid solutions. Many more have been discovered since the publication of their book, including some quite unlike those mentioned above (for example, SbSI, Fatuzzo et al., 1962). It has become clear that ferroelectricity, far from being uncommon, is a widespread phenomenon.

1.5. Methods and problems in structural studies

The methods employed in structural studies are commonly those of X-ray and neutron elastic scattering experiments. Both techniques yield the unit cell dimensions and space group symmetry of

the crystal concerned.

In principle the time-averaged distribution of electron density in the unit cell, $\rho(\underline{r})$, is obtainable from X-ray data. In practice, on the assumption that the electron distribution in an atom is spherically symmetric about its nucleus, the maxima of $\rho(\underline{r})$ are identified with the positions, $n(\underline{r})$, of the nuclei of the constituent atoms. This is not a good approximation for covalently bonded light atoms, or for atoms executing pronounced thermal motion. Further advances in the treatment of scattering from real crystals, and in the representation of scattering from vibrating atoms and bonding electrons, are required before the full potential of the X-ray method can be realised. The chief advantages of the X-ray method are that the data is relatively easy, quick and cheap to obtain, and that it is capable of giving the absolute configuration of a polar structure. The latter information has been used in the study of both KDP and TGS (Jona and Shirane, 1962, p.379).

From neutron data one derives the time-averaged distribution of the neutron scattering density of the unit cell. The maxima (and, in some cases, minima) of this function are identified with the nuclear positions, $n(\underline{r})$. There are several advantages to the neutron method: it actually does yield $n(\underline{r})$, atoms of low atomic weight may be readily located in the presence of atoms of high atomic weight, the isotropic scattering offers the possibility of much better high angle data and so better resolution (Frazer, 1962), and during refinement parameters are often less affected by correlation than with X-ray data (see below). In data collection neutrons are less likely than X-rays to cause

radiation damage (see below).

The problems encountered in structural studies of ferroelectric transitions chiefly arise from the pseudo-symmetric nature of the structure in the ferroelectric phase. A pseudo-symmetric structure is one in which the atomic positions are displaced by only small amounts (pseudo-symmetric displacements) from ones which satisfy a higher symmetry. Such a structure is to be expected in a ferroelectric phase as a corollary to the requirement that the polarisation be reversible by an externally applied electric field.

A pseudo-symmetric structure may present considerable difficulties in the initial stages of structure analysis if the true unit cell is larger than the pseudo-symmetric cell (see chapters 3 and 5). Further problems may be encountered even when a broadly correct trial structure has been found, because pseudo-symmetry often introduces a high degree of parameter interaction (or 'correlation') during a refinement using X-ray data. A classic example is to be found in the X-ray diffraction study of the tetragonal ferroelectric phase of barium titanate by Evans, 1952. After attempting a full-matrix least-squares refinement, Evans concluded that the structure was essentially indeterminate — despite an R-factor of less than 5% (Evans, 1961). Geller, 1961, also investigated this problem. He agreed that, although an extreme case, it is indeed possible for a structure to be known in general features and yet remain indeterminate in detail; he included the ferroelectric phase of GASH with that of barium titanate in the then studied examples. In barium titanate the interaction may be attributed to the insensitivity

of the structure factors to small pseudo-symmetric displacements of the titanium and oxygen atoms in the presence of the relatively high scattering from the barium atoms. In neutron diffraction all scattering lengths are of a similar order of magnitude so that the problem may be expected to be reduced (see Jona and Shirane, 1962, pp.377-378). Parameter correlation is discussed further in chapter 7 in relation to the refinement of the ammonium hydrogen sulphate structure.

A perhaps unexpected problem that may be encountered in the study of a pseudo-symmetric structure is that of radiation damage. X-ray experiments on the ferroelectric phase of Rochelle salt did not detect the expected (0k0) reflections with k odd: neutron experiments did detect them (Frazer, 1962). At first this was taken to indicate that only hydrogen atoms were involved in the transition, but further neutron experiments established that this was not the case. Eventually Boutin et al., 1963, were able to show that radiation dosages small compared with those normally received by a crystal during collection of X-ray data were sufficient to reduce the initial intensity of these (0k0) reflections practically to zero. It must be concluded that the structure of Rochelle salt in its ferroelectric phase cannot be determined by current X-ray methods. The possibility of a similar effect in TGS has been suggested by Chynoweth, 1959.

The problems of parameter interaction, in both barium titanate and Rochelle salt, and the radiation damage suffered by Rochelle salt in an X-ray beam, the subsequent attempts to overcome these difficulties with neutron experiments, and the general advantages of neutron experiments in the study of ferro-

electric or other pseudo-symmetric structures have been reviewed by Frazer, 1962. As he points out, small as the pseudo-symmetric displacements in a ferroelectric structure may be, it is from these that the spontaneous polarisation arises and they must be accurately determined in any meaningful study.

Thus, radiation damage aside, there are two principal problems to be expected in a structural study of a transition in a 'soft' ferroelectric: first the accurate determination of small pseudo-symmetric displacements, and secondly the accurate location of light atoms. Both are more difficult in X-ray experiments. 'Soft' ferroelectrics may present extra experimental difficulties, arising from their physical fragility and the fact that many of them are at least slightly deliquescent.

1.6. Some structural studies of phase transitions in 'soft' ferroelectrics

Perhaps the classic example of a successful structural study of a ferroelectric phase transition is that carried out on KDP by Bacon and Pease, 1955, using neutron diffraction techniques. They were able to demonstrate conclusively the ordering of the protons onto asymmetric sites between the phosphate ion tetrahedra in the ferroelectric phase, and the movement of the protons to the alternative sites upon polarisation reversal.

Some more recent studies of particular interest are two using neutron diffraction, viz., one on thiourea (Elcombe and Taylor, 1968) and one on ammonium sulphate (Schlemper and Hamilton, 1966), and a third using both X-ray and neutron methods on diglycine nitrate (DGN) (Sato, 1968). These studies are

particularly pertinent to the present work: all three were carried out in both the non-ferroelectric and the ferroelectric phase, and all the materials fall into the category of 'soft' ferroelectrics containing hydrogen.

Within this category each represents a different type of transition. Thiourea is interesting in that it may "represent the closest example to a realisation of the classical picture of rigid semi-rotatable macrodipoles in a three-dimensional lattice." (Jona and Shirane, 1962, p.351). In ammonium sulphate the spontaneous polarisation is attributed to NH_4^+ ions distorted by relatively strong hydrogen bonding to neighbouring sulphate ions (O'Reilly and Tsang, 1967). The transitions in both these materials are first-order, associated with a change in the inter-ion hydrogen bonding. However, in thiourea the molecules are themselves strongly polarised and only weakly bonded to each other; in ammonium sulphate the NH_4^+ ions are relatively weakly polarised and are strongly bonded to neighbouring ions. DGN is akin to KDP in having a short but asymmetric hydrogen bond which seems to be closely associated with the second-order, order-disorder phase transition in this material (Sato, 1968).

Elcombe and Taylor were able to account for both the magnitude and direction of the spontaneous polarisation in thiourea in terms of the refined low temperature structure. Furthermore they showed that the change in orientation of the molecules at the transition is consistent with the molecular thermal motion in the non-ferroelectric phase. They associated the transition with the strengthening of one of a pair of hydrogen bonds which

are symmetrically equivalent in the non-ferroelectric phase.

Schlemper and Hamilton's approach was almost entirely structural. They presented a detailed description of the structure of ammonium sulphate in both its non-ferroelectric and its ferroelectric phase. Regarding the transition itself they remarked only that it "is not of the order-disorder type but rather involves a change in the hydrogen bonding of the ammonium ions to the sulphate ions" which "results in stronger hydrogen bonds and less distorted ammonium ions, both of which would seem to be energetically favourable.". From their finding that, within error, the sulphate ion is distorted in neither phase while the NH_4^+ ion is quite significantly distorted in both, one may conclude that the source of the spontaneous polarisation is to be found in the orientation of the NH_4^+ ions. They did not pursue this aspect of their results.

Sato was able to attribute the spontaneous polarisation in DGN to the glycine ions, but considered these too complex to permit an estimation of the magnitude of the spontaneous polarisation. He described the transition as an ordering of the disordered non-ferroelectric phase, and identified the ordering of a proton in the short hydrogen bond between the two glycine ions as an important aspect of this process.

These three studies are representative of the accurate structural studies that can now be made of transitions in 'soft' ferroelectrics. They illustrate the nature and scope of the structural approach, which can provide accurate information regarding the static character of a transition but only a starting point (though a valuable one) for a quantitative understanding of its dynamics.

The latter requires a model for the interatomic forces. Nevertheless, the structural changes occurring at the transition may be interpreted in terms of a dynamical model as explained in section 1.3. As seems to be quite general, the authors of the three studies described above adopted this approach only in so far as they correlated high thermal vibrations with the atomic displacements at the transition. A direct interpretation of structural information in the terms of section 1.3. has been made in the case of some perovskite-type ferroelectrics by Cochran and Zia, 1968.

1.7. Ammonium hydrogen sulphate

Ammonium hydrogen sulphate (hereafter, AHS), NH_4HSO_4, was shown to be ferroelectric by Pepinsky et al. in 1958. It exhibits a large dielectric anomaly in passing from a non-ferroelectric to a ferroelectric phase at -3°C (the 'upper transition') and another small but sharp anomaly on passing to a second non-ferroelectric phase at -119°C (the 'lower transition').

The symmetry and cell dimensions of each of the three phases, as determined by Pepinsky et al., are tabulated in table 1.7.1.. The pseudo-orthorhombic cell is included because of its convenience and importance in the structural work described later.

It is the dielectric constant measured along the c-axis (ϵ_c) which shows the anomalies referred to above (fig. 1.7.1.). Those along the b-axis and the pseudo-orthorhombic a-axis exhibit no anomaly at either transition. Below -3°C the spontaneous polarisation along the c-axis increases, at first rapidly and then more slowly, to 0.8 microcoulombs/cm^2 before dropping

Table 1.7.1.

[Axial lengths given in Å units;
Z = number of formula units per cell]

Room temperature (centrosymmetric)	T = -30°C (polar, ferroelectric)	T = -140°C (polar, non-ferroelectric)
Monoclinic cell	Monoclinic cell	Triclinic cell
a = 14.51	a = 14.26	a = 14.24
b = 4.54	b = 4.62	b = 4.56
c = 14.90	c = 14.80	c = 15.15
β = 120° 18'	β = 121° 18'	β = 123° 24'
		$\alpha \approx 90°$, $\gamma \approx 90°$
space group $P2_1/c$	space group Pc	space group P1
Z = 8	Z = 8	Z = 8
Monoclinic, pseudo-orthorhombic cell	Monoclinic, pseudo-orthorhombic cell	Triclinic, pseudo-orthorhombic cell
a = 24.90	a = 24.37	a = 24.43
b = 4.54	b = 4.62	b = 4.56
c = 14.90	c = 14.80	c = 15.15
β = 90° 18'	$\beta \approx 90°$	β = 91° 12'
		$\alpha \approx 90°$, $\beta \approx 90°$
space group $B2_1/a$	space group Ba	space group B1
Z = 16	Z = 16	Z = 16

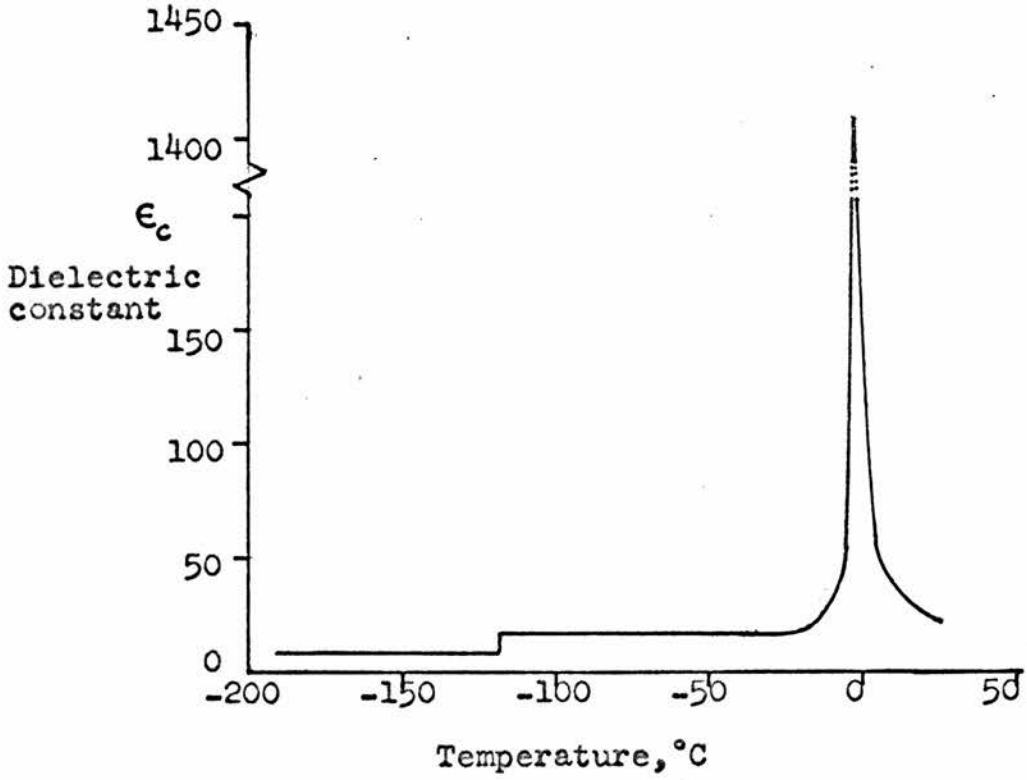

Fig. 1.7.1. (Fig.1., Pepinsky et al., 1958)

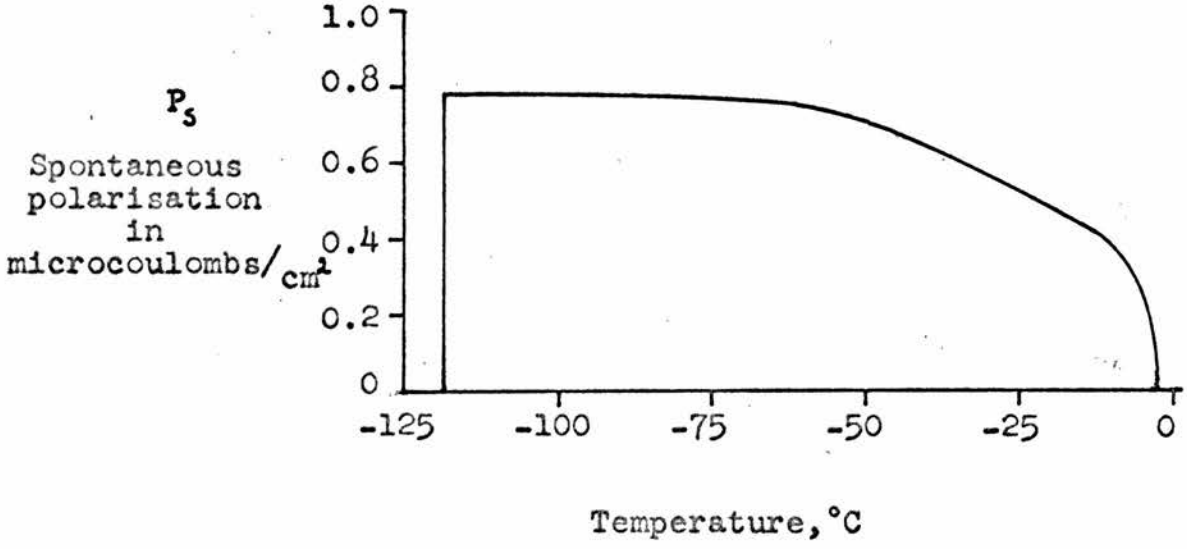

Fig. 1.7.2. (Fig.2., Pepinsky et al., 1958)

abruptly to zero at -119°C (fig. 1.7.2.).

Pepinsky et al. concluded from their measurements that the upper transition is second-order and that the lower transition is first-order.

Prior to the discovery of its ferroelectric properties AHS was the subject of very little published work. Details of its morphology, axial ratios and optical characteristics were given by Groth, 1908. Couture and Riche, 1949, studied the Raman spectrum of AHS; they concluded that there might be three symmetrically inequivalent SO_4^{2-} ions and that the structure must be "fort complexe".

Since 1958 AHS has been the subject of several Raman scattering, infrared absorption and nuclear magnetic resonance (NMR) experiments (Raman scattering: Bazhulin et al., 1959; infrared absorption: Myasnikova, 1962; Myasnikova and Yatsenko, 1962; Oden, 1966; NMR: Burns, 1961; Miller et al., 1962), and also a neutron inelastic scattering experiment (Rush and Taylor, 1965). There is general agreement from this work that the internal vibrations of the NH_4^+ ion do not change in passing through the upper transition, though the lower transition may be associated with an ordering of these ions (Miller et al., 1962). Both transitions appear to be chiefly accompanied by a change in the character of hydrogen bonding in the structure. The internal vibrations of the SO_4^{2-} ions are reported to show no change at either transition (Myasnikova, 1962; Myasnikova and Yatsenko, 1962; Bazhulin et al., 1963). Some recent deuteron magnetic resonance (DMR) experiments on ND_4DSO_4, at the upper transition, show weak changes in the signals from the DSO_4^- ion, which have

yet to be interpreted, and detect no change in those from ND_4^+ (J.A.S. Smith, 1968, private communication). The results of Rush and Taylor, 1965, suggest that the rotational freedom of the NH_4^+ ion is quite high. The DMR results also indicate that the ion is in rotation, and, further, that it is either unsymmetrical or has unequal lifetimes in its various configurations (loc. cit.). Some unsuccessful attempts have been made to detect low frequency optical modes of AHS and some related ferroelectrics in spectra from Raman scattering and infrared absorption (Bazhulin et al., 1963, Myasnikova and Arefev, 1964).

Other aspects of the behaviour of AHS have been studied. Strukov et al., 1964, investigated its polarisation reversal characteristics, which they found to be 'normal'. Further to the measurements of Pepinsky et al., 1958, the temperature dependence of ϵ_c and the spontaneous polarisation have been redetermined in the vicinity of the upper transition (Strukov et al., 1962). The results differed only slightly from those of Pepinsky et al. A careful measurement of the temperature dependence of the specific heat of AHS in the range -70°C to +14°C revealed a sharp peak in the immediate vicinity of the transition; this was attributed to non-negligible polarisation fluctuations (Strukov and Danilycheva, 1963). Both this work and that of Strukov et al., 1962, confirmed that the upper transition is second-order. Polandov et al., 1969, have studied the ferroelectric properties of AHS as a function of hydrostatic pressure. The peak value of ϵ_c decreases with increasing pressure and the transition temperature rises. The temperature of the lower transition rises more rapidly with pressure, and the results

suggest that the ferroelectric phase disappears at high pressures (above 1000 kg/cm^2).

1.8. The present work

Pepinsky et al., 1958, reported that the structures of all three phases of AHS were under investigation in Osaka University by K. Ogawa and I. Nitta. Any results that may have been obtained remain unpublished. As far as is known, no other attempts to solve the structure of any of the phases have been undertaken. The only information on the structure of AHS available, prior to the results reported in this thesis, was the estimation of the coordinates of the rubidium atoms in $RbHSO_4$ by Bengtssen, 1941: AHS and $RbHSO_4$ are isomorphous (Pepinsky and Vedam, 1960).

The succeeding chapters comprise an account of the solution of the structure of AHS in its room-temperature, non-ferroelectric phase.

CHAPTER 2

SPECIMEN PREPARATION

2.1. Introduction

Four specimens were used in this study of AHS: one (designated SC) for the preliminary X-ray studies (chapter 3), two (SD1 and SD2) for the collection of full three-dimensional X-ray data (chapter 4), and one (SN) for the collection of neutron data (chapter 6). In this chapter the techniques of preparing and mounting these specimens are described.

Crystal planes and orientation are referred to the pseudo-orthorhombic cell.

Occasional reference is made to features of the four-circle diffractometer used to collect the full three-dimensional X-ray data and the neutron data. This instrument is described in chapter 4.

2.2. Source of specimens

All four specimens were obtained directly or indirectly (SN) from AHS supplied in crystalline form by British Drug Houses Ltd. (BDH), at laboratory reagent purity. The maximum levels of impurity stated by the manufacturer were

chloride	0.005%,
iron	0.002%,
lead	0.001% and
non-volatile matter	0.2%.

The large, formless crystals, as supplied, will be referred to as 'source crystals'.

2.3. Physical characteristics

The physical properties of AHS relevant to specimen preparation are its excellent cleavage in the (001) plane, its relatively poor cleavage in the (010) plane, and its marked deliquescence. At room temperature (~22°C), in relative humidities greater than 50%, the solid phase disappears completely in a few minutes. In the laboratory conditions obtaining during the preliminary work (2.4.1. and chapter 3) the material could be handled only in a dry-box. Later, air-conditioning maintained the relative humidity below 50%, and it became possible to work satisfactorily with an ordinary 60-watt lamp close over the specimens.

2.4. Preparation and preservation of specimens for X-ray data collection

2.4.1. Investigation of methods of preservation; preparation of specimen SC

Methods of preventing specimens from deliquescing were investigated in three general categories:

(i) coating the specimen directly,

(ii) maintaining the specimen in a dry atmosphere, and

(iii) enclosing the entire mount (the specimen and its supporting fibre) in a suitable, water-tight vessel.

For accurate data collection there are two principal conditions to be fulfilled by any acceptable method of specimen preservation: first, deterioration of the specimen must be negligible over a

period of several months, and secondly the method should introduce negligible, or small but isotropic, absorption of the incident and reflected beams.

For early experiments in the above categories clean, clear cleavage flakes were obtained by crushing source crystals in the dry-box. Suitable specimens were selected by checking the flakes for optical singularity under a polarising microscope mounted in the dry-box. Coating materials used in experiments (i) were shellac, "Durofix", nail varnish, "Bostik No. 1", polyurethane varnish, "Valspar" varnish, and methyl methacrylate monomer polymerised by warming at about 60°C for 2-3 days. None of these preserved specimens for more than a few days, except for excessively thick coatings of varnish. The solvents of "Durofix", nail varnish and "Bostik No. 1" actually attacked the specimens.

Two methods of type (ii) were investigated. First a specimen was mounted in a jet of nitrogen gas dried through "Molecular Sieve" and silica gel columns. This was successful only with a gas flow so fast as to cause the mount to vibrate. The method was modified by enclosing the mount in half of a gelatine capsule, introducing and extracting the dried gas through a brass base-plate. This also failed; at the relative humidities then obtaining in the laboratory the capsules were too highly pervious to atmospheric water-vapour. Attempts were made to render the capsules sufficiently impervious by coating them with the materials used in experiments (i). The polyurethane varnish was effective enough to suggest proceeding directly with experiments of type (iii).

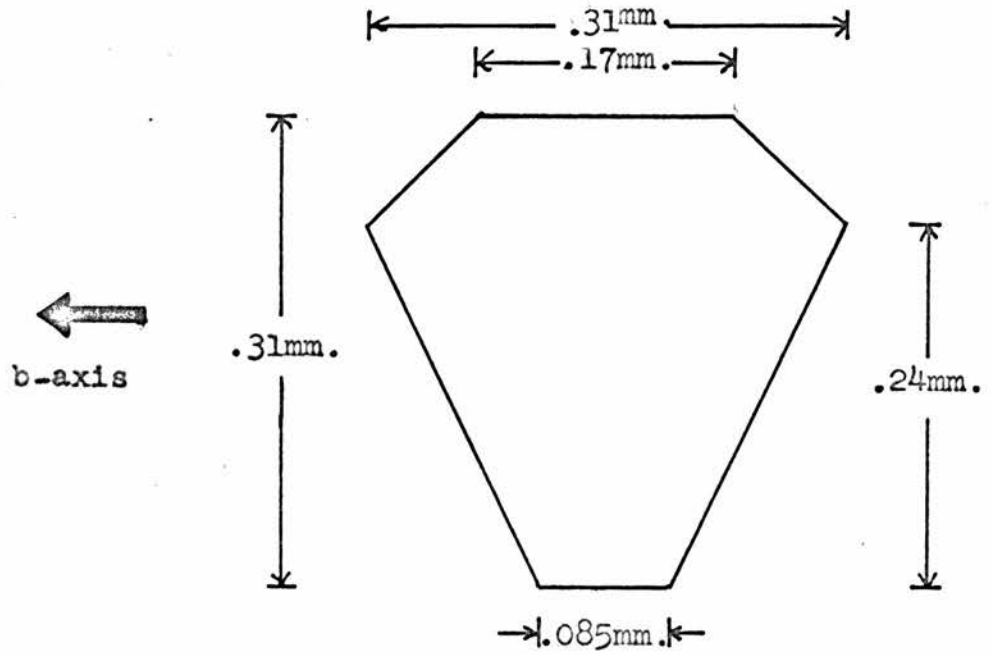

The (001) cleavage plane is in the plane of the diagram
The flake has a uniform thickness of 0.04mm.
All dimensions were measured to ±0.01mm. with a travelling microscope

Fig. 2.4.1.

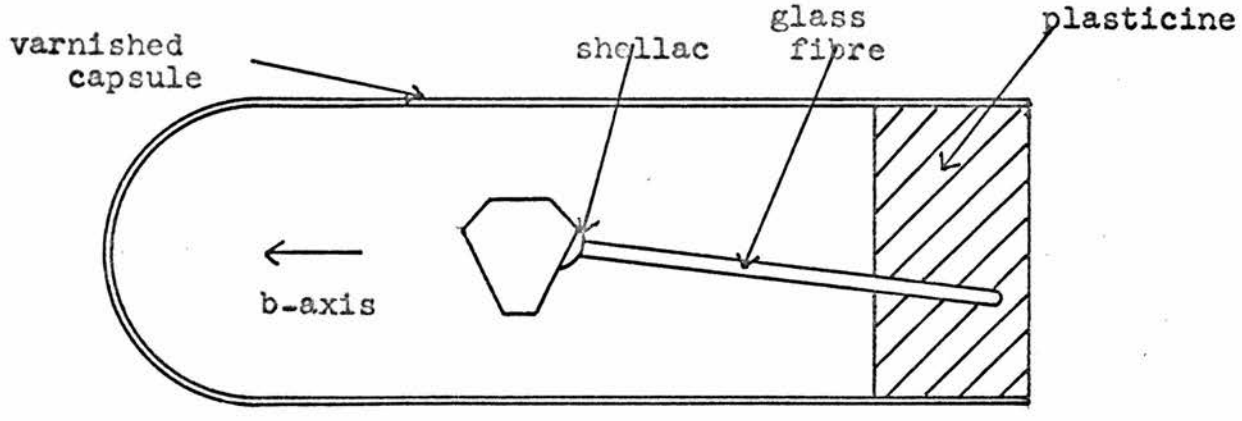

(the mount is enlarged in proportion to the capsule)

Fig. 2.4.2.

The capsules were coated evenly by dipping them repeatedly in thinned varnish and drying them with their side-walls vertical. Specimens were mounted on a glass fibre, using shellac as an adhesive (its solvent does not attack AHS). The fibre was supported in plasticine. Fragments of calcium chloride, to act as a drying agent, were imbedded in the plasticine around the base of the fibre. A coated capsule was placed over the mount, including the calcium chloride, and the seal into the plasticine painted over with varnish. Specimens were often preserved well for several weeks – but not dependably: they sometimes deteriorated badly for no obvious reason.

This technique was considered suitable for the collection of zero-layer data about an axis coaxial with a capsule of uniform wall-thickness (higher-layer data would require a correction for the increased effective wall-thickness), and it was used to preserve specimen SC. Specimen SC was one of the (001) cleavage flakes produced as described above; its shape and dimensions are shown in fig. 2.4.1. The specimen was mounted on the end of a thin glass fibre, with shellac adhesive, such that the b-axis was coaxial with the enclosing capsule (fig. 2.4.2.).

2.4.2. Further development of preservation techniques; the preparation of specimens SD1 and SD2

The technique used to preserve SC was not suitable for specimens to be used in the collection of accurate three-dimensional data. The method was, as said, unreliable, and the absorption by the capsule would have been non-isotropic and, possibly, rather uncertain.

To obtain dependable long-term protection from atmospheric water-vapour, it was decided to enclose the whole mount in a glass bulb. Provided the bulb wall-thickness were uniform, and the bulb close to spherical with the specimen located centrally in it, all beams, incident and reflected, would suffer the same absorption. To reduce the absorption losses and complementary background scattering, it was desirable that the bulb walls be as thin as possible. The conditions of relatively low X-ray absorption and high physical strength were met by fused silica. Karel Hackl of London manufactured, to order, a number of thin-walled, transparent, fused-silica bulbs (fig. 2.4.3.), each with a diameter constant to within $\pm$1.5%.

The uniformity of wall-thickness of these bulbs was tested by changing their orientation in a reflected beam from a standard crystal on the diffractometer, and measuring the variation in recorded intensity. A beam passing along AB (fig. 2.4.3.) had an intensity $\sim$5% less than that of the uninterrupted beam; MoKα radiation was used for these tests. None of the bulbs caused a variation in intensity of more than 1% as it was rotated or tilted, until, for the beam along a diagonal such as CF, F was within 4mm. of H (fig. 2.4.3.). Then the intensity dropped by a further 3-6%, reflecting the expected thickening of the silica around the apex (J) and stem of the bulb.

Hence, the variation in absorption arising from irregularities in the bulb wall-thickness would be negligible if both the incident and the reflected rays lay within the shaded area in fig. 2.4.4. From the mode of operation of the diffractometer, it follows that no reflection would be affected by the increased

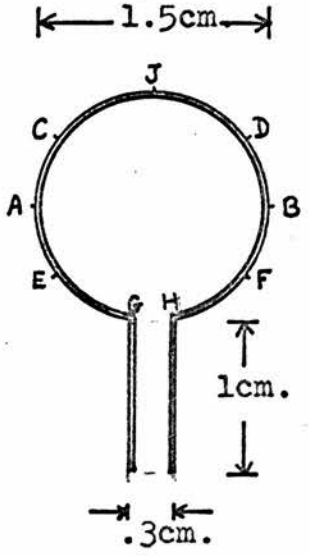

The wall thickness ~ 0.05mm.

The given dimensions vary between different bulbs by < ± 0.5mm.

Fig. 2.4.3.

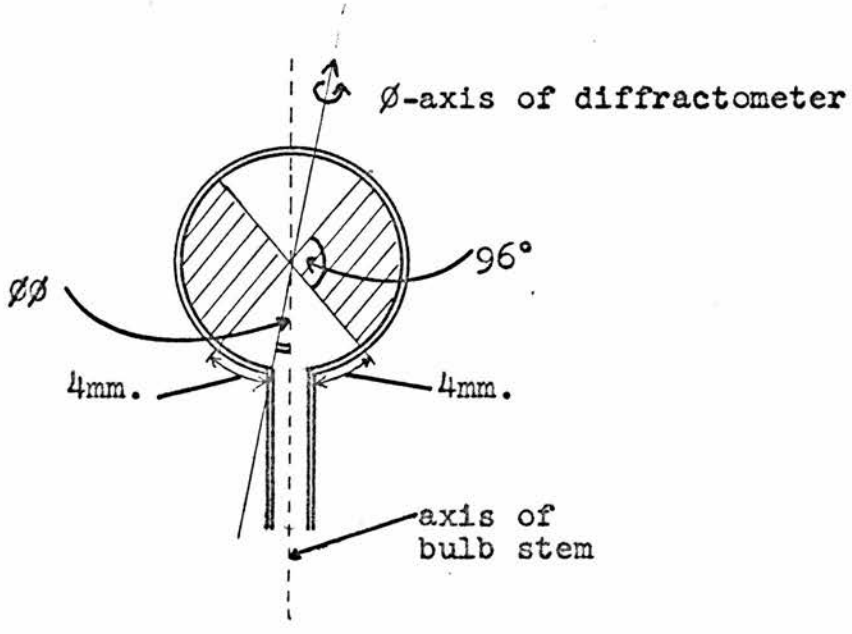

This is any cross-section through the bulb;the diffractometer Ø-axis is shown for the particular cross-section in which it lies in the plane of the cross-section

Fig. 2.4.4.

wall-thickness if the maximum Bragg angle included in data collection were less than (48° - ØØ); ØØ is the angle between the stem of the bulb and the Ø-axis of the diffractometer (fig. 2.4.4.).

It was found later that, for SD1 and SD2, ØØ did not exceed 10° with the specimens oriented for data collection; the maximum Bragg angle included in collecting data from these specimens should not exceed 38°.

With suitable **impervious** enclosing vessels to hand, the following mounting technique was developed:

(i) Source crystals were cleaved in (001) with a razor blade to obtain clean, clear 'slabs'; they were checked for optical singularity under the polarising microscope. These and subsequent operations were performed in the open air under an electric lamp (see section 2.3.). With care the 'slabs' could be cleanly cleaved in (010), and then, rather less often, in a plane close to (100). A day's work would usually produce three or four cuboids with plane faces and sharp edges. The cutting technique limited the specimen dimensions to edge lengths of 0.2 - 0.3mm. This range is somewhat less than that suggested by the approximate criterion, $\mu R = 1$ (Willis and Arndt, 1966, p.240); μ is the linear absorption coefficient (6.4cm.$^{-1}$ for AHS with MoKα radiation – chapter 4), and R is a typical dimension – strictly the radius of a spherical specimen. The uniform beam area readily obtainable with the diffractometer also limited the specimen size – to, at the most, twice the above range.

(ii) after mounting as described below, Laue photographs were taken of these specimens to select the few which gave good clean photographs – indicating that they had suffered no deterioration or damage during mounting. A week's work would yield two or three good specimen crystals – well shaped, the right size, and single. On these criteria, SD1 and SD2 were the best specimens obtained also having the required orientation after mounting (see (iv)).

(iii) glass-fibres to support the specimens were made relatively thick for most of their length, with a sharp taper at the specimen end (fig. 2.4.5.). This design provided a rigid support, to minimise vibrations of the specimen caused by the motion of the diffractometer shafts, and yet presented only a very small amount of glass to the incident beam. The fibre was imbedded in low melting-point (30°C) vacuum wax at its 'lower' end.

(iv) the most convenient orientation for a monoclinic crystal on the diffractometer is with the b-axis parallel to the Ø-axis. Hence, AHS specimens should be mounted with the b-axis parallel to the supporting fibre. The (001) face of each cuboid was easily identified by its very clean, bright appearance. The (010) and '(100)' faces could not be identified by direct observation. A good specimen was too valuable to risk any deterioration in attempting to orient it under the polarising microscope: the 50% chance of selecting the preferred orientation was accepted. The specimens were mounted on the tapered end of a glass fibre with shellac adhesive. One of the faces perpendicular to (001) was set normal to the

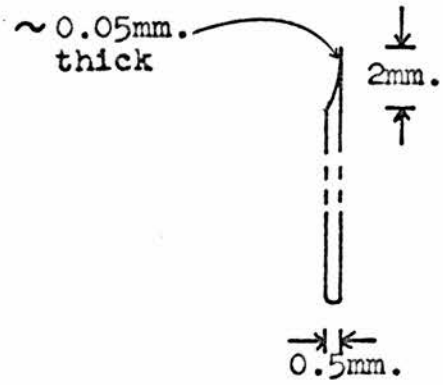

Fig. 2.4.5.

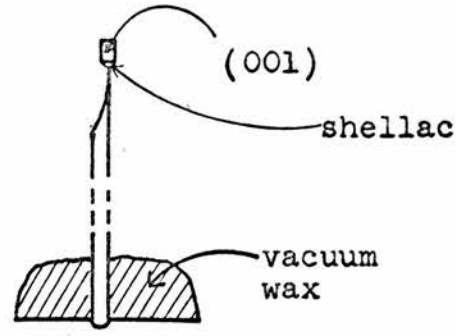

Fig. 2.4.6.

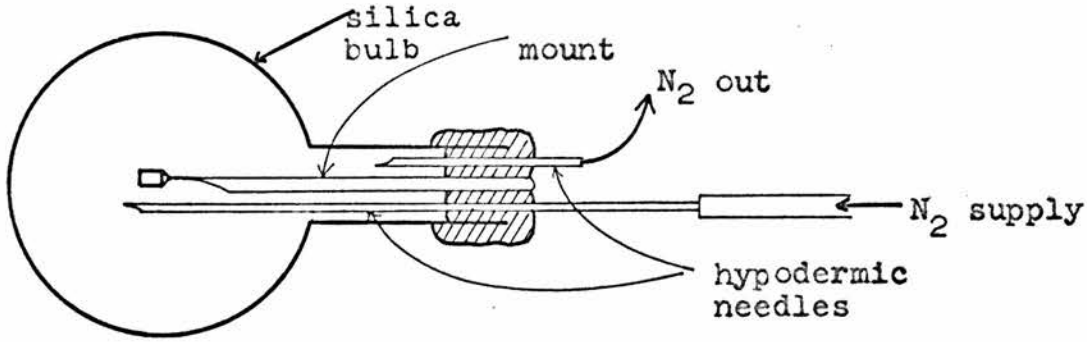

Fig. 2.4.7.

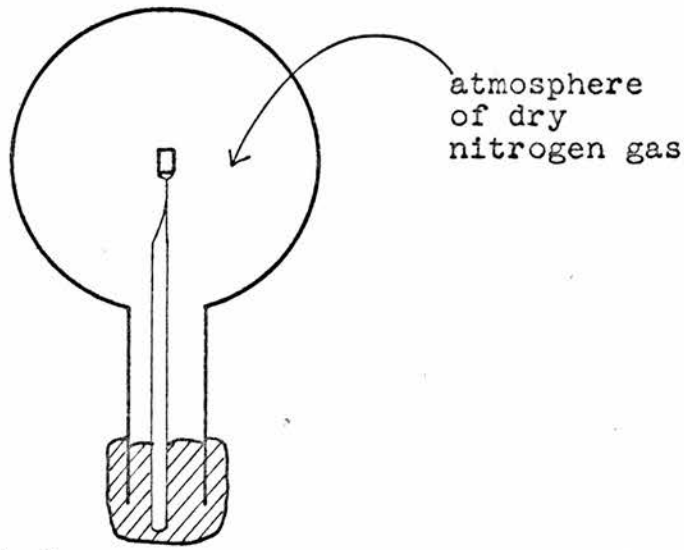

Fig. 2.4.8.

fibre (fig. 2.4.6.).

(v) when the shellac had set, the electric lamp was brought close over the mount to soften the vacuum wax. Two hypodermic needles were inserted through the wax, close to the fibre. One needle, attached to a supply of nitrogen gas dried through "Molecular Sieve" and self-indicating silica gel columns, extended just beyond the specimen; the other just passed through the wax (fig. 2.4.7.). With the gas supply on, a silica bulb was placed over the mount and needles, and the neck of the bulb pushed into the softened wax (fig. 2.4.7.). The bulb was thoroughly flushed out with the dry gas. Then the needles were withdrawn and the wax was immediately sealed over. The electric lamp was raised, and, as the wax started to set, the position of the specimen was adjusted to be central in the bulb. Once the wax had set, the base of the mount was dipped in molten wax to thicken the seals where the needles had been withdrawn.

The enclosed mount after the completion of these procedures is illustrated in fig. 2.4.8.. The technique here described has been found to be effective and reliable: specimen SD2 showed no detectable deterioration eight months after mounting.

The dimensions and orientation of SD1 and SD2 are given in section 4.3..

2.5. Preparation and preservation of specimens for neutron data collection

The collection of neutron data required a specimen of dimensions somewhat larger than could be obtained from the source

crystals. A specimen of AHS, cut to a cube of side 0.5cm., was ordered from Semi-Elements Incorporated. The specimen arrived and was treated with appropriate care. It was found to be ammonium sulphate.

The best method of growing large crystals of AHS is by crystallisation from the melt (Pepinsky et al., 1958), but there was insufficient time to develop the technique. The standard methods of crystallisation from solution are (loc. cit.):

(i) slow cooling of ammonium sulphate dissolved in concentrated sulphuric acid, and

(ii) slow hydrolysis of chloroacetamide in dilute sulphuric acid with a one to one molar ratio of $C\ell CH_2CONH_2$ and H_2SO_4.

Method (ii) was tried without success: a variant of (i) produced usable crystals.

A room-temperature saturated solution of the source crystals, in water, was prepared. From this, blade-shaped crystals of AHS appeared when sufficient concentrated sulphuric acid was added to the mother-liquor to reduce its pH below 4. The sulphuric acid used was BDH "Analar" grade. Three recrystallisations were performed to purify the original material. Concentrated sulphuric acid was added slowly to a saturated solution of the purified AHS until a few small blade-shaped crystals appeared. Some of the mother-liquor was put into each of several crystallisation bottles. One of the crystals was suspended in each bottle by a glass fibre attached to a sealing cap. Every day, two drops of mother-liquor and one of concentrated sulphuric acid were added to all the bottles. After five days a large crystal had formed

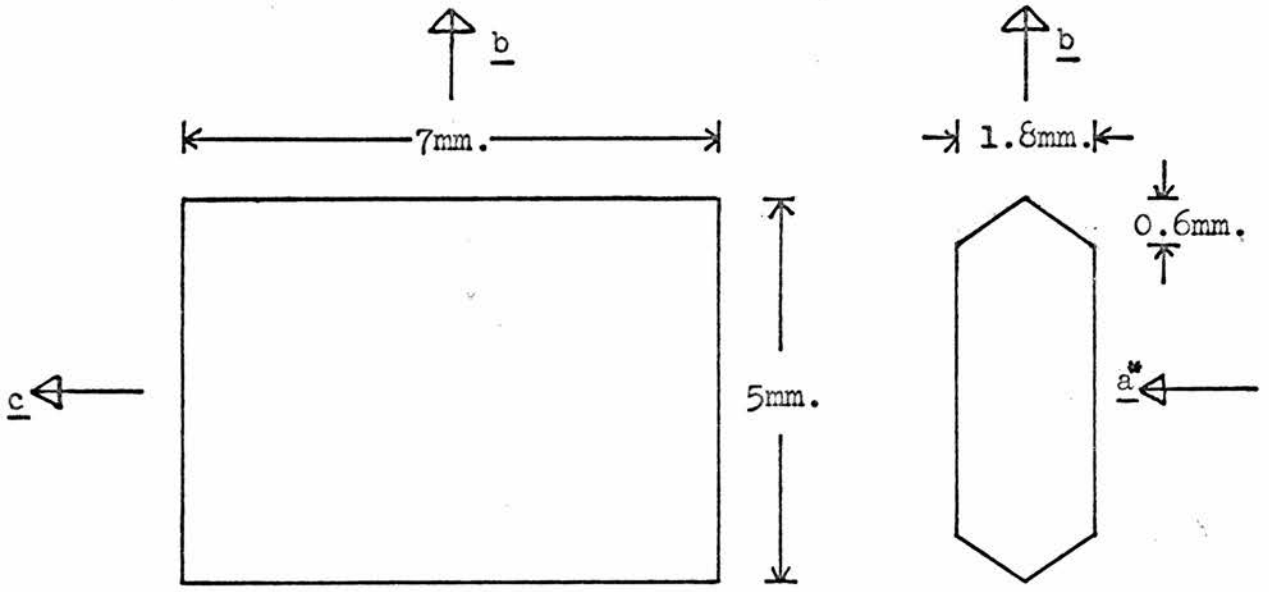

Dimensions measured to ± 0.1mm. with a travelling microscope

Fig. 2.5.1.

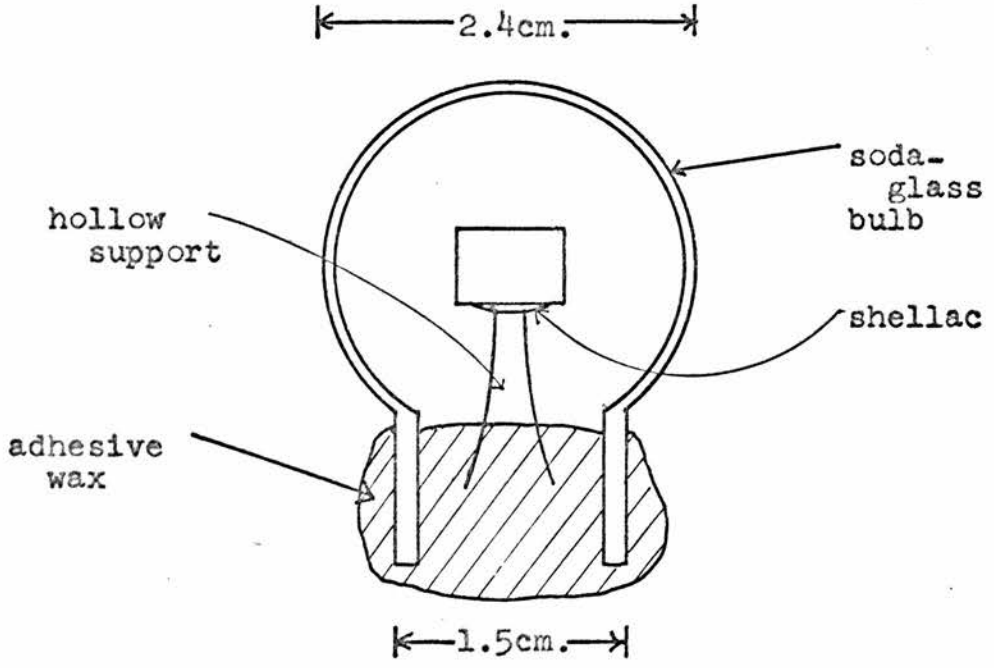

Fig. 2.5.2.

in each bottle; most were ill-formed or had a mass of smaller crystals attached. One, however, was free from parasitic crystals and of a usable, if not ideal, size and shape (fig. 2.5.1.). This was selected for the collection of neutron data, and designated specimen SN.

For neutron work the conditions to be set upon specimen enclosing vessels are not so stringent as with X-ray work. Most materials absorb thermal neutrons very weakly, so that very thin, uniform walls are not required. Bulbs were blown from soda-glass (harder glasses contain boron which is highly absorbing for neutrons) by Mr. J.J. Broom of the Chemistry Department, Edinburgh. A few of these bulbs appeared to be particularly uniform in wall-thickness and nearly spherical; one was chosen to enclose SN.

The specimen was mounted on a short, broad, hollow plastic tube with shellac adhesive (fig. 2.5.2.). BDH "Sira" adhesive wax was used in the place of vacuum wax (section 2.4.2.). The specimen was of sufficient size to be negligibly affected by the small amount of water-vapour included when the mount was enclosed under an electric lamp. The specimen was centred as the wax set after removing the lamp. The enclosed mount is illustrated in fig. 2.5.2..

2.6. Preliminary X-ray examination of specimens

SC, SD1, SD2 and SN were all examined with X-rays before being accepted as suitable specimens for data collection. Laue, oscillation and Weissenberg photographs were taken of SC, SD1 and SD2. The photographs were searched for any evidence that these

crystals were not single or had suffered any deterioration during or after mounting. The three specimens were satisfactory. Back-reflection Laue photographs of SN were used to check that it was single, and to orient it approximately. The photographs showed that SN had been correctly mounted with the b-axis coaxial with the supporting tube (fig. 2.5.2.).

CHAPTER 3

PRELIMINARY X-RAY STUDIES

3.1. Introduction

For this preliminary study two-dimensional photographic data was collected from specimen SC. From the data the broad features of the structure in the (010) projection were determined. Furthermore, the nature of the problems to be faced in a complete structure determination became apparent. The latter information was used later in planning the collection of full three-dimensional data.

3.2. Orientation, cell dimensions and space groups

The b-axis of SC was oriented parallel to the rotation axis of an oscillation camera. Oscillation and Weissenberg photographs, about the b-axis, were taken to determine the cell dimensions and space group.

The previously published cell dimensions and space groups of the three phases of AHS are presented in table 1.7.1. The dimensions given for the room-temperature monoclinic and pseudo-orthorhombic cells are not compatible. Taking the given dimensions of the monoclinic cell, those of the pseudo-orthorhombic cell were calculated to be

a'_o = 25.06 Å

b'_o = 4.54 (subscript o denotes the

c'_o = 14.90 pseudo-orthorhombic cell)

β'_o = 90° 36'

which do not agree with the dimensions in table 1.7.1. The axes of the pseudo-orthorhombic cell are related to those of the monoclinic cell (denoted by the subscript m) by

$$\underline{a}'_o = -(2\underline{a}_m + \underline{c}_m)$$
$$\underline{b}'_o = \underline{b}_m$$
$$\underline{c}'_o = \underline{c}_m \ .$$

The reversal of the sense of $\underline{a}'_o$ relative to $\underline{a}_m$, with respect to the common c-axis — presumably so that β'_o should be greater than 90° — seems an unnecessary deference to convention. It is proposed here to adopt the pseudo-orthorhombic cell given by

$$\underline{a}_o = 2\underline{a}_m + \underline{c}_m \qquad (a_o = 25.06 \text{ Å})$$
$$\underline{b}_o = \underline{b}_m \qquad (b_o = 4.54\ )$$
$$\underline{c}_o = \underline{c}_m \qquad (c_o = 14.90\ )$$
$$(\beta_o = 89° 24')$$

(fig. 3.2.1.). This cell will be assumed and used hereafter. Later, it will be seen to simplify the description and discussion of many important features of the AHS structure to refer them to the pseudo-orthorhombic cell. This cell will be referred to as the 'pseudo cell'.

The dimensions of the pseudo cell as determined from oscillation and Weissenberg photographs of SC were

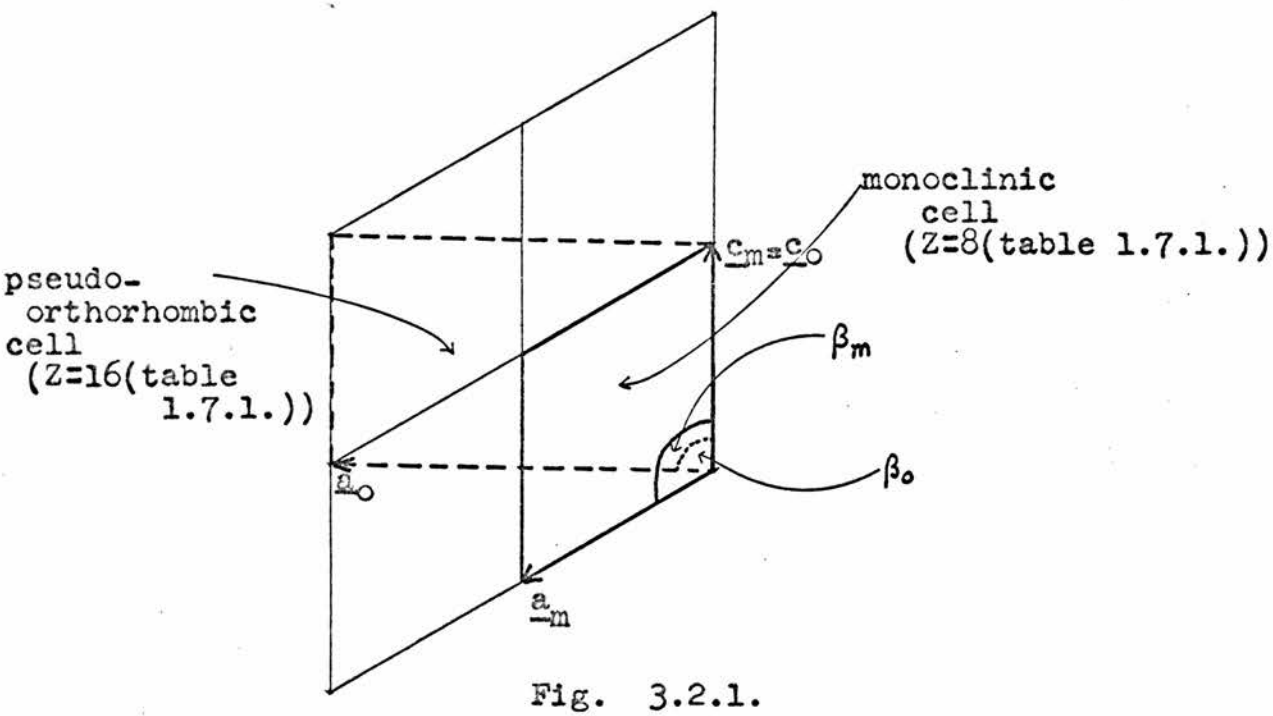

Fig. 3.2.1.

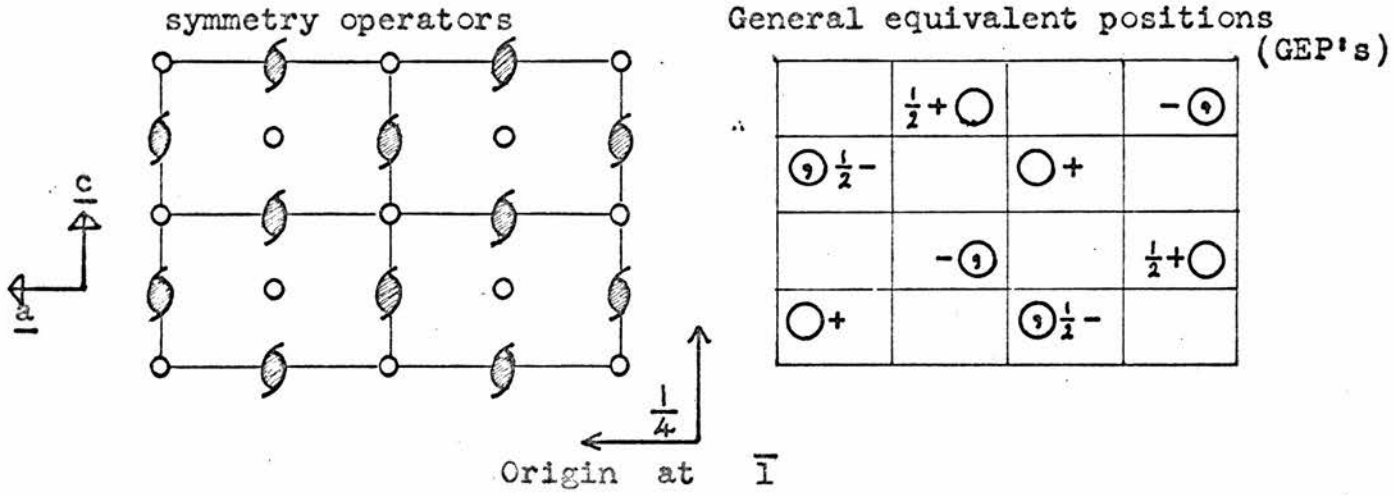

Four sets of four-fold special positions on centres of symmetry

(For the space group symbols and other nomenclature see the International Tables, 1962)

Fig. 3.2.2.

a_o = 24.66 Å

b_o = 4.59

c_o = 14.81

β_o = 89° 41' .

These are in agreement with those measured later on the diffractometer (section 4.3.); the latter differ significantly from the dimensions listed in table 1.7.1. Hereafter a_o, b_o, c_o and β_o will be referred to simply as a, b, c and β.

The systematic absences found in the Weissenberg photographs confirmed the space group as $B2_1/a$. This space group is illustrated in fig. 3.2.2..

3.3. Intensity measurements

The b-axis of AHS is very short (4.6 Å); a projection of the structure into (O1O) may be expected to show most atoms resolved from one another. With the specimen SC already correctly mounted for the collection of (h0ℓ) data, it was transferred to a Nonius Integrating Weissenberg camera (Wiebenga and Smits, 1950). The X-ray source was a Philips fine-focus copper tube.

Intensities were recorded on a series of multiple film packs, using CuKα radiation. Each pack comprised three Ilford "Industrial G" films only. All films were developed and fixed for the same lengths of time.

It was required to record all but the weakest reflections measurably, and all the strong reflections in the range over which the optical density on the film was approximately proportional to

intensity. A sufficient overlap of measurably recorded reflections between films was needed to be able to bring the intensities on all the films to a common scale. For these purposes, four packs were exposed for one, two, six and twelve times the period of one integrating cycle – 12 hours. There were thus twelve films in all. The oscillation range was 200°: 275 reflections were recorded out to $\sin\theta/\lambda = 0.64$ on each half of the film. 130 of these 275 were symmetrically inequivalent.

A scale of spots of the same size and shape as those on the films was prepared on a strip of "Industrial G" film, with exposures of $\frac{1}{2}$, 1, 2, 3..... 25 time units. The time unit and the number of spots were adjusted so that a maximum range of optical densities was covered, with the weakest spot just visible and the difference in optical density between adjacent spots clearly detectable over the whole scale.

The intensities of spots on one half (θ = 0° to 90°) of each film were read by eye-estimation against this scale. First, the scale strip was moved so as to bring successively weaker spots alongside the film spot. When the scale spot was not clearly stronger than the film spot the scale value ($\frac{1}{2}$, 1, 2.... 25) was recorded. The procedure was repeated moving the strip the other way; the value of the strongest spot which was not clearly weaker than the film spot was recorded. The intensity of the film spot was taken as the average of these two readings. Spots which were discernible but weaker than $\frac{1}{2}$ were recorded as $\frac{1}{4}$. Where there was partial separation of the $K\alpha_1$ and $K\alpha_2$ spots (α_1/α_2 separation), the intensities of the two separate parts and of the overlapping part were all obtained. The measurement

was repeated if there was a significant discrepancy between the sum of the intensities of the separate parts and the intensity of the overlapped portion. Otherwise these were averaged. Where the α_1/α_2 separation was complete each spot was measured and the intensity taken as the sum of the two. The intensity of a spot mounted on a Laue streak was measured with the scale spot also on the streak.

After measuring the intensities on the twelfth film, all the spots on the first two films were re-read as a check on the reproducibility of the intensity estimation. Of the 400 with intensities $\leq$ 25, 360 differed by $<$ 1, 30 by 1–2 and 10 by 2–2.5. This was considered satisfactory. On the remaining ten films a few spots, picked at random in each of the intensity ranges $>$ 20, 15–20, 10–15, 5–10 and 5, were re-read. The agreement was very similar to that detailed above. These checks afforded an estimation of the standard deviation on intensities (table 3.3.1.).

Table 3.3.1.

intensity range	s.d. as a %
$I \geq 20$	10
$5 < I < 20$	7.5
$3 \leq I \leq 5$	10
$1 \leq I < 3$	30
$I < 1$	80

The scaling factors, to bring the intensities on each film

to a common scale, were found from the values of $I_i(hO\ell)/I_j(hO\ell)$ - where i and j were the film numbers 1, 2.... 12, $i \neq j$ - for all pairs of $I_i(hO\ell)$ and $I_j(hO\ell)$ in which both values were known sufficiently accurately. From the estimated standard deviations (table 3.3.1.) it follows that the approximate standard deviation will be 15% on ratios involving only $3 \leq I \leq 25$, 30% on ratios involving $1 \leq I < 3$ and $3 \leq I \leq 25$, and 45% on ratios involving only $1 \leq I < 3$. Only ratios in the first two of these classes were used; a relative weight of ¼ was given to those in the second class. The intensities of reflections lying on Laue streaks or a heavy general background, or showing α_1/α_2 separation, were not used. With these limitations all available ratios were calculated for twenty pairs of films.

For each pair of films the weighted mean ratio and its standard deviation were calculated. The values of the ratios N:1 (N is the film number, 2 to 12; 12 designates the film with the weakest intensities) were computed as the weighted mean of the values obtained by all the independent paths which gave reasonable accuracy. The ratio 6:1, for example, was calculated from (5:6, 4:5 and 1:4) and (6:7 and 1:7). The standard deviations on N:1 were calculated in the usual way from those of the ratios used.

The standard deviations of the intensities on each film were estimated according to intensity range (table 3.3.1.), and doubled for spots which lay on pronounced Laue streaks or a very heavy general background, or which showed α_1/α_2 separation. A weighted mean value for the intensity and standard deviation of each of the 275 reflections was calculated after scaling all its observed

values to film 1. The estimated error on the scaling factor was included. This calculation was performed by a computer program which also applied the Lorentz-polarisation correction factor. No other corrections were applied to the data.

3.4. The intensity distribution and the projected structure

The (h0ℓ) intensities, together with those roughly estimated from a few higher layer Weissenberg photographs of SC, showed the following systematic distributions:

in (h0ℓ)	h = 4n, strong
	h = 4n + 2, weak
	(h or ℓ odd, space group absent);
in (h1ℓ), (h2ℓ) etc.	h = 4n, strong
	h = 4n + 2, weak
	h odd, intermediate;
in (h00), (h20) etc.	h = 8n, very strong
	h ≠ 8n, weak;
and in (h10), (h30) etc.	h = 8n + 4, very strong
	h ≠ 8n + 4, weak;

n is any integer. It is evident that the structure of AHS arises from small displacements from a structure of higher symmetry, of unit cell $\underline{a}/4 \times \underline{b} \times \underline{c}$: the true structure is comprised of four closely similar sub-cells which have a pseudo-symmetry higher than the true $B2_1/a$ symmetry. From the intensity distribution in (hk0), and the observation that the intensities of (hkℓ) and ($\bar{h}$kℓ) are always similar when h = 4n, it may be deduced that the sub-cells have a pseudo-symmetry which includes an n-glide plane perpendicular to $\underline{c}$, and a mirror or glide plane perpendicular to $\underline{a}$.

Attention is now focussed on the (0l0) projection. The a- and c-glide planes of $B2_1/a$ become equivalent to translations of $\underline{a}/2$ and $\underline{c}/2$; the two-dimensional unit cell thus has dimensions $\underline{a}/2 \times \underline{c}/2$ and contains four formula units — it is the projection of the shaded area in fig. 3.4.1.. This cell has the oblique two-dimensional space group p2 (fig. 3.4.2.). The corresponding sub-cell can be seen to have dimensions $\underline{a}/4 \times \underline{c}/2$. The pseudo-symmetry of this sub-cell must be that of the rectangular two-dimensional space group pmg (fig. 3.4.3.) — there was no intensity distribution indicating a pseudo-glide plane perpendicular to $\underline{a}$.

As already seen, the $(h0\ell)$ intensities may be divided into 'strong' ($h = 4n$) and 'weak' ($h = 4n + 2$) reflections. Since $\rho(x,z)$, the electron density at (x,z), is centrosymmetric,

$$\rho(x,z) = \frac{1}{A} \sum_{\substack{h \\ \ell}}^{\text{and}} F(h0\ell) \cos 2\pi(hx + \ell z). \qquad (3.4.1.)$$

A, is the area of the unit cell; the other symbols have their usual meaning. Now the electron density at $(x + {}^1/_4, z)$ is given by

$$\rho(x + {}^1/_4, z) = \frac{1}{A} \sum_{\substack{h \\ \ell}}^{\text{and}} F(h0\ell) \cos 2\pi(hx + h/4 + \ell z) \qquad (3.4.2.)$$

$$= -\rho(x,z) \quad \text{for} \quad h = 4n + 2, \text{ and}$$

$$= \rho(x,z) \quad \text{for} \quad h = 4n.$$

Hence,

$$[\rho(x,z) + \rho(x + {}^1/_4, z)] = \frac{2}{A} \sum_{\substack{\ell \\ h=4n}}^{\text{and}} F(h0\ell) \cos 2\pi(hx + \ell z), \qquad (3.4.3.)$$

and

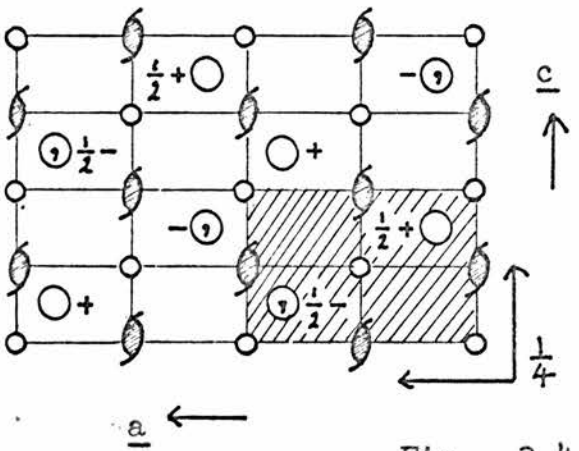

$B2_1/a$ (origin at $\bar{1}$)

8 GEP's

16 formula units in cell

Fig. 3.4.1.

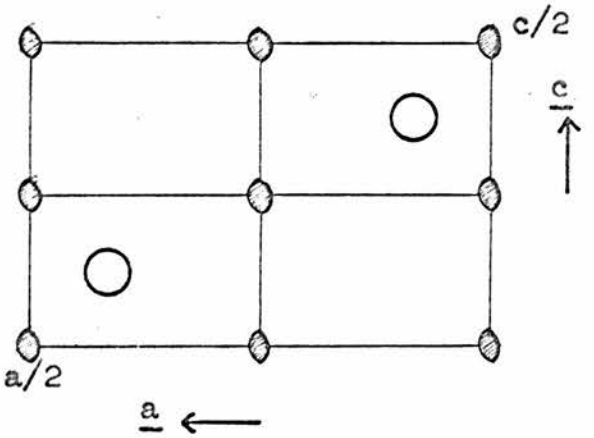

p2 (origin at 2)

2 GEP's

4 formula units in cell

Fig. 3.4.2.

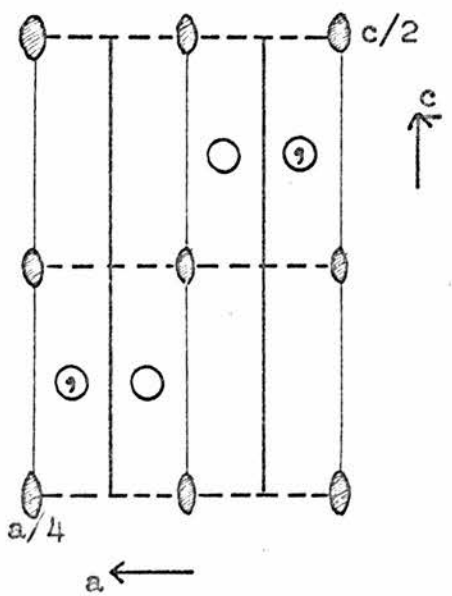

pmg (origin at 2)

4 GEP's

2 formula units in cell

Fig. 3.4.3.

$$[\rho(x,z) - \rho(x + \tfrac{1}{4},z)] = \frac{2}{A} \sum_{\substack{\ell \text{ and} \\ h=4n+2}} F(h0\ell) \cos 2\pi(hx + \ell z). \quad (3.4.4.)$$

Thus, the 'strong' reflections transform to the 'average structure', $[\rho(x,z) + \rho(x + \tfrac{1}{4},z)]$: the 'weak' reflections transform to the 'difference structure', $[\rho(x,z) - \rho(x + \tfrac{1}{4},z)]$. The 'average structure' is seen to be the contents of the sub-cell ($a = 0$ to $a = \tfrac{1}{4}$) x $\underline{c}/2$, superposed on the sub-cell ($a = \tfrac{1}{4}$ to $a = \tfrac{1}{2}$) x $\underline{c}/2$. It has the pseudo-symmetry pmg, the true symmetry p2, and a <u>true</u> unit cell of $\underline{a}/4$ x $\underline{c}/2$. This is illustrated diagrammatically in fig. 3.4.4.. The 'difference structure' is the difference between the contents of the above two sub-cells. It has a true unit cell of $\underline{a}/2$ x $\underline{c}/2$ (fig. 3.4.4.). The symmetry of the 'difference structure' is p2 with the addition of centres of anti-symmetry (fig. 3.4.4.). The structure in the (010) projection is, of course, the sum of the 'average' and 'difference' structures.

The function

$$P_a(u,w) = \frac{1}{A} \sum_{\substack{\ell \text{ and} \\ h=4n}} |F(h0\ell)|^2 \cos 2\pi(hx + \ell z) \quad (3.4.5.)$$

is the Patterson function (Lipson and Cochran, 1966, chapter 7) corresponding to the 'average structure'. This is discussed in the following section. The function

$$P_d(u,w) = \frac{1}{A} \sum_{\substack{\ell \text{ and} \\ h=4n+2}} |F(h0\ell)|^2 \cos 2\pi(hx + \ell z) \quad (3.4.6.)$$

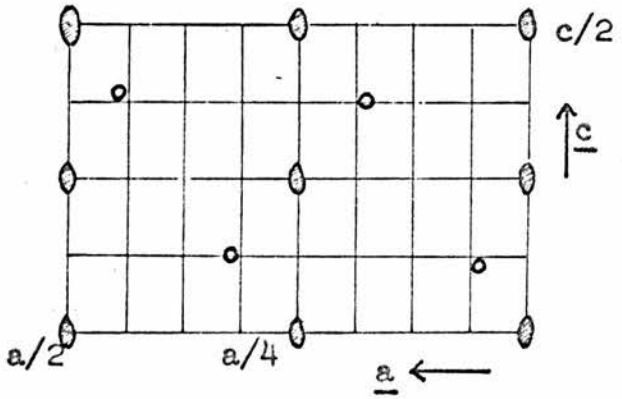

p2
2 GEP's
4 formula units in cell

true unit cell is
$\underline{a}/2 \times \underline{c}/2$

pseudo-cell is
$\underline{a}/4 \times \underline{c}/2$

A diagrammatic structure, $\rho(x,z)$, with atoms at o

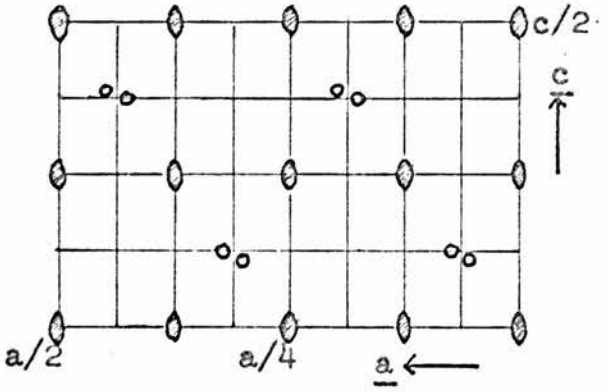

p2, the true symmetry

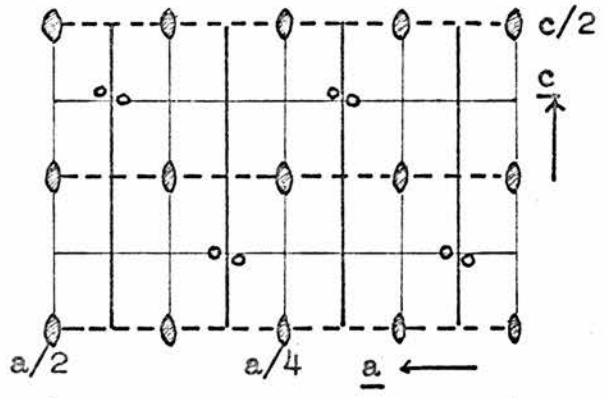

pmg, the pseudo-symmetry

the true unit cell is $\underline{a}/4 \times \underline{c}/2$

$\left[\rho(x,z)+\rho(x+1/4,z)\right]$, the 'average structure', corresponding to $\rho(x,z)$ above

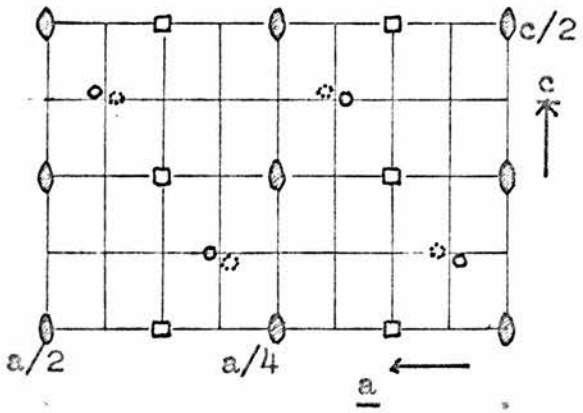

○ signifies a negative peak

□ is a centre of anti-symmetry

the true unit cell is
$\underline{a}/2 \times \underline{c}/2$

$\left[\rho(x,z)-\rho(x+1/4,z)\right]$, the 'difference structure', corresponding to $\rho(x,z)$ above

Fig. 3.4.4.

is the Patterson function corresponding to the 'difference structure'. As is discussed in the following section, a solution to this function was not found with the photographic data. A fuller discussion of this function, the 'difference structure' itself, and their solution, appears in chapter 5.

The separation of the two-dimensional structure into two components – the 'average' and 'difference' structures – was an important step in the solution of the AHS structure. Similar techniques are likely to be helpful for any pseudo-symmetric structure (Qurashi, 1963).

3.5. The solution and refinement of the 'average structure'

A program was written to compute the function $P_a(u,w)$ from the observed intensities, $|F_o(hO\ell)|^2$. The corresponding 'sharpened' Patterson function, $SP_a(u,w)$, was also computed (Lipson and Cochran, 1966, p.165).

For the function $SP_a(u,w)$ the 'sharpened' intensities, $|SF_o(hO\ell)|^2$, were prepared as follows. The scale factor, k, to bring the observed intensities to an absolute scale was found by Wilson's method (Wilson, 1942). The compution of mean values of $|F_o(hO\ell)|^2$ in ranges of $\sin\Theta$ could not be extended reliably below $\sin\Theta = 0.2$. The mean value at $\sin\Theta = 0$ was taken to be $k^{-1} \Sigma Z_j^2$, where Z_j is the atomic number of the j^{th} atom. The summation extended over the contents of the $\underline{a}/4 \times \underline{c}/2$ cell. The values of all $|F_o(hO\ell)|^2$ were then adjusted, by a factor depending on $\sin\Theta$, to $|SF_o(hO\ell)|^2$ such that mean values of the latter, taken over ranges of $\sin\Theta$, lay on the Gaussian $[k^{-1} \Sigma Z_j^2] \exp[-\frac{\pi^2}{p} . S^2]$; S is $2\sin\Theta/\lambda$ and p is a

constant. The value of p was set at 7.25; $\overline{|SF_o(hO\ell)|^2}$ at $\sin\Theta = 1.0$ is then a tenth of its value at $\sin\Theta = 0$. In practice, this has been found to be the best degree of 'sharpening' (Lipson and Cochran, 1966, pp.165-168). Then,

$$SP_a(u,w) = \frac{1}{A} \sum_{\substack{\ell \text{ and} \\ h=4n}} |SF_o(hO\ell)|^2 \cos 2\pi(hx + \ell z). \qquad (3.5.1.)$$

The 'sharpened' function corresponding to $P_d(u,w)$ is

$$SP_d(u,w) = \frac{1}{A} \sum_{\substack{\ell \text{ and} \\ h=4n+2}} |SF_o(hO\ell)|^2 \cos 2\pi(hx + \ell z). \qquad (3.5.2.)$$

Some symmetry considerations helped in the solution of $SP_a(u,w)$. The pseudo-symmetry of the sub-cells is pmg (section 3.4.). This generates four G.E.P.'s, but the sub-cells contain only two formula units. Therefore the nitrogen and sulphur atoms had to lie either close to the pseudo-mirror planes, or else close to the diads. The second possibility could be ruled out for the sulphur atoms: those diads which are screw diads in the three-dimensional structure would place two sulphate tetrahedra above each other in 4.6Å, and this is not possible. The positioning of the sulphur atoms on or close to the pseudo-mirror planes required that the tetrahedral sulphate ion be oriented with its mirror plane coincident, or nearly coincident, with the pseudo-mirror plane.

No features were resolved by $SP_a(u,w)$ that were not also resolved by $P_a(u,w)$; but the positions of peaks in the former

were more clearly defined. With the help of the above observations regarding the positions of the sulphur and nitrogen atoms and of the sulphate groups, the solution of $SP_a(u,w)$ was straightforward. The 'average structure' deduced is shown diagrammatically in fig. 3.5.1.. The fractional coordinates, referred to the cell $\underline{a}/4 \times \underline{c}/2$, are listed in table 3.5.1.. Each 'atom' in the structure is actually composed of two atoms with their centres slightly separated about the given coordinates. The hydrogen atoms were not considered.

The overall temperature factor, B, (eqn. 3.5.3.), was estimated by Wilson's method (Wilson, 1942) as 1.25Å^2. The value found for the scale factor, k, was 120. The errors associated with parameters found by Wilson's method are typically of the order of 30% (Lipson and Cochran, 1966, p.134). The atomic coordinates (table 3.5.1.), temperature and scale factors, and the atomic scattering factors for neutral sulphur, oxygen and nitrogen atoms (International Tables, 1962, Vol. III, table 3.3.1.A.) were used to calculate the structure factors, $F_c(h0\ell)$, for the 'strong' reflections. $F_c(h0\ell)$ is given by

$$F_c(h0\ell) = k^{-\frac{1}{2}} \sum_{\text{unit cell}} f_j \cos 2\pi(hx_j + lz_j)\exp[-B.\ \sin^2\Theta/\lambda^2]. \quad (3.5.3.)$$

f_j is the value of the scattering factor of the j^{th} atom, for reflection $(h0\ell)$. The conventional R-factor — $\Sigma\big||F_o(h0\ell)| - |F_c(h0\ell)|\big| / \Sigma|F_o(h0\ell)|$ — was 36% for the 'strong' reflections, with the above parameters.

A Fourier synthesis (section 5.2.) of the 'average structure'

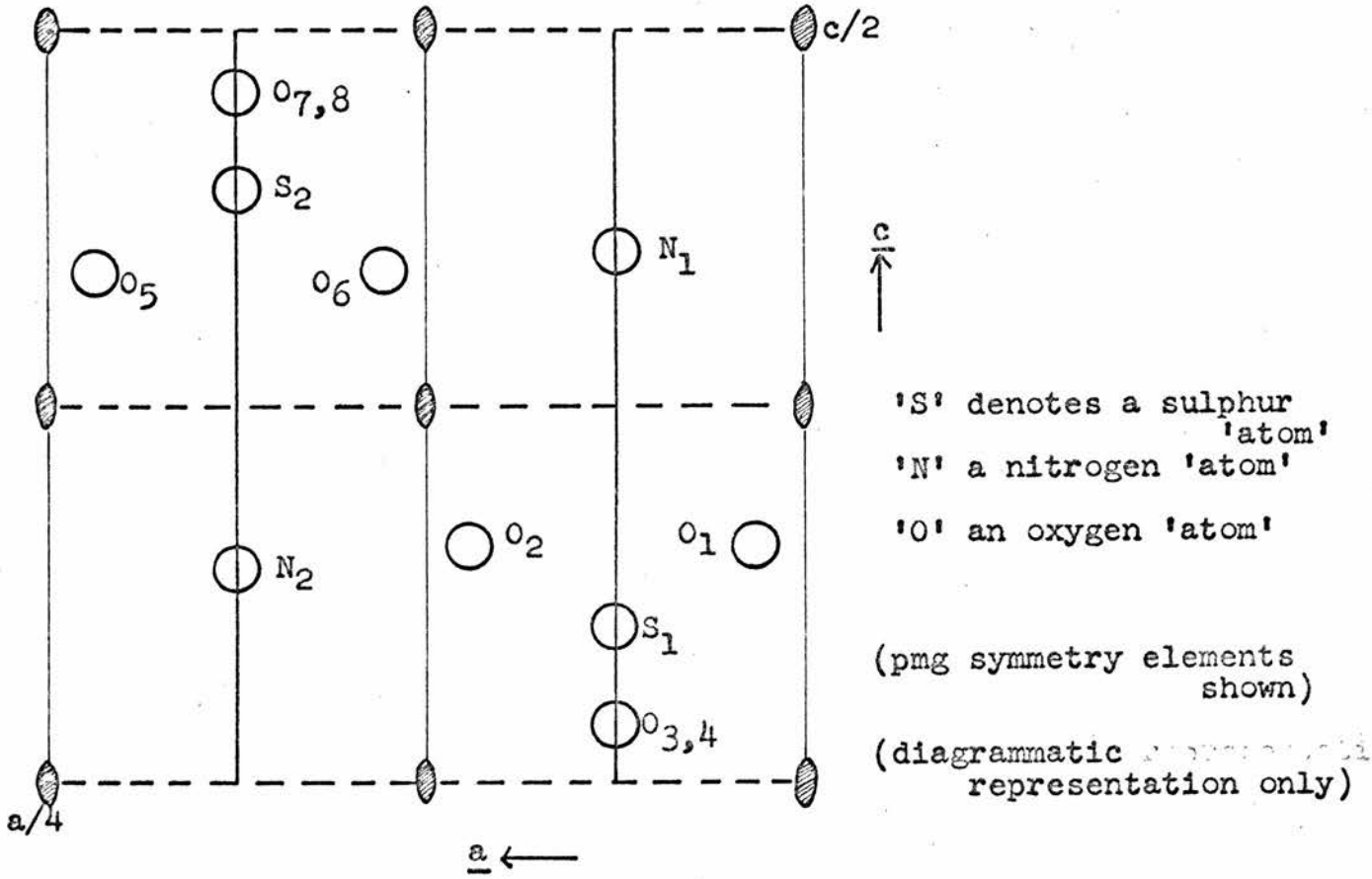

Fig. 3.5.1.

Table 3.5.1.

	x	z		x	z
S_1	.25	.21	S_2	.75	.79
O_1	.06	.32	O_5	.94	.68
O_2	.44	.32	O_6	.56	.68
$O_{3,4}$	.25	.08	$O_{7,8}$	.75	.92
N_1	.25	.71	N_2	.75	.29

x and z are fractional coordinates referred to the cell $\underline{a}/4 \times \underline{c}/2$

was calculated from $|F_o(h0\ell)|$ given the same signs as the corresponding $F_c(h0\ell)$. The pairs of oxygen 'atoms', $O_{7,8}$ and $O_{3,4}$ showed marked broadening perpendicular to the pseudo-mirror plane (fig. 3.5.1.). The R-factor was very sensitive to small symmetric displacements of these pairs into separate oxygen 'atoms' lying off the plane, but relatively insensitive to any symmetric displacement of the sulphur or nitrogen 'atoms'. Successive structure factor calculations, with coordinates improved by reference to the corresponding Fourier synthesis, reduced the R-factor to 18%.

A scattering factor (*f*-curve) for the ammonium ion in free rotation (Webb, 1965) was substituted for the nitrogen *f*-curve in an attempt to reduce the R-factor further. It increased. Davis and Whitaker, 1966, have since published a more accurate *f*-curve for the ammonium ion; they gave reasons for supposing Webb's results to be incorrect. With this *f*-curve, the R-factor remained at 18%.

At this stage no attempt had been made to refine the overall temperature factor or to give individual temperature factors to each 'atom'. The two superposed atoms in each 'atom' had not been allowed to separate. In principle, the separations could be found from $P_d(u,w)$ – a correct determination of these separations being equivalent to solving the 'difference structure'. $P_d(u,w)$ was computed from the observed 'weak' intensities (eqn. 3.4.6.), but neither $P_d(u,w)$ nor the corresponding 'sharpened' function, $SP_d(u,w)$, was interpreted. These functions and the problem of interpreting them are discussed further in chapter 5. Again, in principle, the separations could emerge from a refinement

of the 'average structure' itself. However, for small separations, the correlation between temperature factors and atomic coordinates would be very high – as was confirmed later in attempting to refine the 'average structure' from the diffractometer data (chapter 5). It did not seem worthwhile, then, to pursue attempts to solve the 'difference structure' any further; the problem was taken up again later with the more extensive and accurate diffractometer data. The fractional coordinates of the 'average structure' at this stage are listed in table 3.5.2..

Table 3.5.2.

	x	z		x	z
S_1	.25	.21(2)	S_2	.75	.78(8)
O_1	.06(5)	.32(2)	O_5	.93(5)	.67(8)
O_2	.43(8)	.32(2)	O_6	.56(2)	.67(8)
O_3	.20	.07(9)	O_7	.80	.92(1)
O_4	.30	.07(9)	O_8	.70	.92(1)
N_1	.25	.71(6)	N_2	.75	.28(4)

Fractional coordinates referred to the cell $\underline{a}/4 \times \underline{c}/2$

The limited objectives of the preliminary study had been achieved; attention was turned to the collection of full three-dimensional data in the possession of useful information regarding the nature of problems to be met and with a starting point for further refinement of the AHS structure.

CHAPTER 4

COLLECTION AND PROCESSING OF THE THREE-DIMENSIONAL X-RAY DATA

4.1. Introduction

Full three-dimensional X-ray intensity data was collected on the Hilger and Watts Y230 Mk III four-circle automatic diffractometer. A Philips fine-focus molybdenum tube was the X-ray source. The AHS specimens were prepared and mounted as already described in chapter 2. This chapter comprises an account of the experimental procedures adopted in collecting the data, and the subsequent problems and methods of data reduction.

4.2. The diffractometer

The machine is automatic to the extent that it is controlled by instructions read from paper tape. This 'control-tape', prepared from data provided by the experimenter, includes shaft setting orders, reflection measuring orders, shaft datum checks, and 'rescue sequences'. Datum checks are performed to ensure that shaft setting orders have been correctly punched on the control-tape and correctly read therefrom. 'Rescue sequences' are designed to enable the machine to locate the datum positions of all the shafts and continue collecting data if the

control-tape is mis-read. As a check on experimental stability the control-tape also includes orders for recording periodically the profile of a reflection chosen to be the 'standard'.

Reflection profiles (see fig. 4.6.1.) may be collected in any desired order from all accessible parts of reciprocal space. The number of profiles recorded with each control-tape is limited only by the size of the latter to about five hundred. The machine may be operated manually by typing in orders at a teleprinter. Under either manual or automatic operation there are two output streams: a printout on the teleprinter, and the same information punched in Ferranti computer code on 5-hole tape. The output includes everything read from the control tape or typed in by hand, the reflection profiles in six-digit counts, and the shaft setting errors at datum checks.

The diffractometer uses normal-beam equatorial diffraction geometry (Willis and Arndt, 1966, p.37). This and the disposition of the four 'circles' of the diffractometer are illustrated diagrammatically in fig. 4.2.1. (a reproduction of Fig. 3 of Willis and Arndt, 1966). The crystal is positioned by rotation about the ϕ-, χ- and ω-shafts, each of which can be set to a precision of 0.01°; the counter moves on the 2θ-shaft and can be positioned to a precision of 0.02°. The settings of all four shafts are maintained by a feed-back servo-system.

Before commencing data collection the alignment of the machine was checked. The check requires first that, when the χ-shaft is at its datum position, the ϕ-, ω- and 2θ- axes coincide and intersect the χ-axis normally — within the permitted tolerance. This intersection defines the 'machine centre'.

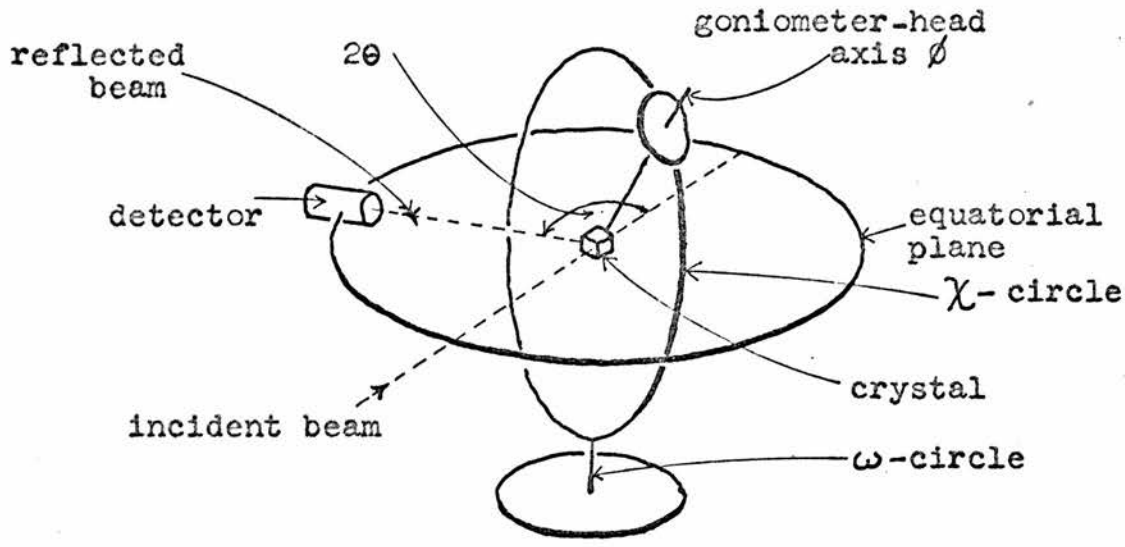

Normal-beam equatorial geometry. The crystal is mounted on a goniometer-head attached to the ϕ-axis; the ϕ-circle moves round the vertical χ-circle, and the ϕ-χ assembly rotates as a whole about the vertical ω-axis. The detector moves in the horizontal, equatorial plane and the incident beam is normal to the crystal oscillation axis ω. The detector moves about the 2θ-axis, which is parallel to and independent of the ω-axis.

(This figure is copied from Fig. 3 of Willis and Arndt, 1966)

Fig. 4.2.1.

With these conditions satisfied, a fine collimator held in the counter arm is adjusted so as to be coaxial with the χ-axis when the 2θ- and ω-shafts are at datum. The X-ray source is adjusted in position to lie on the line defined by the counter collimator and the machine centre. A subsequent and sufficient check on the alignment of the machine and source, and the setting of the shafts, is that reflection peaks should show no systematic deviation from the centre of their scans – assuming that the cell dimensions have been obtained with the machine after alignment, and that the crystal is properly aligned.

The intensity distribution in reciprocal space may be scanned by stepping any of the shafts singly, or ω and 2θ together, and counting the detected quanta at each position for a pre-set period timed by an internal crystal-oscillator clock. The quanta are detected by a counting chain composed of a NaI(Tℓ) scintillator crystal, and a photomultiplier tube (PMT) from which the pre-amplified signals must pass through a pulse-height analyser (PHA) before being recorded as 'counts'.

All aspects of the diffractometer are fully described and discussed by Willis and Arndt, 1966.

4.3. The specimens

The preparation of the two specimens of AHS to be used for data collection has been described in chapter 2.

The cell dimensions of the first specimen, SD1, were determined from MoKα_1 peak positions in ω-scans through high angle reflections as

$a = 24.66 \pm 0.02$ Å

$b = 4.60 \pm 0.01$

$c = 14.82 \pm 0.02$

$\beta = 89.87 \pm 0.01°$

$\alpha = \gamma = 90.00 \pm 0.01°$

(compare section 3.2., and table 1.7.1.). Datum checks were performed after each scan; the specimen alignment was checked after the final scan. The cell dimensions of SD2 were found to agree within the above errors.

The most convenient orientation for a monoclinic crystal on the diffractometer is with the b-axis (standard setting) coincident with the Ø-axis. This orientation was chosen. The Ø-datum was adjusted so that the reciprocal lattice +a*-axis was directed towards the source and coincident with the χ-axis when all shafts were at datum (hereafter, 'machine datum'). Both specimens were found to be mounted with the -b-axis upwards at machine datum: the control-tape production program assumes a right-handed axial system.

The specimens were cuboids. Their dimensions, measured with a travelling microscope, were

SD1: 0.28 mm. along a*
0.34 mm. along b
0.22 mm. along c, and

SD2: 0.25 mm. along a*
0.30 mm. along b
0.21 mm. along c.

There was an error of ±0.01 mm. on each measurement. The cuboid shape was only judged by eye through the telescope. Similarly, directions such as 'along a*' were not precisely determined. However, the crystal shows excellent cleavage in (001) and also cleaves quite well in the perpendicular (010), and these cleavage faces could be seen.

Having determined the cell dimensions and orientation of SD1 a control-tape was prepared to scan a number of general (hkℓ) reflections. These were selected to span the range of intensities and the range of sin θ/λ over which data was to be collected. The profiles of these reflections were plotted out and examined for any indication that the specimen was damaged or twinned. None was found. The same procedure was repeated with SD2. In both cases the reflections selected included those necessary to check the reported space group of AHS.

4.4. Alignment, accuracy and experimental precautions

The alignment of the machine and source have been described. A small degree of machine misalignment is tolerated and determines the amount by which the specimen, located at the machine centre, moves as the shafts are rotated through their full range. The area of uniform intensity of the primary beam must be sufficient to accommodate this movement, the measured dimensions of the specimen and the maximum tolerated misalignment of the specimen itself. This last misalignment is limited by the counter aperture and, more severely, by the uniformity of response of the scintillator crystal.

The stops of the beam collimator were adjusted to obtain a

primary beam of sufficient uniform area, with a minimum penumbra, centred on the machine centre. Photographs of the beam taken at the machine centre were scanned with a microdensitometer to check the uniformity of the intensity in the 'uniform area' and to measure the penumbra. Throughout data collection on both SD1 and SD2 the beam at the machine centre had the form and dimensions illustrated in fig. 4.4.1..

The specimen was brought to the chosen orientation using the goniometer-head arcs and the adjustable Ø-datum position, and was located at the machine centre in the uniform area of the primary beam.

The E.H.T. on the photomultiplier tube (PMT) and the upper and lower limits of the PHA 'window' depend on the particular scintillator crystal and PMT, and on the radiation being used. The energies of the photons emitted by the scintillator in response to the arrival of an X-ray quantum show a Gaussian-like distribution (International Tables, 1962, p.148). The E.H.T. was adjusted to bring the peak of this distribution into the centre of the range of 'window' settings; the latter were chosen so as to exclude less than 0.5% of the area under the 'Gaussian' at each of its extremes. These settings were determined with the X-ray tube at working potential and current.

The axis of the PMT is off-set from the χ-axis by about 0.3cm. at machine datum. By turning the PMT in its holder different parts of the scintillator crystal, mounted on the front of the PMT, can be used for detection. The counter moves in a horizontal equatorial plane (fig. 4.2.1.). If the machine is properly aligned this plane passes through the machine centre and bisects the counter aperture. The response of the

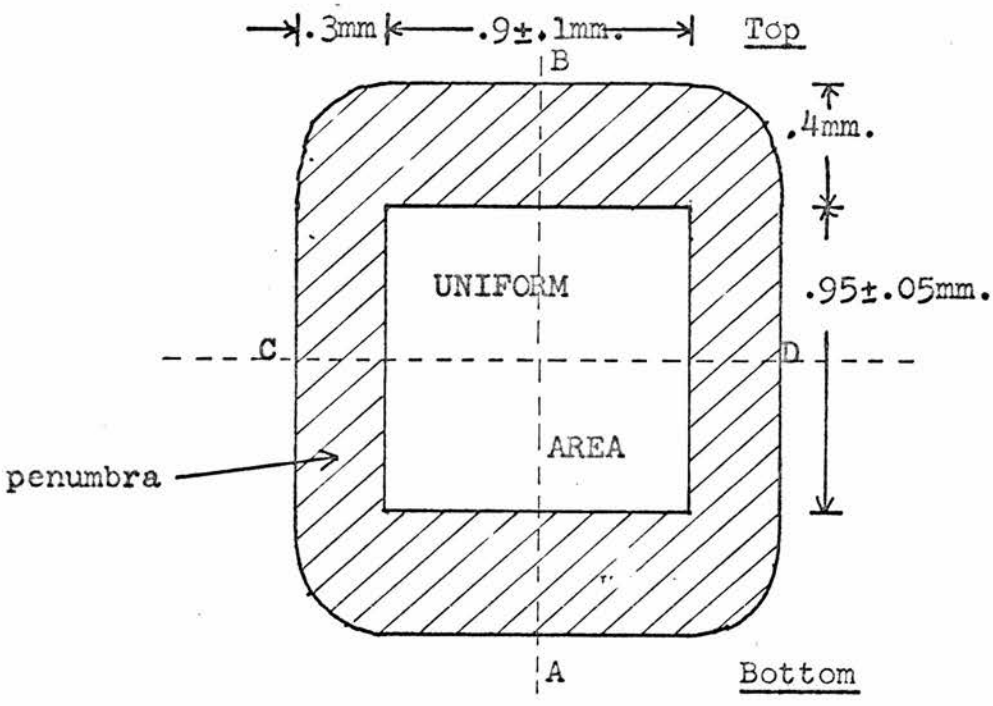

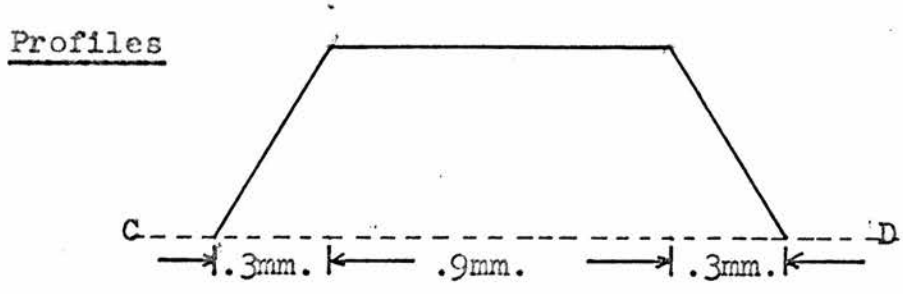

(Diagrammatic only)

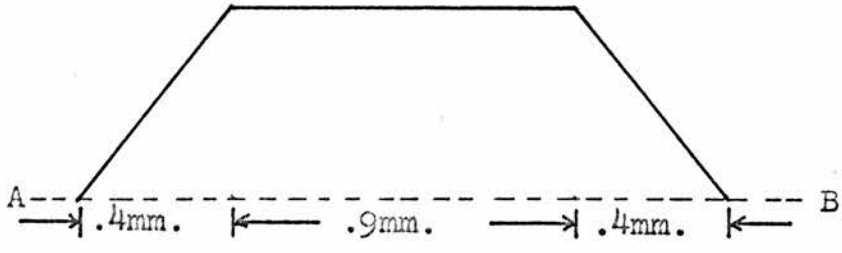

Fig. 4.4.1.

scintillator along the line of its intersection with this plane, integrated over the area of the reflected beam, may be obtained as the variation in peak height of ω-scans through a chosen reflection – the counter position being moved on a small amount before each scan. The scintillator response should be uniform – at least over the area being used for detection.

The scintillator used for the first set of data was replaced when a 10% dip in its response profile was found close to the detecting region (appendix 1). Profiles for the replacement were recorded at 10° intervals for a full rotation of the PMT. Over one range of 30°, which was scanned again at 5° intervals, the maximum variation in response was $\pm$1%; the PMT was set at the centre of this range. Calculations showed that if the specimen were kept correctly oriented to within $\pm$0.05° on both the goniometer arcs and on the Ø-datum setting, the reflected beam would fall well within the area of this uniform response. 0.05° was the tolerance already adopted at the start of data collection.

Direct checks of the machine and source alignment and of the primary beam were made only after mechanical servicing, replacement of the X-ray tube, and at the end of data collection. The PHA settings were checked monthly and not found to vary. The scintillator response profiles were checked only once, two months after the installation of the new scintillator. They were found to be unchanged. The specimen orientation was checked at least twice a day.

An indirect check on all these aspects of experimental stability was afforded by the measurement of a 'standard'

reflection once every hour. Under ideal conditions the peak of this or any reflection should always appear at the same point in the scan and its integrated intensity be constant within statistical error. The degree to which this is observed in practice is also a check on the stability of the source and the counting chain, and on the condition of the specimen. The latter being the object of particular concern, it was checked occasionally by taking oscillation photographs on the diffractometer, and daily by direct observation – looking for the maintenance of sharp edges and bright cleavage faces.

In addition to the careful attention paid to the 'standard' reflection all of the measured profiles were looked through for spurious or displaced peaks.

The present limit on the reproducibility of intensity measurements is about 2-3% – as experience with repeated measurements of the 'standard' reflection and the results of the A.C.A. Single-Crystal Intensity Project (Abrahams et al., 1967) have shown. This figure was taken throughout as a guide to whether a particular aspect of experimental accuracy was or was not satisfactory. Otherwise, every effort was made to be aware at all times of the nature of the conditions under which data was being collected and to optimise these conditions.

4.5. Data collection

The intensity data was collected at room-temperature (18-22°C) over a complete hemisphere of reciprocal space out to $\sin\Theta/\lambda = 0.81$ ($\Theta = 35°$, see section 2.4.2.). Preliminary measurements showed that beyond $\Theta = 35°$ excessive counting times

would have been required to obtain useful intensity measurements. The hemisphere which kept the supporting fibre away from the incident and reflected beams was chosen (h^{+}_{-}, $k \leq 0$, l^{+}_{-}).

There are ~15,000 reflections from AHS in a sphere out to $\Theta = 35°$ for MoKα radiation. The intensities of (hkl), ($\bar{h}k\bar{l}$), ($h\bar{k}l$) and ($\bar{h}\bar{k}l$) are symmetrically equivalent. Thus ~8000 intensities were to be measured in the defined hemisphere, of which ~4000 were symmetrically inequivalent.

The data was collected in the form of a single* stepped-scan through each peak, including background level counts on both sides. The machine was used in the $\omega/2\Theta$, half-angling scanning mode: the crystal and counter move together through the reflecting position, the displacements of the 2Θ- and ω-shafts from datum always being in the ratio 2:1 (fig. 4.5.1.).

Control-tapes were produced with a program system developed by Dr. E.R. Cowley of this Department from a program by Powell, 1966. The tapes were prepared for half of each layer (hOl, $h\bar{1}l$, ...$h\bar{7}l$: h^{+}_{-} $l \geq 0$); reflections with $l \leq 0$ were collected with the same control tapes after turning the Ø-datum position through 180°. The half-layers were collected in no particular order:

---

*Another commonly used method involves three separate scans for each reflection: a short scan with long counting times through low angle background, a scan through the peak region, and a second background scan on the high angle side of the peak.

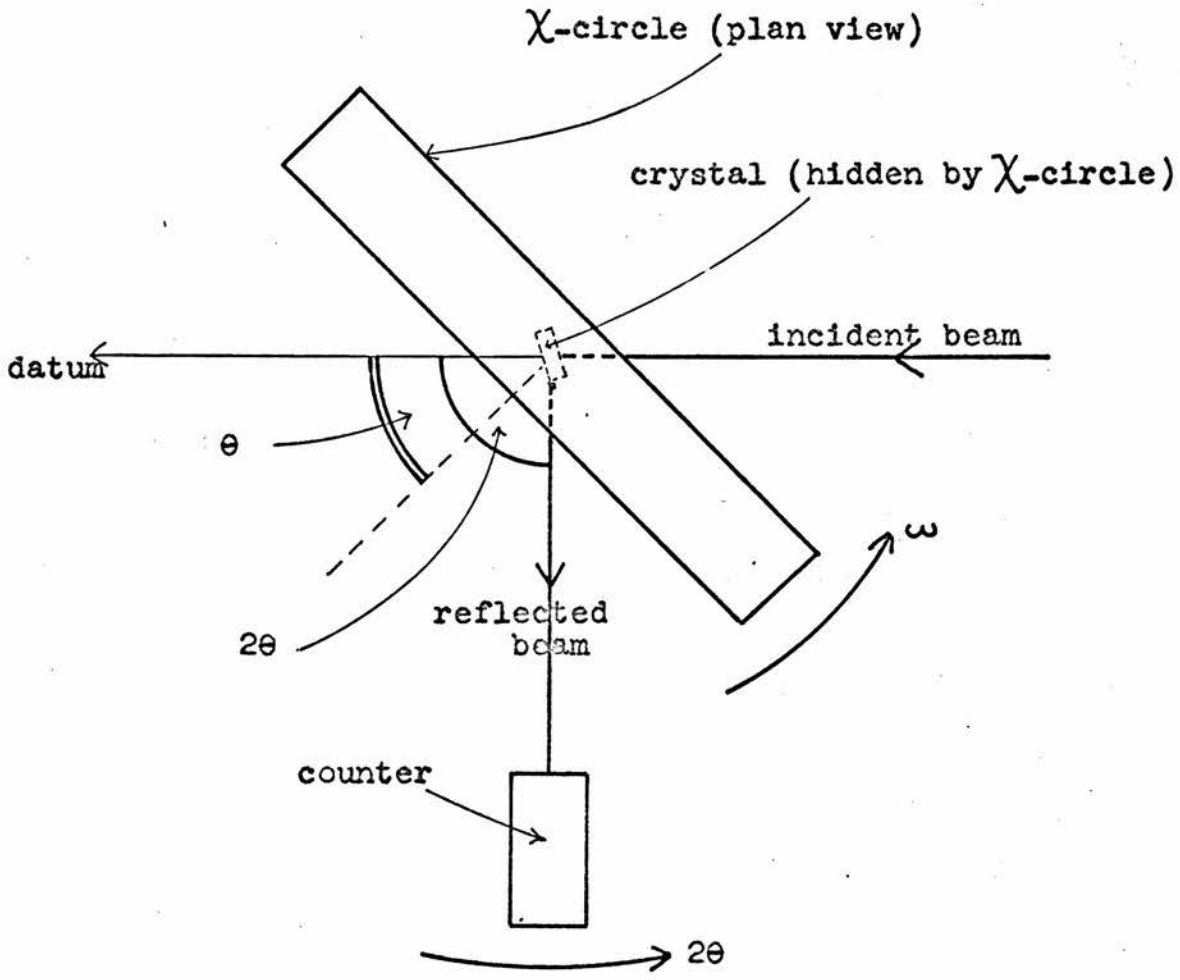

Fig. 4.5.1.

the symmetrically equivalent intensities $I(h\bar{k}\ell)$ and $I(\bar{h}k\bar{\ell})$, later to be used as checks on the internal consistency of the data, were often measured at well separated times, sometimes under different conditions, and even on different specimens.

Within each half-layer the 'weak' reflections ($h = 4n + 2$) were collected separately. They were given three times as long a counting time per scan step as the non-'weak' reflections. This factor of three was estimated to be sufficient to make the average absolute error on the 'weak' reflections from counting statistics, comparable with that on moderate intensities (peak intensity ~5000 cps with the X-ray tube at working kV/mA) among the non-'weaks'.

The final R-factor for a structure is of the order of the average percentage error on the observed $|F_o(hO\ell)|$. Considering the nature of the structure to be solved, and the particular experimental difficulties to be met, a final R-factor of 7-10% was considered a reasonable aim. On this basis, knowing from the preliminary survey (section 4.3.) the approximate counting rates and peak-widths to be expected, it was estimated that a counting time of six seconds per step was required (eighteen seconds for the 'weak' reflections). The step-width was chosen such that the lowest angle reflections were sampled at eight points on the peak. The peak-width, including the α_1 and α_2 components, increases with Θ; scans were always at least twice the expected peak-width.

The chosen values of counting time and scan-width were such that 8000 reflections could have been collected in five weeks with a 66% machine efficiency. A brief summary of the

log of the data collection is presented in appendix 1. A high degree of faulting in the equipment grossly increased the time required to collect the data from five weeks to five months. The first specimen, SD1, lasted three months; SD2, mounted at the same time, was still well prserved after eight months. The changes of specimen, X-ray tube, scintillator and PMT, PHA settings, and source power necessitated considerable overlap of the data collected, so that the five different data sets (see appendix 1) could be brought to a common scale. Furthermore, all data collection performed under suspect conditions was repeated. In all, a total of 15,000 reflections were scanned.

4.6. Data reduction

4.6.1. Counting losses

For a certain time after the arrival of an X-ray or neutron quantum any detector — apart perhaps from photographic film — is insensitive to further incident quanta. Quanta arriving during the insensitive period, or 'dead time', are not detected. They constitute counting losses for which the observed count must be corrected. The length of this period of insensitivity, usually termed the 'resolution time', is characteristic of the type of detector used. For the scintillation and proportional counters currently in use it is of the order of a few microseconds.

If the rate of arrival of quanta at the detector is random in time the proportion of lost counts increases continuously with counting rate; there is no range in which the observed counting rate is strictly proportional to the intensity incident on the detector. However, with a resolution time of a few

microseconds the counting losses will usually be negligible compared with the error from counting statistics.

The diffractometer has a NaI(Tℓ) scintillator crystal, a PMT and a pre-amplifier in the counting-arm assembly. The signal from the pre-amplifier must pass through a pulse-height analyser before being registered as a count. The counting losses depend on the effective resolution time of the whole counting chain, and this may be greater than that of the detector (the scintillator and PMT) itself – indeed it is preferable that it should be so. The PHA is designed to have a 'paralysis-time', τ, slightly larger than the recovery time of the detector; the PHA then determines the resolution time of the whole chain. This feature is incorporated in the FA150 counting chain of the Hilger-Watts diffractometer (W.A. Wood, 1968, private communication). Since the paralysis time is defined by circuit component values, accurate counting loss corrections can be made if these values are known. At the time of data reduction the paralysis time for the FA150 chain was not known and had to be found experimentally (section 4.6.1.1.).

If the observed counting rate is n_o counts per second (cps), and the effective resolution time is $k\tau$ seconds (Willis and Arndt, 1966, p.145), the system is insensitive to the arrival of quanta for $n_o k\tau$ seconds in each second. Hence, if the true counting rate is n cps, $nn_o k\tau$ counts are 'lost' each second, and

$$n = n_o + nn_o k\tau \qquad (4.6.1.)$$

$$\text{or} \quad n = \frac{n_o}{1 - n_o k\tau} \qquad (4.6.2.)$$

This affords a first-order correction; it becomes a poor approximation if the counting losses exceed 10%, because at very high counting rates a significant number of quanta arrive as the detector recovers — giving too weak a signal to pass the PHA but prolonging the dead time (Willis and Arndt, 1966, pp. 144-145).

The experimental determination of the resolution time described below finds the value of the effective resolution time directly, and avoids the problem of considering k, the form factor of the source (Willis and Arndt, 1966, p. 145). The voltage supply to the diffractometer is well smoothed and stabilised, so k will be close to unity. Hereafter the effective resolution time will be referred to as τ .

4.6.1.1. Experimental determination of τ

Two reflections from SD2 were chosen, (402) and (006); at the working tube power of 55kV and 14mA these had very high (50,000 cps) and moderate (8000 cps) peak counting rates, respectively. The peaks of both reflections were scanned in the order (402), (006), (402), (006) for each value of the tube current in three different but overlapping ranges of incident beam intensity. The three sets of data were obtained with

i) 55kV, beam unattenuated, and the tube current varied from 4 to 14mA in steps of 2mA,

ii) 55kV, two beam attenuators inserted, and the tube current varied as in i), and

iii) 35kV, two beam attenuators inserted, and the tube current varied from 4 to 20mA in steps of 2mA.

The specimen crystal was kept centred in the uniform beam and correctly oriented to ensure that the same part of the scintillator surface was used throughout the experiment.

The intensity of each peak was found by drawing a free-hand curve through the points of the stepped $\omega/2\theta$ scan. The values found for the two scans of both reflections at each tube current setting were averaged. The error on the intensity was estimated from the scatter of points about the best smooth curve and the difference between the heights of the two peaks. To check the long term stability a few of the scans were repeated. There was agreement within two 'standard deviations' in every case.

From eqn. 4.6.2.

$$n = \frac{n_o}{1 - n_o \tau} \quad , \qquad (4.6.3.)$$

where τ is now the effective resolution time. Let

$$n(402) = \alpha(402).\ I \ , \qquad (4.6.4.)$$

where n(402) is the counting rate at the peak of (402), $\alpha(402)$ is a constant and I is the incident intensity. Similarly,

$$n(006) = \alpha(006).\ I \ . \qquad (4.6.5.)$$

For (006) the counting losses were small and

$$I = \frac{n(006)}{\alpha(006)} \doteq \frac{n_o(006)}{\alpha(006)} \ . \qquad (4.6.6.)$$

It then follows that

$$\frac{1}{n_o(402)} = \tau + \frac{\alpha(006)}{\alpha(402)} \ . \ \frac{1}{n_o(006)} \ . \qquad (4.6.7.)$$

τ may be found as the value of $n_o(402)^{-1}$ as $n_o(006) \rightarrow \infty$.

$n_o(402)^{-1}$ was plotted against $n_o(006)^{-1}$ as a check on the data. The points from all three sets fell on the same straight line within statistical error.

A least-squares program was written to find the best fit to the straight line of eqn. 4.6.7., and hence the value and standard deviation of τ . The observations were weighted according to their estimated error. Although the counting losses for (006) were small the problem was solved iteratively; the value of $n_o(006)$ was corrected each cycle with the current value of τ , until no further significant change in the value of τ occurred.

The final value found for τ was

$$2.6 \pm 0.9 \text{ microseconds.}$$

This is in agreement with the value of the paralysis time of the FA150 counting chain, subsequently quoted by the manufacturer as being in the range 2-3 microseconds (W.A. Wood, 1968, private communication).

4.6.2. The background

4.6.2.1. The linear truncation procedure

The integrated intensities were extracted from the recorded reflection profiles by locating the peak, summing the recorded counts over the peak range and subtracting the contribution from non-characteristic radiation by a linear truncation between the background levels on either side of the peak.

The linear truncation procedure is an approximation. It ignores the fact that inelastic scattering from the lattice

vibrations – thermal diffuse scattering (TDS) – makes a significant contribution at the Bragg positions. It is possible to make a correction for the TDS contribution, although the computations are lengthy and complex (see, for example, Cochran, 1969, and Willis, 1969). Furthermore, normal truncation procedures involve the assumption that the observed peak profile decays rapidly at its extremes. This profile is a convolution of functions describing the beam divergence, the spectral dispersion and the crystal mosaicity. The exact form of the spectral function has yet to be accurately determined (L.E. Alexander, 1968, private communication) but is known to be Cauchy-like (Alexander and Smith, 1962). Such a function decays slowly, and unless the scan range is very large considerable underestimation of the integrated intensity may be made (see Alexander and Smith, 1962, p.989 and figs. 11, 12 and 15). Ladell and Spielberg, 1966, and J. Ladell, 1968 (private communication), take issue with Alexander and Smith for assuming a Cauchy-like spectral function when attempting to estimate the 'truncation error' in data collected with β-filtered radiation and pulse-height analysis: the true spectral function is complex and asymmetric (Ladell and Spielberg, 1966, fig. 1(b)). They argue that the problem is intractable unless crystal-monochromatised radiation is used to produce a truncated Cauchy-like spectral function (loc. cit., fig. 1(c)), and scorn attempts to derive anything but approximate results with zirconium-filtered Mo radiation. L.E. Alexander, 1968 (private communication), agrees that an exact correction is impossible with β-filtered radiation. However, he asserts that, given the white radiation profile under

the characteristic spectral line is linear or slowly varying, the results of Alexander and Smith, 1962, are valid indications of the order of magnitude of the 'truncation error' as a function of 2Θ, under the average conditions assumed (see their fig. 18).

There is little doubt that one may conclude that

i) the 'truncation error' increases with 2Θ, and very rapidly at high values of 2Θ and

ii) this error increases as the separation of the points between which truncation is made decreases.

For the AHS data the separation of these points varied from 0.5° for low angle reflections to 0.9° at Θ = 35°. A crude estimation from fig. 18 of Alexander and Smith, 1962, suggests that the 'truncation error' increases from 4% at Θ = 10° to 15% at Θ = 35°. This error should be a function of Θ only, and so mainly affect the accuracy of the atomic temperature factors. J. Ladell, 1968 (private communication), supports this contention.

It should be noted that a 'truncation error' may also arise in data collection. For ω/2Θ scanning this will only occur if the receiving aperture is less than the total angular width of the convolution of the non-dispersive elements of the reflection profile. These are the angular widths of the source at the crystal and of the crystal at the source, and the crystal mosaic spread. The latter is usally assumed to be adequately described by a Gaussian function. However, Ladell and Spielberg, 1966, report that there is evidence that mosaic spread is more properly described by a Cauchy-like function, in which case an appreciable detection 'truncation error' would be incurred with any practicable receiving aperture. The size of the aperture used in collecting

the AHS data was large enough to make this possible error small, and certainly less than that incurred in data reduction.

4.6.2.2. The β-filter absorption edge

To simplify the discussion in this section the problems raised in the preceding section are ignored.

The data for AHS was collected with Zr-filtered Mo r diation. For strong reflections there is a pronounced rise in the white radiation level at the filter absorption edge (fig. 4.6.1.). At low Bragg angles this rise is close to or even within the low angle limit of the peak. The problem of obtaining a good approximation to the white radiation background to be subtracted in such cases has not, so far as is known, been the subject of any published work, although attention was drawn to this difficulty by Alexander and Smith, 1962.

To a good approximation the profile of the non-characteristic part of the Zr-filtered Mo spectrum, after passing through the PHA, is as illustrated in fig. 4.6.2.. The profile of the observed background, arising from Bragg reflection of this spectrum, is obtained by convoluting the above function (fig. 4.6.2.) with one which represents the combined effects of beam divergence and crystal mosaicity. The latter function may be approximated empirically by the profile of an observed peak at a low Bragg angle, assuming the characteristic spectral line to be relatively very narrow, and analytically by a Gaussian of similar dimensions.

The problem to be solved is represented in fig. 4.6.3.. To subtract the background from I_o the equation of the line AB and the position of A in the profile must be found. Then, integrating

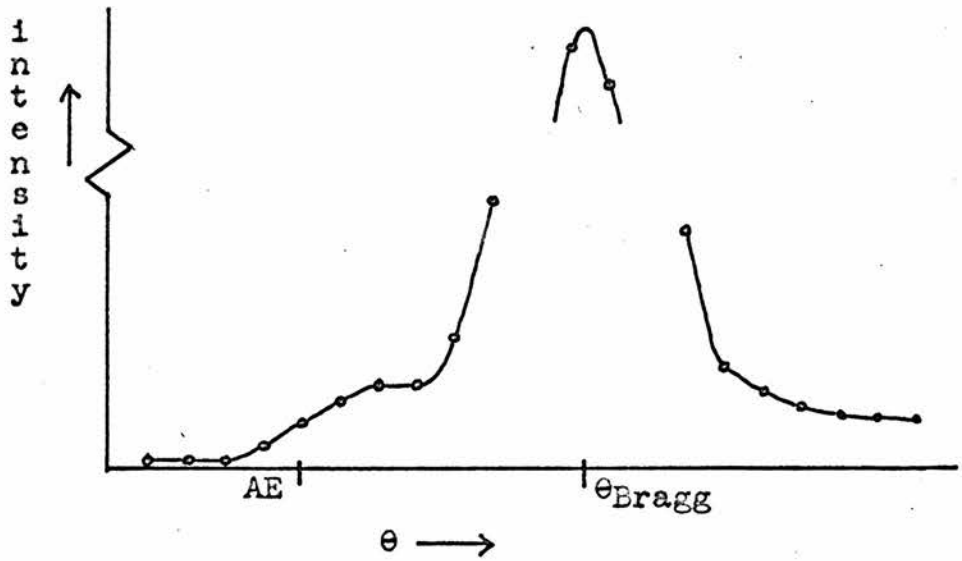

Observed reflection profile. AE is the absorption edge
o mark the position at which a count is made

Fig. 4.6.1.

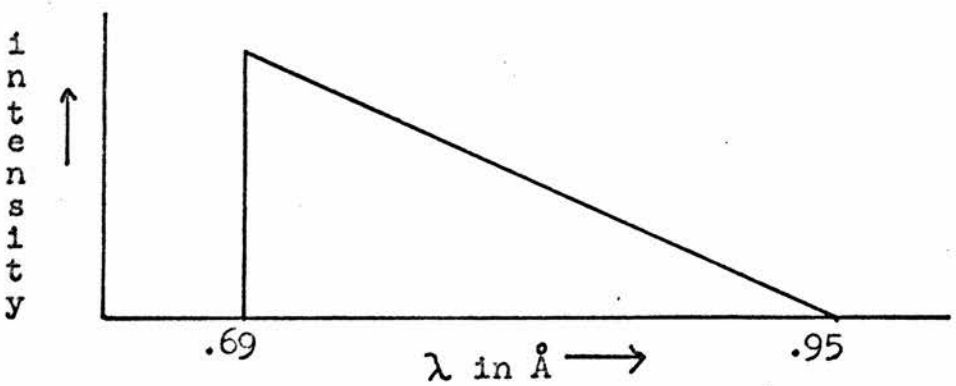

(after Ladell and Spielberg, 1966, fig.1(b))

Fig. 4.6.2.

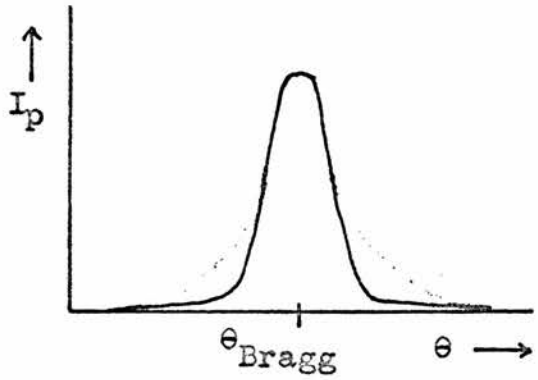

The characteristic peak --- from MoKα radiation only

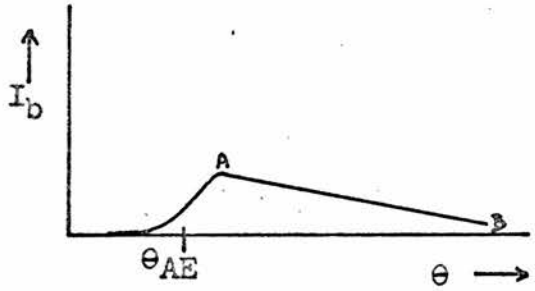

The white radiation:the observed background arising from Bragg reflection of the spectrum in fig.4.6.2.. θ_{AE} is the angle at which the filter cut-off wavelength is reflected

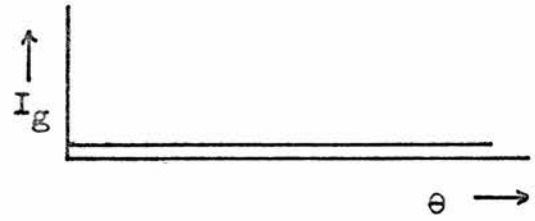

The general background level

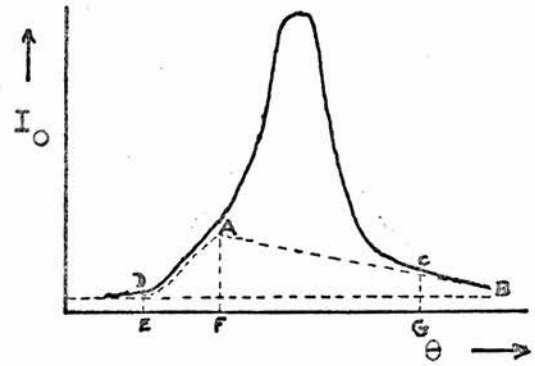

The observed profile

$$I_o = I_p + I_b + I_g$$

Fig. 4.6.3.

the peak from E to G, the background to be removed is closely approximated by the sum of the areas of the trapeziums ADEF and AFGC.

The first problem tackled was that of locating A. The approximated background spectrum (fig. 4.6.2.) was convoluted analytically with a Gaussian of dimensions derived from observed low angle reflections. The analysis proved to be very cumbersome. The cruder approximation was made of replacing the Gaussian with a triangle of the same width at half-height. The profile obtained was of the form shown in fig. 4.6.4.. The portions CA and BD are general cubics in Θ, and AB is a straight line. An analytical expression for the position of A' relative to Θ_{AE} was obtained in terms of R, the interval CA' as $\Theta_{Bragg} \rightarrow \infty$, and L, the separation between the angles at which the wavelengths at the extremes of the background (fig. 4.6.2.) are reflected by the reflection considered. Because L was so large in comparison to CA', except at very low angles ($\Theta < 2°$), CA' was sensibly constant for $\Theta > 10°$. Hence the value of R could be found experimentally from the profiles of reflections in which the rise in the background, C $\rightarrow$ A (fig. 4.6.4.), was well clear of the peak. Since Θ_{AE} is at the centre of the interval CA' as $\Theta_{Bragg} \rightarrow \infty$, and CA' is almost constant down to low angles, the separation of Θ_{AE} and A' differs from $\frac{1}{2}$R by a very small amount. Therefore, although the theory, as developed, contains several crude approximations, its use to locate A' cannot introduce significant errors into the background correction. The main result of the theory derives from the close agreement between the form of the predicted profile for I_b and the parts of I_b observed experimentally:

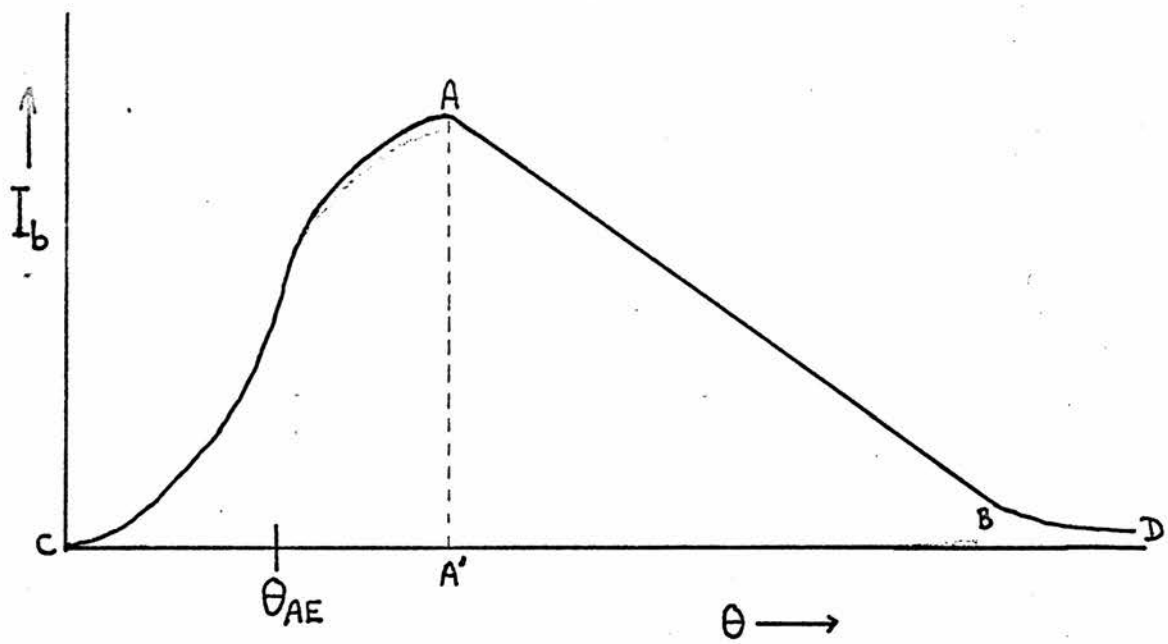

Fig. 4.6.4.

this agreement lends assurance to the removal of a background profile of the predicted form when only one part of I_b is experimentally accessible – the line AB beyond the high angle limit of the peak.

Apart from A', the position of A in the scan, the required parameters were derived experimentally. The principle parameters are R and those defining the line AB. The latter may be determined by a least-squares fit to the background counts on the high angle side of the peak. In practice it was found that these spanned an insufficient range of Θ to determine AB well, often giving clearly wrong results. A general background level count at the point at which AB, extrapolated, falls to that level can be used as an 'observation' in the least-squares procedure, to give a more accurate gradient for AB. The position of this 'observation' in the extrapolated scan may be characterised by a wavelength. The best value of this wavelength was found to be 1.0Å, during the tests described below.

The complete procedure for background subtraction was developed as a routine, 'absorption edge', of the data reduction program (section 4.6.3.). The routine was tested on a large number of AHS reflections. Many of those selected for this purpose had the rise C → A (fig. 4.6.4.) well clear of the low angle limit of the peak. For them, a comparison between the integrated intensities found by 'absorption edge' and by simple truncation showed good agreement – within $\pm$3% for reflections with > 1000 cps at the peak centre – which <u>improved</u> as Θ_{Bragg} decreased. For those where the rise C → A lay partially or completely within the peak, the scan was plotted out and the

background profile generated by 'absorption edge' was removed graphically. In all cases a satisfactorily symmetric peak was obtained.

It was concluded that 'absorption edge' gave a correct value of the integrated intensity to within 2-3% or better for reflections with > 1000 cps at the peak centre. For weaker reflections the error involved in ignoring the rise C → A was found to be 1% at most.

4.6.3. The data reduction program

A data reduction program has been written and developed to process the 'raw' 5-hole tape output from the diffractometer. The program as written will accept only single scan profiles (footnote p.50), and assumes that all scans are made in the direction of increasing Θ. The procedures used to locate the peak in the scan and the detailed features and facilities of the program are entirely due to the author. The program has been written to minimise the degree to which the data tape must be correctly punched, and, by adjustment of the parameters of the processing algorithm, to provide a considerable range of adaptability to the requirements of each user's data. This flexibility is essential in view of the fairly high incidence of punching errors with the present equipment – many of which are unimportant for the purposes of data processing, the almost unlimited range of 'unusual' character sequences that may appear on the tape, the wide range of data collection strategies available to the user, and the variety of peak widths and shapes that may be obtained from different materials.

The performance of the program has been thoroughly tested on the 15,000 reflections collected from AHS. After locating the peak in the scan the calculation of the background corrected integrated intensity is very straightforward, except in the cases where the separately described and tested 'absorption edge' routine is used; the calculation of the standard deviation of the intensity is more complex. The part of the program which calculates the standard deviation has been carefully checked both by the author and independently by Mr. P. Bradfield of this Department. The intensity and standard deviation for several reflections have also been checked by 'hand' calculation.

The method and output information of the program are summarised in the following sections, and a typical example of the program output is to be found in appendix 2. A detailed 'write-up' of all the pertinent aspects of the program has been prepared in the form of a users' manual.

4.6.3.1. Method

In the following summary parameters supplied to the program before the 5-hole data tape is read are marked P, or P(Θ) if the parameter is a function of Θ.

Reflections are processed in batches of thirty. The details of the analyses are printed out on one output page, and the corresponding reflection profiles on the following page (see appendix 2). In normal operation the reflection processing procedure may be summarised as follows:

i) the start of a reflection measuring sequence is located;

ii) the number of the reflection on the control-tape (hereafter

referred to as the 'index'), h, k, ℓ and Θ are read;

iii) the measuring order is located and read to find the counting time per step, the number of steps in the scan and the step width;

iv) the reflection profile is read, any mis-punching of the six-digit counts is recorded, and an optional correction for counting losses is applied to each count if required (P);

v) the position of the peak in the profile is located by

a) subtracting off an approximate background from the observed profile by a linear interpolation between the averages of the first two and of the last two counts in the scan,

b) 'smoothing' this secondary profile by summing the counts in groups which cover a range of about half (P) the intrinsic peak width (the peak width as the α_1/α_2 separation $\rightarrow 0°$), the first group starting at the first count in the scan, the second group at the second count and so on,

c) finding the first moment of the secondary profile over a range centred on the highest point in the 'smoothed' profile, this range being greater than the expected peak width (P(Θ)) by a variable factor (P),

and d) adding the known separation (P(Θ)) between the position of the first moment and the peak centre (midway between the centres of the α_1 and α_2 peaks):

if the reflection is found to be too weak to locate a statistically significant (P) 'smoothed' peak, or the first moment with sufficient accuracy (P), the peak is taken to be located at the centre of the scan and the expected peak width increased by a variable amount (P)

to allow for any error in this assumption;

vi) having located the peak centre in the scan, the primary profile (as found in (iv)) is used to calculate the integrated intensity. The peak counts are summed over the expected peak width centred on the peak centre as located in (v). The background contribution is removed by a linear truncation between the mean background levels on the low and high angle sides of the peak. On the low angle side the counts used are only those between the top of the rise in the background level at the filter absorption edge and the beginning of the peak. If the absorption edge is too close to (P) or within the peak, and the peak intensity is above a pre-set level (P), the background is removed by 'absorption edge';

vii) the integrated intensity is corrected for the Lorentz-polarisation factor: the corrected integrated intensity for a 'standard' reflection is brought to a pre-chosen scale (P);

viii) the random error on the integrated intensity is computed from the counting statistics error and the error (P) on the lost counts correction, if applied;

ix) the values of h, k, ℓ, the integrated intensity (from (vii)) and its standard deviation (from (viii)), and a parameter which may be used to label the batch of data are 'packed' into a single number to be stored on magnetic tape — unless the integrated intensity is negative or the standard deviation is greater than or equal to the intensity;

x) faults found at any stage of the above procedure are printed out: some of these will necessarily terminate the processing of a reflection at the stage then reached.

Other features included in 'normal' processing are:

xi) datum checks are recognised and any errors printed out: datum checks occurring in 'rescue sequences' are ignored unless the 'rescue' was performed;

xii) the program allows the extra facility of reading, and printing in the output, information typed in at the teleprinter.

The counting loss correction in step (iv) was not incorporated in the program when the AHS data was processed (see section 4.8.2.).

4.6.3.2. Output

The information presented to the user is illustrated in appendix 2.

The reflection index, h, k, ℓ and Θ, and the duration, number and size of the scan steps are given. Then follows information relating to the progress of the peak location procedure and the calculation of the integrated intensity and its standard deviation. This information, taken with the faults printed out for the reflection, simplifies the determination of the reason for any termination of processing and the location of faults in the data tape. If the processing is completed the integrated intensity, its standard deviation, and their filing location on magnetic tape are given.

The accompanying profiles afford an immediate check that peaks have been properly located by the program, show the position of any mispunched counts, and enable the user to keep a constant check on spurious or displaced peaks. Further details of the output, particularly the exact source and interpretation of the various faults, would be out of place in this account. They are fully discussed in the users' manual.

4.7. Sources of error

There are several recognised sources of significant systematic error in measured integrated intensities. In the reduction of the AHS data corrections for two of these — counting losses (section 4.8.2.) and the Lorentz-polarisation factor — were applied. The error arising from linear truncation procedures and its effect on the results of structure analysis have been discussed. The problem of scattering from lattice vibrations has also been mentioned. As has been said (Cochran, 1969), "a correction which can be as large as 25% should not be ignored", but it is pointed out (loc. cit.) that the form of the correcting factor implies that the effects of failing to make the correction will be largely taken up in the atomic temperature factors (see also Willis and Arndt, 1966, p.226).

Reduction of the kinematical integrated intensity by primary and secondary extinction has become the subject of renewed theoretical and experimental interest with the increasing accuracy of data collection. A recently developed general theory of X-ray diffraction in crystals (Zachariasen, 1967 and 1968), despite some approximations, has proved very successful even for reflections showing high extinction (Zachariasen, 1968a, 1968b, 1968c and 1969; Chandrasekhar et al., 1969). The proper application of this theory to correct for extinction effects requires intensity data collected with two different wavelengths: the AHS data was collected with MoKα radiation only. Earlier methods of applying extinction corrections give rather approximate results when the error is $> 5\%$, and the "safest procedure for dealing with extinction is to ignore those reflections for which extinction

is suspected" (Willis and Arndt, 1966, p.251). This, of course, can only be done when structural parameters are being refined by the method of least-squares; it is the procedure adopted in the case of the AHS refinement.

No absorption corrections were applied to the AHS data. For AHS the calculated linear absorption coefficient (International Tables, 1962, Vol. III, p.157) for MoKα is 6.4cm^{-1}: this value is unusually low. Furthermore, both AHS specimens were approximately equi-dimensional, so absorption errors may be expected to depend mainly on θ. Even when the crystal shape is far from equi-dimensional, it has been found that failure to apply an absorption correction will affect the atomic temperature factors markedly but the positional parameters very little (Srivastava and Lingafelter, 1966). An estimation of the absorption factor for maximum and minimum path lengths through the larger specimen of AHS showed that intensities of reflection at high angles ($\theta \sim 35°$) were reduced by $\lesssim$ 10% relative to those at low angles.

The elimination of multiple reflections (Coppens, 1968) was not attempted. There are, however, indications that this particular source of error was not serious: none of the space group absent reflections was significantly 'present', and the results of least-squares refinement (chapter 7) do not appear to show a significant systematic overestimation of the observed intensities of weak reflections (Post, 1969).

Of the sources of systematic error discussed,

i) counting losses,

ii) the Lorentz-polarisation factor,

iii) linear truncation of background,

iv) thermal diffuse scattering,

v) extinction,

vi) absorption, and

vii) multiple reflections, proper corrections to the data have been applied only for (i) and (ii), and the effects of (vii) appear to be negligible. Those reflections strongly affected by (v) are to be omitted in structure refinement. It has been argued that (iii), (iv) and (vi) mainly affect the atomic temperature factors and not the positional coordinates. This study is principally concerned with establishing the positional coordinates of the atoms in the AHS structure; temperature factors are currently the objects of intensive research and, in the meantime, considerable scepticism as to their accuracy (see, for example, Acta Crystallographica A25, part 1). The corrections applied are considered sufficient and appropriate for the stated objectives.

4.8. Checking, correcting and sorting the processed data

4.8.1. Initial sorting and minor corrections

The values of h, k and ℓ, the integrated intensity and its percentage error, and a parameter designating the specimen (SD1 or SD2) and orientation ($\ell \geq 0$ or $\ell \leq 0$), for each of the 15,000 collected reflections which had been successfully processed, was stored in duplicate on magnetic tape (file 1). The data reduction was performed in no particular order. There were no empty locations for reflections on which processing had been terminated, or for which the calculated intensity was negative or non-significant (having a percentage error $\geq$ 100).

A second file (file 2) was prepared with the reflections in the precise order in which they had been collected, including all repeats and 'standards'. The data in file 1 was re-filed into this. Empty locations appeared wherever reflections had yet to be processed; they appeared also wherever the calculated intensity had been negative or non-significant – the 'accidentally absent' reflections. Each of these gaps was accounted for and filled either with the calculated intensity and error, or with zero intensity for the accidentally absent reflections. File 2 was then printed out and marked with the detailed log of the experiment, including the results of specimen orientation checks and the duration of breaks in data collection. Thus the prevailing experimental conditions and result of every complete observation made during the five months of data collection were compiled into a single record.

All data collected under poor experimental conditions was either removed from file 2 or given an appropriately increased percentage error. The latter was estimated from the variation in the 'standard' intensity and the nature of the 'poor experimental conditions'. Every reflection was measured at least once under acceptable experimental conditions.

The silica bulb enclosing the specimens gave rise to a broad peak in the general background near $\Theta = 4°$. All weak reflections with $\Theta < 5°$ were plotted out to remove the background graphically. In several cases large corrections were necessary to the result produced by the data reduction program.

4.8.2. Correction for counting losses

At the time of processing the AHS data the data reduction program did not apply a counting loss correction: another method of correction was devised to avoid reprocessing all those reflections for which the correction was significant.

It may be assumed that significant losses will occur only at Bragg angles low enough that the peak is sensibly single. If the measured intensity at the peak centre is n_o cps, then the integrated intensity, I, after subtracting the background is given by

$$I = \alpha n_o$$

for counts of one second per step. α is of the order of the peak width at half-height. The background may be assumed to carry a negligible counting loss error for all intensities normally encountered.

The true peak count rate, n, is $n_o/(1 - n_o\tau)$ (eqn. 4.6.3.). Hence the counting loss at the peak is $nn_o\tau$ cps. The curve representing the counting losses per second has a peak height of $nn_o\tau$; it clearly falls off from its peak faster than the reflection profile for which it is the correction. Therefore, the area under this curve is

$$\alpha nn_o\tau /\beta, \text{ where } \beta > 1.$$

Let I_t be the integrated intensity corrected for background and for counting losses. Then

$$\frac{I_t - I}{I_t} = \frac{\alpha nn_o\tau /\beta}{\alpha n_o + \alpha nn_o\tau /\beta} , \qquad \text{or}$$

$$\frac{I_t - I}{I_t} = \frac{\tau}{\beta} \cdot n_o + \frac{(\beta-1)n\tau}{\beta + n\tau} \cdot \frac{\tau}{\beta} \cdot n_o \cdot \qquad (4.8.1.)$$

Since β is of the order of unity and $n\tau \leq 0.1$ the second term may be neglected. Thus, to this approximation, $(I_t - I)/I_t$ is a linear function of n_o.

Sixteen reflections were chosen ranging in observed peak intensity from 7000 cps to that of the most intense AHS reflection, 75,000 cps. They were also selected to span the range of Bragg angles over which reflections of this strength occurred. Values of I_t were computed using the full counting loss correction later included in the data reduction program. $(I_t - I)/I_t$ was plotted against n_o; all the points lay on a straight line through the origin, within one standard deviation.

The observed integrated intensities, I, were corrected using this line. The standard deviation on τ was about $\tau/3$ (section 4.6.1.1.). The absolute error on I_t was increased over that on I by a third of the correction made – as an approximation to the inclusion of error in I_t arising from the uncertainty of τ . The corrected intensities and errors were inserted in file 2.

It is shown in appendix 3 that, to a good approximation, the line described above can be used for any crystal – provided τ remains the same. This provides justification for using the same line to correct integrated intensities measured on two different specimens under different working conditions, given only that the paralysis time of the PHA remained constant.

Before correcting intensities by the method here described it was necessary to decide the minimum peak intensity for which

the correction would be significant. As previously discussed, the minimum expected error on any integrated intensity is not less than 2% with present equipment and techniques (Abrahams et al., 1967). For the known value of τ the counting loss correction becomes greater than 2% at a peak intensity of 10,000 cps. It was decided to err on the side of industry: the correction was applied to all reflections with a peak intensity greater than 5000 cps.

4.8.3. Final checking and sorting

The integrated intensities of the 1200 'standard' reflections measured during data collection were plotted out to look for significant long or short term variations — particularly where the scintillator, the beam, the X-ray tube power, or the PHA settings had been changed.

Data sets (1), (2) and (3) were collected on specimen SD1, and (4) and (5) on SD2 (see appendix 1). The maximum variation of the 'standard' intensity during set (1) was $\pm$3%. There was a significant long term variation, but of a magnitude no greater than that often found between successive 'standards'. No meaningful correction could be applied in such circumstances. The variation was, in any case, no greater than the expected minimum error in the recorded intensities. The results and conclusions for set (2), although differing in detail, were broadly similar and no correction was applied.

Several factors led to a decision not to use the data in set (3): the machine alignment was suspect (see appendix 1), there was a sudden drop of 5% in the mean level of the 'standard'

intensity, and the stability of the specimen alignment was very poor. For similar reasons set (4) was also removed from file 2.

The maximum variation of the 'standard' intensity during the six weeks spent collecting set (5) was $\pm$3%. In that period the mean level of the 'standard' intensity dropped by 1%. Again neither variation was considered to warrant a correction.

The data to be used was thus on three different scales: sets (1) and (2) collected under different conditions from SD1, and set (5) collected from SD2. For each set a list comprising the intensity and error – with repeated measurements, if made – of each reflection was printed out alongside those of the symmetrically equivalent reflection (i.e. $h\bar{k}\ell$ and $\bar{h}\bar{k}\ell$). Disagreements in intensity among repeats of the same reflection or between the symmetrically equivalent pairs were investigated. Some were traced to a faulty value of Θ on the data tape which had passed undetected; file 2 was corrected accordingly. Otherwise where one value disagreed with the others by more than three standard deviations it was removed. In the few cases where symmetrically equivalent pairs disagreed their standard deviations were increased according to the magnitude of the disagreement.

For each reflection ($h\bar{k}\ell$) measured in each data set, a single weighted mean intensity and error was calculated from the repeats of that and the symmetrically equivalent reflection ($\bar{h}\bar{k}\ell$). The intensities and errors of the 'weak' reflections were scaled down by the factor of three by which the counting time for these reflections had been increased. This data was stored on paper tape (file 3) for later use with the least-squares refinement program. It comprised, with overlap between data sets, the

intensities and errors of 6500 symmetrically inequivalent reflections with $h \geq 0$, $k \leq 0$ and $\ell^{\pm}$, lying in the range $0° \leq \Theta \leq 35°$.

For preliminary structure analysis in the (010) projection (chapter 5) the three sets of data were scaled together approximately by the mean 'standard' intensity for each set. This data was stored on magnetic tape in file 4.

CHAPTER 5

STRUCTURE ANALYSIS

5.1. Introduction

The general features of the two-dimensional 'average structure' have been found already using photographic data (chapter 3). With the more accurate diffractometer data, extending to a somewhat higher value of $\sin\Theta/\lambda$, this 'average structure' was refined further as a preliminary to attempts to solve the two-dimensional 'difference structure'. The solution of the latter led directly to a good trial structure for the three-dimensional structure which was refined by full-matrix least-squares techniques.

5.2. Methods and the further refinement of the two-dimensional 'average structure'

The two-dimensional 'average structure' is the Fourier transform of the systematically strong ($h0\ell$) structure factors (eqn. 3.4.3.). The refinement of this structure from the crude results obtained with the photographic data (table 3.5.2.) proceeded by the minimum residual method of Bhuiya and Stanley, 1963, combined with a study of the Fourier synthesis and the difference synthesis obtained with the structural parameters at each stage of the refinement. The data used was that in file 4.

5.2.1. Methods

5.2.1.1. 'Pangloss'

Bhuiya and Stanley's method was specifically developed to refine projections of structures in which overlap of atoms makes difficult the use of Fourier techniques to locate parameters in the correct 'holes' in parameter space, and makes the least-squares method ineffective because of high parameter correlation. It appeared to be ideally suited to the problems posed by the two-dimensional 'average structure' and 'difference structure' of AHS.

The method involves stepping the value of each parameter in turn through pre-set increments, calculating some residual index for each value, and setting the parameter at the value which minimises this residual. The residual index chosen was

$$RI = \Sigma(|F_o(hO\ell)| - |F_c(hO\ell)|)^2,$$ where the summation was over all the measured structure amplitudes. The $|F_c(hO\ell)|$ were calculated from the current trial structure parameters, and the same f-curves as were used in the final stage of refining the photographic data.

The advantages of the method derive from the pre-determination of the range of parameter variation. This allows the right parameters for an approximately correct structure to be found when these are separated from their starting values by several false minima in parameter space. This situation is particularly likely to arise when atoms overlap in projection. The disadvantages, with regard to the convergence of the refinement, of constraining parameters to move in turn along pre-set lines,

instead of cooperatively towards a minimum in parameter space, are found in practice to be much less serious than might be supposed (Bhuiya and Stanley, 1963, p.983).

A computer program based on this method was developed by Mr. L. Sawyer of this Department. It was further and specifically developed by the author for application to AHS. This program and the method it incorporates will be referred to as 'Pangloss'.

5.2.1.2. The F_o-synthesis

The standard Fourier synthesis

$$\rho(xyz) = \frac{1}{V} \sum_{\substack{h,k \\ \text{and } \ell}} |F_o(hk\ell)| \exp 2\pi i(hx + ky + \ell z + \alpha) \qquad (5.2.1.)$$

using the observed structure amplitudes $|F_o(hk\ell)|$, and the phases α calculated from a trial structure, will be referred to as the F_o-synthesis. The summation is over all observed $(hk\ell)$ – out to a limiting value of $2\sin\Theta/\lambda$ designated S. Because it incorporates the trial structure phases the F_o-synthesis will partly reproduce the features of that structure: atomic centres will appear displaced from their 'true' positions towards the trial structure positions. For a non-centrosymmetric structure in which all the $F_o(hk\ell)$ have general phase angles it can be shown (Lipson and Cochran, 1966, p.318) that

$\rho_o \doteq \frac{1}{2}(\rho_t + \rho_c)$, where ρ_o is the F_o-synthesis, ρ_c is the trial structure and ρ_t is the 'true' structure – towards which ρ_c is being refined. If an atom is at $\underline{r}$ in ρ_c and at $\underline{r} + d\underline{r}$ in

ρ_o it should be moved to $\underline{r} + 2d\underline{r}$ for the new ρ_c. For a centrosymmetric structure when ρ_c is approximately correct, the signs for most $|F_o(hk\ell)|$ will be correct so that

$$\rho_o \doteq \rho_t.$$

The positions to be assumed for the new ρ_c are more nearly those of ρ_o than in the general non-centrosymmetric case.

Cochran, 1948, has shown that the solution obtained by successive F_o-syntheses is "a special case of the least-squares solution in which the weight given to each observation is inversely proportional to the magnitude of the corresponding atomic scattering factor". This is a disadvantage: excessive weight is given to the probably poorly determined high order $|F_o(hk\ell)|$ and the weighting cannot be adjusted according to the accuracy of each $|F_o(hk\ell)|$. Also diffraction ripple errors are introduced by the termination of the data series at a finite S. However, the method has the advantage that assumptions about the electron distribution in atoms are less important than in the least-squares method; for centrosymmetric structures the atomic scattering factors need only be known with sufficient accuracy to obtain the correct sign for each $|F_o(hk\ell)|$. Fourier synthesis is, of course, the only method that can be used if the actual electron density distribution in the unit cell is required.

5.2.1.3. The difference synthesis

Cochran, 1951, introduced the $(F_o - F_c)$-synthesis, now more usually referred to as the 'difference synthesis'. It is defined by

$$D(xyz) = \frac{1}{V} \sum_{\substack{h,k \\ \text{and } \ell}} (F_o(hk\ell) - F_c(hk\ell))\exp 2\pi i(hx + ky + \ell z), \qquad (5.2.2.)$$

or for a centrosymmetric structure by

$$D(xyz) = \frac{1}{V} \sum_{\substack{h,k \\ \text{and } \ell}} (F_o(hk\ell) - F_c(hk\ell))\cos 2\pi(hx + ky + \ell z). \qquad (5.2.3.)$$

This synthesis is used in the final stages of refinement: in the centrosymmetric case $F_o(hk\ell)$ is assumed to have the same sign as $F_c(hk\ell)$. The difference synthesis was a development from the earlier 'error synthesis' introduced by Bunn (Crowfoot et al., 1949).

When $D = 0$, $(\frac{\partial D}{\partial r})_{r=0} = 0$ and $(\frac{\partial^2 D}{\partial r^2})_{r=0} = 0$ for all atomic sites, where r is the distance from an atomic centre, the scale factor, the atomic coordinates and the thermal parameters respectively are 'correct' in that they minimise the function

$$\phi_j = \sum_{\substack{h,k \\ \text{and } \ell}} (\frac{1}{f_j})(F_o(hk\ell) - F_c(hk\ell))^2, \qquad (5.2.4.)$$

where f_j is the value of the j^{th} atomic scattering factor for the reflection $(hk\ell)$. The theory of errors (section 5.4.1.) gives as the correct function to minimise

$$R_1 = \sum_{\substack{h,k \\ \text{and } \ell}} \omega(hk\ell)(|F_o(hk\ell)| - |F_c(hk\ell)|)^2, \qquad (5.2.5.)$$

where the weight $\omega(hk\ell)$ is inversely proportional to the variance of $|F_o(hk\ell)|$. The introduction of appropriate weights into the difference synthesis is possible but is more conveniently performed in the least-squares refinement method discussed later.

It is usual to use the difference synthesis as defined above and hence to minimise $\emptyset_j$.

The chief use of the difference synthesis is thus not to achieve the 'best' final parameters, but show up inadequacies of the trial structure in the later stages of refinement. For this purpose an important feature of the synthesis is that it is not affected by series termination ripples. Analytical expressions in terms of D(xyz) for the corrections to be applied to the scale factor and to positional and thermal parameters have been derived by Cochran, 1951. However, in this work the difference synthesis was always used in conjunction with either Pangloss or the least-squares method. It was, therefore, only qualitatively interpreted, as illustrated in Figs. 335, 336 and 337 of Lipson and Cochran, 1966. It was used thus to suggest probable separations of atoms in the two-dimensional 'average structure' and 'difference structure', to study inadequacies remaining in trial structures after refinement by Pangloss or least-squares, and, later, to look for hydrogen atoms in the three-dimensional structure.

5.2.2. Refinement of the two-dimensional 'average structure'

Starting with the coordinates obtained with the photographic data (table 3.5.2.) and allowing individual isotropic temperature factors, the R-factor for the two-dimensional 'average structure' dropped from 17% to 10% in three cycles of Pangloss. Anisotropic temperature factors could not be introduced because of the very high correlation that would occur between them and the separation of the centres of superposed pairs of atoms. Difference syntheses

showed that appreciable correlation existed even with isotropic temperature factors. Attempts were made to refine the coordinates and the temperature parameters separately, deciding on the next 'move' each time after studying the difference synthesis corresponding to the previous stage in the refinement. The R-factor could not be reduced below 9.5%.

In this refinement the atomic coordinates were referred to the true two-dimensional cell, $\underline{a}/2 \times \underline{c}/2$ – even though the true cell for the 'average structure' is $\underline{a}/4 \times \underline{c}/2$. It was convenient to consider the asymmetric unit as comprising the two molecules situated about the pseudo-mirror planes at $\underline{a}/16$ and $5\underline{a}/16$, rather than one of the 'double' molecules in the actual 'average structure' as was done in the photographic work. The pairs of symmetrically inequivalent atoms which superpose in the 'double' molecules of the 'average structure' were thus separated and yet the members of each pair had approximately the same z-coordinate. All this simplified the representation of the problem of solving the 'difference structure' – which was essentially to find the correct allocation of members of each such pair of atoms between the molecules at $\sim\underline{a}/16$ and $\sim 5\underline{a}/16$ – and saved having to change later from the true 'average structure' cell to the true 'difference structure' cell ($\underline{a}/2 \times \underline{c}/2$).

The fractional coordinates and isotropic temperature factor parameters, B, of the refined (R = 9.5%) 'average structure' were:

Table 5.2.1.

	x	z	B in Å^2		x	z	B in Å^2
S_1	.127	.226	1.4	S_2	.624	.205	1.9
O_1	.037	.339	1.8	O_5	.524	.306	1.8
O_2	.212	.344	2.0	O_6	.724	.310	1.9
O_3	.084	.094	3.4	O_7	.604	.062	4.5
O_4	.165	.099	3.1	O_8	.650	.063	4.5
N_1	.124	.702	2.2	N_2	.625	.704	2.0

The implied separation into two molecules is, of course, entirely arbitrary.

The separations between superposing atoms (e.g. O_1 at $x = .037$, $z = .339$ and O_5 at $x = .024$ ($\equiv .524$), $z = .306$) had been in essentially the same directions throughout the above refinement; it was assumed that the 'difference structure' could be solved simply by finding which of the 32 possible allocations of the atoms between the two molecules at $\sim \underline{a}/16$ and $\sim 5\underline{a}/16$ gave the best fit to the 'weak' $|F_o(h0\ell)|$ data. A computer program was written to calculate the R-factor for each allocation using the 'weak' $|F_o(h0\ell)|$ only. These R-factors all lay between 75% and 85%, and it was clear that the separations found in the 'average structure' were incorrect. The high correlations between the positional parameters of superposed atoms and also between their positional and thermal parameters made the 'average structure' essentially indeterminate.

The general features of the 'average structure' were known; but other methods had to be found to solve the 'difference structure'.

5.3. Methods and the refinement of the two-dimensional 'difference structure'

5.3.1. The Patterson function

The first step in a direct attempt to solve the 'difference structure' was to compute its Patterson function $P_d(u,w)$ (eqn. 3.4.6.), using all the observed 'weak' ($hO\ell$) intensities. Before attempting to interpret this function it was necessary to study the characteristics of the corresponding Fourier synthesis (eqn. 3.4.4.) – the 'difference structure' itself.

Consider, for example, the oxygen atoms O_1 and O_5 with the coordinates given above:

	x	z
O_1	.037	.339
O_5	.524	.306 .

The 'difference structure' will have

	x	z
O_1	.037	.339
$-O_5$	.024	.306
$-O_1$	.537	.339
O_5	.524	.306 ,

where a negative sign indicates an atom with negative electron density. The resultant electron density for O_1 and $-O_5$ is shown diagrammatically in fig. 5.3.1.. The Fourier synthesis of the 'difference structure' thus shows an anti-symmetric pair of peaks for each superposing pair of atoms. The peaks may be distorted if different atom pairs are close together in projection.

The next step was to investigate how the separation and height

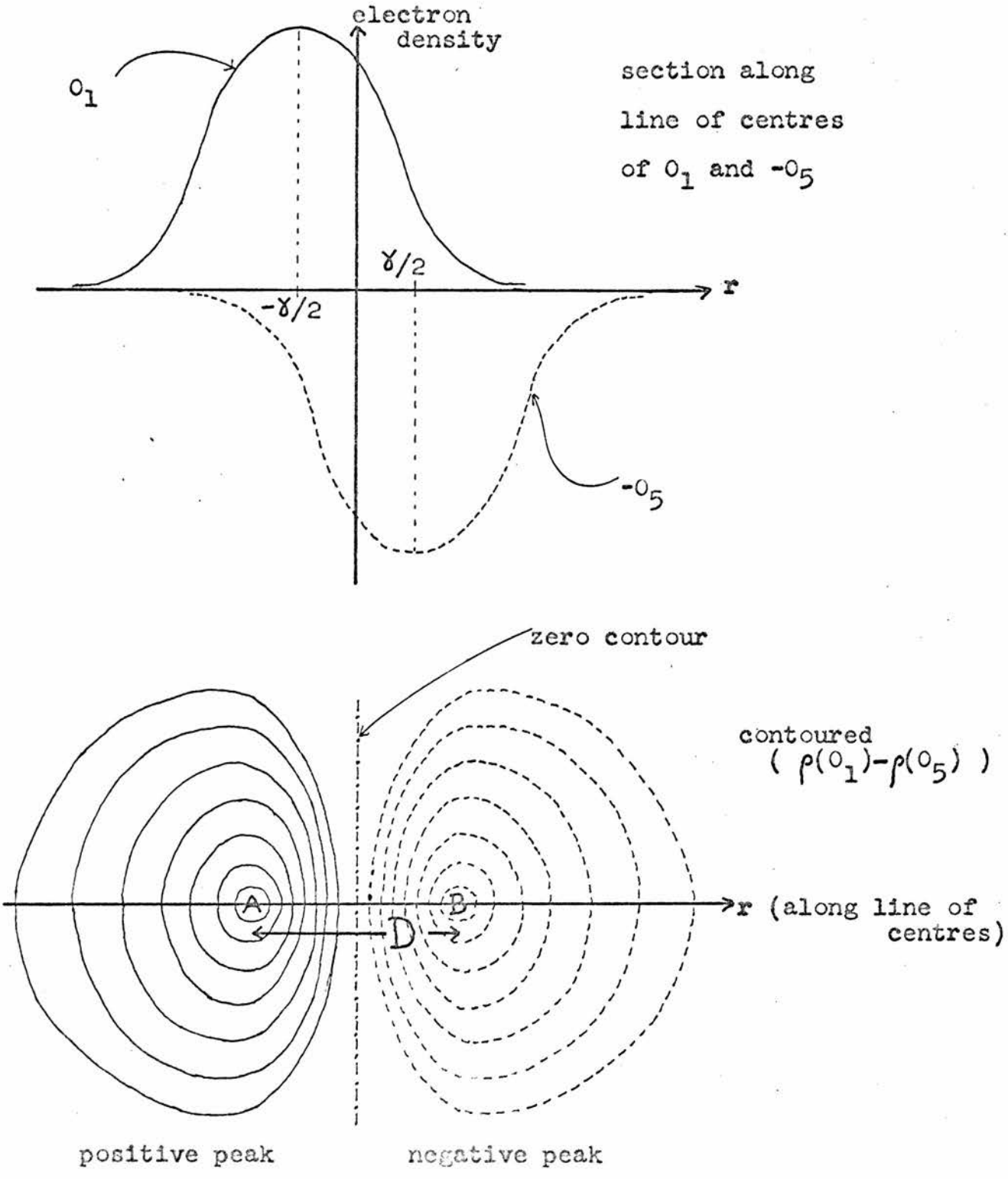
electron density
O_1
section along line of centres of O_1 and $-O_5$
$\gamma/2$
$-\gamma/2$
r
$-O_5$
zero contour
contoured ($\rho(O_1)-\rho(O_5)$)
A
B
D
r (along line of centres)
positive peak
negative peak

Fig. 5.3.1.

of the anti-symmetric pair of peaks depended on the separation, γ, between atomic centres (see fig. 5.3.1.). To a good approximation the electron density near the centre of an atom may be represented by a Gaussian function; the peak height of the function is approximately proportional to the atomic number, Z, and its width at half-height depends to some extent on Z and also on the temperature factor (Lipson and Cochran, 1966, p.321). A Gaussian function was drawn out and the 'subtraction-curves' resulting from subtracting an identical function (fig. 5.3.2.) were plotted for varying separations, s, of the peaks of the two functions. The height, h, of the positive peak in this anti-symmetric subtraction-curve was plotted against s; so also was the separation, d, of the positive and negative peaks of the subtraction-curve (fig. 5.3.3.). It can be seen that h depends linearly on s nearly up to the half-width of the Gaussian at half-height; d changes only very slowly with s and may be taken to be approximately constant.

Hence, for small separations of the superposed atoms in the 'difference structure', the separation of the positive and negative peaks, D (fig. 5.3.1.), is approximately constant — with a value which depends on the type of atom considered; the 'heights' of the peaks are equal, opposite and proportional to the separation of atomic centres, γ. In the Patterson function $P_d(u,w)$, therefore, the negative 'self-peaks', arising from each pair of anti-symmetric peaks, are at distances from the origin which are characteristic of the type of atom involved, and are of a height proportional to $(\gamma Z)^2$. It is assumed that the values of γ will all be small enough for these approximations to be valid.

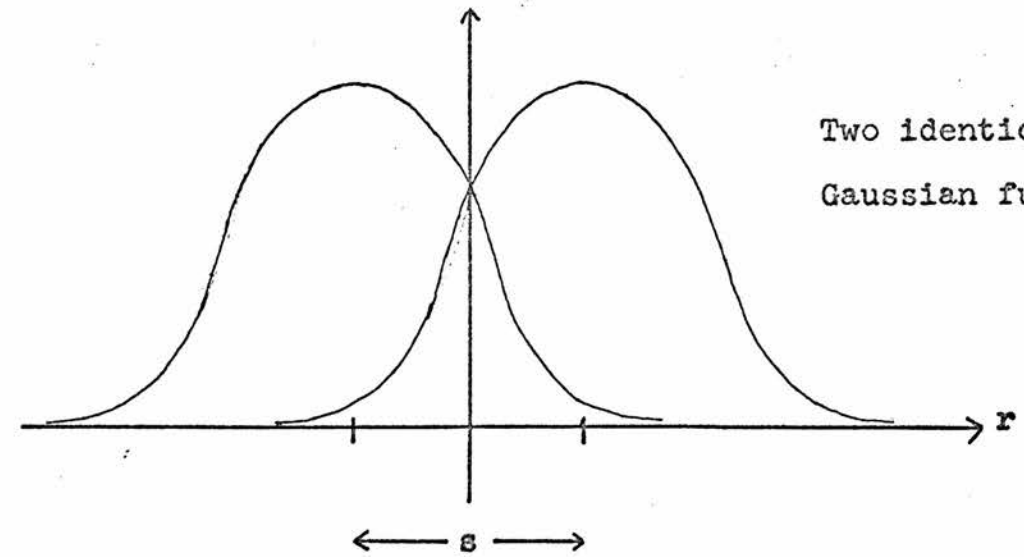
Two identical
Gaussian functions
r
s

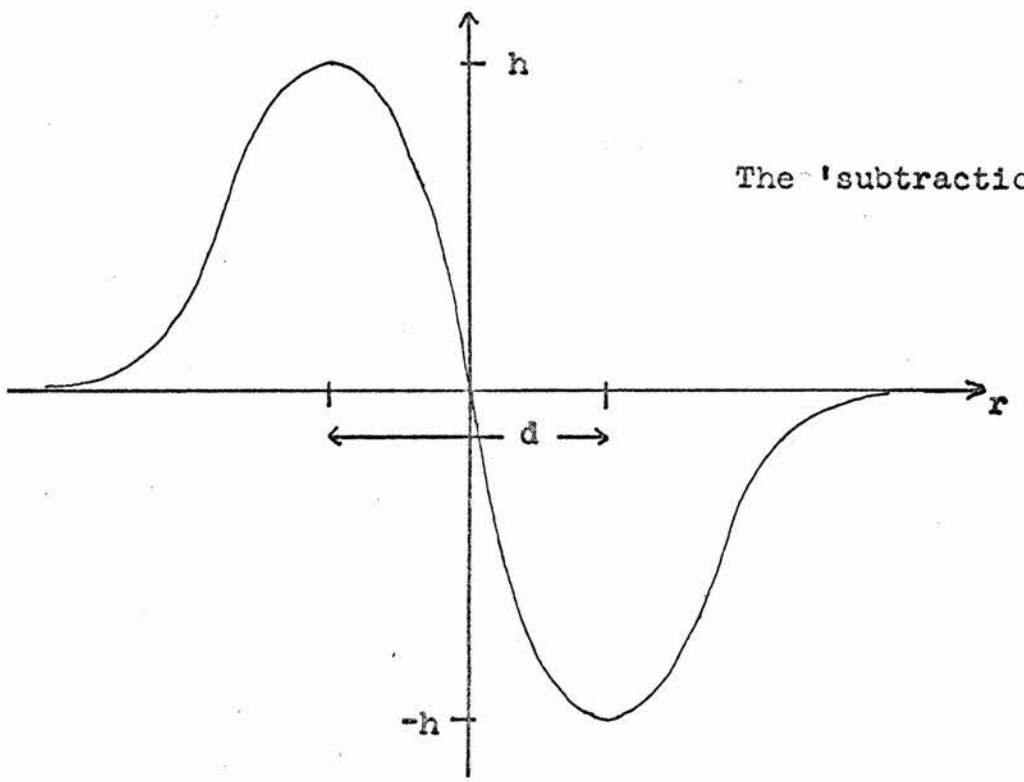
h
The 'subtraction-curve'
r
d
-h

Fig. 5.3.2.

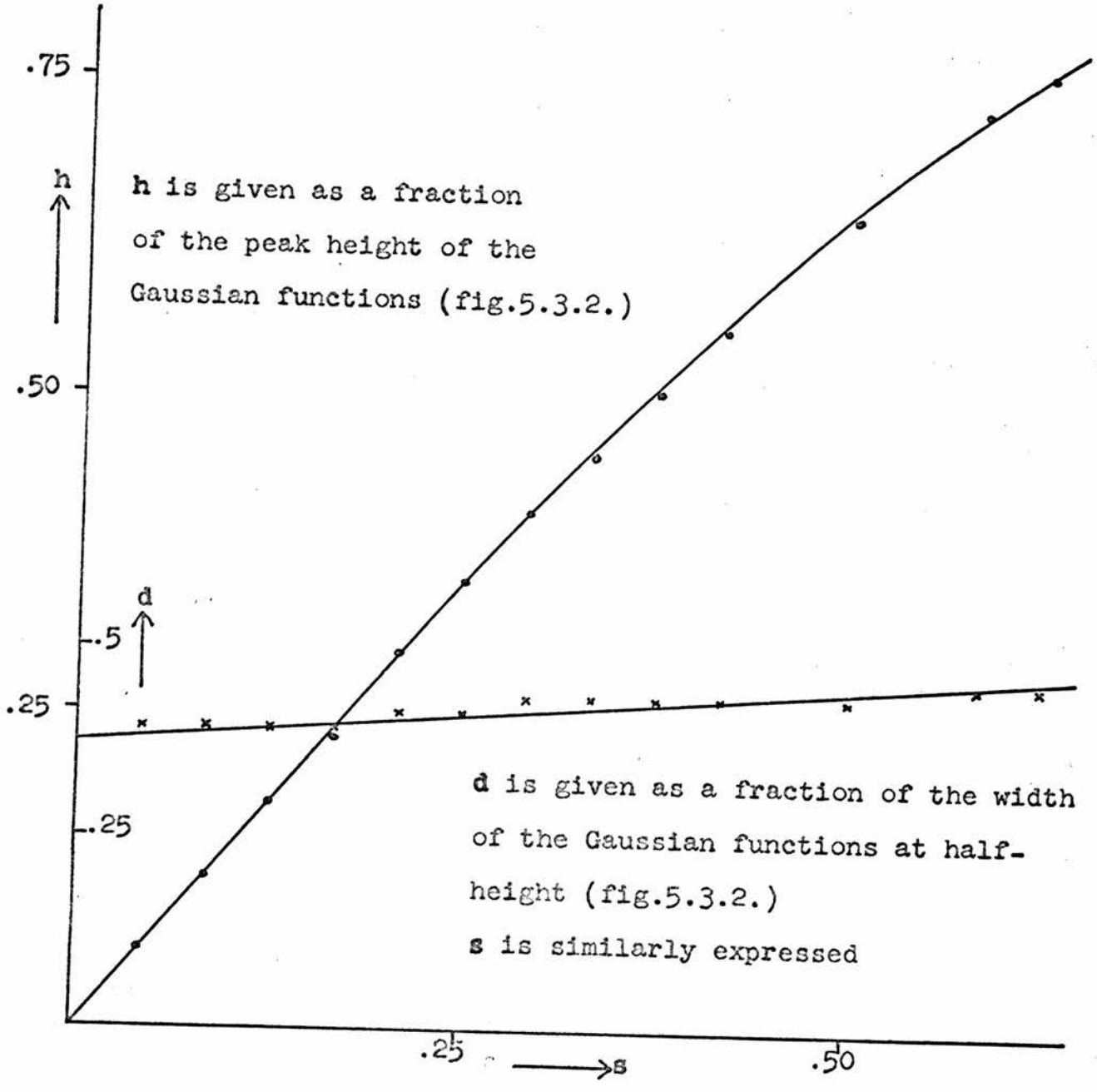

The dependence of **h** on **s** is shown by the curve through the points o
The dependence of **d** on **s** is shown by the curve through the points ×
(see fig. 5.3.2. for 'd', 'h' and 's')

Fig. 5.3.3.

It was later found that the anti-symmetric component of Patterson and Fourier functions in problems involving small atomic shifts from positions of higher symmetry had already been investigated by Qurashi, 1963. Essentially the same conclusions were reached.

In the light of this analysis an attempt was made to interpret $P_d(u,w)$. Taking the widths at half-height as found from F_o-syntheses of the 'average structure'

$\sim 0.54\mathring{A}$ for oxygen and nitrogen

$\sim 0.46\mathring{A}$ for sulphur

as approximate measures of the relative dimensions of these atoms, it follows from the preceding discussion that the sulphur 'self-peaks' were nearer the origin of $P_d(u,w)$ than those of oxygen and nitrogen. In the refined 'average structure' at that stage all oxygen atom pairs showed separations, γ, of $\sim 0.3\mathring{A}$; both the sulphur and the nitrogen pairs showed separations, γ, of $\sim 0.1\mathring{A}$. From these values the approximate relative 'self-peak' heights were estimated as

sulphur	4
oxygen	16
nitrogen	1 .

The actual rather than relative distances of the 'self-peaks' from the origin could not be obtained without accurate knowledge of the form of the actual electron density function for each atom. However, for the function $SP_d(u,w)$ (eqn. 3.5.2.), the Patterson function computed from the 'sharpened' 'weak' intensities, the artificial scattering factors

$$f = Z \exp[-\frac{\pi^2}{2p} . \ s^2]$$

were introduced for each atom, with p=7.25 (see chapter 3, pp.37-38). The Fourier transform of this Gaussian function gave the Gaussian artificial electron density function for each atom. The expected distances of the 'self-peaks' from the origin of $SP_d(u,w)$ are then seen from fig. 5.3.3. to be approximately the same as the half-width at half-height of these functions.

Although the features of $SP_d(u,w)$ were more clearly defined than those of $P_d(u,w)$, the better knowledge regarding the distance of the 'self-peaks' from the origin led to no solution. Further investigations of other features to be expected in $P_d(u,w)$ and $SP_d(u,w)$ were made but bore no fruit. Attempts to find a solution were eventually suspended; it became apparent that the relatively strong oxygen 'self-peaks' dominated the region around the origin but, being displaced in different directions from the origin, appeared as a weakly featured ring rather than as separate peaks. In the regions away from the origin there were too many peaks all of similar magnitudes for the function to be interpretable.

5.3.2. Direct methods

The 'weak' reflections correspond to a definite structure: the 'difference structure' is an electron density function which gives rise to the 'weak' reflections only. Some thought was given as to whether direct methods might be applied to the solution of this structure. 'Direct methods' are usually taken

to be "those methods which attempt to derive the phases of the structure factors directly by mathematical means from the X-ray diffraction data" (Woolfson, 1961, p.2).

These methods vary in complexity; but they are all concerned with finding a relationship between the phases of the structure factors $F(\underline{h})$, $F(\underline{h}')$ and $F(\underline{h} + \underline{h}')$, or $F(\underline{h})$, $F(\underline{h}')$ and $F(\underline{h} - \underline{h}')$ (Woolfson, 1961). They appeal to the premise that the electron density in crystals is everywhere positive (Cochran, 1952).

The probability of a phase relationship holding increases with the magnitude of the structure factors involved (Woolfson, 1961). Consider, for example, the simple two-dimensional centrosymmetric structure in fig. 5.3.4.a.. If F(100) and F(101) are positive and strong (in direct methods the strength of a structure factor is measured by the ratio, U, of its magnitude to the maximum possible magnitude for a structure factor at the same value of $\sin\Theta/\lambda$) then the structure is likely to have high electron density at the points marked ● . If $F(\underline{h} + \underline{h}')$, F(201), and $F(\underline{h} - \underline{h}')$, F(001), are strong it becomes more likely that there is high electron density at these points, and it is clear that the signs of these reflections are very probably positive. Had, say, the sign of F(100) been negative then the regions of high electron density would have appeared at □ , and it is clear that the signs of F(201) and F(001) would then be negative.

Thus for centrosymmetric structures, provided $|F(\underline{h})|$ and $|F(\underline{h}')|$ are large ($U > 0.5$), $s(\underline{h}).s(\underline{h}').s(\underline{h} \pm \underline{h}') \approx \pm 1$, provided $|F(\underline{h} \pm \underline{h}')|$ are large ($U > 0.5$), where s denotes 'sign of F' and $\approx$ denotes 'is probably equal to'. $U > 0.5$ is the usual criterion

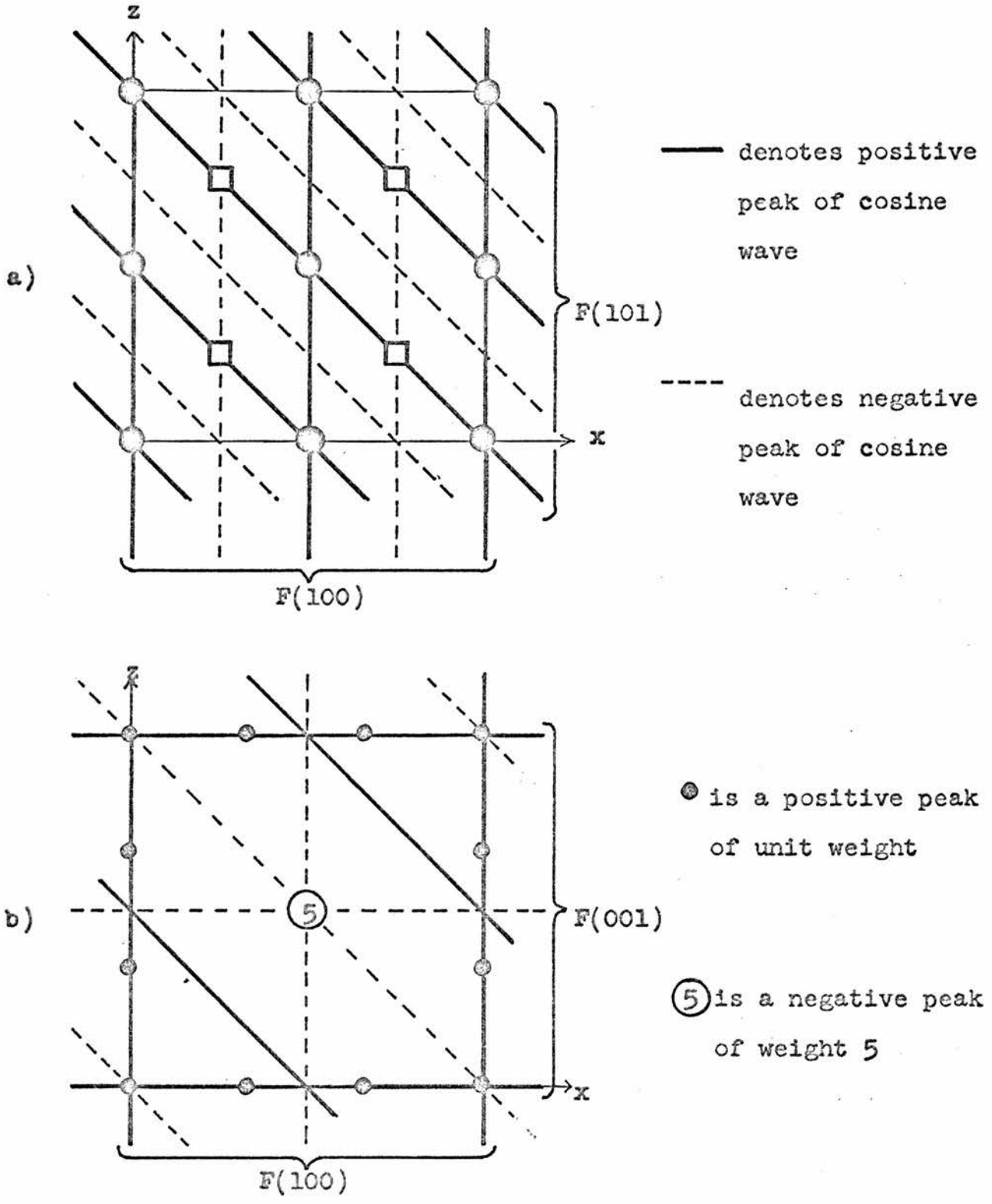
a)
z
x
F(101)
F(100)
denotes positive peak of cosine wave
denotes negative peak of cosine wave
b)
z
x
5
F(001)
F(100)
is a positive peak of unit weight
5 is a negative peak of weight 5

Fig. 5.3.4.

for a 'sufficiently large' $|F|$ (Woolfson, 1961).

Now in a 'difference structure' there are positive and negative peaks of equal amplitude: the physical basis for the phase relationships is lost. It is easy to envisage a structure in which $\int_V \rho(\underline{r})dV = 0$ and the above sign relationships are actually reversed. If F(100) and F(001) in fig. 5.3.4.b. are strong and positive, it is clear that F(101) is likely to be strong and negative. In the particular case of such a structure that is presented by the 'difference structure' of AHS the above sign relationships cannot be applied either way. Structure factors for the 'difference structure' are systematically absent for h even. Hence at least one out of $F(\underline{h})$, $F(\underline{h}')$ and $F(\underline{h} \pm \underline{h}')$ has zero amplitude.

Direct methods appear to be inapplicable to any structure in which $\int_V \rho(\underline{r})dV = 0$, and certainly could not be used for the 'difference structure' of AHS.

5.3.3. Pangloss and F_o-syntheses

Renewed attempts were made to solve the 'difference structure' with Pangloss, helped by the study of F_o-syntheses of the 'weak' reflections. The characteristics of this synthesis have been discussed.

Pangloss, as then written, computed and applied a scaling factor for each cycle. It was realised that this could not be allowed if the program were to be used on the 'weak' reflections alone because of the very high correlation between the scale factor and the separation of atom pairs in the 'difference structure'. With the scale factor fixed at the value found for

the 'strong' reflections, Pangloss was applied to the 'weak' reflections alone with immediate success. Starting positions corresponding to three different allocations of the 'average structure' coordinates (table 5.2.1.) were tried. All three refined to essentially the same structure. In each case the R-factor dropped from ~120% to ~30% in three cycles. The largest movement in these three refinements was 0.4Å. What seemed more remarkable was that in cases where the initial allocation of an atom pair was incorrect (with the initial position of the negative atom close to the final position of the positive atom, and vice versa) the negative and positive atoms moved through each other to their correct positions.

The 'difference structure' was refined through another three cycles of Pangloss to an R-factor of 26%. The structural parameters were:

Table 5.3.1.

	x	z	B in Å^2		x	z	B in Å^2
S_1	.122	.213	2.5	S_2	.625	.205	1.8
O_1	.040	.326	2.4	O_5	.542	.327	1.7
O_2	.229	.324	2.9	O_6	.722	.316	2.5
O_3	.106	.136	4.7	O_7	.592	.082	3.8
O_4	.140	.059	3.7	O_8	.659	.103	3.9
N_1	.123	.709	2.0	N_2	.624	.703	2.3

The two symmetrically inequivalent molecules of the AHS structure had now been correctly distinguished in the (010) projection: the crux of the problem was solved.

During the refinement difference syntheses of the 'difference

structure' were computed at each stage. The interpretation of such syntheses is at best complex, and possibly totally misleading: they are the difference between structures which already contain positive and negative peaks. They were used, therefore, only to obtain indications of the regions of the structure where disagreement remained between the trial and the 'observed' structures.

The 'strong' data did not agree as well with the refined 'difference structure' (R = 28%) as with the previously refined 'average structure' (R = 9.5%). However, it was considered that the coordinates of the full two-dimensional structure must be close to those found for the 'difference structure' – the fit for the latter structure was much more sensitive to small coordinate shifts than the 'average structure' with its high correlation between positional and thermal parameters. The least-squares refinement of the full two-dimensional structure, starting from the final 'difference structure' found by Pangloss, is described in the following section.

5.4. Least-squares refinement of the structure of AHS in the (010) projection

5.4.1. The least-squares method

When measures of a physical quantity differ from each other owing to accidental errors of observation only, the distribution of these measures about the true value, defined as the limit to which the mean of n observations tends when n increases to infinity, is a normal frequency distribution. The best value of the physical quantity is that which renders a minimum the sum

of the squares of the differences between the observational measures and that value. The general least-squares method is based on this principle (Whittaker and Robinson, 1944, Ch. IX).

The application of the method to crystal structure analysis was first suggested by Hughes, 1941, who pointed out that the exact least-squares treatment of a set of linear equations (see Lipson and Cochran, 1966, pp.341-7) could be adapted to an iterative solution for the corrections to be applied to the structural parameters — provided that the parameters were already well enough known that these corrections were small. Then the equations in the parameter corrections, δp_j , can be written

$$\sqrt{W_i} \sum_{j=1}^{m} \frac{\partial |F_c|_i}{\partial p_j} . \delta p_j = \sqrt{W_i} \left(|F_o| - |F_c| \right)_i, \quad i = 1 \text{ to } s. \tag{5.4.1.}$$

There are m parameters, p, and s observed structure amplitudes $|F_o|$. The corresponding calculated amplitudes $|F_c|$ are functions of the rest atomic scattering factors and the current values of the parameters. To each equation the weight $\sqrt{W_i}$ is applied. The correct value for W_i is the reciprocal of the variance of $|F_o|_i$ (Whittaker and Robinson, 1944, section 113).

The quantity to be minimised is

$$R_1 = \sum_{i=1}^{s} W_i (|F_o| - |F_c|)_i^2 . \tag{5.4.2.}$$

Let $$Y_i = (|F_o| - |F_c|)_i - \sum_{j=1}^{m} \frac{\partial |F_c|_i}{\partial p_j} . \delta p_j ,$$

then R_1 is minimised when

$$\sum_{i=1}^{s} W_i \gamma_i \frac{\partial \gamma_i}{\partial (\delta p_{j'})} = 0, \quad j' = 1 \text{ to } m, \text{ and } \delta p_j \rightarrow 0.$$

$$\frac{\partial \gamma_i}{\partial (\delta p_{j'})} = - \frac{\partial |F_c|_i}{\partial p_{j'}} \quad , \text{ so that}$$

$$\sum_{i=1}^{s} W_i \frac{\partial |F_c|_i}{\partial p_{j'}} \left[(|F_o| - |F_c|)_i - \sum_{j=1}^{m} \frac{\partial |F_c|_i}{\partial p_j} \cdot \delta p_j \right] = 0, \quad j' = 1 \text{ to } m,$$

or

$$\sum_{j=1}^{m} \left[\sum_{i=1}^{s} W_i \frac{\partial |F_c|_i}{\partial p_{j'}} \cdot \frac{\partial |F_c|_i}{\partial p_j} \cdot \delta p_j \right] = \sum_{i=1}^{s} W_i \frac{\partial |F_c|_i}{\partial p_{j'}} (|F_o| - |F_c|)_i \quad ,$$

$$j' = 1 \text{ to } m. \qquad (5.4.3.)$$

Equations 5.4.3. may be written in matrix form as $\underline{\underline{M}} . \underline{\delta p} = \underline{E}$, which in full is

$$\begin{bmatrix} \sum_{i=1}^{s} W_i \frac{\partial |F_c|_i}{\partial p_1} \cdot \frac{\partial |F_c|_i}{\partial p_1} & \sum_{i=1}^{s} W_i \frac{\partial |F_c|_i}{\partial p_1} \cdot \frac{\partial |F_c|_i}{\partial p_2} & \cdots & \sum_{i=1}^{s} W_i \frac{\partial |F_c|_i}{\partial p_1} \cdot \frac{\partial |F_c|_i}{\partial p_m} \\ \sum_{i=1}^{s} W_i \frac{\partial |F_c|_i}{\partial p_2} \cdot \frac{\partial |F_c|_i}{\partial p_1} & \sum_{i=1}^{s} W_i \frac{\partial |F_c|_i}{\partial p_2} \cdot \frac{\partial |F_c|_i}{\partial p_2} & \cdots & \sum_{i=1}^{s} W_i \frac{\partial |F_c|_i}{\partial p_2} \cdot \frac{\partial |F_c|_i}{\partial p_m} \\ \vdots & \vdots & & \vdots \\ \sum_{i=1}^{s} W_i \frac{\partial |F_c|_i}{\partial p_m} \cdot \frac{\partial |F_c|_i}{\partial p_1} & \sum_{i=1}^{s} W_i \frac{\partial |F_c|_i}{\partial p_m} \cdot \frac{\partial |F_c|_i}{\partial p_2} & \cdots & \sum_{i=1}^{s} W_i \frac{\partial |F_c|_i}{\partial p_m} \cdot \frac{\partial |F_c|_i}{\partial p_m} \end{bmatrix} \cdot \begin{bmatrix} \delta p_1 \\ \delta p_2 \\ \vdots \\ \delta p_m \end{bmatrix}$$

$$
\equiv\equiv \quad
\begin{bmatrix}
\sum_{i=1}^{s} W_i \frac{\partial |F_c|_i}{\partial p_1} \left(|F_o| - |F_c| \right)_i \\
\sum_{i=1}^{s} W_i \frac{\partial |F_c|_i}{\partial p_2} \left(|F_o| - |F_c| \right)_i \\
\vdots \\
\sum_{i=1}^{s} W_i \frac{\partial |F_c|_i}{\partial p_m} \left(|F_o| - |F_c| \right)_i
\end{bmatrix}
\qquad (5.4.4.)
$$

The required solution is then $\underline{\delta p} = \underline{\underline{N}}.\underline{E}$, where $\underline{\underline{N}} = \underline{\underline{M}}^{-1}$. Since the $|F_c|$ and the $\partial |F_c| / \partial p_j$ are functions of the parameters, p_j, this procedure has to be iterated until every δp_j is small compared with its standard deviation.

The parameters p_j, $j = 1$ to m, are the positional coordinates of the atoms and the isotropic or anisotropic temperature factor parameters. In addition, a scale factor is introduced, unless the $|F_o|$ are measured on an absolute scale, to bring $|F_c|$ to the same scale as $|F_o|$. This is treated as another parameter in the refinement.

The correct choice of absolute weights is, as said, $W_i = [\sigma^2 (|F_o|_i)]^{-1}$. In practice relative weights rather than absolute weights are likely to be used:

$$W_i = \epsilon^2 / \sigma^2 (|F_o|_i) , \qquad (5.4.5.)$$

where ϵ^2 may be estimated from the parameters at the end of the

refinement as

$$\epsilon^2 = \sum_{i=1}^{s} W_i \gamma_i^2 / (s-m) \qquad (5.4.6.)$$

(Whittaker and Robinson, 1944), and $\gamma_i = (|F_o| - |F_c|)_i$ on the assumption that $\delta p_j \rightarrow 0$ for all j. The introduction of the constant factor ϵ^2 into W_i does not affect the least-squares calculation, because it appears as a factor on both sides of equation 5.4.3..

The standard deviation on parameters at the end of refinement are obtained from

$$\sigma^2(\delta p_j) = \sigma^2(p_j) = \epsilon^2 \cdot N_{jj}$$

(Whittaker and Robinson, 1944), so that

$$\sigma(p_j) = [N_{jj} \sum_{i=1}^{s} W_i \gamma_i^2 / (s-m)]^{\frac{1}{2}} . \qquad (5.4.7.)$$

Cruickshank, 1965 (p.113), underlines the fact that equation 5.4.7. is only correct if the weights have been correctly chosen. If absolute weights have been found – perhaps by repeated observations of each $|F_o|$ – the resulting $\sigma(p_j)$ only cover the random errors associated with this process. Where weights have been chosen to give constant values of $\overline{W\gamma^2}$ taken over ranges of $\sin\theta/\lambda$ or $|F_o|$ (see section 5.5.2.2.) the resulting $\sigma(p_j)$ will cover a larger range of possible errors. It follows from equation 5.4.6. that the expectation value of $\sum_{i=1}^{s} W_i \gamma_i^2$ at the end of refinement is (s-m) if absolute weights have been applied; this provides a test in such a case that the only significant errors are indeed the random experimental ones.

It may happen that the fit of the model to the data is

affected in almost exactly the same way by a change in one parameter as it is by a change in one or more of the other parameters. Such parameters are said to be strongly correlated. In terms of the least-squares equation $\underline{\underline{M}}.\underline{\delta p} = \underline{E}$, correlation arises between p_j and $p_{j'}$ if $M_{ij}/M_{ij'}$ is approximately the same for all i. Since $N_{jj} \propto 1/\det|M|$ (Whittaker and Robinson, 1944), and $\det|M|$ is small under the above conditions, the standard deviation on correlated parameters is higher than on relatively uncorrelated ones. Indeed if $M_{ij}/M_{ij'} \rightarrow$ a constant for all i, then $N_{jj} \rightarrow \infty$ and p_j and $p_{j'}$ cannot be separately determined. The degree of correlation between parameters is estimated by the correlation coefficient

$$\lambda_{ij} = \frac{\text{covariance } (p_i, p_j)}{\sigma(p_i) \cdot \sigma(p_j)}$$

$$= \frac{N_{ij} \cdot \epsilon^2}{(N_{ii} \cdot \epsilon^2 . N_{jj} \epsilon^2)^{\frac{1}{2}}} = \frac{N_{ij}}{(N_{ii} . N_{jj})^{\frac{1}{2}}} . \qquad (5.4.8.)$$

λ_{ij} is thus immediately obtainable from the matrix $\underline{\underline{N}}$. If $\lambda_{ij} = 1$, p_i and p_j are completely correlated: if $\lambda_{ij} = 0$, they are completely uncorrelated.

5.4.2. Refinement

Least-squares refinement of the (010) projection of the AHS structure commenced from the 'difference structure' parameters in table 5.3.1. The data used were the 370 independent reflections in file 4. No further consideration was given at this stage to the appropriateness of the scattering factors; the neutral sulphur and oxygen atom f-curves and the ammonium ion f-curve

were retained. All observations were given unit weight. Anisotropic temperature factor parameters were refined from the thermal parameters given in table 5.3.1. The refinement was performed by a full-matrix least-squares program written by Dr. G.S. Pawley of this Department.

The R-factor fell in one cycle from 28% to 15% (13.5% on the 'strongs' and 26.5% on the 'weaks'). The refined coordinates preserved the size and direction of the atom pair separations found for the 'difference structure', but moved the pairs a little. A further two cycles reduced the R-factor to 11% (9% on the 'strongs' and 19% on the 'weaks').

The matrix of the correlation coefficients was extracted. Correlation between the scale factor and thermal parameters was not high — usually 0.1, and at most 0.3. Otherwise, as expected, the highest correlations appeared between the parameters of atoms which partially overlapped in the (010) projection. None of these was greater than 0.5. The only other correlation coefficients greater than 0.1 appeared between the thermal parameters of each atom: for every atom the β_{11}/β_{33} coefficient was $\sim$0.2. None of these correlations was large enough to suggest that the structure was in any way indeterminate (see section 7.2.). The larger ones, arising from overlap in projection, were expected to be reduced considerably in the three-dimensional refinement.

A final refinement of the projected structure was performed with the file 3 data. Scale factors for the two different zero layer data sets in file 3 (data (1) and data (5) — see appendix 1) were introduced as separate parameters. There were 338 independent observations on SD1 (data (1)) and 374 on SD2 (data (5)).

Absolute weights were applied to the observations with the estimated standard deviations as compiled for file 3. One further cycle with this data decreased the R-factor to 8.5%. This could be broken down as follows:

Data (1)	R-factor
'strong' reflections	5.5%
the same after removing 5 very strong reflections	3.7%
'weak' reflections including $\|F_o\| = 0$	18%
the same excluding $\|F_o\| = 0$	13%
Data (5)	
'strong' reflections	8.2%
the same after removing 6 very strong reflections	5.0%
'weak' reflections including $\|F_o\| = 0$	16.5%
the same excluding $\|F_o\| = 0$	12%

The 'very strong reflections' in each case were those which appeared to suffer from pronounced extinction effects in that $|F_c|$ was much greater than $|F_o|$. For (004) on SD2 the ratio $|F_c| / |F_o|$ was 1.3. The 'weak' reflections included many with intensities too weak to be measured. There was some interest in seeing how much the removal of these affected the R-factor. The overall R-factor was reduced from 8.5% to 7.7% by omitting all these accidentally absent $|F_o|$.

The refined structural parameters were:

Table 5.4.1.

	x	z	β_{11}	β_{22}	β_{31}	
S_1	.124	.222	.004	.013	.001	
O_1	.030	.320	.005	.018	.003	
O_2	.219	.330	.006	.023	-.003	
O_3	.105	.125	.012	.043	.007	
O_4	.145	.060	.010	.015	.005	
N_1	.124	.706	.004	.012	0	with all $\delta p \lesssim \sigma(p)$
S_2	.627	.214	.003	.010	0	
O_5	.533	.322	.005	.015	.003	
O_6	.713	.321	.005	.013	-.003	
O_7	.590	.075	.007	.013	-.003	
O_8	.663	.098	.006	.013	0	
N_2	.625	.700	.005	.009	0	

where the anisotropic temperature factor, W_A, in

$$F_c(h0\ell) = \sum_{\text{unit cell}} f_j \cos 2\pi(hx_j + \ell z_j).W_A \qquad (5.4.9)$$

(compare eqn. 3.5.3.) is given by

$$W_A = \exp[-(h^2\beta_{11} + \ell^2\beta_{33} + 2\ell h\beta_{31})] \qquad (5.4.10.)$$

An F_o-synthesis and difference synthesis of the 'average structure' were computed from the 'strong' data (1) with the signs and $|F_c|$ calculated from the above parameters. The difference synthesis showed several positive regions of height 10 units, and a negative regions of 25 units around the position of the sulphur

atom pair. On the same scale the peak height of the sulphur atom pair in the F_o-synthesis was 750 units. A subsequent difference synthesis calculated with $|F_o| - |F_c|$ set equal to zero for the five very strong reflections had no features above 10 units. It was particularly featureless around the nitrogen positions, suggesting that the NH_4^+ f-curve was adequate.

Attention was now turned to the solution of the full three-dimensional structure of HS.

5.5. Solving and refining the three-dimensional structure

5.5.1. Solving the structure

A survey of the intensity distribution in the first three layers (h1ℓ, h2ℓ, h3ℓ) confirmed the conclusions reached with the photographic data. The intensity distributions

(i)	in (h00), (h20) etc.	h = 8n are very strong
		h ≠ 8n are weak
(ii)	in (h10), (h30) etc.	h = 8n+4 are very strong
		h ≠ 8n+4 are weak
(iii)	in (h1ℓ), (h2ℓ) etc.	h = 4n are strong
		h = 4n+2 are weak
		h odd are intermediate

held at least up to the third layer, although the proportion of the total intensity in the 'weak' reflections (h = 4n+2) did increase from 2% in the first layer to 7% in the third.

From (i) and (ii) it follows that there is a pseudo-n-glide plane, with displacements $\underline{b}/2$ and $\underline{a}/8$, perpendicular to $\underline{c}$ in the three-dimensional structure; from (iii) it follows that

$\rho(x,y,z)$ and $\rho(x + \frac{1}{4},y,z)$ are closely similar even in three dimensions.

Consider first the relatively strongly scattering sulphur atoms. They are known to be situated in special positions in the pseudo-symmetric sub-cell, and may be expected to satisfy the above conditions quite closely. In fig. 5.5.1., one set of symmetrically equivalent sulphur atoms (S_1) is shown O; the other set (S_2) is shown □ . It can be seen that in satisfying the condition $\rho(x,y,z) = \rho(x + \frac{1}{4},y,z)$ by putting A and B at approximately the same height, the pseudo-n-glide planes also arise.

Assuming the SO_4^{2-} ion to be an approximately regular tetrahedron, certain deductions can be made about the y-coordinates of the oxygen atoms. The $S_1 - O_1$, $S_1 - O_2$, $S_2 - O_5$ and $S_2 - O_6$ separations in the (010) projection were found to be between 1.38Å and 1.46Å. The average S – O distance in the SO_4^{2-} ion is given as 1.49Å in the International Tables, 1962, Vol. III, Table 4.1.9. Thus O_1 and O_2, and O_5 and O_6 have about the same y-coordinates as S_1 and S_2 respectively. The approximate disposition of these atoms is illustrated in fig. 5.2.2. in the asymmetric unit containing A and B.

For both N_1 and N_2 the distance to the nearest oxygen atom was about 1.9Å measured in the (010) projection. The average $NH_4^+ - O$ distance for four nearest neighbours, and the average N....O hydrogen bond length are both about 2.9Å (International Tables, 1962, Vol. III, Tables 4.1.1. and 4.1.12.). The maximum separation between a nitrogen atom and a neighbouring oxygen atom is obtained when $y_N = y_O + \frac{1}{2}$. With the b-axis length of 4.6Å,

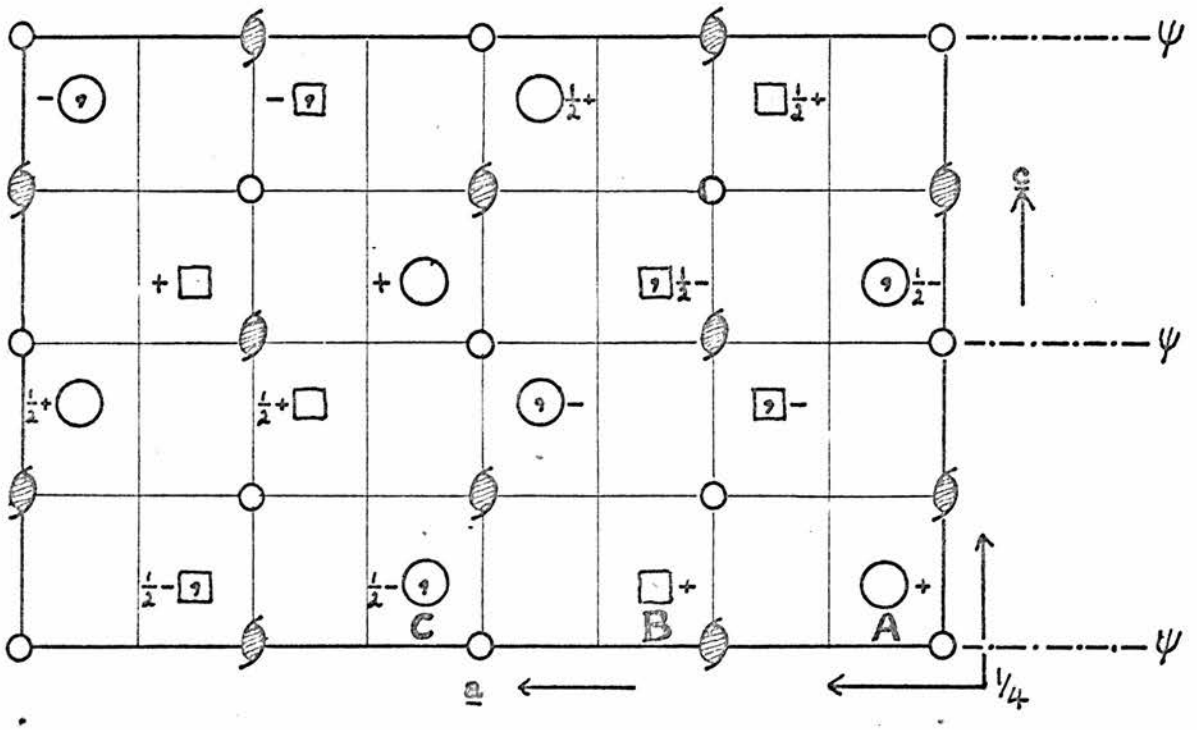

$B2_1/a$ space group elements shown; Z = 16 ; ψ ≡ 'pseudo-'

Fig. 5.5.1.

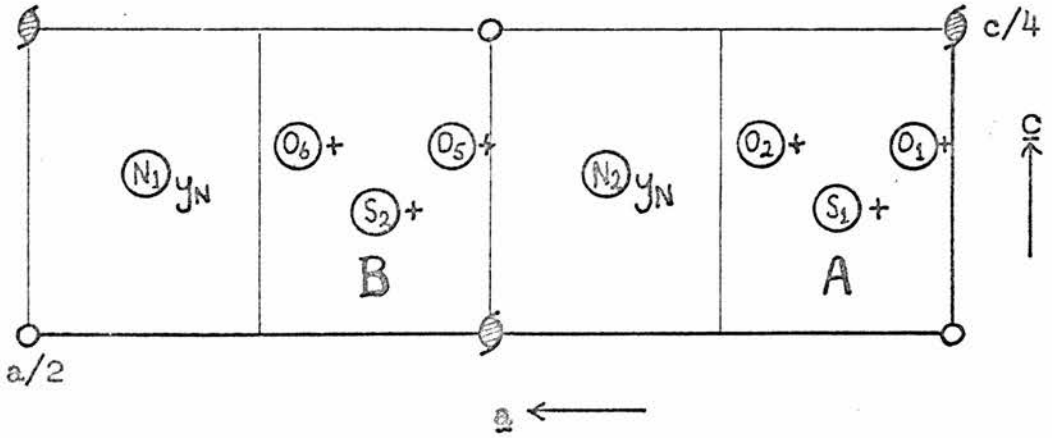

Fig. 5.5.2.

the N – O separation is then 3.0Å – which is close to the expected value. y_N in fig. 5.5.2. may thus be put equal to $\frac{1}{2}+$. With these postulated y-coordinates, S_1, S_2, N_1, N_2, O_1, O_2, O_5 and O_6 all satisfy the pseudo-n-glide plane and the condition $\rho(x,y,z) = \rho(x + \frac{1}{4},y,z)$.

If now the above relationship between the y-coordinates of N and its near-neighbour oxygen atoms be applied to N_1 between B and C (figs. 5.5.1. and 5.5.2.) it is seen that $\frac{1}{2}+$ (the height of N_1) and $\frac{1}{2}-$ (the height of C and its O_1 atom) must differ by 0.5. Hence N_1 is at $y \doteqdot 0.25$ and C is at $y \doteqdot 0.75$. The alternative choice corresponds to a change of origin to $(0,\frac{1}{2},0)$. It follows that S_1, S_2, O_1, O_2, O_5 and O_6 are all at $y \doteqdot 0.75$, and N_1 and N_2 are at $y \doteqdot 0.25$.

There remain the oxygen atoms O_3, O_4, O_7 and O_8. Given the average S – O distance of 1.49Å and the tetrahedral angle of 109°, the average O – O distance in the SO_4^{2-} ion is 2.45Å. O_4 and O_3 were separated in the (010) projection by 0.7Å, and O_7 and O_8 by 0.9Å; their expected separations in the y-direction were thus 2.35Å and 2.28Å respectively. Approximate y-coordinates for these atoms were calculated by taking them to be equally displaced above and below the sulphur atoms at $y \doteqdot 0.75$.

The structure thus deduced is illustrated in fig. 5.5.3.. The two symmetrically inequivalent molecules are shown, in which S_1, S_2, O_1, O_2, O_5, O_6, N_1 and N_2 are all at $y \doteqdot 0.75$. O_3 and O_7 are taken as being at $y > 0.75$, and O_4 and O_8 at $y < 0.75$. This is indicated by the + and - signs. The positions of the symmetrically equivalent sulphur atoms are shown with the relative disposition of the O_3, O_4 and O_7, O_8 atoms indicated

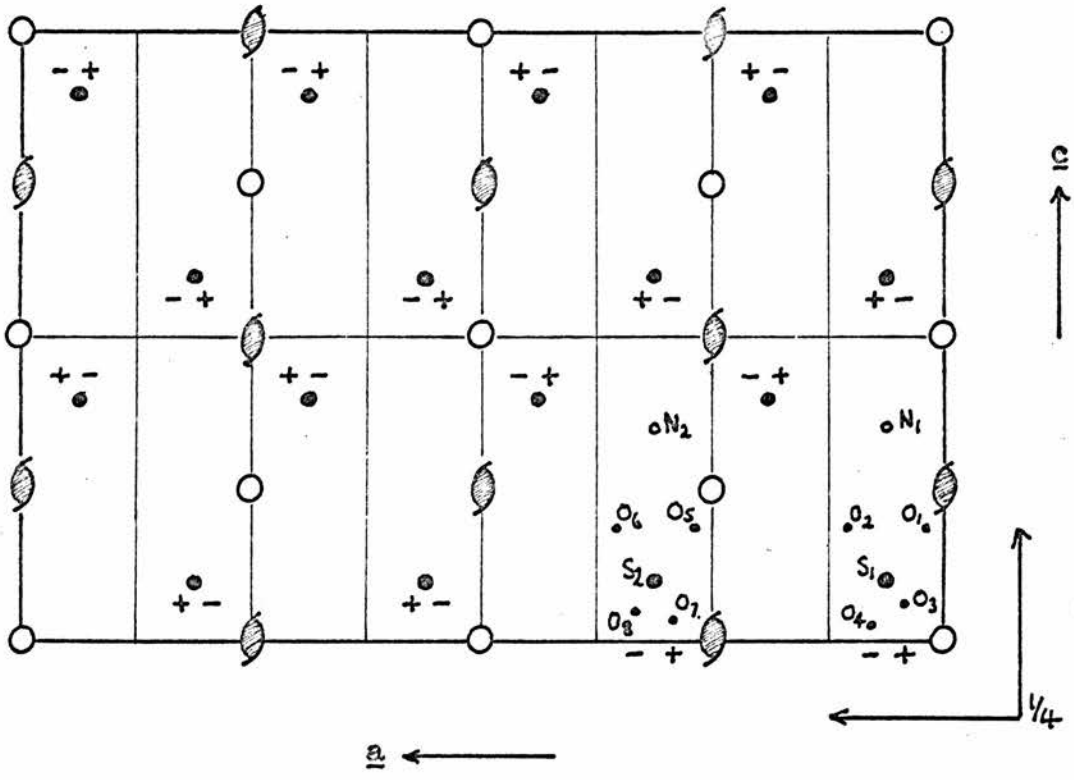

● represents a sulphur atom,

• an oxygen atom, and

○ a nitrogen atom

($B2_1/a$ space group elements are shown)

Fig. 5.5.3.

by + and - signs. This illustrates that these oxygen atoms, while satisfying the condition $\rho(x,y,z) = \rho(x + \frac{1}{4},y,z)$, cannot satisfy the pseudo-n-glide plane. The choice of O_3 and O_7 as being at $y > 0.75$ is arbitrary. The alternative choice of O_4 and O_8 at $y > 0.75$ is equivalent to moving the origin to $(\frac{1}{2},0,0)$.

The program Pangloss was altered to carry out a refinement in three dimensions. As only an approximate refinement was required no alteration was made to incorporate anisotropic temperature factors. The x- and z- coordinates were taken as those found by the least-squares refinement of the (010) projection (table 5.4.1.), and the thermal parameters as those found at the end of the refinement of the 'difference structure' (table 5.3.1.). All these parameters were kept fixed while the y-coordinates, starting from those deduced above, were refined using 156 low angle reflections collected on SD2. The R-factor fell from 30% to 16% in four cycles as the y-coordinates refined thus:

Table 5.5.1.

	initial y	final y		initial y	final y
S_1	.75	.72	S_2	.75	.77
C	.75	.60	O_5	.75	.69
O_2	.75	.70	O_6	.75	.89
O_3	1.03	1.01	O_7	.96	1.02
O_4	.47	.50	O_8	.54	.51
N_1	.75	.63	N_2	.75	.79

The S — O bond lengths in the two SO_4^{2-} ions were calculated to check that reasonable y-coordinates had been found. They were

all ~ 1.5Å. The fit was considered good enough to commence a least-squares refinement of the three-dimensional structure.

5.5.2. Refining the structure

5.5.2.1. The atomic scattering factors

Before starting the refinement some consideration was given to the atomic scattering factors to be used. The f-curves in use at the time were those for the neutral sulphur atom (Dawson, 1960), the neutral oxygen atom (Freeman, 1959) and the rotating ammonium ion (Davis and Whitaker, 1966).

It seemed unlikely that the ammonium ion formed any single stable configuration of bonds to neighbouring oxygen atoms: the latter do not form an even approximately tetrahedral environment. Recent deuteron magnetic resonance work on deuterated AHS found that the ND_4^+ group was in rotation (section 1.7.). The two-dimensional difference map was featureless in the region of the NH_4^+ ion after full refinement with the Davis and Whitaker f-curve. For these reasons it was decided that the latter curve was adequate.

The use of neutral atom f-curves for sulphur and oxygen, however, seemed unrealistic. The SO_4^{2-} ion has several of the outer electrons of all five atoms involved in strong covalent S – O bonds. The negative charge of the ion is expected to be located near the more electronegative oxygen atoms; Pringle and Broadbent, 1965, in refining the structure of sodium hydrogen sulphate monohydrate used an $O^{\frac{1}{2}-}$ f-curve – presumably to allow for this charge location. However, it is clear that the outer electrons of the sulphur and oxygen atoms must be considerably distorted from a spherically symmetric distribution by the strong

S — O valence bonds. The effect of the hydrogen atom included in the actual HSO_4^- ion of AHS could not be estimated without some knowledge of its position. It was expected that the S — O(H) bond would be significantly longer than the S — O bonds of the ion (Cruickshank, 1961).

In the presence of these distortions of the atomic electron density from spherical symmetry it seemed that any attempt to correct for charge redistribution simply by using non-neutral atom f-curves was in fact not realistic. Even if there were a significantly increased charge in the region of the oxygen atoms, the probable errors arising from the use of any spherical atom f-curve would be somewhat larger than those incurred by ignoring this charge increase. Furthermore, any error that could be corrected by a small 'ionisation' of the spherical neutral atom f-curves could be equally well accommodated by changes in the scale factor and the atomic temperature factors. The latter have already been acknowledged to be affected by several other sources of error. It was concluded that, so long as spherical atom f-curves were to be used, there was no significant advantage to be gained in attempting to modify those for the neutral atoms.

It may be remarked here that the problem of treating and refining structures in terms of discreet small molecules or molecular ions (e.g. NH_4^+ and SO_4^{2-}) has recently been investigated by Groenewegen and Feil, 1969. They cite the NH_4^+ f-curves of Webb, 1965, and Davis and Whitaker, 1966, as the only previous attempts to use molecular scattering factors calculated from ab initio molecular wave functions.

The neutral sulphur and oxygen atom f-curves then in use were

checked against those published by Cromer and Mann, 1968. These authors gave no explicit indication of the probable accuracy of their results. However, Doyle and Turner, 1968, independently published atomic scattering factors which agreed with those of Cromer and Mann to within 0.01 electrons for sulphur and 0.003 electrons for oxygen. Doyle and Turner stated that the third, and probably also the second, decimal places of their f-curves had no physical significance. Since both of these independent f-curves agreed with the oxygen one in use to within 0.01 electrons it was left unchanged. There did, however, seem to be significant differences between the 'new' f-curves for sulphur and the one in use. There was a difference of 0.18 electrons at $\sin\theta/\lambda = 0.15$. Although only two other differences were > 0.1 electrons, the majority were > 0.05 electrons – taken at intervals of 0.05 in $\sin\theta/\lambda$ out to $\sin\theta/\lambda = 1.0$. However, the greatest difference was within $\pm 0.5\%$, and no correction was applied at this stage.

The atomic scattering factors discussed above are based on the assumption that there is no dispersion – all the electrons in the atom are taken to scatter with the same amplitude and phase as a free electron. The errors introduced by this assumption may be taken into account by representing the atomic scattering factor, f, as the complex number

$$f = f_o + \Delta f' + i\,\Delta f'' , \qquad (5.5.1.)$$

where f_o is the uncorrected scattering factor, and $\Delta f'$ and $\Delta f''$ are the real and imaginary parts of the dispersion correction (Templeton, 1962). Templeton warns that the tabulated values

of $\Delta f'$ and $\Delta f''$ are subject to errors which cannot be assessed as yet.

For MoKα radiation both $\Delta f'$ and $\Delta f''$ for oxygen and nitrogen are < 0.05 electrons, while for sulphur $\Delta f'$ is 0.1 electrons and $\Delta f''$ is 0.2 electrons. These were all considered negligible in view of the recognised inadequacies of the scattering curves.

5.5.2.2. Refinement

The initial values of $x, y, z, \beta_{11}, \beta_{33}$ and β_{31} for each atom were taken from tables 5.4.1. and 5.5.1., and adjusted to the full cell ($\underline{a} \times \underline{b} \times \underline{c}$). The three-dimensional anisotropic temperature factor, W_A, in

$$F_c(hk\ell) = \sum_{\text{unit cell}} f_j . \cos 2\pi(hx_j + ky_j + \ell z_j) . W_A \qquad (5.5.1.)$$

is given by

$$W_A = \exp[-(h^2\beta_{11} + k^2\beta_{22} + \ell^2\beta_{33} + 2k\ell\beta_{23} + 2\ell h\beta_{31} + 2hk\beta_{12})]. \qquad (5.5.2.)$$

The β_{22} parameters were given the values found by the input of isotropic temperature factor parameters to the two-dimensional least-squares refinement (section 5.4.2.). The β_{23} and β_{12} parameters were given initial values of zero.

The 6500 reflections in file 3 were on three different scales - data (1), data (2) and data (5) (appendix 1). Separate scale factors for data (1) and data (5) had already been obtained in the last stage of the two-dimensional refinement. An initial value for the data (2) scale factor was estimated from the mean 'standard'

intensity of that data set.

With 6500 symmetrically inequivalent observed intensities, derived from the 15,000 recorded profiles, a total of 111 parameters were to be refined: there were three positional and six thermal parameters for each of twelve atoms — continuing to treat the NH_4^+ groups as 'atoms' labelled N_1 and N_2 — and three scale factors. The 6500 observations included repeats in the different data sets of some of the $\sim$4000 symmetrically inequivalent $|F_o(hk\ell)|$ measured. The estimated standard deviation of each $|F_o(hk\ell)|$ was used to give absolute weights to the observations in the least-squares calculation.

Before committing all 6500 observations to the refinement, a preliminary refinement of the y, β_{22}, β_{12} and β_{23} parameters and the scale factor for data (2) was carried out with data selected at random from all three data sets. Then two cycles were performed using all 6500 observations to refine all of the 111 parameters. The R-factor fell from 11.4% to 9.0% (7.0%, excluding the accidentally absent reflections). At this stage a third of the parameters were still changing by more than one standard deviation, and some by three. However, it was decided to do no further refinement (which took 100 minutes for each cycle) until consideration had been given to the treatment of strong reflections affected by extinction and accidentally absent reflections, and to the appropriateness of the weighting scheme.

The three data sets (1), (2) and (5) in file 3 were brought to a common scale, ten times the absolute scale. Each set was multiplied by 10/Sc, where Sc was the scale factor for that set as found in the second cycle above. Weighted means were computed

of structure amplitudes appearing in more than one set. This produced a single set of the 3720 symmetrically inequivalent structure amplitudes with $h \geq 0$, $k \leq 0$ and $\ell \pm$, lying in the range $0° \leq \Theta \leq 35°$. For each such $|F_o(hk\ell)|$ the corresponding standard deviation was calculated. This included the counting statistical error, the stability error as judged from variations in the 'standard' intensity, and the uncertainty in the lost counts correction. The complete data set of $|F_o(hk\ell)|$ and $\sigma\,(|F_o(hk\ell)|)$ will be referred to as file 5.

A computer program, 'weight test', was written to calculate structure factors from the trial structure parameters. The same program computed values of $(|F_o(hk\ell)| - |F_c(hk\ell)|)^2/\sigma^2(|F_o(hk\ell)|)$, or $W\gamma^2$, for each reflection; values of $W\gamma^2$ were summed in ranges of $\sin\Theta/\lambda$ and $|F_o(hk\ell)|$ to investigate the dependence of $\overline{W\gamma^2}$ on these two variables.

The output showed that for the 38 reflections with $|F_o(hk\ell)| > 1100$ (file 5), $|F_c(hk\ell)|$ was greater than $|F_o(hk\ell)|$. This was attributed to extinction effects, and these 38 reflections were removed from the data.

In dealing with accidentally absent reflections the method commonly employed has been to estimate $|F_o(hk\ell)|$ as $\frac{1}{2}F_{lim}$, where F_{lim} is the minimum $|F_o(hk\ell)|$ which could have been detected in that part of the spectrum, and to give each a weight adjusted in accordance with the weighting of other reflections (Cruickshank and Pilling, 1961, p.46). If there are N measurably observed reflections the inclusion of n accidentally absent reflections may be expected to decrease the standard deviation of refined parameters by approximately $[N/(n + N)]^{\frac{1}{2}}$ (loc. cit.).

Very recently, Dunning and Vand, 1969, have pointed out that implicit in this treatment of the accidentally absent reflections is the false premise that the 'true' values of their structure amplitudes are normally distributed about a mean of $\frac{1}{2}F_{lim}$. In fact these reflections are in the region of the tail of the distribution of $|F_o(hk\ell)|$ and their amplitudes should be uniformly distributed. The authors show, both in principle and with an experimental example, that the previous method is incorrect and also that the improvement in parameter standard deviations is illusory.

It is pointed out that when $|F_c(hk\ell)| > F_{lim}$ the experimental observation that $|F_o(hk\ell)| < F_{lim}$ carries information relevant to the refinement. It is suggested that such 'observations' should be included with $|F_o(hk\ell)|$ set equal to zero or F_{lim} and be given a weight

$$W = c(|F_c(hk\ell)|_a - F_{lim})^2. \qquad (5.5.3.)$$

c is an arbitrary constant except that its value is found in practice to affect the rate of convergence. $|F_c(hk\ell)|_a$ is the calculated structure amplitude for an accidentally absent reflection. When $|F_c(hk\ell)|_a < F_{lim}$ no further information can be obtained — the parameters are consistent with the observation that $|F_o(hk\ell)| < F_{lim}$, and the 'observation' should be left out of the refinement. In practice these observations must be left in with small weights, otherwise the refinement oscillates, possibly bringing $|F_c(hk\ell)|_a > F_{lim}$ again. At the end of refinement most $|F_c(hk\ell)|_a$ should be less than F_{lim} and hence have very low weighting. Thus the choice of weights for

these observations should not affect the final result. As has been said, the accidentally absent reflections should be excluded from the calculation of standard deviations of parameters: the fact that the latter satisfy a certain limit carries no further information about their accuracy. The degree to which this limit is satisfied does, however, contribute to the assessment of the agreement between $|F_o(hk\ell)|$ and $|F_c(hk\ell)|$. It is suggested that the usual R-factor should be quoted for the measurably observed $|F_o(hk\ell)|$ alone, together with the proportion of accidentally absent reflections for which $|F_c(hk\ell)| < F_{lim}$.

The authors admit that there are objections in principle to this method in that the suggested weights are not the 'minimum variance' weights required for least-squares refinement and that they depend on $|F_c(hk\ell)|_a$. They have so far achieved only an approximate treatment of the non-normal error distribution involved. However, they found the suggested method to work well in practice; and previous methods are certainly incorrect. The procedures outlined above were adopted initially in the refinement of the AHS structure. Later, in the final refinement discussed in chapter 7, some of Dunning and Vand's method is called into doubt and the procedure modified accordingly.

F_{lim} was estimated at a constant value of 25 for all ranges of $\sin\Theta/\lambda$ by inspection of the listed $|F_o(hk\ell)|$ in file 5. The 435 reflections with $|F_o(hk\ell)|$ recorded as zero were removed from file 5 and listed separately. They were given 'standard deviations' such as to weight then according to the

value of $|F_c(hk\ell)|_a$ (eqn. 5.5.3.). File 5 amended by the removal of strong reflections affected by extinction, and by the separate listing of accidentally absent reflections, will be referred to as file 6.

The initial R-factor for file 6 was 7.1% on the measurably observed reflections, with 62% of the $|F_c(hk\ell)|_a < F_{lim}$. On the first refinement cycle the R-factor increased to 8.7%. $\Sigma_{\text{file 6}} wy^2$ decreased – but chiefly through a decrease in the initially very high contribution from the accidentally absent reflections. The weights of the latter were adjusted according to the new $|F_c(hk\ell)|_a$. In the next cycle most of the relatively large parameter changes of the previous cycle were reversed. The R-factor dropped again to 7.6%, with 66% of $|F_c(hk\ell)|_a < F_{lim}$. It seemed clear that the accidentally absent reflections were too highly weighted and were causing the refinement to oscillate. A further cycle was performed without altering their weights. This gave an R-factor of 7.6%, and 68% of $|F_c(hk\ell)|_a < F_{lim}$.

It seemed that by increasing the percentage of accidentally absent reflections which satisfied the condition $|F_c(hk\ell)| < F_{lim}$ the R-factor for the remainder was increased. This difficulty was overcome in the final refinement (chapter 7) when the weighting for the accidentally absent reflections was changed.

The standard deviations of the observed $|F_o(hk\ell)|$ listed in file 6 took into account the counting statistical error, the stability error estimated from the fluctuations in the 'standard' reflection intensity, and the error in correcting for lost counts. They were expected to be good estimates of the true random errors, and hence to give absolute weights. If absolute weights are

applied the expected value of $\sum_{i=1}^{s} W_i \gamma_i^2$ at the end of refinement is (s-m), where there are s observations and m parameters (section 5.4.1.). For any weighting scheme, values of $\overline{W\gamma^2}$ taken over ranges of, say, $\sin\theta/\lambda$ or $|F_o(hk\ell)|$ should be constant at the end of refinement (Cruickshank, 1965, p.113). Program 'weight-test' obtained the values of $\overline{W\gamma^2}$ in ranges of these two variables. The dependence on $|F_o(hk\ell)|$ was quite flat except for a decrease in $\overline{W\gamma^2}$ for $|F_o(hk\ell)| < 100$. The dependence on $\sin\theta/\lambda$ was less satisfactory; $\overline{W\gamma^2}$ showed a pronounced decrease for $\sin\theta/\lambda > 0.35$ and reached a level near unity at high angles. The latter suggested that the lower angle reflections were relatively over-weighted because, for absolute weights, $\overline{W\gamma^2}$ should be close to unity in all ranges. The apparently pronounced dependence of $\overline{W\gamma^2}$ on $\sin\theta/\lambda$, with its value very much greater than unity except at high angles, is an abiding puzzle in view of the care with which seemingly absolute weights were derived. The use of an incorrect weighting scheme can lead to estimated parameter variances in error by 15% or so, and has strong effects on the scale factor and the thermal parameters; it is less important for positional parameters (Cruickshank, 1965, p.113 and p.115). The weighting scheme was not grossly incorrect, the computer time required to test different schemes was not readily available and the positional parameters were the principal objects of interest. The weights were not changed; but the possible underestimation of parameter variances and the yet further source of error in the thermal parameters are to be noted. The weighting scheme is discussed further in chapter 7: the dependence of $\overline{W\gamma^2}$ on $|F_o(hk\ell)|$ and $\sin\theta/\lambda$ was essentially the same after the last

refinement as it was here, and is illustrated in section 7.2..

The final refinement of the AHS structure from X-ray data is discussed in chapter 7. The final structural parameters and their errors are given there. In order to include the hydrogen atoms in this final refinement, attention was now turned to the location of these atoms from X-ray and neutron diffraction data.

CHAPTER 6

THE HYDROGEN ATOMS

6.1. Introduction

The methods brought to bear on locating the hydrogen atoms in the room-temperature AHS structure, and the results obtained, are discussed.

6.2. Information from the X-ray results

The three-dimensional structure, as refined from the X-ray data, gave the following lengths for the S – O bonds in the two symmetrically inequivalent SO_4^{2-} ions:

Table 6.2.1.

$S_1 - O_1$	1.43 ± 0.01Å	$S_2 - O_5$	1.44 ± 0.01Å
O_2	1.42	O_6	1.44
O_3	1.43	O_7	1.56
O_4	1.55	O_8	1.45

According to Cruickshank, 1961, it is a general rule that in crystals the effect of a hydrogen atom attached to an SO_4^{2-} group is to lengthen the S – O(H) bond with respect to the other S – O bonds. The latter shorten such that the average S – O distance is preserved at 1.49 ± 0.01Å. The bond lengths given

above yield the same average S – O distance for both ions – 1.46 ± 0.01Å for the S_1 ion and 1.47 ± 0.01Å for the S_2 ion. The bonds $S_1 - O_4$ and $S_2 - O_7$ are both lengthened significantly by 0.12Å relative to the other S – O bonds in their respective ions. The above bond lengths compare quite well with those found by Cruickshank, 1961, for the structure of $KHSO_4$, in which the S – O(H) length was 1.56 ± 0.015Å and the average S – O length was 1.49 ± 0.015Å.

It was deduced that the SO_4^{2-} groups were linked along the b-axis direction by the hydrogen bonds

$$O_3 \ldots\ldots H''_9 - O''_4 \qquad \text{and}$$
$$O_7 - H''_{10} \ldots\ldots O''_8 \ .$$

The double prime denotes an atom in a cell adjacent along b to that containing the unprimed atoms. As indicated, the hydrogen atom is asymmetrically placed in each bond, being more closely attached to O''_4 and O_7.

The distances $O_3 \ldots O''_4$ and $O_7 \ldots O''_8$ were calculated to be 2.51 and 2.59 ± 0.02Å respectively. Hamilton, 1962, investigated 22 compounds with O – H ....O bonds in which the oxygen separation r(O ....O) lay in the range 2.49 – 2.90Å. He found the following relationship between the oxygen – hydrogen separation, r(O – H), and r(O ....O),

$$r(O - H) = 1.574 - 0.2145 \ r(O \ldots O) \qquad (6.2.1.)$$

by a least-squares fitting procedure. The standard deviation on a value of r(O – H) obtained from equation 6.2.1. was found to be 0.03Å. From this relationship the distances $O''_4 - H''_9$ and $O_7 - H''_{10}$ were estimated to be 0.99 and 0.98 ± 0.03Å, respectively,

and hence the approximate coordinates of H_9 and H_{10} were found. This information was used later in refining the neutron data (section 6.4.).

No information regarding the hydrogen atoms (H_1, H_2, ...H_8) of the NH_4^+ ions was available beyond the observation that the use of the X-ray scattering factor for a freely rotating ammonium ion gave a featureless two-dimensional difference synthesis in the region of that ion.

6.3. Neutron data collection

6.3.1. Instrumentation and techniques

Data collection from specimen SN was carried out at room-temperature (22.5°C) on the DIDO reactor at A.E.R.E., Harwell. The preparation of SN has been described in chapter 2. The instrument used for data collection was the Hilger and Watts Mk II four-circle diffractometer. This instrument, a prototype to the Mk III model used in the X-ray data collection, was essentially the same in its mode of operation and use.

Some differences of instrumentation and techniques are necessary for the collection of neutron data. The primary beam is a narrow bandwidth selected from the continuous thermal neutron spectrum by a monochromating crystal. Compared with X-ray experiments, the low incident beam flux (10^5 to 10^6 neutrons/cm^2/sec) and the very low absorption of neutrons by most materials, respectively require and allow the use of relatively large specimens; and even then, longer counting times are generally needed to obtain a low counting statistics error. The counter which detects the reflected neutron beam must be

shielded against the γ-ray and fast neutron general backgro nd. The consequently massive construction of the counter compared with those used in X-ray experiments necessitates some reduction in the speed with which the 2θ-shaft is moved. Because of the generally higher counting times this does not constitute an increase in the proportion of 'wasted' time. The total energy liberated in the counter is practically independent of the incident neutron energy, and so different neutron wavelengths cannot be discriminated. The contribution of the $\lambda/2$ component to the primary beam — of peak wavelength λ — is minimised firstly by selecting a moderately high-angle reflection from the monochromator, which reduces the bandwidth reflected, and secondly by setting the monochromator so as to reflect a mean wavelength below that corresponding to the peak of the thermal neutron spectrum. In normal operation, because the intensity of the beam incident on the monochromator fluctuates somewhat, the detecting circuit counts against the collection of a pre-set number of counts by a low-efficiency monitor in the beam from the monochromator — rather than against a pre-set time as in X-ray experiments (Willis and Arndt, 1966, chapters 4 and 7).

The peak wavelength used in data collection from AHS was 1.042Å. The detector was a $^{10}BF_3$ gas-filled proportional counter (see Willis and Arndt, 1966, chapter 4).

Another factor introduced by the use of a monochromating crystal is the 'focusing' or 'defocusing' of the neutron beam as it passes through the monochromator and the specimen. The beam is 'focused' when the 'parallel' arrangement is used, in which

the beam incident on the specimen is reflected back towards the direction of the beam incident on the monochromator. This was the arrangement for the AHS data collection. At a value of 2Θ which depends on the monochromator setting the reflected peak width, as a function of Θ, is independent of the collimation angle of the beam incident on the monochromator. It depends solely on the mosaic spreads of the monochromator and the specimen, and the 'focusing' is a maximum. It is preferable that this condition should be satisfied for the high-angle range of the data to be collected, because it improves the signal-to-background ratio (see Willis and Arndt, 1966, pp.208-212). For the AHS experiment maximum 'focusing' occurred at 2Θ = 90°.

6.3.2. Data collection

The collection of data from SN was performed under less stringent conditions of accuracy than the X-ray data collection described earlier. Specimen SN was not of an ideal shape, volume or quality; but the purpose of the neutron study was the limited one of locating the hydrogen atoms in the (010) projection of the AHS structure. Moreover, the time available was limited to one three-week reactor cycle, with a known average diffractometer breakdown record of at least 25% of the available time.

Checking of the machine alignment was restricted to determining the datum positions of the χ-, ω- and 2Θ-shafts with respect to the directions defined by the incident beam and the normal to the plane in which the counter aperture moved.

Specimen SN was mounted and aligned. The -b-axis was set parallel to the Ø-axis and found to be directed upwards at

machine datum — as in the X-ray experiments. The Ø-datum was adjusted to bring the $-a^*$-axis coincident with the incident beam direction at machine datum. The AHS cell dimensions were confirmed to the extent that reflections appeared at the expected Bragg angles.

The horizontal and vertical dimensions of the beam incident on the specimen could be adjusted by stops on the end of the incident beam collimator nearer the specimen. In collecting (h0ℓ) data the specimen presented maximum horizontal and vertical dimensions of 7mm. and 5mm. respectively. The direct beam was scanned with a slit on the counter 0.2mm. wide and 6mm. high. The profile was flat over a range which could not be increased by opening the horizontal stops further, and which was less than the required width. The stops were finally adjusted to produce a profile which was uniform to within $\pm$5% over a range of 1cm. at the counter. By photographing the beam at the counter and at the specimen position, the equivalent range at the specimen was estimated to be 8mm. Outside this range the profile showed the desirable characteristic of a rapid fall-off — minimising unwanted background.

Having set the horizontal beam stops, the vertical stops were adjusted with reference to photographs of the beam taken at the specimen position. The setting was later tested by recording a reflection with the crystal raised and lowered 1mm. from its central position. The recorded intensity showed a decrease of only 1.5%. Because of the shape and orientation of the crystal and the intention to collect only (h0ℓ) data, it was thought unnecessary to attempt to investigate the variations of

the beam in the vertical direction.

SN was centred carefully at the machine centre. The direct beam was scanned with the longer dimension of the specimen (7mm.) parallel to the incident beam. The absorption peak showed the specimen to be well centred in the incident beam. The centring was invariant under a rotation of 180° about the Ø-axis.

A selection of reflections, spanning the expected range of intensities and the range of Θ to be covered, were scanned. The 'focusing' effect was found to reduce the width of the peak at half-height from 0.40° at low angles to 0.08° at Θ = 50°. Accordingly, the scan width and scan step width were reduced for the higher angle reflections in data collection.

Control-tapes were prepared to collect (h0ℓ) data in two half-layers out to Θ = 55° ($\sin\Theta/\lambda$ = 0.78) — $h^{\pm}$ and $\ell \geq 0$, and the symmetrically equivalent $h^{\pm}$ and $\ell \leq 0$. The programs used were written by M.J.D. Powell and N.A. Curry of A.E.R.E., Harwell. The systematically weak reflections were again collected separately with three times the counting time per step given to the systematically strong reflections. A separate tape was produced to scan a few randomly selected space group absent reflections.

The volume of SN was insufficient to give good 'weak' reflection data in the time available. The above preliminary survey demonstrated that the 'strong' reflections showed the pseudo-mirror plane symmetry found with X-rays, and that the 'weak' reflections were indeed systematically weak. It was concluded that the hydrogen atoms, like the others, were in closely similar positions in the pseudo-symmetric sub-cells (section 3.4.), and

that attention could and should be concentrated on the 'strong' reflections. Accordingly, the scan width of the 'weak' reflections was reduced to a minimum, leaving very little scope for displacement of the peak by specimen mis-setting. One of the half-layers of the 'weak' reflections ($h\bar{+}$, $l \leq 0$) was only collected in the range $0° < \theta < 40°$, and then with only twice the time per step given to the corresponding 'strong' reflections.

As with X-ray data collection a 'standard' reflection was measured at regular intervals. The strong reflection ($\bar{4}02$) was chosen for this purpose.

The counter aperture was kept fully open. This increased the background detected: but it conferred the advantage of being able to tolerate the frequently occurring datum errors of up to 0.15° on the ω- and 2θ-shafts, and also a higher degree of mis-setting of the specimen than was allowed during X-ray work. A 2θ-scan through the ($\bar{4}02$) peak showed that the counter received the full reflected beam over a range of 2° in 2θ.

The orientation of the specimen was checked regularly and corrected when necessary. Throughout the experiment the Ø-datum held its initial setting to within 0.02°. The maximum error found on the goniometer-head arcs was 0.12°.

No direct check was made of the performance or reliability of the counting chains. The 'standard' reflection afforded a check on the combined effects of instability in the counting chains of both the detector and the monitor, and of mis-setting of the specimen. The 'standard' intensity, with a standard deviation of $\pm$1%, showed a maximum long term variation of $\pm$4%. Over a period of a few hours the maximum variation was $\pm$3%.

There seemed no reasonable way of applying a correction for these variations, and there was thus a minimum error of the order of $\pm$4% on all recorded intensities.

Reflections missed because of equipment malfunction or scanned when datum errors were worse than those given above were all re-scanned. Every reflection out to $\Theta = 55°$ was scanned at least once, in one or other of the two half-layers, under acceptable experimental conditions.

6.3.3. Data reduction

The computer program to process the data tapes was written by N.A. Curry of A.E.R.E., Harwell. The diffractometer was used in the mode of operation in which the low-angle background is scanned in five steps, followed by a stepped scan through the peak region and another five step background scan on the high-angle side (see footnote, p.50). The data reduction program produced the integrated intensities corrected for general background by a linear truncation between the averages of the high- and low-angle five step scans. A correction was also applied for the Lorentz factor; in neutron diffraction there is no polarisation effect associated with nuclear scattering (Willis and Arndt, 1966, p.284). When the highest count was less than a pre-set amount above the background level for that reflection, the program made an estimate of the intensity — by a method not explained in the program 'write-up' — and set the standard deviation at one third of this intensity.

The intensities of the randomly selected space group absent reflections were all zero within experimental error, confirming

the glide plane of $B2_1/a$. Of the others there were 380 symmetrically inequivalent reflections out to $\Theta = 55°$. These had been scanned in four groups – the systematically weak and strong reflections separately and in the two ranges $0° < \Theta < 40°$ and $40° \leq \Theta < 55°$. For each group the symmetrically equivalent group had been collected, except for the 'weak' reflections in the range $40° \leq \Theta < 55°$. A total of 690 different reflections had been scanned – some more than once. The data reduction results showed that the intensities of 'weak' reflections with $\Theta \geq 40°$ were not significant. This left a total of 620 reflections comprising 380 'strong' reflections in the range $0° < \Theta < 55°$ and 240 'weak' reflections in the range $0° < \Theta < 40°$. Of the 'strong' reflections, 140 had standard deviations from counting statistics of < 4%: this was true of only 20 of the 'weak' reflections.

The data reduction program produced values of $|F_o(h0\ell)|$ and the counting statistics standard deviation on an arbitrary scale. Weighted means of the structure amplitudes and errors of those reflections scanned more than once were calculated to produce a single list of $|F_o(h0\ell)|$ and $\sigma(|F_o(h0\ell)|)$ for the 620 reflections. Symmetrically equivalent pairs were scrutinised for any significant disagreements. All agreed within a maximum of two standard deviations, with the exception of pairs of 'weak' reflections in which one member was just strong enough to be computed directly from the recorded counts while the other, its highest count being a little smaller, was estimated by the unspecified procedure mentioned above. In such cases the value calculated from the counts was taken. For the remainder a

weighted mean of the symmetrically equivalent $|F_o(hk\ell)|$ was calculated. Thus one set of symmetrically inequivalent observed structure amplitudes was produced comprising 190 'strong' and 120 'weak' reflections.

6.3.4. Errors in the data

The expected errors in the neutron data were considerably greater than those in the X-ray data. The only corrections applied were the linear truncation of the general background and the Lorentz factor.

As has been said, the 'standard' reflections revealed a stability fluctuation of $\pm$4%. The incident beam was not uniform: no correction was applied, though an approximate correction could have been obtained from the measured beam profile. Both the monitor and the detector circuits could operate at 10,000 cps with only a 1% loss (Bunce and Wheeler, 1965). The maximum count rate measured from SN was 150 cps, so counting losses were negligible. Similarly, extinction effects were expected to be small with such weak reflections. No correction was applied for thermal diffuse scattering, which is expected to affect mainly the temperature factors (section 4.7.). No investigation was made of the possibility of multiple reflection effects, though this problem is expected to be greater in neutron diffraction than in X-ray diffraction (Willis and Arndt, 1966, p.251). Quite high absorption was to be expected in AHS, mainly from the very high incoherent scattering cross-section of hydrogen. The linear absorption coefficient for AHS was estimated from the absorption peak in the scan across SN centred in the beam (section 6.3.2.)

as being of the order of $1cm.^{-1}$. The specimen was far from equi-dimensional in the a.c plane – being approximately a rectangle 7mm. by 1.8mm. – and the maximum absorption errors were estimated to be as high as 25%. Nevertheless, the conclusion of Srivastava and Lingafelter, 1966, that absorption errors are almost entirely taken up in the temperature factors, was expected to apply.

The possible errors in the neutron data are seen to be considerable, and not all of known magnitudes. Corrections could in principle be applied for the non-uniformity of the beam, for absorption and, with more work, for thermal diffuse scattering. However, the principle objective was to locate the hydrogen atoms in the (010) projection and it has been argued that their positional parameters should not be strongly affected by the errors discussed. An approximate measure of their accuracy may be obtainable from a comparison of the x- and z-coordinates for the other atoms in the structure as obtained from X-ray and neutron data.

6.4. Neutron data analysis

The 'strong' reflection data was used to locate the hydrogen atoms in the two-dimensional 'average structure'. The techniques of the Pangloss program, F_o-syntheses, difference syntheses, and least-squares refinement were employed.

The sulphur, oxygen, and nitrogen atoms were given the positional and thermal parameters found by X-ray analysis. These parameters were also used to suggest initial positions for the hydrogen atoms, H_9 and H_{10}, linking the SO_4^{2-} ions (section 6.2.).

Scattering lengths for the oxygen, nitrogen and hydrogen nuclei were taken from table 2 of Bacon, 1962. For sulphur the value was taken as that found by E.N. Maslen, 1966 (private communication), and confirmed subsequently by Elcombe and Taylor, 1968. The Neutron Diffraction Commission have recently published an up-to-date table of scattering lengths (N.D.C., 1969). The values given agree with those used, except that the magnitude of the hydrogen scattering length is now reported to be 2% less than previously supposed.

The hydrogen atoms H_9 and H_{10} refined satisfactorily. Some difficulty was experienced with those in the NH_4^+ ions; the data was fitted equally well by a distribution of eight half atoms with isotropic temperature factors (fig. 6.4.1.a.) and by four single atoms with a large thermal anisotropy (fig. 6.4.1.b.).

F_o-syntheses, although showing H_9 and H_{10} clearly, displayed an irregular negative scattering region encircling the nitrogen atoms in the (010) projection. The model illustrated in fig. 6.4.1.b. seemed the more reasonable: there was no reason to suppose that the ammonium ion had just two preferred orientations, and the separation of the hydrogen atoms represented in fig. 6.4.1.a. was larger than expected for superposing atom pairs in the 'average structure' in view of the weakness of the 'weak' reflections.

The positional but not the thermal parameters of the sulphur, oxygen and nitrogen atoms were allowed to refine. At this stage, those 'weak' reflections were introduced into the refinement which had at least one of the pair $|F_o(h0l)|$ and $|F_o(h0\bar{l})|$ with a standard deviation of less than 30%. With this data an attempt

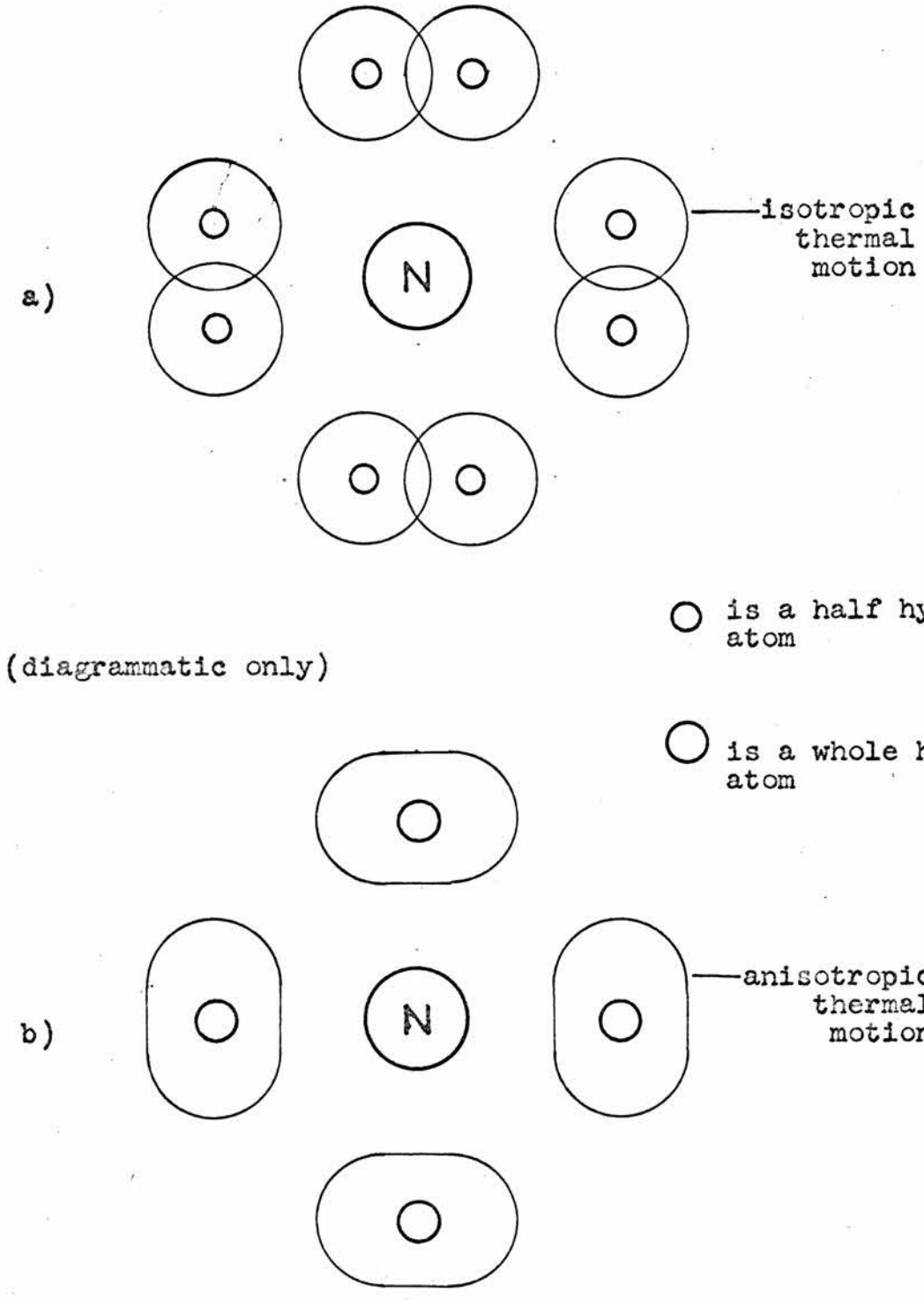
a)
N
isotropic thermal motion
O is a half hydrogen atom
(diagrammatic only)
O is a whole hydrogen atom
b)
N
anisotropic thermal motion

Fig. 6.4.1.

was made to refine the two-dimensional structure. The hydrogen atoms of the two symmetrically inequivalent ammonium ions were given the same initial coordinates except for a mutual displacement of (¼,0,0) – referred to the full unit cell. H_9 and H_{10} were allocated between the two symmetrically inequivalent molecules on the basis of their closeness to the lines joining O_4 and O_3, and O_7 and O_8 in projection. A reasonable fit to these 'weak' reflections was found, refining to R-factors of 13% on the 'strong' reflections and 26% on the 'weak' reflections.

A further least-squares cycle was performed with all the 'weak' data included. The final R-factors were 13% on the 'strong' reflections and 30% on the 'weak' reflections. These could have been reduced by allowing the thermal parameters of the sulphur, oxygen and nitrogen atoms to refine; still further improvement would probably have been accomplished by finding a correct weighting scheme instead of the unit weighting actually used. However, it is doubtful whether any further information of physical significance for the problem in hand could have been gained thereby.

Of the 780 non-self-correlation coefficients between the parameters of the ten symmetrically inequivalent hydrogen atoms, all but six were less than 0.5; these six were less than 0.6. They are not large enough to suggest that any of the parameters were essentially indeterminate (section 7.2.).

An F_o-synthesis and a difference synthesis of the two-dimensional cell were calculated using all the data. The F_o-synthesis showed H_9 and H_{10} well resolved; the difference synthesis was featureless in the regions of H_9 and H_{10}, and showed

only weak detail near three of the remaining hydrogens. The latter tended to support the earlier contention that the model of fig. 6.4.1.a. could not be interpreted as showing the separation of superposing atoms in the 'average structure'. Other features of the difference synthesis were mainly in the vicinity of oxygen atoms.

It was concluded that the positioning of the hydrogen atoms H_9 and H_{10} suggested by the X-ray results was correct, and that the NH_4^+ ions were executing pronounced thermal motion as illustrated diagrammatically in fig. 6.4.1.b..

The refined X-ray and neutron positional parameters of the sulphur, oxygen and nitrogen atoms were compared, firstly to see if any displacement of electron charge in bonds was detectable, and secondly as a possible check on the accuracy of the neutron values. The displacements between the X-ray and neutron positions were:

Table 6.4.1.

	Å		Å
S_1	.01	S_2	.04
O_1	.04	O_5	.04
O_2	.04	O_6	.04
O_3	.02	O_7	.04
O_4	.08	O_8	.08
N_1	.06	N_2	.04

The directions of these displacements were not such that they could be interpreted as arising from bonding effects. The displacements were all attributed mainly to errors in the X-ray

and neutron positional parameters; the errors in the latter were expected to be somewhat greater. The size of the displacements suggested that the calculated standard deviations on the H_9 and H_{10} coordinates – $\pm$0.02Å on both x and z – were probably underestimated. A conservative estimate of $\pm$0.04Å was taken. The refined fractional coordinates of H_9 and H_{10}, referred to the cell $\underline{a} \times \underline{c}$, were:

Table 6.4.2.

	x	z
H_9	.066 $\pm$ .002	.053 $\pm$ .003
H_{10}	.313 $\pm$ .002	.049 $\pm$ .003

Otherwise the results of the neutron experiment were interpreted qualitatively. The actual values for the positional parameters of H_1, H_2.... H_8, and the thermal parameters of all the hydrogen atoms are of doubtful physical significance. They are not quoted.

6.5. Other information on the hydrogen atoms

6.5.1. The hydrogen bonds: neutron results

The refined positions of H_9 and H_{10} in the (010) projection (table 6.4.2.) lie significantly off the lines joining O_3 and O_4'', and O_7 and O_8''. Hamilton, 1962, pointed out that although the hydrogen bond is generally assumed to be linear, and the closeness of X–H.... X bond angles to 180° in a large number of compounds tends to support the hypothesis that the linear bond is energetically the most favourable, it is not a strict

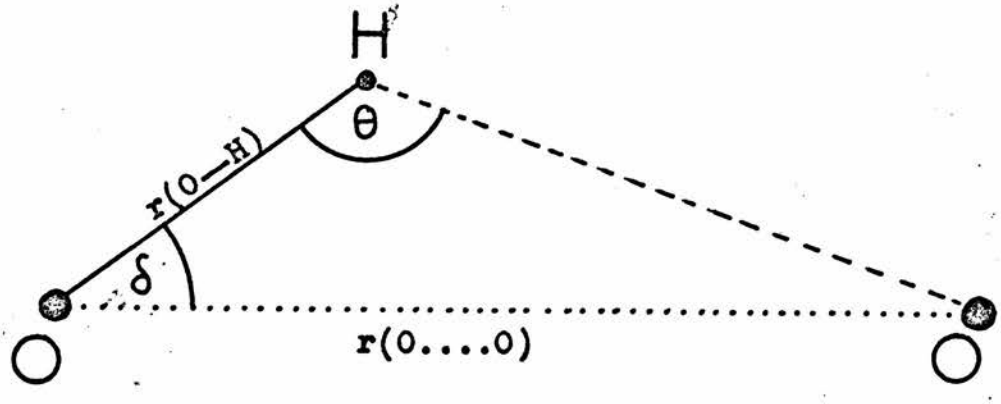

Fig. 6.5.1.

requirement. With data from the same 22 O — H.... O bonds as he used to obtain the relationship between r (O — H) and r (O....O) (eqn. 6.2.1.), Hamilton found the following relationship between Θ(O — H....O) (see fig. 6.5.1.) and r (O....O),

$$\Theta(O - H....O) = 277.7 - 40.08\ r\ (O....O)\ . \qquad (6.5.1.)$$

The least-squares calculation gave a standard deviation of 6° on any value of Θ derived from this relationship. From equation 6.5.1. and the known values of r (O....O), the expected values of $\Theta(O_3....H''_9 - O''_4)$ and $\Theta(O_7 - H''_{10}....O''_8)$ were obtained as 177 ±6° and 174 ±6° respectively.

More recently Chidambaram and Sikka, 1968, took up a comment made by Hamilton, 1962, that the bending of hydrogen bonds is evidence that the energy of bending of these bonds is comparable with the energy gains available from, say, favourable van der Waals packing in the crystal. They argued that there is no physical significance in the suggestion embodied in equation 6.5.1. that there is a favoured bonding angle for each particular r (O....O) — which they felt must always be 180° in the absence of other effects — but that it gives an indication of the bending that can be tolerated for that r(O....O). They showed values of δ (fig. 6.5.1.) for r(O....O) in the range 2.4 to 3.0Å. These were obtained from 100 independent O — H....O bonds occurring in 35 compounds studied by neutron diffraction. It was clear that the range of δ increased linearly with increasing r(O....O). The points were more concentrated near a line which bisected this

range – a line close to that found by Hamilton – but there were bonds with $\delta \leq 1°$ up to oxygen separations, $r(O....O)$, of 2.9Å. With the known $r(O_3....O_4'')$ and $r(O_7....O_8'')$ the expected range of δ for $O_3....H_9'' - O_4''$ and $O_7 - H_{10}'' .... O_8''$ were obtained as 0° – 7° and 0° – 9° respectively.

Combining the $r(O....O)$ distances found from X-ray results, the estimated $r(O - H)$ distances (section 6.2.), and the x- and z-coordinates and standard deviations for H_9 and H_{10} found in the neutron studies, the following results were obtained:

Table 6.5.1.

	$\Theta_{expected}$	$\Theta_{observed}$	$\delta_{expected}$	$\delta_{observed}$
$O_3.... H_9'' - O_4''$	177 ± 6°	164 ± 5°	0° – 7°	10 ± 3°
$O_7 - H_{10}''.... O_8''$	174 ± 6°	168 ± 4°	0° – 9°	7.5 ± 2°

It appears that the H_{10} bond is in agreement both with the expected mean Θ value from equation 6.5.1. and with the expected range of δ. The H_9 bond does not agree with the expected mean Θ within one standard deviation and seems to show a significantly high value of δ. This may indicate an unusually bent bond. Otherwise, the error on the H_9 position is higher than estimated; this could be caused by the relatively strong correlation between the positional parameters of H_9, O_3 and O_4 (which overlap more in the (010) projection than do H_{10}, O_7 and O_8).

The estimated positions of H_9 and H_{10}, as calculated above, yielded an estimate of their y-coordinates. Including these estimates, their fractional coordinates, referred to the full

cell, were:

Table 6.5.2.

	x	y	z
H_9	.066	.298	.053
H_{10}	.313	.207	.049

6.5.2. Difference syntheses and the X-ray data

The program used earlier to calculate F_o-syntheses and difference syntheses in two dimensions was extended to perform three-dimensional calculations with the X-ray data. The structural parameters used were those reached in the refinement of the file 6 data (section 5.5.2.2.). Values of $F_c(hk\ell)$ were calculated for all reflections in file 6 in the range $0 < \sin\theta/\lambda < 0.5$ $\mathring{A}^{-1}$. Three-dimensional difference syntheses were computed from these $F_c(hk\ell)$ and the corresponding $|F_o(hk\ell)|$. There were 740 reflections ($h \geq 0$, $k \leq 0$, $\ell^{\pm}$) in the given range. The $\sin\theta/\lambda$ limitation could be made because the principal objective was to look for hydrogen atoms. Although there is significant scattering from hydrogen beyond $\sin\theta/\lambda = 0.5$ $\mathring{A}^{-1}$ (see fig. 7.2.1.) it represents a small proportion of that below this value, and it is a common practice to terminate at $\sin\theta/\lambda = 0.5$ $\mathring{A}^{-1}$ the data used to look for hydrogen atoms in X-ray difference syntheses (see, for example, Liminga, 1968; Nahringbauer, 1968).

The program calculated

$$\rho(xyz) = \frac{2}{sc.V} \sum_{\substack{h\geq 0,\\ k\leq 0, l\pm}} F(hk\ell)\,[\cos 2\pi(hx+ky+\ell z)+\cos 2\pi(hx-ky+\ell z)]. \qquad (6.5.2.)$$

sc is the scale factor required to bring $|F_c(hk\ell)|$ to the same scale as $|F_o(hk\ell)|$, V is the volume of the unit cell, and $F(hk\ell)$ is $F_o(hk\ell)$ $\left[\text{i.e. } F_o(hk\ell) \times (\text{sign of } F_c(hk\ell))\right]$ for an F_o-synthesis and $(F_o(hk\ell) - F_c(hk\ell))$ for a difference synthesis. Hence $\rho(xyz)$ was given in electrons per cubic angstrom. F_o-syntheses were computed to test the program. They showed atoms at the expected positions with correct electron densities.

Difference syntheses of the regions containing the two symmetrically inequivalent SO_4^{2-} groups showed the following features:

i) at the positions of both sulphur atoms there were peaks containing about -0.3el. (electrons): this suggested that the scaling was slightly in error, probably because some $|F_o(hk\ell)|$ reduced by small extinction effects were still included;

ii) the oxygen atoms O_1, O_2 and O_4 had associated with them weak positive peaks ($\sim$0.15el.) and much weaker negative peaks. O_3 showed larger discrepancies, with a positive peak, at the same height as the atom but displaced from its x- and z-coordinates towards those of S_1, of $\sim$ 0.2el., and also a negative peak of $\sim$ 0.1el.;

iii) in the region of each of O_5, O_6, O_7 and O_8 there were positive peaks containing about 0.1 el.;

iv) at the same height as S_2, but displaced from its x- and z-coordinates towards those of O_5, was a positive peak of ~0.2 el.;

v) significant peaks containing ~0.25 el. appeared near the expected H_9 and H_{10} positions: these hydrogen positions were between SO_4^{2-} groups along b and there were no other features of a comparable magnitude in these regions of the unit cell.

The fractional coordinates of the centres of the H_9 and H_{10} peaks estimated from the difference syntheses were:

Table 6.5.3.

	x	y	z
H_9	.072	.299	.056
H_{10}	.316	.185	.052

These are to be compared with those given in tables 6.4.2. and 6.5.2.. The difference syntheses may be expected to show a maximum electron density close the positions of the protons (Lipson and Cochran, 1966, p.352). It will be seen that the H_{10} x- and z-coordinates obtained here agree with those found from the neutron diffraction data to within two standard deviations on the latter values; the x- and z-coordinates of H_9 found here agree within one standard deviation on z but disagree significantly on x. However, the positions of the peaks in the difference syntheses which were identified with these hydrogen atoms may be somewhat in error. They were not far from peaks of a comparable magnitude arising from inadequacies in the parameters of the other atoms. No meaningful comment can be

made on the agreement between the estimated y-coordinates (table 6.5.2.) and those found here.

The difference syntheses thus showed significant peaks very close to the H_9 and H_{10} positions expected from other information. They were the only significant peaks in those regions of the difference syntheses. These peaks had a low electron content of $\sim$0.25 el.. This may be significant; it may indicate that much of the hydrogen electron cloud is located in the region of the attached oxygen and has been partially accounted for both by a small shift of that atom and by a change in its thermal parameters. Otherwise, the low electron content may, possibly, arise from the failure to include the relatively small contribution from $\sin\theta/\lambda > 0.5$ $\mathring{A}^{-1}$, and a superposition of any negative peaks caused by inadequacies in the parameters of adjacent oxygen atoms.

Difference syntheses were also computed for the regions containing the two symmetrically inequivalent NH_4^+ ions. These syntheses showed weak peaks, both positive and negative, containing $\sim$0.05 el., in a region corresponding to the extent of the nitrogen atom. They were otherwise featureless. This result gave further support to the contention (section 5.5.2.1.) that the NH_4^+ ion scattering factor was adequate, to the resolution of the data used, and hence was in accord with the conclusion of the neutron study, and other work (section 5.5.2.1.), that the ion was in rotation.

There was, then, qualitative agreement between the X-ray and neutron results concerning the nature of the NH_4^+ ion motion. The X-ray data afforded good quantitative agreement with the

positions of H_9 and H_{10} deduced from neutron work. It was now possible to proceed to a final refinement of the X-ray data (file 6) with H_9 and H_{10} included.

CHAPTER 7

THE ROOM-TEMPERATURE STRUCTURE OF AMMONIUM HYDROGEN SULPHATE

7.1. Introduction

In this concluding chapter the results of chapters five and six are drawn together in a final structure refinement with the X-ray data. The structure is described and discussed. The future work required to elucidate the nature of the ferroelectric transition is outlined in relation to some other recent work on similar ferroelectrics.

7.2. The final refinement

7.2.1. Refinement

Structure refinement with the file 6 X-ray data proceeded from the point reached at the end of chapter 5. The hydrogen atoms, H_9 and H_{10}, linking SO_4^{2-} groups along b were included with the initial positional coordinates found from X-ray difference syntheses (table 6.5.3.). They were each given an initial isotropic temperature factor parameter of 2.5 $\AA^2$.

The hydrogen atom scattering factor used was that published by Stewart et al., 1965, (fig. 7.2.1.). Jensen and Sundaralingam, 1964, pointed out that, using a free hydrogen atom f-curve, the amplitudes of thermal motion of bonded hydrogen

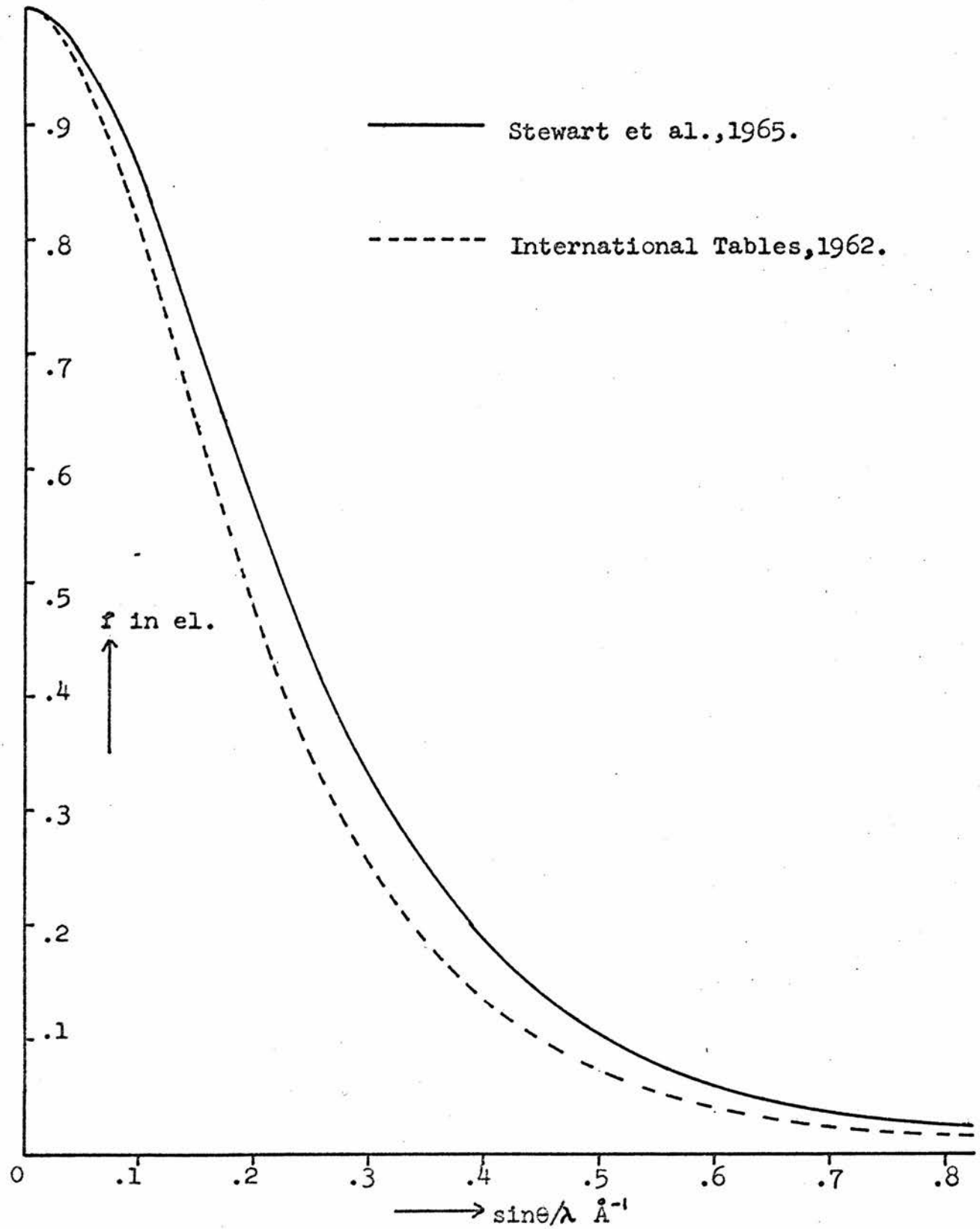
Stewart et al.,1965.
International Tables,1962.
f in el.
.9
.8
.7
.6
.5
.4
.3
.2
.1
0
.1
.2
.3
.4
.5
.6
.7
.8
sinθ/λ Å⁻¹

Fig. 7.2.1.

atoms in well determined structures appeared to be spuriously low – suggesting that the electron cloud is more localised than in the free atom. Mason and Robertson, 1965, reported similar conclusions and a least-square refinement of an experimental f-curve for bonded hydrogen. Stewart et al. (loc. cit.) derived their scattering factor analytically for the hydrogen atom in the hydrogen molecule. This f-curve is currently accepted as the best available from the point of view of obtaining reasonable thermal parameters (G.B. Robertson, 1968, private communication; L.H. Jensen, 1968, private communication; Hamilton and La Placa, 1968). However, least-squares refinement will always place the hydrogen atom closer to the atom to which it is bonded than the corresponding nuclear separation, unless non-spherical scattering factors are used (Stewart et al. (loc. cit.); Hamilton and La Placa (loc. cit.)). This is, of course, just an extreme case of a problem presented by the outer, bonding electrons of all atoms. Inadequacies in the representation of these electrons for the other atoms in the structure may contribute to the displacement of the hydrogen atoms.

The same oxygen atom and ammonium ion scattering factors were used as previously; the sulphur atom scattering curve was replaced by that published by Cromer and Mann, 1968, (see section 5.5.2.1.).

The first least-squares cycles showed, as expected, that the parameters for S_1, S_2, O_1, O_2, O_5, O_6 and the ammonium ions were not significantly affected by the inclusion of H_9 and H_{10}. The largest changes appeared in the positional and thermal parameters of O_4 and O_7 – to which these hydrogen atoms are more strongly

bonded in the two hydrogen bonds. The other members of these bonds, O_3 and O_8, showed a significant change only in their y-coordinates. The thermal parameters of both hydrogen atoms became absurdly high. This was interpreted as an indication that, in agreement with the features of the difference syntheses (section 6.5.2.), the occupancy of the hydrogen atom sites was less than unity.

An attempt was made to refine the occupancy and the thermal parameter of each hydrogen atom. This proved to be as difficult as expected in view of the high correlation between these two parameters. The final values obtained were:

Table 7.2.1.

	Occupancy	B in $\AA^2$
H_9	0.6 ± 0.1	3.5 ± 1.0
H_{10}	0.7 ± 0.1	3.0 ± 1.0

It appeared that the weights previously given to the accidentally absent reflections were too high (section 5.5.2.2.). They were reduced so that $\overline{w\gamma^2}$ for these reflections lay on the extrapolated curve of $\overline{w\gamma^2}$ against $|F_o(hk\ell)|$ produced by 'weight-test' (section 5.5.2.2.). Furthermore, the procedure whereby the weights for these reflections were made dependent on $|F_c(hk\ell)|$ (eqn. 5.5.3.) was discontinued. It is, in principle, incorrect: the value of $|F_o(hk\ell)|$ might be subject to an unsuspected error, and $|F_c(hk\ell)|$ itself might carry a particularly high model-dependent error. It remains acceptable that the criterion should be that

as many as possible of the $|F_c(hk\ell)|_a$ should be less than F_{lim} (section 5.5.2.2.). The procedure adopted was to give a very low weight to those reflections for which $|F_c(hk\ell)|_a$ was less than F_{lim} and a constant weight of the order of F_{lim}^{-2} – but adjusted as described above – to those for which $|F_c(hk\ell)|_a$ was greater than F_{lim}.

To ascertain whether the data still included reflections significantly affected by extinction, $|F_o(hk\ell)|$ for the strongest reflections in file 6 were compared with the corresponding $|F_c(hk\ell)|$ at the end of the previous least-squares cycle. The calculated amplitudes were not systematically stronger, and none of the reflections in file 6 was removed from the refinement.

The refinement was continued until δp_j was less than $\sigma(p_j)$ for all j. The R-factor, excluding the accidentally absent reflections, was 6.9%; 72% of the $|F_c(hk\ell)|_a$ were less than F_{lim}.

The final values of the structural parameters are given in table 7.3.1.. The complete list of $|F_o(hk\ell)|$, and $F_c(hk\ell)$ at the end of refinement, is given in appendix 4.

7.2.2. The weighting scheme

The weighting scheme for this refinement and the general problem of selecting a correct scheme were discussed in section 5.5.2.2.. The dependence of $\overline{w\gamma^2}$ at the end of refinement on $\sin\theta/\lambda$ and on $|F_o(hk\ell)|$ are illustrated in fig. 7.2.2.. Both are unsatisfactory: but the dependence on $|F_o(hk\ell)|$ is quite flat except at low values of $|F_o(hk\ell)|$ – which is

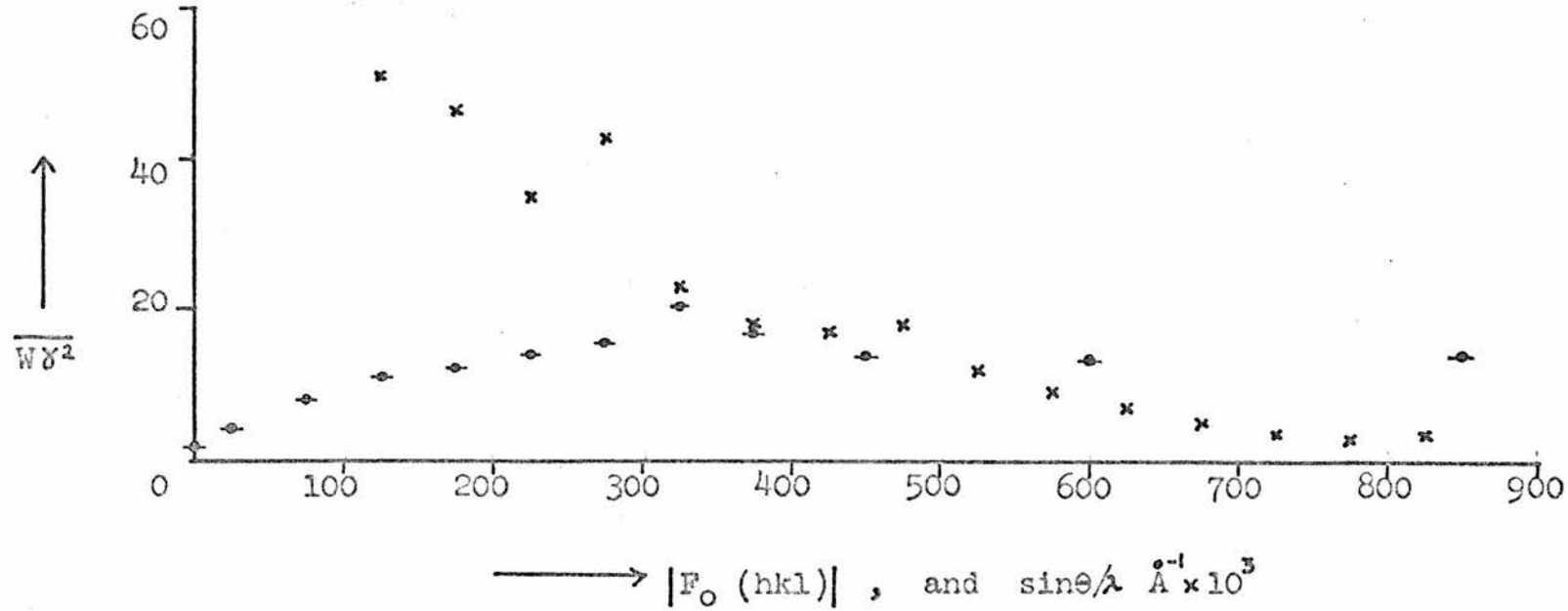

-⊕- show the dependence of $\overline{W\gamma^2}$ on $|F_o\ (hkl)|$

× show the dependence of $\overline{W\gamma^2}$ on $\sin\theta/\lambda$

Fig.7.2.2.

probably a reflection of the relatively low weighting given to the high-angle data. One may conclude that the weighting depends mainly on $\sin\Theta/\lambda$. In such circumstances, as has been said already (section 5.5.2.2.), the effects will be taken up almost entirely in the atomic temperature factors.

The final value of $\sum_{i=1}^{s} W_i \gamma_i^2/(s-m)$ was 9.5. For absolute weights it is expected to have a value close to unity. The discrepancy remains a puzzle.

7.2.3. The correlation matrix

The matrix of correlation coefficients between the 117 structural parameters (the six thermal and three positional parameters for the two sulphur atoms, the eight oxygen atoms and the two NH_4^+ ions, the one thermal and three positional parameters for the two hydrogen atoms, and the scale factor) was extracted after each cycle. The coefficients involving the occupancies and the thermal parameters of the two hydrogen atoms were found in a separate refinement. Most of the 7021 non-self-correlation coefficients were < 0.05: 83 were > 0.2 and are listed in table 7.2.1.. The following comments are made:

i) there is the expected high correlation between the scale factor and principal thermal parameters (β_{11}, β_{22} and β_{33}) - particularly those of the sulphur atoms;

ii) eighteen of those listed are between the corresponding parameters of atoms related by the pseudo-symmetry (see section 1.5.): with one exception the parameters involved are all x,z, β_{11}, β_{33} and β_{31} - reflecting the closer pseudo-symmetry in the (010) projection;

Table 7.2.1. (Continued overleaf)

[Sc = scale factor; Occ = occupancy; λ = correlation coefficient]

p_i/p_j	λ_{ij}	p_i/p_j	λ_{ij}	p_i/p_j	λ_{ij}	p_i/p_j	λ_{ij}
$Sc/\beta_{11}S_1$	.4	zO_2/zO_6	.3	$\beta_{11}O_4/\beta_{31}O_4$	.3	$\beta_{32}O_7/zH_{10}$	-.4
$Sc/\beta_{22}S_1$	.4	$\beta_{11}O_2/\beta_{22}O_2$	.2	$\beta_{11}O_4/yH_9$	.3	$\beta_{12}O_7/BH_{10}$	.2
$Sc/\beta_{33}S_1$	.4	$\beta_{11}O_2/\beta_{33}O_2$	.2	$\beta_{22}O_4/\beta_{33}O_4$	-.2	$\beta_{12}O_7/xH_{10}$	-.3
$Sc/\beta_{11}S_2$	.5	$\beta_{22}O_2/\beta_{23}O_2$	.2	$\beta_{22}O_4/BH_9$	.3	$\beta_{12}O_8/\beta_{33}O_8$	-.2
$Sc/\beta_{22}S_2$	.5	$\beta_{31}O_2/\beta_{31}O_6$	.3	$\beta_{33}O_4/\beta_{31}O_4$	.3	xN_1/xN_2	.3
$Sc/\beta_{33}S_2$	.5	xO_3/zO_3	.2	$\beta_{33}O_4/zH_9$	-.4	zN_1/zN_2	.3
$Sc/\beta_{22}O_6$	.2	$\beta_{11}O_3/\beta_{31}O_3$	.3	$\beta_{23}O_4/\beta_{12}O_4$	.2	$\beta_{11}N_1/\beta_{22}N_1$	-.2
$Sc/\beta_{11}O_8$	.2	$\beta_{22}O_3/\beta_{23}O_3$	.2	$\beta_{23}O_4/zH_9$	.3	$\beta_{11}N_1/\beta_{33}N_1$	-.3
xS_1/xS_2	.2	$\beta_{22}O_3/\beta_{12}O_3$	.2	$\beta_{23}O_4/BH_9$	-.3	$\beta_{33}N_1/\beta_{33}N_2$	.3
zS_1/zS_2	.3	$\beta_{33}O_3/\beta_{31}O_3$	.3	$\beta_{11}O_5/\beta_{33}O_5$	-.2	$\beta_{31}N_1/\beta_{31}N_2$	.2
$\beta_{11}S_1/\beta_{11}S_2$	.2	$\beta_{23}O_3/\beta_{12}O_3$	.2	$\beta_{11}O_6/\beta_{31}O_6$	-.3	$\beta_{11}N_2/\beta_{22}N_2$	-.2
$\beta_{22}S_1/\beta_{22}S_2$	.2	xO_4/zO_4	.2	xO_7/xH_{10}	-.3	$\beta_{11}N_2/\beta_{33}N_2$	-.3
$\beta_{33}S_1/\beta_{33}S_2$	.3	$xO_4/\beta_{12}O_4$	-.2	xO_7/yH_{10}	.3	$OccH_9/BH_9$	.8
xO_1/xO_5	.3	xO_4/xH_9	-.5	xO_7/BH_{10}	.2	$OccH_9/OccH_{10}$	.7
zO_1/zO_5	.3	yO_4/yH_9	.3	yO_7/xH_{10}	.3	$OccH_9/BH_{10}$	.5
$\beta_{11}O_1/\beta_{22}O_1$	-.2	yO_4/zH_9	-.2	yO_7/yH_{10}	.2	yH_9/yH_{10}	-.3
$\beta_{11}O_1/\beta_{33}O_1$	-.2	yO_4/BH_9	-.3	yO_7/BH_{10}	.3	zH_9/zH_{10}	.3

Table 7.2.1. Contd.

p_i/p_j	λ_{ij}	p_i/p_j	λ_{ij}	p_i/p_j	λ_{ij}	p_i/p_j	λ_{ij}
$\beta_{22}O_1/\beta_{12}O_1$	-.2	zO_4/yH_9	-.3	zO_7/zH_{10}	-.5	$BH_9/OccH_{10}$	.5
$\beta_{33}O_1/\beta_{31}O_1$	.2	zO_4/zH_9	-.2	$\beta_{11}O_7/xH_{10}$	-.3	BH_9/BH_{10}	.5
$\beta_{31}O_1/\beta_{31}O_5$	.2	zO_4/BH_9	.3	$\beta_{22}O_7/xH_{10}$	.2	$OccH_{10}/BH_{10}$	.8
xO_2/xO_6	.4	$\beta_{11}O_4/\beta_{22}O_4$	-.3	$\beta_{32}O_7/\beta_{12}O_7$	-.2		

$\beta_{11}S_1$ = β_{11} parameter of atom S_1; xS_1 = x parameter of S_1, etc.

iii) there are high correlations between the positional and thermal parameters of H_9 and O_4, to which H_9 is 'attached': the same is true of H_{10} and O_7;

iv) apart from the correlation between the occupancies and thermal parameters of the hydrogen atoms no coefficient is greater than 0.5 in magnitude: all but 12 are 0.3 or less;

v) in view of the argument often put forward that although many sources of error reside in the thermal parameters the positional parameters are little affected, it is worthy of note that apart from hydrogen atom parameters there is only one listed case of correlation between a positional and a thermal parameter.

When refinement has proceeded by a full-matrix least-squares method the parameter standard deviations, $\sigma(p)$, include the effects of correlation; the importance of an examination of the correlation matrix lies in gaining confidence that the refined structure is as well determined as it appears to be. As discussed in section 1.5., it is possible for a structure to have a low R-factor and yet be essentially indeterminate because of high parameter interaction. In such cases, however, correlation coefficients have been of the order of 0.8 – 1.0 (Geller, 1961). The correlation coefficients found for AHS do not suggest that the structure is in any way indeterminate. Pseudo-symmetry does not appear to have produced the problems in AHS that it did in $BaTiO_3$ and GASH (Geller, 1961).

7.2.4. Difference syntheses

The difference syntheses computed to look for hydrogen atoms (section 6.5.2.) were re-calculated. $F_c(hk\ell)$ were computed from

the parameters at the end of the refinement (table 7.3.1.). As before, only data out to $\sin\theta/\lambda = 0.5$ Å^{-1} was used. These syntheses showed peaks closely similar to those found before except that the two identified with H_9 and H_{10} were now absent.

A difference synthesis of the whole asymmetric unit, $\underline{a}/4 \times \underline{b} \times \underline{c}/2$, was prepared using all the data. Although the features of this synthesis were broadly the same as those found above, there were more minor peaks and the principal peaks were stronger. This was to be expected: higher angle data is generally less accurate and, more importantly, small inadequacies of the structural model – in its refined parameters and assumed scattering factors – will show up mainly in the high-angle $F_c(hk\ell)$. Pertinent features of this synthesis were:

i) that the peaks identified with H_9 and H_{10} in the earlier syntheses were still absent, confirming that the principal contributions to these peaks had come from data below $\sin\theta/\lambda = 0.5$ Å^{-1};

ii) both sulphur atoms lay on moderate negative peaks – probably indicating a small scale factor error caused by the inclusion of reflections slightly affected by extinction;

iii) both ammonium ions were in regions of only weak features even with the high-angle data included;

iv) some mis-placing of oxygen atoms was apparent: O_3 was on a strong gradient, O_4 on a slightly less strong gradient and O_2 on a weak gradient; the remainder were associated with relatively very weak features.

In relation to (iv) it may be remarked that O_3 and O_4 were the only atoms listed in table 7.2.1. as showing a significant correlation between their positional parameters: $\lambda(xO_3/zO_3)$ and

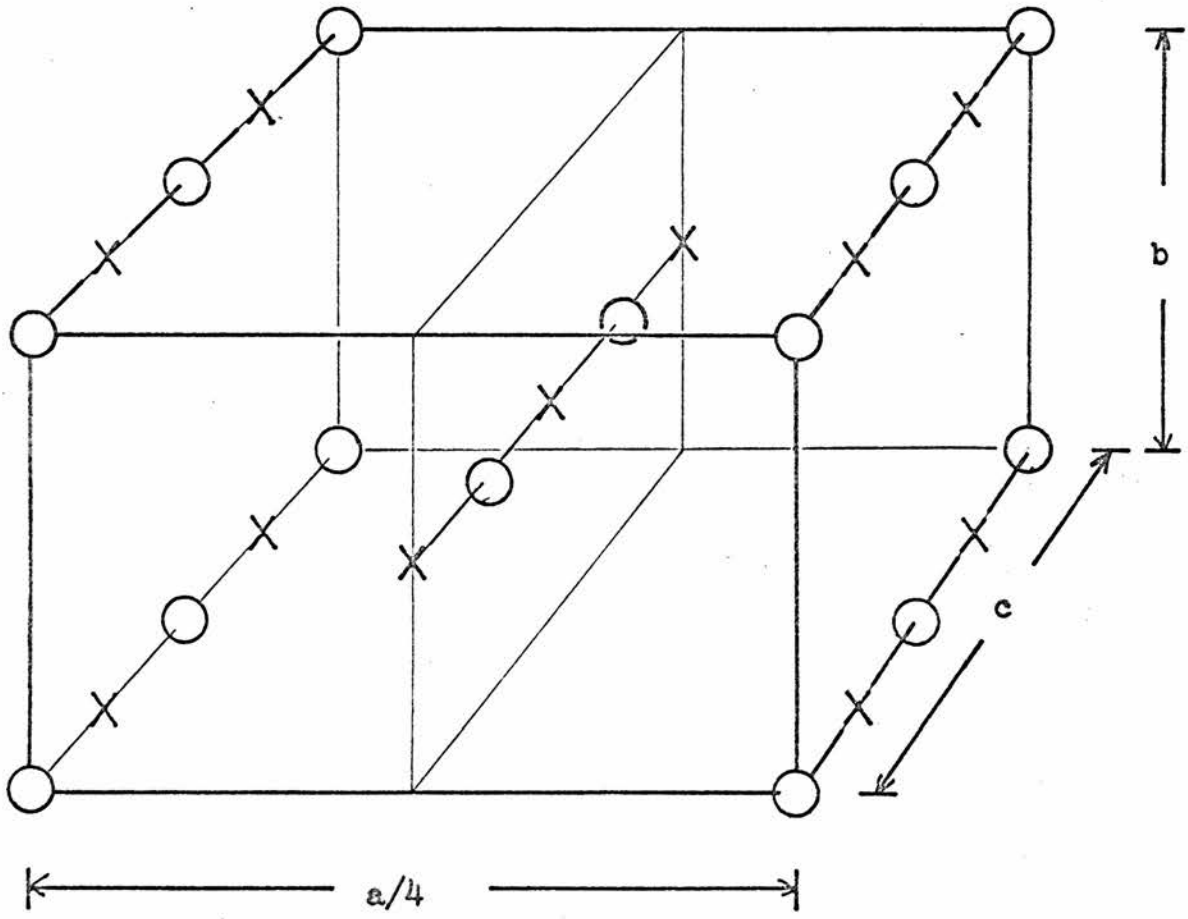

○ are sulphur atoms (the origin is moved to a sulphur atom)

X are nitrogen atoms

Fig. 7.3.1.

$\lambda(xO_4/zO_4)$ were both 0.2.

7.3. The structure

The room-temperature structure of AHS that has emerged from this study can be described as being composed of distorted sulphate tetrahedral ions linked into chains along b by short hydrogen bonds in which the protons are in ordered acentric positions, these chains alternating in both the a and c directions with rows, along b, of ammonium ions. The two structural elements are presumably bound together chiefly by ionic forces and hydrogen bonding between the sulphate and ammonium ions. The latter appear to be in free rotation at room-temperature. The relative disposition of the sulphur and nitrogen atoms is shown schematically in fig. 7.3.1..

7.3.1. Parameters and errors

The positional and thermal parameters are given in table 7.3.1. for the atoms in the asymmetric unit. The given errors are 'correct' standard deviations in the sense that they were calculated by a complete solution of the least-squares equations. In principle, these error estimates may be considered to be conservative (Geller, 1961). This, however, is true only if the weighting scheme is unbiassed, and the atomic scattering and temperature factors of the model completely describe anharmonic components of the thermal motion of the atoms and non-spherical components of their electron distributions. It has been recognised already that neither of these conditions obtain. The biassed weighting scheme, it has been said, may cause the standard

Table 7.3.1.

	x	y	z	β_{11}	β_{22}	β_{33}	β_{23}	β_{31}	β_{12}
S_1	.06208(2)	.71422(9)	.11079(3)	.00107(1)	.02160(19)	.00355(2)	-.00098(5)	.00031(1)	-.00054(3)
S_2	.31343(1)	.76186(9)	.10707(2)	.00084(1)	.02100(16)	.00237(1)	.00048(5)	-.00008(1)	-.00051(3)
O_1	.01521(5)	.61791(36)	.15926(9)	.00134(2)	.05505(94)	.00445(7)	-.00231(23)	.00079(3)	-.00255(12)
O_2	.10986(6)	.70472(51)	.16386(11)	.00137(3)	.1112(170)	.00582(9)	-.00586(34)	-.00049(4)	-.00134(17)
O_3	.05250(9)	.98660(39)	.06552(15)	.00411(6)	.03212(87)	.00981(14)	.00605(30)	.00238(7)	.00353(17)
O_4	.07093(8)	.51118(40)	.02896(11)	.00300(4)	.03886(87)	.00350(7)	-.00233(22)	.00124(4)	-.00190(16)
O_5	.26636(5)	.68751(34)	.15988(9)	.00116(2)	.05329(91)	.00372(6)	.00044(20)	.00057(3)	-.00204(11)
O_6	.35675(5)	.88429(30)	.15996(8)	.00121(2)	.03728(69)	.00316(6)	.00064(17)	-.00062(3)	-.00190(10)
O_7	.29432(6)	.99568(32)	.03814(10)	.00162(3)	.02373(60)	.00403(7)	.00185(18)	-.00089(3)	-.00061(10)
O_8	.33160(5)	.52234(27)	.05042(9)	.00144(2)	.02413(59)	.00385(6)	-.00102(16)	.00009(3)	.00061(9)
N_1	.06223(5)	.63909(38)	.35245(10)	.00097(2)	.03649(77)	.00347(7)	-.00007(20)	-.00005(3)	-.00024(11)
N_2	.31258(5)	.79758(38)	.34988(10)	.00118(2)	.04439(96)	.00282(6)	.00007(21)	.00007(3)	-.00065(13)
H_9	.0691(140)	.3614(890)	.0502(240)	*					
H_{10}	.3057(100)	.1299(650)	.0449(190)	*					

*The thermal parameter and occupancy of each of these atoms are given elsewhere (table 7.2.1.).

The fractional coordinates, x, y and z, and thermal parameters, β_{ij}, are referred to the full cell, $\underline{a} \times \underline{b} \times \underline{c}$.

Standard deviations on parameters are given in brackets, $\times 10^5$.

deviations on parameters to be incorrect by 5 – 10%. The effect of inadequate scattering factors has not been assessed; positional parameters are likely to be affected though not as severely as thermal parameters (Hamilton, 1969).

Of course, the standard deviations will not give a meaningful indication of the accuracy of parameters if systematic errors are present. Several of these have been recognised in the AHS data (section 4.7.). They will chiefly render the thermal parameters incorrect – but by an amount that is difficult to estimate. It is probable, however, that the relative magnitudes of these parameters will be nearly correct for each atom; the effects, apart perhaps from those of absorption, will mainly be taken up in the overall isotropic temperature factor (Lipson and Cochran, 1966, p.355). The thermal motion of a molecular or ion group can cause an apparent displacement of atoms at the extremes of the group towards its 'centre'. The correction for this particular systematic error, the so-called 'riding correction', is typically of the order of 0.01 Å at room-temperature (Lipson and Cochran, 1966, p.354).

Hamilton, 1969, recently reviewed the problem of random and systematic errors in currently obtainable values of $|F_o(hk\ell)|$ and $F_c(hk\ell)$. He assessed their effect on positional thermal parameters both theoretically and, by comparing the results of X-ray and neutron structure analyses, empirically. It is suggested that, with current methods, standard deviations estimated in least-squares refinement will often be small by a factor of two. Giving examples of systematic error, Hamilton pointed to the recognised misplacing of hydrogen atoms with X-ray data, and

the significant differences which persist between X-ray and neutron thermal parameters — which are generally larger for X-rays. He attributed these effects to the inadequacies of the free-atom approximation used for current f-curves. It is concluded that at present, with really careful accurate work,

i) 'heavy' atom coordinates can be found to within 0.001 — 0.002 Å by both neutron and X-ray methods;

ii) hydrogen atom coordinates can be found to within 0.001 — 0.002 Å by neutron and 0.01 — 0.02 Å by X-ray methods;

iii) root-mean-square (rms) vibration amplitudes can be found to within 0.001 — 0.002 Å (0.01 — 0.02 Å for hydrogen atoms with X-ray data), which is about 1% of the usual amplitudes at room temperature.

Hamilton further suggested that the maximum amount of systematic error, not included in the above 'random' errors, remaining in the best diffractometer experiments may cause errors of 0.006 Å both in coordinates and in rms amplitudes. So far these are, at best, careful estimates.

The results in table 7.3.1. show that the estimated errors on atomic coordinates are of the order of 0.0005 Å for the sulphur atoms, 0.0015 Å for the oxygen atoms and the ammonium ions, and 0.03 Å for the hydrogen atoms. These should perhaps be doubled to obtain a more realistic 'random' error (see (i) above). The estimated errors on the thermal parameters are somewhat larger than Hamilton found: they are 0.004 Å or more on all rms amplitudes — which is an error in the range 2 — 4%.

Many possible sources of systematic error in the data have

been discussed which are likely to have affected the thermal parameters — without being included in the above 'random' errors. It is proposed that the actual values of all of these parameters, and their standard deviations, be regarded with suspicion. The relative magnitudes of these parameters are likely to retain some significance. As has been said, the various systematic errors, both in the data and in the model, are unlikely to have affected positional parameters strongly. Nevertheless it appears that realistic errors may be as much as four or five times greater (see above) than those given in table 7.3.1..

This is as much as can be said at the present time. Further research, like that of the American Crystallogrphic Association's Single Crystal Intensity Project (Abrahams et al., 1967), is required to identify and quantify all the many systematic errors that may affect diffractometer experiments (Hamilton, 1969; Mathieson, 1969).

7.3.2. Bond lengths and angles

A computer program was written to calculate bond lengths and bond angles from the refined positional parameters (table 7.3.1.) and the measured cell dimensions (section 4.3.). To check the program it was used to calculate some of the results given for thiourea by Elcombe and Taylor, 1968. The method used to calculate the errors on bond angles was a crude one. It overestimated the errors by a factor of not more than three. With this qualification, the calculated errors correctly combined those given in table 7.3.1. and the estimated errors on the cell dimensions. The increments in parameter errors suggested in the

preceding section were not included. The increases would have been arbitrary and would not have altered the uncertainty in the accuracy of the results obtained.

All pertinent bond lengths and angles are given in table 7.3.2.. The method of labelling symmetrically equivalent atoms is illustrated in fig. 7.3.2.. The disposition of the atoms involved in the listed bond lengths and angles is illustrated diagrammatically in an (010) projection in fig. 7.3.3..

No 'riding correction' was applied to the bond lengths. Firstly the thermal parameters were very uncertain, and secondly no argument is put forward which turns on a correction of the order of 0.01 Å. As said, the quoted errors do not take account of the possible 'factor of four or five' discussed in the preceding section; it is possible that the listed bond lengths, apart from those involving hydrogen atoms, are already in error by 0.01 – 0.02 Å before considering the 'riding correction'. The latter is only expected to affect S – O distances in the AHS structure; for these the correction would probably be somewhat less than 0.01 Å. It will be in the same direction and of a closely similar magnitude for all S – O bonds, and so will not affect any of the following comparisons of bond lengths.

Even if the 'standard deviations' are incremented by a factor of ~ 5 it is clear that both sulphate tetrahedra are distorted, and that they differ in dimensions and distortion. Taking an error of $\pm$0.01 Å on the S – O bond lengths, the average length of S_1 – O bonds is 1.460 $\pm$ 0.005 Å and that of S_2 – O bonds is 1.473 $\pm$ 0.005 Å – on the assumption that any systematic errors will affect the two ions similarly so that the errors on the

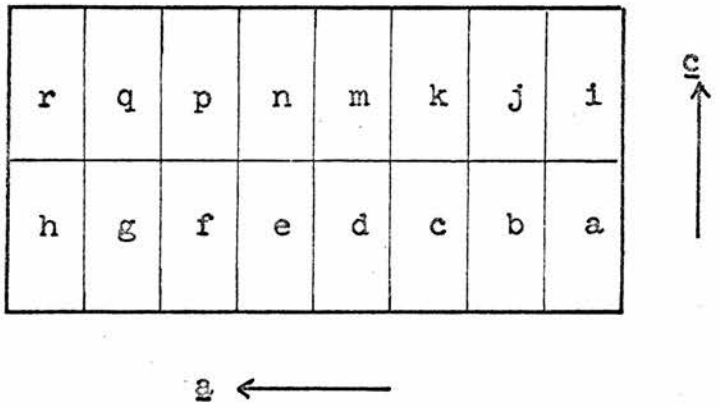

The full cell $\underline{a} \times \underline{b} \times \underline{c}$ is divided into sixteen 'sub-cells', $\underline{a}/8 \times \underline{b} \times \underline{c}/2$, each containing one formula unit. These cells are labelled 'a' to 'r' :

S_1, O_1, O_2, O_3, O_4, N_1, and H_9 are in 'a' ;

S_2, O_5, O_6, O_7, O_8, N_2, and H_{10} are in 'c' .

Symmetrically equivalent atoms in 'b' would be designated S_2b, O_5b etc. Atoms in the adjacent unit cell along $\pm x$, $\pm y$, or $\pm z$ are shown by single, double and triple primes respectively.

e.g. $(O_1h')''$ is the atom symmetrically equivalent to O_1 in the 'h' sub-cell of the unit cell next to the principal one along x and next to this second cell along y.

Fig. 7.3.2.

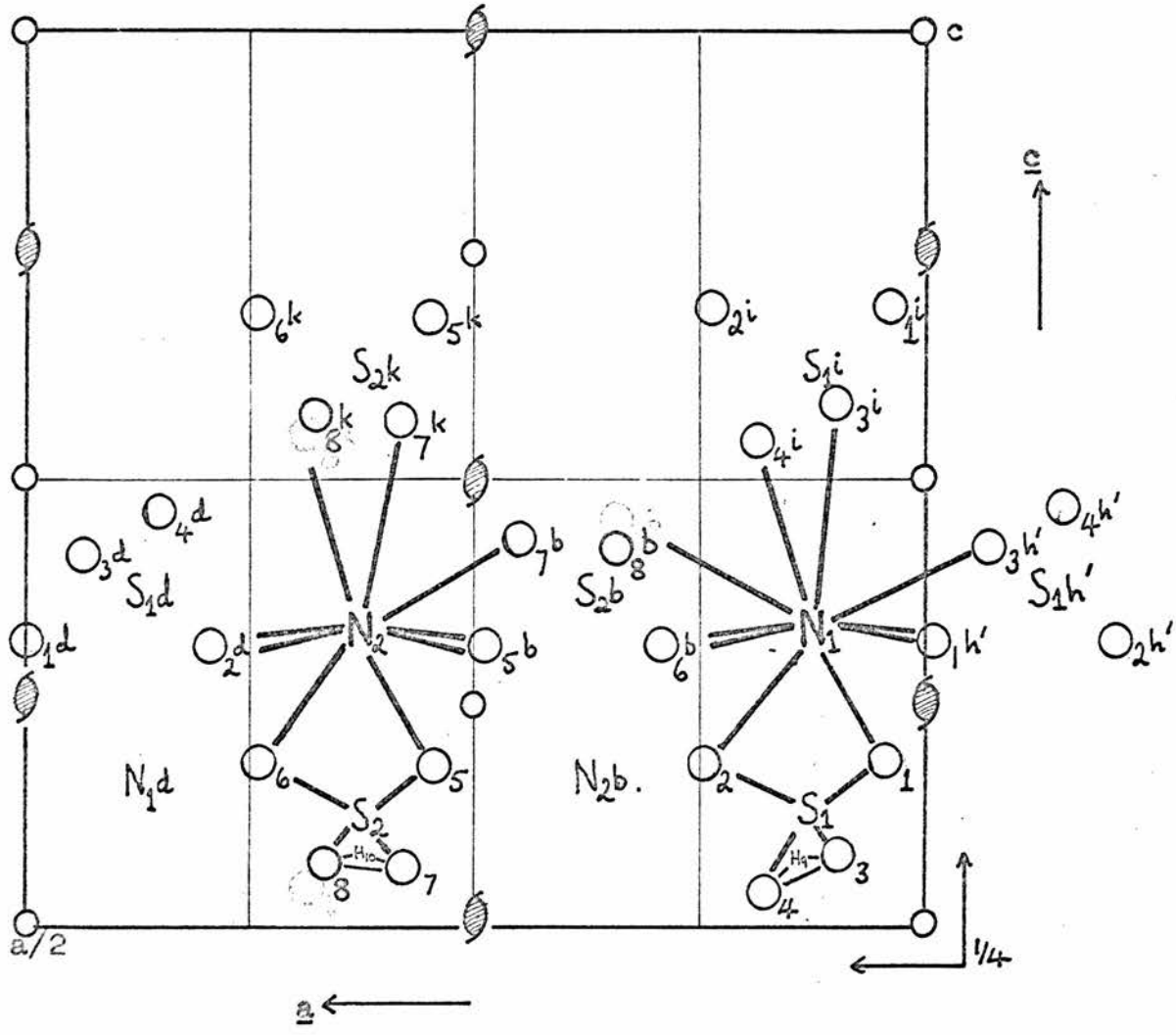

All bonds whose lengths are listed in table 7.3.2. are marked by solid lines joining atoms

($B2_1/a$ space group symmetry elements are shown)

Fig. 7.3.3.

Table 7.3.2.

[Bond lengths in Å; errors given in brackets x 10^3 Å]

$S_1 - O_1$	1.430(2)	$S_2 - O_5$	1.440(2)
O_2	1.419(2)	O_6	1.441(2)
O_3	1.441(3)	O_7	1.557(2)
O_4	1.546(3)	O_8	1.455(2)
$N_1 - O_6b$	3.134(5)	$N_2 - O_5b$	2.965(4)
O_6b''	2.972(4)	O_5b''	3.070(5)
O_1h'	3.070(5)	O_2d	3.006(5)
$(O_1h')''$	2.921(4)	O_2d''	2.990(5)
O_4i	3.079(4)	O_7k	3.131(4)
O_3i	3.219(5)	O_8k	3.122(4)
O_1	3.093(4)	O_5	3.082(4)
O_2	3.044(4)	O_6	3.042(4)
O_8b	3.081(3)	O_7b''	3.254(3)
O_3h'	3.156(3)		
$O_3 - H_9''$	1.790(41)	$O_7 - H_{10}''$	0.690(30)
$H_9'' - O_4''$	0.760(40)	$H_{10}'' - O_8''$	1.920(30)
$O_3 - O_4''$	2.514(6)	$O_7 - O_8''$	2.598(5)

[Bond angles in degrees; errors given in brackets x 10 degrees]

$O_1 - S_1 - O_2$	112.5(1)	$O_5 - S_2 - O_6$	113.3(1)
$O_1 - S_1 - O_3$	111.7(1)	$O_5 - S_2 - O_7$	106.0(1)
$O_1 - S_1 - O_4$	108.6(1)	$O_5 - S_2 - O_8$	112.4(1)
$O_2 - S_1 - O_3$	115.0(1)	$O_6 - S_2 - O_7$	108.2(1)
$O_2 - S_1 - O_4$	107.5(1)	$O_6 - S_2 - O_8$	112.5(1)
$O_3 - S_1 - O_4$	100.5(1)	$O_7 - S_2 - O_8$	103.8(1)
$O_3 \cdots H_9'' - O_4''$	160 ± 4°	$O_7 - H_{10}'' \cdots O_8''$	172 ± 6°

S – O distances may be treated as random errors in the averaging process. The lengthening of the S – O(H) bond is clearly significant in both ions. According to Cruickshank, 1961, the other S – O bonds shorten by an amount which preserves the ion's average bond length of 1.49 ± 0.01 Å. He instanced $KHSO_4$ in which the S – O(H) bond length is 1.56 ± 015 Å and the S – O bond lengths are 1.47 ± 0.015 Å. In AHS the length of the S – O(H) bond is the same as that in $KHSO_4$; but the average bond length is significantly less than 1.49 ± 0.01 Å. Nevertheless, all the individual S – O bond lengths fall within the ranges given for the sulphate ion S – O bonds in the International Tables, 1962, Vol. III, Tabl 4.1.9..

With regard to bond angles, the S_1 ion shows a markedly greater distortion than the S_2 ion. It is interesting that it is O_3 rather than O_4 which is involved in bonds showing the greatest deviation from the regular tetrahedral angle. In the other ion O_8 is similarly involved in more distorted bonds than O_7, but the difference is far less marked.

The International Tables (loc. cit.), Tables 4.1.1. and 4.1.12., give the range of NH_4^+ – O distances as 2.8 – 3.4 Å and the range of N.... O separations in hydrogen bonds as 2.7 – 3.2 Å. All N – O separations less than 3.5 Å in AHS are listed in table 7.3.2.. The environments of the two ammonium ions are very similar. Both are almost at the centre of a square array of oxygen atom neighbours. $N_1 - O_6b$, O_6b'', O_1h' and $(O_1h')''$ are 3.13, 2.97, 3.07 and 2.92 Å respectively. With a conservative error on each of ±0.02 Å, the mean of these is 3.02 ± 0.01 Å. $N_2 - O_5b$, O_5b'', O_2d and O_2d'' are 2.96, 3.07, 3.01 and 2.99 Å

respectively, and their mean is 3.02 ± 0.01 Å. The effects of systematic error are expected to be the same in each case. Each ammonium ion has neighbouring oxygen atoms displaced from it approximately along ± c, and the N – O distances are again quite similar:

$N_1 - O_4i$	3.08 ± 0.02 Å	$N_2 - O_7k$	3.13 ± 0.02 Å
O_3i	3.22	O_8k	3.12
$N_1 - O_1$	3.09 ± 0.02 Å	$N_2 - O_5$	3.08 ± 0.02 Å
O_2	3.04	O_6	3.04

The only difference to be noticed is that N_1 has two other near neighbours, O_3h' and O_8b, at distance of 3.16 and 3.08 Å respectively, while N_2 has only O_7b'' at a distance of 3.25 Å.

The bonding of oxygen atoms to the ammonium groups differs slightly between the two sulphate ions. It is seen that in the S_1 ion O_1 and O_2 are triply bonded, O_3 is doubly bonded and O_4 is singly bonded; in the S_2 ion O_5 and O_6 are triply bonded, and O_7 and O_8 are doubly bonded. The average O – N distance for the S_1 ion is 3.064 ± 0.007 Å, and for the S_2 ion is 3.084 ± 0.007 Å – again assuming systematic errors to affect the environments of the two sulphate ions similarly. The O(H) oxygen atoms, O_4 and O_7, are involved in possible bonding to the ammonium ions. So also are the other members of the hydrogen bonds linking sulphate groups, O_3 and O_8. This may contribute to the distortions of the sulphate ions and their linking hydrogen bonds.

The two hydrogen bonds are illustrated in fig. 7.3.4.. The

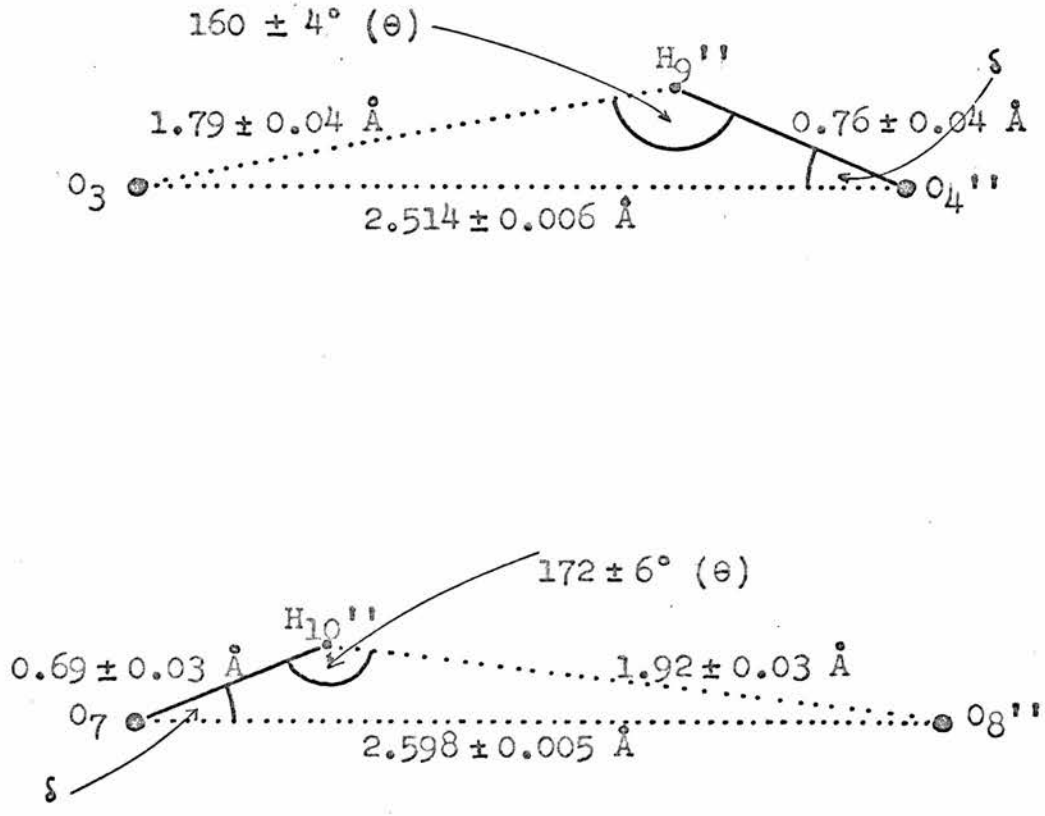

The given dimensions for each bond are as found from the X-ray refinement

Fig. 7.3.4.

hydrogen atom fractional coordinates found from neutron results (tables 6.4.2. and 6.5.2.) were:

		x	y	z
i)	H_9	.066 ± .002	.298	.053 ± .002
	H_{10}	.313 ± .002	.207	.049 ± .002

where the y-coordinates were estimated from the O.... O separation. The X-ray difference syntheses located the hydrogen atoms at (table 6.5.3.):

		x	y	z
ii)	H_9	.072	.299	.056
	H_{10}	.316	.185	.052

The final least-squares refinement with the X-ray data placed them at:

		x	y	z
iii)	H_9	.069 ± .002	.361 ± .009	.049 ± .002
	H_{10}	.305 ± .001	.130 ± .007	.045 ± .002

The differences between (i) and (iii) appear chiefly in the y-coordinates and are attributable to the apparent shortening of the O — H distance in the least-squares refinement ((iii)).

From equation 6.2.1. (Hamilton, 1962) the expected O — H

nuclear separations for the values of r(O....O) obtained from the X-ray refinement are:

$r(O_4'' - H_9'')$	$r(O_7 - O_{10}'')$
0.99 ± 0.03 Å	0.98 ± 0.03 Å

The corresponding O — H separations refined from the X-ray data were:

0.76 ± 0.04 Å	0.69 ± 0.03 Å

Even if the random errors on the X-ray results were underestimated by a factor of two or three, the X-ray results place H_9 and H_{10} nearer to O_4 and O_7, respectively, by a minimum of 0.15 Å. The probable displacement is nearer 0.25 Å. Lipson and Cochran, 1966 (p.352), pointed out that a Fourier synthesis of X-ray data should show the maximum in the electron density of hydrogen atoms undisplaced from their nuclei. The coordinates found from the difference syntheses do place the hydrogen atoms nearer to their estimated nuclear positions than do the least-squares refinement results (compare (i), (ii) and (iii) above).

From the studies of Hamilton, 1962, and Chidambaram and Sikka, 1966, (section 6.5.1.) the 'expected' values of Θ and ranges of δ (fig. 7.3.4.) are:

		Θ	δ
a)	$O_3 ....H_9'' - O_4''$	177 ± 6°	0° - 7°
	$O_7 - H_{10}''....O_8''$	174 ± 6°	0° - 9°

The values found from least-squares refinement of the X-ray data were:

		Θ	δ
b)	$O_3 \ldots H''_9 - O''_4$	$160 \pm 4°$	$14 \pm 3°$
	$O_7 - H''_{10} \ldots O''_8$	$172 \pm 6°$	$6 \pm 4°$

which are in agreement with those found earlier (table 6.5.1.) by combining the refined neutron x- and z-coordinates with the O — H distances estimated from equation 6.2.1. (Hamilton, 1962). If it is assumed that the X-ray refinement displaces the hydrogen atoms along a line joining the proton position to the relevant oxygen nucleus, and the O — H distances are increased along this line to their 'expected' values of ~ 0.98 Å (see above), the δ values remain the same, of course, but the Θ values become:

		Θ
c)	$O_3 \ldots H''_9 - O''_4$	$158 \pm 4°$
	$O_7 - H''_{10} \ldots O''_8$	$171 \pm 6°$

Comparing (a), (b) and (c) it seems clear that while the $O_7 - H''_{10} \ldots O''_8$ bond is bent by an 'expected' amount for the given $O_7 \ldots O''_8$ separation, the $O_3 \ldots H''_9 - O''_4$ bond is abnormally strongly bent. There is no reason to suppose that the $O_3 \ldots O''_4$ separation is incorrect to a degree that would vitiate this conclusion; and the strong bending is apparent in both the neutron and the X-ray results.

7.3.3. A summary

The following conclusions have been reached regarding the

room-temperature structure of AHS:

i) the two symmetrically inequivalent sulphate ions show significant differences in distortion and dimensions – though the difference in the latter is small;

ii) both sulphate ions show one very significantly lengthened S – O bond, while the three other bonds are, within error, of equal lengths;

iii) the length of this longer S – O bond is, within error, the same as that found for S – O(H) bonds in other structures containing HSO_4^- ions;

iv) both of the symmetrically inequivalent ammonium ions are in very similar asymmetric environments: with one exception there is no significant difference to be found in the two sets of N – O separations;

v) although the evidence is not conclusive, it all suggests that the ammonium ions are in free rotation;

vi) the two symmetrically inequivalent O – H.....O hydrogen bonds are significantly different: both are short and the shorter of the two is abnormally strongly bent;

vii) the hydrogen atoms in these bonds are in ordered acentric positions.

With the exception of (v) above no conclusions are reached regarding the thermal motion of atoms in the structure. The thermal parameters are subject to too many sources of error – though their relative magnitudes are expected to be meaningful. No conclusion has been reached as to the character of the bonding between the ammonium ions and sulphate groups.

7.4. Conclusion: the structure, the transition, future work

By the nature of the problem as stated at the outset, there can be no 'conclusion' as such at this stage. But the first part of the project has been successfully completed and at least some aspects of the transition are already clear.

The structure of AHS in its room-temperature non-ferroelectric phase has two unusual features: first it is pseudo-symmetric, and secondly the protons are already ordered in acentric positions in hydrogen bonds which are expected to play some rôle in the transition. It is more usual for a ferroelectric to become pseudo-symmetric in its ferroelectric phase, and for protons to be disordered in such bonds in the non-ferroelectric phase.

The pseudo-symmetry of the structure suggests the existence of a higher symmetry phase at a higher temperature. In the case of AHS the following considerations show that such a phase does not in fact exist below its melting point (at 1 atmos. pressure). It is known that single crystals of AHS may be grown from the melt (Pepinsky et al., 1958). The pseudo-symmetry includes a mirror plane perpendicular to a. Hence the higher symmetry is orthorhombic. If an orthorhombic phase existed below the melting point, then on passing to a room-temperature phase symmetry-twinning would occur. Yet the growth of single crystals is reported.

A very much studied example of a ferroelectric having a proton disordered in a short hydrogen bond in its non-ferroelectric phase is KDP. The motion of the proton in the non-ferroelectric phase has been interpreted as an overdamped oscillation somewhat analogous to a phonon mode. It has been investigated as such with both Raman scattering experiments on KDP itself (Kaminow and

Damen, 1968), and neutron scattering experiments on deuterated KDP (Buyers et al., 1968). Kaminow and Damen fitted their results to a simple harmonic oscillator model with a temperature-dependent damping constant. From this they extracted a temperature-dependent characteristic frequency which dropped towards zero as T_c was approached. The neutron experiments initially looked for a transverse optic mode whose frequency fell as T_c was approached. Such a mode was not found. Instead, quasi-elastic scattering around Bragg peaks was detected which peaked up strongly as T_c was approached. The latter results do not distinguish between descriptions of the scattering as from a very overdamped oscillation or from an order-disorder transition described by an Ising model.

Experiments of a similar kind may be attempted on AHS. The present indications are that the structure is ordered, except for the ammonium ions which seem to play no part in the upper transition (section 1.7.). Hence it is probable that the transition will prove to be associated with a well defined transverse optic mode, rather than with a very overdamped oscillation as in KDP. If that proves to be the case then neutron inelastic scattering and, possibly, Raman scattering methods could be used to look for a transverse optic mode with a strongly temperature-dependent frequency.

Another line of attack on the dynamics of the transition is provided by the deuteron magnetic resonance experiments mentioned earlier. The results should throw light onto exactly which elements of the structure show a change in dynamical behaviour associated with the transition.

From the structural point of view the immediate programme is, of course, to determine the structure of AHS in its ferroelectric phase. It may be possible to interpret the structural changes occurring at the transition directly in terms of a 'frozen-in' mode (section 1.3.).

In summary, then, the room-temperature non-ferroelectric structure of AHS has been determined; this provides a basis for meaningful investigations of the dynamics of the upper transition, by methods such as those outlined above; a determination of the structure in the ferroelectric phase will provide a more complete basis for models of the dynamical behaviour at the transition, and immediate knowledge of the static changes which occur.

APPENDIX 1

A summary of the data collection experiment

Explanatory notes:

i) the five sets of data collected under the different conditions are labelled (1) to (5)

ii) the inclusive dates for the collection of each set are given

iii) the data collected is designated by the layer number (where a control tape included more than one layer this is shown by 5/6 or 4/5/6/7), followed by (1) or (2) to label the two orientations, or half-layers. Orientation (2) is the half-layer with ℓ negative

iv) if the layer number(s) is followed by W this designates the separately collected 'weak' reflections

v) the 'strong' reflections were first collected out to $\Theta = 30°$. The remainder were collected in two ranges: $30° < \Theta \leq 33°$ (HA2) and $33° < \Theta \leq 35°$ (HA3)

vi) "(repeats)" following a half-layer label signifies the remeasurement of that part of the half-layer previously measured unsatisfactorily or not completed

vii) all 'strong' reflections out to $\Theta = 15°$ were measured together on tape LA - (1)

viii) the dimensions of the uniform area of the primary beam are given measured horizontally ($\leftrightarrow$) and vertically ($\updownarrow$)

ix) 'tube at 55/12' means that the X-ray tube E.H.T. and current settings were 55kV and 12mA respectively.

The summary:

Machine and source aligned. Beam set at $\overleftrightarrow{0.8}$ x 0.9$\updownarrow$mm.

Tube at 55/12. Specimen SD1.

4.2.67. O-(1),
OW-(1), 1-(1), 1W-(1), OW-(2), } (1)
21.2.67. O-(2).

Scintillator response profile shows 10% dip near detecting area.

Beam profile shows reduced uniform area.

PMT and scintillator replaced. X-ray tube replaced. Source re-aligned. Beam set at $\overleftrightarrow{1.0}$ x 1.0$\updownarrow$ mm. Best position on scintillator surface located. PHA settings determined. Tube at 55/14.

13.3.67. 1-(2),
1W-(2), 2-(2), 2W-(2), 2-(1), 3-(1), } (2)
26.3.67. 4-(1) (incomplete)

Complete mechanical and electrical servicing. Counter collimator re-aligned. Source re-aligned. Beam set at $\overleftrightarrow{0.8}$ x 0.9$\updownarrow$ mm. PHA settings checked. Tube at 55/14.

28.4.67. 2W-(1),
3W-(1), 5/6-(1), } (3)
2.5.67. 4/5/6/7W-(1)

Specimen SD2 put on. Otherwise conditions as for (3).

3.5.67. 3-(2) (incomplete) } (4)

Machine centre drops 0.7 mm. following incorrect re-assembly after

mechanical servicing.

χ-datum error of +0.30° discovered and also attributed to faulty re-assembly.

Counter collimator re-aligned. Source re-aligned.

Beam set at $\overleftrightarrow{0.9}$ x $0.9\updownarrow$ mm. Scintillator response profiles checked. PHA settings checked. Tube at 55/14.

<u>16.5.67.</u> 3-(2), 3W-(2), 4-(2), 4/5/6/7W-(2), 1W-(2), 5/6-(2), 2-(2), 4/5/6/7W-(1) (repeats), 5/6-(1) (repeats), 2W-(1) (repeats), miscellaneous repeats, LA-(1), 3W-(1) (repeats), 0-(1) (repeats), 0W-(1) (repeats), 4-(1) (repeats), 1W-(1) (repeats), 1-(1) (repeats), 2-(1) (repeats), HA2-(2), HA3-(2), HA3-(1),

<u>1.7.67.</u> HA2-(1). } (5)

<u>7.7.67.</u> Determination of PHA 'paralysis' time for counting loss corrections.

<u>31.8.67.</u> Four low angle reflections ((002), (00$\bar{2}$), (200) and ($\bar{2}$00)), wholly or partly obscured by the backstop in normal working conditions, measured with the backstop removed.

<u>1.9.67.</u> Alignment of the source, and the beam profile checked and found to be unaltered.

APPENDIX 2

An example of the data reduction program output

Notes

On the first page the details of the reflection processing appear. After the index, h, k, ℓ and theta in hundredths of a degree, the parameters of the reflection measuring order are given: the counting time of each step in seconds, the number of steps, and their size in degrees. 'Diff' is the difference, in numbers of steps, between the highest point of the 'smoothed' profile and the centre of the scan. 'C-M' is the difference, similarly expressed, between the final peak centre, as located by the program, and the centre of the scan. 'E' gives the step number in the scan at which the centre of the rise in the white radiation at the absorption edge occurs. Then follow the mean background levels on the low and high angle sides of the peak, and the integrated intensity corrected for background. The standard deviation on this intensity ('Err') includes the counting statistics error, and the uncertainty in the counting loss correction if applied. The intensity is corrected by the Lorentz-polarisation factor and given together with its standard deviation expressed as a percentage. The magnetic tape location, where h,k,ℓ, the integrated intensity and the error for the reflection are stored, is given under 'File'. For reflections processed by the routine 'absorption edge', the intercept and

gradient of the least-squares fit to the high angle background counts are labelled A and B. The errors on these are given under 'Faults', labelled EA and EB. Following EB are the expected and calculated angles, in hundredths of a degree, at which the line intercepts the general background level. For all reflections faults, in sensu latu, are listed. A key to these appears at the bottom of the page. Any datum errors which occur are given after 'Datum' which signifies that a datum check has been performed. 'Standard' reflections are labelled 'St Ref' under 'Index'.

On the second page the reflection profiles as read from the diffractometer tape (and corrected for counting losses if required) are given. Each profile is headed by its index. Pertinent features of the reflection processing are marked: 'M' is the highest point of the 'smoothed' profile; 'G' is the position of the 'centre of gravity' of the counts in the peak region; '+' is the centre of the peak as located by the program; 'S' indicates that 'G' and '+' occur at the same point; 'E' is the position of the white background rise at the absorption edge; '-' marks the extremes of the peak assumed by the program in calculating the integrated intensity. Although none appear in the example given, any count mis-punched on the diffractometer tape appears as 'Nondig' in the profile.

INDEX	H	K	L	THETA	STEPS SECS	NO	SIZE	DIFF	C-M	E	LOWBG	HIGHBG	INT	ERR	LPINT	%ERR	FILE		FAULTS
258	4	[illegible]	16	2279	6	24	0.04	1	2	-6	185	187	20253	161	9709	0.8	56		
259	4	[illegible]	18	2578	6	26	0.04	1	3	-7	69	65	348	51	196	14.8	57		4
260	4	[illegible]	20	2884	6	26	0.04	0	2	-12	63	63	1879	62	1235	3.3	58		
261	8	0	0	661	6	20	0.04	0	0	5	15045A	-183B	1027257	25233	120616	2.5	59	AER	DATUM 2EA 4EB 933 932 23
262	8	[illegible]	2	714	6	20	0.04	0	0	4	4925A	-51B	384836	3734	49094	1.0	60	AER	3EA 6EB 1011 1010 23
263	8	[illegible]	4	860	6	22	0.04	0	0	4	1488	1222	102018	475	15773	0.5	61		23
264	8	[illegible]	6	1060	6	22	0.04	0	1	3	1508	1338	146690	597	28379	0.4	62		23
265	8	0	8	1290	6	22	0.04	1	1	2	595	672	46138	255	11091	0.6	63		DATUM
266	8	0	10	1540	6	22	0.04	1	1	-1	400	414	28734	200	8466	0.7	64		
267	8	[illegible]	12	1802	6	24	0.04	1	1	-2	296	287	22589	173	8036	0.8	65		
268	8	[illegible]	14	2075	6	24	0.04	1	1	-4	184	196	15752	146	6687	0.9	66		
269	8	[illegible]	16	2357	6	24	0.04	-2	F3	-8	79	79	79	69	39	87.3	67		DATUM 3 14
270	8	[illegible]	18	2649	6	26	0.04	1	1	-9	71	62	1261	57	739	4.6	68		
271	8	0	20	2950	6	26	0.04	0	2	-12	56	51	696	50	472	7.1	69		4
272	12	0	0	995	6	22	0.04	0	-2	1	1493	949	1590	269	287	16.9	70		4 13 17
ST REF	0	0	6	824	6	22	0.04	1	1	6	2993A	-26B	153632	1958	22763	1.3	71	AER	DATUM 9EA 13EB 1167 1165
274	12	0	2	1032	6	22	0.04	0	F3	3	263	265	174	112	33	64.5	72		3 5 14 15 17
275	12	[illegible]	4	1138	6	22	0.04	0	0	2	2697	2419	323162	1898	67568	0.6	73		23
276	12	0	6	1297	6	22	0.04	0	0	1	369	323	6235	125	1508	2.0	74		
277	12	[illegible]	8	1493	6	22	0.04	0	1	-1	1091	1144	140735	498	39991	0.4	75		
278	12	[illegible]	10	1716	6	24	0.04	0	1	-2	418	454	39932	226	13385	0.6	76		DATUM
279	12	0	12	1957	6	24	0.04	1	1	-3	407	478	49057	248	19335	0.5	77		
280	12	[illegible]	14	2214	6	24	0.04	1	1	-6	117	122	4722	90	2179	1.9	78		
281	12	[illegible]	16	2489	6	26	0.04	1	2	-7	94	101	5047	88	2711	1.7	79		
282	12	0	18	2765	6	26	0.04	-2	1	-11	60	62	157	45	98	28.6	80		DATUM
283	12	0	20	3059	6	26	0.04	0	2	-14	49	44	491	47	349	9.6	81		4
284	16	0	0	1332	6	22	0.04	0	0	0	1363	1157	156234	615	38941	0.4	82		
285	16	[illegible]	2	1360	6	22	0.04	0	0	0	259	243	2238	91	571	4.1	83		
286	16	0	4	1443	6	22	0.04	0	0	-1	842	793	100681	382	27501	0.4	84		DATUM
287	16	0	6	1573	6	22	0.04	0	1	-2	259	244	6537	115	1975	1.8	85		

KEY TO FAULTS

1 = DIFF GREATER THAN VAR1
2 = EF X WIDTH EXCEEDS SCAN
3 = ERR(COFG) GREATER THAN VARERR,OR MOMENT OR MASS LTOET 0
4 = CENTRE-SCAN MIDDLE GT VAR4
5 = EDGE TOO NEAR SIGNAL
6 = NO TERMINATING BLANK
7 = NON-DIGIT IN COUNT
8 = RESTART INDEX FOUND
9 = FAULT IN H K OR L
10 = PLUS MISSING
11 = THETA FAULTY
12 = FAULT IN ORDER
13 = SLOPING BACKGROUND
14 = WEAK PEAK, MUDDLE=SCAN MIDDLE
15 = BIGGEST NUMBER NOT IN MUDDLE
16 = SIGNIFICANT PEAK DISPLACED FROM CENTRE
17 = HIGH BACKGROUND
18 = FAULT? TWICE
19 = SIGNAL EXCEEDS SCAN
20 = MUDDLE NOT SET
21 = ONLY ONE BG COUNT IN A.E. ROUTINE
22 = EDGE TOO NEAR SCAN LIMIT
23 = POSITIVE GRADIENT BACKGROUND

PROFILES M = MUDDLE - = SIGNAL LIMITS G = COFG + = CENTRE S = G ON + E = EDGE

258	259	260	261	262	263	264	265	266	267	268	269	270	271	272
14*	80	57	1494	826	465	319	337	360	276	154	92	66	60	1590E
174	79	64	1513	835	515	438	414E	354	265	192	73	59	54	1567
169	72	56	1963	1064	506	8405	491	383	285	182	79	65	49	1493
177	62	67	4275	2374E	696E	1178	562	420	312	200	72	56	43	1446-
189	74	65	11001E	4809	1065	1422	587	430	296	185	62-	79	56	1471
211	59	57	17999-	7023-	1488	1595	637	450	321	190	73	94	51	1404
227	62	76	23951	8959	1700-	1782-	693-	513-	317	228-	81	76	70	1326
277-	66	77-	52554	32482	2646	2923	921	771	349-	277	96	76-	68	1340
429	69-	75	221886	98560	7115	8737	2325	2099	567	406	94	90	54-	1392S
1281	69	82	3631025	137134S	24208	30705	7850	6311	1254	1223	92M	98	55	1641
3878	97	220	297074	85022	33825S	43435G	13166	7511	4263	3357	103	132	108	1700M
5031	141	491	111521	36477	26702	38164+	11623S	5471S	5892	3823	97	312	206	1463
3074G	123	476M	26327	9059	11028	19044	7643	4623	4092S	2116S	83	359	200-	1230-
1573+	114M	213G	16961	5827	4176	7318	4572	3028	3174	1746	89	216S	137	1064
2706	94G	128+	14674-	5004-	2677	4166	1636	1144	3184	2384	98	126	77S	1003
2472	118+	169	13271	4661	1763-	3415	1377	820	1599	1399	87	164	97	958
1034	120	325	12345	4232	1472	2799-	1284-	730	700	565	67	223	117	953
433	85	241	11698	3944	1290	1769	952	598-	588	448	68	147	120	981
259	5*	119	11357	3889	1156	1400	732	554	425-	258-	68	90	97	963
225-	6*	82	10892	3804	1160	1172	564	397	372	239	76	79	54	863
227	66	65-			1108	1149	552	336	352	226	85-	74-	69	900
206	65-	63			1144	1201	561	371	276	206	84	63	54-	853
144	63	72							232	161	77	69	55	
171	7*	63							205	150	75	43	57	
	70	64										65	46	
	5*	54										69	46	

273	274	275	276	277	278	279	280	281	282	283	284	285	286	287
2791	259	568	365E	907	386	361	117	90	55	50	940	231	761	237
2464	272	1217F	368	982	396	403	103	66	66	50	1194	249	816	269
2572	259E	2114	385	980	414	372	114	93	57	49	1248	254	850	270
2525	305-	2617	343	1070	435	365	120	72	76	45	1361	292	853	257
2628	285	2778	380	1202	406	402	121	99	49	62	1647	243	929	260
3169E	285	3536-	400-	1402	469	430	124	107	59	43	1840-	268-	1114-	309-
3743	285	4343	378	1739-	556-	518	117-	115	62-	53	2263	282	1565	274
3750-	257	7928	540	3656	716	662-	166	110	63	45-	5338	285	3194	439
4975	290	34140	1035	12334	1294	1306	254	111-	82	46	19417	474	12794	882
12791	279	81656	1930	33244	4769	3515	646	227	73	68	45885	815	27212	1764
37475	284	91444S	1785S	35711G	10090	10700	1269	531	80M	127	41179S	812S	24621S	1725G
51779S	278	68608	1495	24611+	8897G	12000	1069	1253	88	147	28731	709	17966	1291+
38091	273	39998	1064	21031	5594+	6245S	485S	1185	78G	116M	17123	504	13692	1212
14344	285	10439	556	11336	6131	6412	595	470G	73+	64G	5007	325	4693	689
5343	257	5790	450	4215	3703	6726	756	398+	69	73+	1891	280	1711	375
3960	272	3571-	405-	2915	1491	3515	402	703	70	85	1465-	253-	1106-	323
3792-	259	2832	348	2233-	1102	1509	226	641	75	109	1365	235	979	269-
3205	260-	2415	301	1715	827-	1034	161	351	74	86	1261	268	873	247
2726	251	2375	321	1182	703	766-	125-	194	56	66	1104	230	788	242
2412	273	2304	330	975	567	741	134	133	72-	54	1111	229	726	253
2252	256	2213	315	976	409	609	158	116-	68	54	1056	251	713	231
2286	270	2178	325	870	343	411	110	118	58	44-	1047	247	679	248
					361	321	102	99	65	44				
					340	309	104	101	69	38				
								100	51	49				
								85	62	44				

APPENDIX 3

Generality of the counting loss correction method

So long as the reflection peak remains sensibly single, the peak profile can be approximated in shape by a Gaussian function. The area under this curve can be reasonably approximated by that under a triangle of the same height and the same width at half-height.

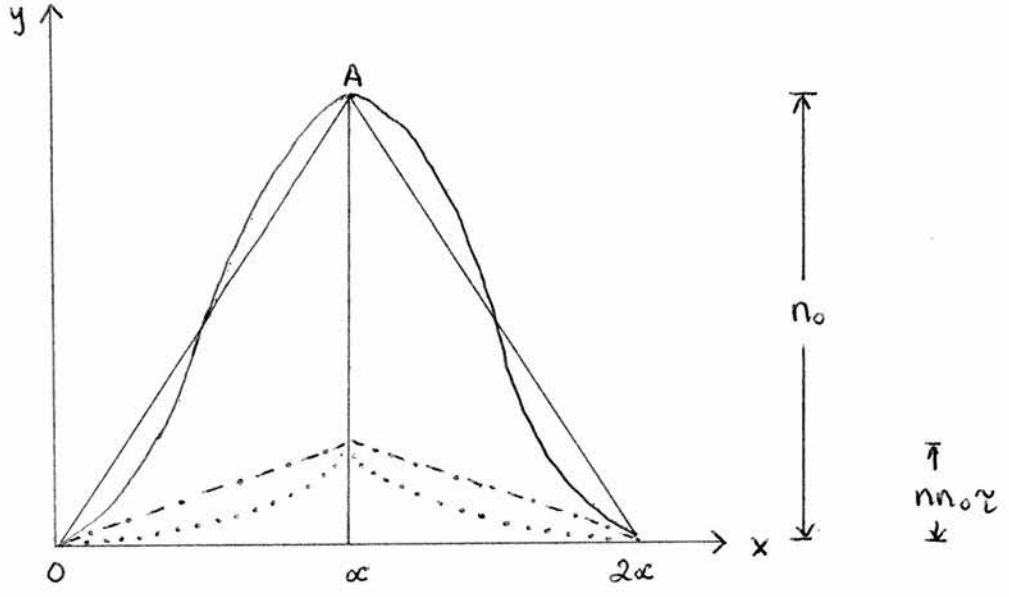

n_o is the observed peak counting rate; n is the corrected peak counting rate.

OA is given by $y = (n_o/\alpha) . x$

The counting loss curve (.....) corresponding to the triangular 'peak' is given, for $0 \leq x \leq \alpha$, by

$y = N - N_o = NN_o\tau$,

where $N_o = (n_o/a).\ x$ and $N = N_o/(1 - N_o\tau)$.

Hence

$$y = (n_o/a)^2.\ x^2.\ \tau\ [1 - (n_o/a).x.\ \tau\ ]^{-1}$$

$$= (n_o/a)^2.\ x^2.\ \tau\ (1 + (n_o/a).x.\tau),$$

neglecting terms in $(n_o\tau)^2$. Even for the highest recorded count rate of 7.5×10^4 cps $n_o\tau = 0.2$. For this same count rate

$$n_o^2\tau \doteqdot 1.5 \times 10^3 \text{ sec.}^{-1}$$

and $n_o^3\tau^2 \doteqdot .4 \times 10^3$ sec.$^{-1}$, so that, apart from the few extremely strong reflections, the $n_o^3\tau^2$ term may be neglected. Then

$$y = (n_o/a)^2.\tau\ .\ x^2,$$

so that the area under the curve(.....) is

$$2\int_o^a (n_o/a)^2.\tau\ .\ x^2\ dx = \frac{2}{3}.\ n_o^2.\tau.a.$$

The area under the triangle shown -.-.- is $n_o^2.\tau.a$. β, the ratio of these two areas, is given by

$$\beta = n_o^2.\tau\ .a \Big/ \frac{2}{3}.\ n_o^2.\tau\ .a = {}^3/_2,$$

a constant which is independent of peak width and Bragg angle (on both of which a depends). This approximate result is in reasonable agreement with the gradient of the empirical line (see below equation 4.8.1.) which gives

$$\beta = 2.6/2.$$

Hence the line used for counting loss corrections (see equation 4.8.1.),

$$(I_t - I) / I_t \doteq (\tau/\beta) \cdot n_o,$$

depends only on the value of the PHA paralysis time, τ .

APPENDIX 4

The observed structure amplitudes, and the calculated structure factors at the end of refinement

Overleaf are listed the indices and observed structure amplitudes, $|F_o|$, of the 3721 independent reflections measured on AHS. With each reflection is given the corresponding structure factor, F_c, calculated from the structural parameters at the end of refinement. Both $|F_o|$ and F_c are on a scale ten times the absolute scale. The 'accidentally absent' reflections ($|F_o| = 0$) are listed separately; so also are those reflections left out of the refinement because they were expected to be significantly affected by extinction.

Within each of these three groups reflections are listed by layer (k = 0, -1, ... -7). Each layer is separated into the systematically strong reflections (h = 4n), followed by the systematically weak reflections (h = 4n + 2) and the intermediate reflections (h odd). The latter are space group absent in the zero layer (k = 0). In each of these three categories, reflections (hkℓ) and (hk$\bar{\ell}$) are adjacent, except where one of the pair appears in another of the two groups of reflections.

h	k	l	|Fo|	Fc
36	0	0	25	-25
36	0	2	131	-125
36	0	-2	139	134
36	0	4	141	-136
36	0	-4	150	137
36	0	6	159	158
36	0	-6	171	-178
36	0	8	217	217
36	0	-8	256	-256
36	0	10	122	-118
36	0	-10	109	116
32	0	0	237	242
32	0	-2	105	102
32	0	4	295	-311
32	0	-4	318	-319
32	0	6	226	-213
32	0	-6	276	-273
32	0	8	246	246
32	0	-8	272	271
32	0	10	237	234
32	0	-10	254	243
32	0	12	141	-119
32	0	-12	101	-97
32	0	14	123	-118
32	0	-14	109	-117
28	0	2	237	266
28	0	-2	229	-248
28	0	4	168	174
28	0	-4	204	-211
28	0	6	333	-370
28	0	-6	329	319
28	0	8	462	-455
28	0	-8	513	499
28	0	10	148	145
28	0	-10	111	-126
28	0	12	379	367
28	0	-12	425	-427
28	0	14	56	-97
28	0	-14	25	32
28	0	16	203	-200
28	0	-16	217	211
24	0	0	928	-981
24	0	2	180	173
24	0	-2	163	151
24	0	4	891	915
24	0	-4	864	870
24	0	6	46	-40
24	0	-6	429	-418
24	0	8	399	-386
24	0	-8	247	-231
24	0	10	312	-248
24	0	-10	93	-79
24	0	12	139	-122
24	0	-12	204	189
24	0	14	259	259
24	0	-14	121	98
24	0	16	146	140
24	0	-16	152	-159
24	0	18	217	-204
20	0	2	985	-1010
20	0	-2	940	965
20	0	4	62	29
20	0	-4	59	-12
20	0	6	753	750
20	0	-6	704	-694
20	0	8	366	375
20	0	-8	417	-388
20	0	10	178	-150
20	0	-10	149	167
20	0	12	492	-481
20	0	-12	554	534
20	0	14	121	-97
20	0	-14	150	141
20	0	16	286	290
20	0	-16	328	-328
20	0	18	43	24
20	0	-18	56	-58
20	0	20	227	-221
20	0	-20	226	218
16	0	2	160	139
16	0	-2	295	266
16	0	6	306	-307
16	0	-6	399	-367
16	0	8	780	755
16	0	-8	831	840
16	0	10	455	437
16	0	-10	514	490
16	0	12	149	-131
16	0	-12	198	-199
16	0	14	245	-260
16	0	-14	322	-324
16	0	16	125	-131
16	0	-16	152	-144
16	0	18	156	173
16	0	-18	152	154
16	0	20	130	128
16	0	-20	159	153
12	0	0	113	-2
12	0	2	29	10
12	0	-2	51	-12
12	0	6	269	-275
12	0	-6	277	297
12	0	10	819	755
12	0	-10	853	-872
12	0	12	971	962
12	0	-12	1012	-1130
12	0	14	330	-340
12	0	-14	336	347
12	0	16	356	-372
12	0	-16	386	389
12	0	18	71	82
12	0	-18	90	-89
12	0	20	135	136
12	0	-20	107	-118
12	0	22	91	87
12	0	-22	102	-95
8	0	4	893	923
8	0	-4	967	983
8	0	8	737	-757
8	0	-8	757	-765
8	0	10	642	-672
8	0	-10	622	-655
8	0	12	628	615
8	0	-12	622	619
8	0	14	573	563
8	0	-14	624	637
8	0	16	59	16
8	0	-16	93	72
8	0	18	188	-211
8	0	-18	218	-213
8	0	20	157	-135
8	0	-20	174	-152
8	0	22	127	114
8	0	-22	111	107
4	0	0	33	8
4	0	6	241	-210
4	0	-6	291	245
4	0	8	342	369
4	0	-8	235	-256
4	0	10	564	-541
4	0	-10	481	499
4	0	12	921	-913
4	0	-12	933	943
4	0	14	132	117
4	0	-14	77	-58
4	0	16	638	674
4	0	-16	746	-725
4	0	18	98	93
4	0	-18	123	-122
4	0	20	248	-256
4	0	-20	264	267
4	0	22	43	-53
4	0	-22	37	48
0	0	2	955	1075
0	0	6	1018	1021
0	0	8	276	317
0	0	10	544	-527
0	0	12	96	-84
0	0	14	696	-674
0	0	16	421	-429
0	0	18	439	426
0	0	20	236	241
0	0	22	222	-226
38	0	2	25	8
38	0	-4	42	-40
38	0	6	60	-64
38	0	-6	62	-48
34	0	0	49	54
34	0	2	27	40
34	0	-2	53	-36
34	0	-4	45	-39
34	0	-6	62	68
34	0	8	80	-86
34	0	-8	85	84
34	0	10	34	-44
34	0	12	56	69
34	0	-12	55	-55
30	0	0	36	-20
30	0	2	28	58
30	0	-2	36	19
30	0	4	113	128
30	0	-4	58	45
30	0	6	80	82
30	0	-6	59	34
30	0	8	37	10
30	0	10	79	-91
30	0	-10	90	-95
30	0	12	67	-83
30	0	-12	53	-44
30	0	14	55	49
30	0	-14	50	46
26	0	0	49	-56
26	0	2	130	-135
26	0	-2	25	-25
26	0	-4	30	-49
26	0	6	175	211
26	0	-6	96	-94
26	0	8	130	139
26	0	-8	116	-111
26	0	10	95	98
26	0	-10	36	-27
26	0	12	40	16
26	0	-12	87	96
26	0	14	74	-95
26	0	-14	39	44
26	0	16	33	16
26	0	-16	64	-67
26	0	18	62	65
26	0	-18	42	-40
22	0	0	97	-91
22	0	2	129	-146
22	0	-2	91	-39
22	0	4	269	-288
22	0	-4	67	-15
22	0	6	218	-2.5
22	0	-6	76	-39
22	0	8	65	62
22	0	10	124	134
22	0	-10	109	111
22	0	12	127	142
22	0	-12	70	65
22	0	14	71	74
22	0	-14	72	-79
22	0	16	22	-46
22	0	-16	53	-53
22	0	18	53	36
22	0	-18	71	78
18	0	0	249	237
18	0	2	57	27
18	0	-2	125	142
18	0	4	57	-60
18	0	-4	53	-40
18	0	6	189	-230
18	0	-6	82	43
18	0	8	354	-371
18	0	-8	175	177
18	0	10	172	-157
18	0	-10	63	40
18	0	12	37	15
18	0	-12	91	-79
18	0	14	41	55
18	0	16	42	50
18	0	-16	133	133
18	0	18	44	-31
18	0	-18	61	52
18	0	20	33	15
18	0	-20	46	-48
14	0	0	249	161
14	0	2	357	376
14	0	-2	113	-96
14	0	4	209	199
14	0	-4	64	40
14	0	6	267	258
14	0	-6	147	175
14	0	8	123	102
14	0	-8	32	65
14	0	10	261	-294
14	0	-10	74	-45
14	0	12	184	-193
14	0	-12	46	21
14	0	14	32	10
14	0	-14	71	63
14	0	16	42	-15
14	0	-16	57	-32
14	0	18	115	-127
14	0	20	56	-52
14	0	-20	121	-126
14	0	22	36	-24
10	0	0	215	-232
10	0	2	86	-109
10	0	-2	36	-22
10	0	4	165	160
10	0	-4	190	184
10	0	6	121	134
10	0	-6	55	48
10	0	8	234	237
10	0	-8	198	-169
10	0	10	249	230
10	0	-10	86	-95
10	0	12	84	-73
10	0	-12	34	-50
10	0	14	84	-91
10	0	-14	165	-168
10	0	16	58	35
10	0	-16	167	-171
10	0	18	49	37
10	0	-18	68	-59
10	0	-20	47	71
10	0	22	67	-62
10	0	-22	79	99
6	0	0	48	42
6	0	2	120	-114
6	0	-2	66	63
6	0	4	163	-164
6	0	-4	75	-76
6	0	-6	280	-280
6	0	8	100	-93
6	0	-8	238	-241
6	0	10	32	-15
6	0	-10	127	-133
6	0	12	160	158
6	0	-12	65	-56
6	0	14	55	-70
6	0	-14	37	-15
6	0	16	144	-157
6	0	-16	44	55
6	0	18	67	46
6	0	-18	175	197
6	0	20	92	102
6	0	-20	156	162
2	0	0	26	8
2	0	2	44	-7
2	0	-2	92	-93
2	0	4	91	93
2	0	-4	343	-315
2	0	6	49	55
2	0	-6	111	-111
2	0	8	192	189
2	0	-8	114	118
2	0	10	55	55
2	0	-10	154	148
2	0	12	62	-61
2	0	-12	76	94
2	0	14	117	117
2	0	-14	112	133
2	0	-16	229	232
2	0	18	203	-221
2	0	-18	68	60
2	0	20	54	-70
2	0	-20	127	-150
2	0	22	60	69
2	0	-22	65	-72
36	-1	0	256	-264
36	-1	-2	94	-77
36	-1	4	235	230
36	-1	-4	229	229
36	-1	6	101	94
36	-1	-6	149	139
36	-1	8	160	-164
36	-1	-8	168	-167
32	-1	0	42	-29
32	-1	2	151	-153
32	-1	-2	154	141
32	-1	4	219	-217
32	-1	-4	276	277
32	-1	6	142	142
32	-1	-6	149	-147
32	-1	8	322	313
32	-1	-8	361	-358
32	-1	10	169	-165
32	-1	-10	159	160
32	-1	12	254	-245
32	-1	-12	272	264
28	-1	0	490	505
28	-1	2	64	52
28	-1	-2	110	99
28	-1	4	429	-437
28	-1	-4	431	-437
28	-1	6	193	-195
28	-1	-6	246	-234
28	-1	8	268	274
28	-1	-8	253	252
28	-1	10	244	239
28	-1	-10	282	260
28	-1	12	92	-97
28	-1	-12	98	-72
28	-1	14	196	-192
28	-1	-14	224	-220
28	-1	-16	35	-20
24	-1	0	28	5
24	-1	2	648	655
24	-1	-2	631	-644
24	-1	4	134	131
24	-1	-4	153	-150
24	-1	6	414	-420
24	-1	-6	375	382
24	-1	8	317	-310
24	-1	-8	348	346
24	-1	10	142	148
24	-1	-10	102	-99
24	-1	12	370	367
24	-1	-12	419	-416
24	-1	14	69	-11
24	-1	-14	33	-26
24	-1	16	284	-278
24	-1	-16	317	313
24	-1	-18	71	32
20	-1	2	78	73
20	-1	-2	32	41
20	-1	4	1065	1083
20	-1	-4	1039	1055
20	-1	6	54	14
20	-1	-6	460	-466
20	-1	8	449	-449
20	-1	-8	177	-168
20	-1	10	227	-214
20	-1	-10	32	10
20	-1	12	35	-12
20	-1	-12	267	254
20	-1	14	243	246
20	-1	-14	142	137
20	-1	16	160	166
20	-1	-16	227	-220
20	-1	18	236	-231
20	-1	-18	124	-129
20	-1	20	153	-141
16	-1	0	56	-15
16	-1	2	742	-744
16	-1	-2	722	723
16	-1	4	504	-494
16	-1	-4	567	576
16	-1	6	636	641
16	-1	-6	635	-649
16	-1	8	699	697
16	-1	-8	751	-750
16	-1	10	366	-354
16	-1	-10	393	410
16	-1	12	580	-576
16	-1	-12	619	613
16	-1	14	112	117
16	-1	-14	109	-108
16	-1	16	352	359
16	-1	-16	355	-352
16	-1	-18	78	-43
16	-1	20	169	-173
16	-1	-20	153	163
12	-1	0	845	865
12	-1	2	485	440
12	-1	-2	588	576
12	-1	4	547	-520
12	-1	-4	907	-923
12	-1	6	914	-913
12	-1	-6	986	-978
12	-1	8	735	744
12	-1	-8	567	563
12	-1	10	71	726
12	-1	-10	765	769
12	-1	12	393	-392
12	-1	-12	419	-425
12	-1	14	374	-369
12	-1	-14	404	-419
12	-1	16	17	100
12	-1	-16	152	155
12	-1	18	150	138
12	-1	-18	169	152
12	-1	20	9	-93
12	-1	-20	90	-87
8	-1	0	43	46
8	-1	2	136	108
8	-1	-2	155	-124
8	-1	6	576	-578
8	-1	-6	570	595
8	-1	10	638	633
8	-1	-10	603	-619
8	-1	12	919	942
8	-1	-12	953	-953
8	-1	14	302	-338
8	-1	-14	262	274
8	-1	16	454	-465
8	-1	-16	492	498
8	-1	18	45	37
8	-1	-18	40	-24
8	-1	20	177	179
8	-1	-20	190	-184
8	-1	22	89	90
8	-1	-22	75	-76
4	-1	2	81	49
4	-1	-2	110	58
4	-1	6	31	54
4	-1	-6	61	-34
4	-1	8	836	-842
4	-1	-8	802	-792
4	-1	10	394	-408
4	-1	-10	389	-391
4	-1	12	121	126
4	-1	-12	69	66
4	-1	14	487	489
4	-1	-14	527	535
4	-1	16	163	160
4	-1	-16	183	190
4	-1	18	344	-339
4	-1	-18	367	-367
4	-1	20	199	-192
4	-1	-20	191	-189
4	-1	22	173	170
4	-1	-22	178	177
0	-1	4	57	-137
0	-1	6	1024	1039
0	-1	8	389	401
0	-1	10	127	-186
0	-1	12	759	-755
0	-1	14	86	-99
0	-1	16	635	624
0	-1	18	112	112
0	-1	20	319	-321
0	-1	22	78	-81
38	-1	2	47	-34
38	-1	-2	54	50
38	-1	4	39	-19
38	-1	-4	43	43
38	-1	-6	40	-39
34	-1	0	50	52
34	-1	2	41	-3
34	-1	-2	43	38
34	-1	4	61	-57
34	-1	6	43	-51
34	-1	-6	69	-61
34	-1	8	37	-6
34	-1	10	77	81
34	-1	-10	58	53
34	-1	12	25	25
34	-1	-12	25	7
30	-1	2	70	66
30	-1	-2	58	-44
30	-1	4	34	42
30	-1	-4	57	-56
30	-1	6	57	-46
30	-1	-6	76	-71
30	-1	8	97	102
30	-1	10	34	-17
30	-1	-10	27	2
30	-1	12	73	67
30	-1	-12	75	-81
30	-1	14	43	47
30	-1	-14	24	-13
26	-1	0	76	-75
26	-1	2	54	-53
26	-1	4	108	115
26	-1	-4	52	31
26	-1	6	76	75
26	-1	-6	76	68
26	-1	8	53	-44
26	-1	10	66	-56
26	-1	-10	99	-99
26	-1	12	45	-39
26	-1	14	47	39
26	-1	-14	74	71
26	-1	16	61	62
26	-1	-16	45	42
22	-1	2	95	-99
22	-1	-2	57	48
22	-1	4	89	-93
22	-1	-4	90	89
22	-1	6	85	82
22	-1	-6	104	98

h	k	l	|Fo|	Fc
22	-1	-8	115	-111
22	-1	10	31	5
22	-1	-10	29	-32
22	-1	12	51	-38
22	-1	-12	115	120
22	-1	14	55	-66
22	-1	-14	48	49
22	-1	-16	90	-94
22	-1	18	91	93
22	-1	-18	45	-37
18	-1	0	117	123
18	-1	2	87	-77
18	-1	-2	134	128
18	-1	4	59	-41
18	-1	-4	116	-122
18	-1	6	99	-93
18	-1	-6	76	-68
18	-1	8	73	-68
18	-1	-8	57	49
18	-1	10	106	107
18	-1	-10	73	68
18	-1	12	76	77
18	-1	-12	50	39
18	-1	14	66	-61
18	-1	-14	80	-81
18	-1	16	70	-81
18	-1	-16	55	-74
18	-1	18	42	20
18	-1	-18	72	63
18	-1	20	56	65
18	-1	-20	63	54
14	-1	0	170	175
14	-1	2	91	80
14	-1	-2	90	-94
14	-1	4	45	35
14	-1	-4	143	-153
14	-1	6	91	92
14	-1	-6	58	61
14	-1	8	155	-153
14	-1	-8	117	120
14	-1	10	118	-113
14	-1	-10	39	-27
14	-1	12	117	118
14	-1	-12	130	-126
14	-1	14	34	50
14	-1	-14	27	-17
14	-1	16	61	-30
14	-1	-16	101	101
14	-1	18	52	-57
14	-1	-18	54	51
14	-1	-20	43	-46
14	-1	22	68	60
14	-1	-22	42	-43
10	-1	0	142	-142
10	-1	2	43	9
10	-1	-2	145	-143
10	-1	4	75	59
10	-1	-4	47	28
10	-1	6	122	111
10	-1	-6	127	128
10	-1	8	137	144
10	-1	-8	64	-53
10	-1	10	90	-81
10	-1	-10	107	-112
10	-1	12	121	-123
10	-1	-12	56	44
10	-1	14	88	83
10	-1	-14	96	89
10	-1	16	86	93
10	-1	-16	47	40
10	-1	18	54	-30
10	-1	-18	50	-51
10	-1	20	73	-71
10	-1	-20	71	-64
10	-1	-22	38	26
6	-1	0	198	165
6	-1	2	86	-77
6	-1	-2	215	-205
6	-1	4	346	-350
6	-1	-4	170	154
6	-1	6	83	68
6	-1	-6	145	133
6	-1	8	125	103
6	-1	-8	231	-233
6	-1	10	40	35
6	-1	-10	52	27
6	-1	12	36	3
6	-1	-12	187	184
6	-1	14	83	-93
6	-1	-14	50	-32
6	-1	16	33	-1
6	-1	-16	135	-135
6	-1	18	105	109
6	-1	-18	53	-32
6	-1	20	29	33
6	-1	-20	62	66
6	-1	22	92	-56
6	-1	-22	32	41
2	-1	0	65	51
2	-1	2	116	109
2	-1	-2	53	43
2	-1	-4	34	-57
2	-1	6	95	-93
2	-1	-6	81	-97
2	-1	8	57	-65
2	-1	-8	27	31
2	-1	10	46	-44
2	-1	-10	79	91
2	-1	12	131	133
2	-1	-12	44	2
2	-1	14	42	21
2	-1	-14	120	-126
2	-1	16	167	-179
2	-1	-16	46	-41
2	-1	18	34	-11
2	-1	-18	114	119
2	-1	20	115	119
2	-1	-20	57	61
2	-1	-22	67	-65
39	-1	3	37	-45
39	-1	-3	69	-81
37	-1	-1	25	3
37	-1	3	86	84
37	-1	-5	47	-12
37	-1	7	43	1
35	-1	-3	37	-16
35	-1	5	69	-66
35	-1	-5	69	62
35	-1	7	76	-68
35	-1	-7	69	47
33	-1	1	56	-16
33	-1	-1	60	-28
33	-1	3	57	-33
33	-1	-3	83	-56
33	-1	7	94	72
33	-1	-7	78	39
33	-1	13	52	46
31	-1	1	69	68
31	-1	-1	31	23
31	-1	3	50	-49
31	-1	-3	74	-95
31	-1	5	72	75
31	-1	-5	68	50
31	-1	7	69	62
31	-1	-7	45	29
31	-1	9	134	-127
31	-1	-9	130	-117
31	-1	11	56	-46
31	-1	13	40	40
31	-1	-13	66	69
29	-1	1	120	-114
29	-1	-1	93	83
29	-1	3	108	-94
29	-1	-3	77	41
29	-1	5	35	48
29	-1	-5	48	-76
29	-1	7	38	-18
29	-1	-7	45	-6
29	-1	9	44	-26
29	-1	-9	30	11
29	-1	11	62	54
29	-1	-11	46	-17
29	-1	-15	59	-4
27	-1	1	63	-51
27	-1	-1	38	-23
27	-1	3	57	-40
27	-1	-3	58	62
27	-1	5	30	-3
27	-1	7	78	82
27	-1	-7	73	-41
27	-1	-9	36	40
27	-1	11	78	-66
27	-1	-11	94	92
27	-1	-15	47	-32
27	-1	17	42	-39
25	-1	1	87	50
25	-1	-1	51	28
25	-1	3	98	-102
25	-1	-3	96	-105
25	-1	5	76	-62
25	-1	-11	85	65
25	-1	17	37	25
25	-1	-17	82	56
23	-1	1	155	155
23	-1	-1	170	176
23	-1	-3	62	57
23	-1	-5	47	52
23	-1	7	34	-21
23	-1	9	44	25
23	-1	11	76	54
23	-1	-11	40	4
23	-1	13	59	-67
23	-1	-13	96	-109
23	-1	15	78	-58
23	-1	-15	77	-73
23	-1	-17	65	44
23	-1	19	63	-8
21	-1	1	150	134
21	-1	-1	97	-91
21	-1	3	38	20
21	-1	5	190	-207
21	-1	-5	269	277
21	-1	7	97	-97
21	-1	-7	149	147
21	-1	11	57	-14
21	-1	15	43	24
21	-1	-15	53	-55
21	-1	-17	45	-27
21	-1	-19	72	-41
19	-1	1	435	441
19	-1	-1	408	-413
19	-1	3	352	336
19	-1	-3	284	-283
19	-1	5	132	-155
19	-1	-5	79	65
19	-1	7	214	216
19	-1	-7	293	-303
19	-1	9	222	227
19	-1	-9	229	-229
19	-1	11	66	-50
19	-1	-11	42	40
19	-1	13	69	58
19	-1	-13	36	-39
19	-1	15	59	36
19	-1	-15	57	-91
19	-1	17	104	97
19	-1	-17	45	-5
19	-1	19	46	-6
17	-1	1	380	389
17	-1	-1	354	343
17	-1	3	57	-37
17	-1	-3	57	-59
17	-1	5	128	135
17	-1	-5	140	140
17	-1	7	49	46
17	-1	-7	25	-11
17	-1	9	307	-300
17	-1	-9	397	-402
17	-1	11	133	-120
17	-1	-11	164	-169
17	-1	13	78	83
17	-1	-13	64	48
17	-1	15	97	-36
17	-1	-15	75	-66
17	-1	17	63	-34
17	-1	-17	71	-57
17	-1	19	69	37
17	-1	-19	71	35
17	-1	21	45	3
15	-1	1	614	-620
15	-1	-1	603	-616
15	-1	3	256	-235
15	-1	-3	321	-310
15	-1	5	48	-43
15	-1	-5	102	-107
15	-1	7	54	-63
15	-1	-7	25	5
15	-1	9	78	75
15	-1	-9	115	119
15	-1	11	137	152
15	-1	-11	157	166
15	-1	13	143	156
15	-1	-13	165	163
15	-1	15	130	137
15	-1	-15	99	99
15	-1	-17	25	-16
15	-1	19	26	-34
15	-1	-19	36	-31
13	-1	1	234	227
13	-1	-1	331	-330
13	-1	3	326	302
13	-1	-3	320	-299
13	-1	5	254	270
13	-1	-5	328	-310
13	-1	7	402	399
13	-1	-7	512	-523
13	-1	9	45	41
13	-1	-9	29	-25
13	-1	11	210	-216
13	-1	-11	252	270
13	-1	13	92	-78
13	-1	-13	45	51
13	-1	15	70	-36
13	-1	-15	74	60
13	-1	17	95	-72
13	-1	-17	120	117
13	-1	-19	45	38
13	-1	-21	66	30
11	-1	1	131	-151
11	-1	-1	65	59
11	-1	3	592	-582
11	-1	-3	603	698
11	-1	5	601	-568
11	-1	-5	621	617
11	-1	7	203	-204
11	-1	-7	229	232
11	-1	9	382	-407
11	-1	-9	373	371
11	-1	11	287	-315
11	-1	-11	252	262
11	-1	13	57	64
11	-1	-13	30	-75
11	-1	15	60	75
11	-1	-15	65	-72
11	-1	17	47	61
11	-1	-17	37	-19
11	-1	19	62	98
11	-1	-19	58	-32
11	-1	21	43	16
11	-1	-21	56	8
9	-1	1	677	-647
9	-1	-1	715	-676
9	-1	3	68	-42
9	-1	-3	65	-49
9	-1	5	52	6
9	-1	-5	93	75
9	-1	7	242	219
9	-1	-7	272	259
9	-1	9	435	445
9	-1	-9	491	505
9	-1	11	248	233
9	-1	-11	254	258
9	-1	13	34	-55
9	-1	-13	56	-69
9	-1	15	60	-65
9	-1	-15	60	-59
9	-1	17	50	2
9	-1	-17	68	-72
9	-1	19	67	-57
9	-1	-19	98	-99
9	-1	21	68	-77
9	-1	-21	46	-16
9	-1	-23	49	-37
7	-1	1	283	269
7	-1	-1	396	414
7	-1	5	115	96
7	-1	-5	86	77
7	-1	7	364	-357
7	-1	-7	353	-315
7	-1	9	317	325
7	-1	-9	258	271
7	-1	11	175	-190
7	-1	-11	167	-167
7	-1	13	444	-526
7	-1	-13	396	-432
7	-1	15	78	-101
7	-1	-15	41	-36
7	-1	17	46	21
7	-1	-17	30	27
7	-1	19	80	-56
7	-1	-19	77	-70
7	-1	-23	39	-7
5	-1	1	716	724
5	-1	-1	703	-661
5	-1	3	225	-165
5	-1	-3	269	213
5	-1	5	1097	-1098
5	-1	7	80	81
5	-1	-7	124	-95
5	-1	9	327	328
5	-1	-9	384	-382
5	-1	11	57	45
5	-1	-11	65	-62
5	-1	13	251	229
5	-1	-13	245	-243
5	-1	15	194	173
5	-1	-15	142	-137
5	-1	17	37	-36
5	-1	-17	78	76
5	-1	-19	38	-15
5	-1	21	40	34
5	-1	-21	43	-48
5	-1	23	37	-50
5	-1	-23	63	38
3	-1	1	391	414
3	-1	-1	394	-377
3	-1	3	379	400
3	-1	-3	372	-355
3	-1	5	133	106
3	-1	-5	124	-94
3	-1	7	325	296
3	-1	-7	312	-305
3	-1	9	452	470
3	-1	-9	396	-406
3	-1	11	356	378
3	-1	-11	281	-279
3	-1	13	91	86
3	-1	-13	92	-88
3	-1	15	66	-79
3	-1	17	62	-74
3	-1	19	69	-58
3	-1	-19	38	14
3	-1	21	49	-32
3	-1	-23	55	16
1	-1	1	266	-255
1	-1	-1	259	-260
1	-1	3	232	204
1	-1	-3	239	221
1	-1	5	445	-416
1	-1	-5	513	-467
1	-1	7	479	-466
1	-1	-7	514	-509
1	-1	9	90	-88
1	-1	-9	49	-66
1	-1	11	107	-92
1	-1	-11	93	-79
1	-1	13	66	69
1	-1	-13	147	161
1	-1	15	178	177
1	-1	-15	252	259
1	-1	17	55	58
1	-1	19	59	19
1	-1	-19	26	-19
1	-1	21	93	80
1	-1	-21	77	71
1	-1	23	51	38
1	-1	-23	34	3
36	-2	0	32	21
36	-2	2	195	192
36	-2	-2	182	-189
36	-2	4	99	84
36	-2	-4	131	-125
36	-2	6	143	-137
36	-2	-6	121	121
36	-2	8	123	-112
32	-2	0	334	-336
32	-2	2	162	-83
32	-2	-2	142	-131
32	-2	4	242	245
32	-2	-4	224	236
32	-2	6	144	144
32	-2	-6	195	192
32	-2	8	179	-171
32	-2	-8	141	-140
32	-2	10	139	-137
32	-2	-10	152	-147
32	-2	12	103	98
32	-2	-12	92	96
28	-2	0	34	-20
28	-2	2	358	-355
28	-2	-2	349	354
28	-2	4	282	-260
28	-2	-4	329	306
28	-2	6	188	191
28	-2	-6	157	-160
28	-2	8	251	239
28	-2	-8	272	-276
28	-2	10	151	-169
28	-2	-10	162	154
28	-2	12	242	-248
28	-2	-12	267	264
28	-2	14	87	84
28	-2	-14	56	-83
24	-2	0	783	766
24	-2	2	164	152
24	-2	-2	212	179
24	-2	4	495	-498
24	-2	-4	490	-495
24	-2	6	216	-196
24	-2	-6	253	-246
24	-2	8	221	244
24	-2	-8	196	200
24	-2	10	160	171
24	-2	-10	178	195
24	-2	12	147	-155
24	-2	-12	119	-116
24	-2	14	253	-263
24	-2	-14	277	-271
24	-2	16	40	-43
24	-2	-16	72	-47
24	-2	18	147	150
20	-2	0	37	15
20	-2	2	793	771
20	-2	-2	808	-782
20	-2	4	311	292
20	-2	-4	365	-345
20	-2	6	357	-378
20	-2	-6	361	386
20	-2	8	301	-280
20	-2	-8	330	348
20	-2	10	198	226
20	-2	-10	181	-182
20	-2	12	342	351
20	-2	-12	344	-339
20	-2	14	101	-86
20	-2	-14	92	77
20	-2	16	337	-334
20	-2	-16	340	329
20	-2	18	92	-80
20	-2	-18	108	85
16	-2	0	1058	-1031
16	-2	2	100	-86
16	-2	-2	155	-137
16	-2	4	870	867
16	-2	-4	898	905
16	-2	6	336	307
16	-2	-6	397	397
16	-2	8	389	-428
16	-2	-8	409	-432
16	-2	10	314	-310
16	-2	-10	339	-345
16	-2	12	162	180
16	-2	-12	159	155
16	-2	14	353	362
16	-2	-14	339	314
16	-2	16	54	57
16	-2	-16	37	45
16	-2	18	257	-246
16	-2	-18	250	-243
16	-2	20	151	-139
16	-2	-20	165	-156
12	-2	2	536	-538
12	-2	-2	547	544
12	-2	4	412	-382
12	-2	-4	444	435
12	-2	6	746	761
12	-2	-6	757	-796
12	-2	8	857	833
12	-2	-8	911	-922
12	-2	10	314	-351
12	-2	-10	305	315
12	-2	12	550	-572
12	-2	-12	571	564
12	-2	14	172	166
12	-2	-14	169	-169
12	-2	16	398	396
12	-2	-16	379	-375
12	-2	18	66	51
12	-2	-18	48	-30
12	-2	20	166	-161
12	-2	-20	176	172
8	-2	0	427	452
8	-2	2	321	-341
8	-2	-2	370	-339
8	-2	4	596	-569
8	-2	-4	617	-607
8	-2	6	715	691
8	-2	-6	791	788
8	-2	8	739	761
8	-2	-8	800	807
8	-2	10	138	-154
8	-2	-10	95	-88
8	-2	12	349	-375
8	-2	-12	369	-378
8	-2	14	281	275
8	-2	-14	293	299

h	k	l	|Fo|	Fc
8	-2	20	174	156
8	-2	-20	151	138
8	-2	22	120	-102
8	-2	-22	106	-114
4	-2	0	32	-6
4	-2	2	519	552
4	-2	-2	501	-529
4	-2	4	337	-305
4	-2	-4	374	349
4	-2	10	269	272
4	-2	-10	226	-196
4	-2	12	648	673
4	-2	-12	681	-697
4	-2	14	56	-54
4	-2	-14	37	30
4	-2	16	384	-389
4	-2	-16	401	415
4	-2	20	233	230
4	-2	-20	248	-252
4	-2	22	136	117
4	-2	-22	113	-104
0	-2	0	686	-743
0	-2	6	135	153
0	-2	8	1044	-1026
0	-2	10	794	-807
0	-2	12	111	-124
0	-2	14	326	339
0	-2	16	64	64
0	-2	18	335	-336
0	-2	20	168	-162
0	-2	22	151	155
38	-2	0	25	-65
34	-2	2	59	-47
34	-2	-2	65	70
34	-2	4	31	-54
34	-2	-4	60	74
34	-2	6	47	15
34	-2	8	56	49
34	-2	-8	53	-93
34	-2	10	26	-15
30	-2	0	97	101
30	-2	2	82	109
30	-2	-2	69	57
30	-2	6	49	-46
30	-2	-6	96	-115
30	-2	8	63	44
30	-2	10	69	51
30	-2	-10	76	65
30	-2	12	47	-11
30	-2	-12	46	-32
30	-2	14	68	-63
30	-2	-14	46	-45
26	-2	0	137	-136
26	-2	-2	38	-61
26	-2	4	191	207
26	-2	-4	124	-142
26	-2	-6	78	-85
26	-2	8	59	-48
26	-2	-8	136	136
26	-2	10	125	119
26	-2	-10	41	19
26	-2	12	126	117
26	-2	-12	137	-134
26	-2	14	34	15
26	-2	-14	41	2
26	-2	16	40	-40
26	-2	-16	80	77
22	-2	0	232	-264
22	-2	2	146	-162
22	-2	-2	88	-82
22	-2	4	72	-77
22	-2	-4	126	140
22	-2	6	46	-41
22	-2	-6	100	92
22	-2	10	43	-16
22	-2	-10	73	-57
22	-2	14	154	147
22	-2	-14	77	77
22	-2	16	139	136
22	-2	-16	68	58
18	-2	0	41	41
18	-2	2	103	-96
18	-2	-2	310	347
18	-2	4	65	-66
18	-2	-4	117	120
18	-2	6	194	-212
18	-2	-6	91	-85
18	-2	8	78	-97
18	-2	-8	41	-18
18	-2	10	57	-33
18	-2	12	200	-180
18	-2	-12	129	126
18	-2	14	87	-76
18	-2	-14	125	126
18	-2	16	114	117
18	-2	-16	74	-70
18	-2	18	101	112
18	-2	-18	40	-43
18	-2	20	50	32
18	-2	-20	56	70
14	-2	0	450	447
14	-2	2	54	7
14	-2	-2	135	167
14	-2	4	171	151
14	-2	-4	373	-365
14	-2	6	204	202
14	-2	-6	60	5
14	-2	8	140	-149
14	-2	-8	247	238
14	-2	10	39	-28
14	-2	-10	50	63
14	-2	12	68	72
14	-2	-12	53	93
14	-2	14	181	-181
14	-2	-14	48	-50
14	-2	16	139	-168
14	-2	-16	126	-137
14	-2	18	29	30
14	-2	20	79	84
10	-2	0	266	-265
10	-2	2	37	-47
10	-2	-2	57	60
10	-2	4	374	372
10	-2	-4	103	-65
10	-2	6	73	78
10	-2	-6	29	7
10	-2	8	104	-78
10	-2	-8	220	232
10	-2	10	114	96
10	-2	-10	104	-117
10	-2	12	147	119
10	-2	-12	327	-347
10	-2	14	54	49
10	-2	-14	102	-114
10	-2	16	29	-24
10	-2	-16	52	42
10	-2	18	107	-96
10	-2	-18	38	-1
10	-2	20	48	-52
10	-2	-20	54	-34
10	-2	22	51	48
6	-2	0	90	106
6	-2	2	435	-425
6	-2	-2	135	85
6	-2	4	59	38
6	-2	-4	169	-163
6	-2	6	284	257
6	-2	-6	122	124
6	-2	8	121	-107
6	-2	-8	221	-239
6	-2	10	126	-63
6	-2	-10	418	-426
6	-2	12	28	-57
6	-2	-12	39	45
6	-2	14	50	-47
6	-2	-14	165	183
6	-2	16	122	126
6	-2	-16	55	68
6	-2	18	36	43
6	-2	-18	59	50
6	-2	20	110	-101
6	-2	-20	39	32
6	-2	-22	65	54
2	-2	0	384	382
2	-2	2	131	121
2	-2	-2	406	-407
2	-2	4	498	-502
2	-2	-4	159	-89
2	-2	6	144	154
2	-2	-6	78	75
2	-2	8	358	362
2	-2	-8	286	-276
2	-2	10	52	39
2	-2	-10	111	111
2	-2	12	88	-13
2	-2	-12	401	428
2	-2	14	76	-86
2	-2	-14	83	101
2	-2	16	89	-110
2	-2	-16	85	-101
2	-2	18	42	27
2	-2	-18	55	19
2	-2	20	39	21
2	-2	-20	69	54
2	-2	22	94	-79
2	-2	-22	45	-28
37	-2	-1	25	0
37	-2	3	56	42
37	-2	-3	48	42
37	-2	5	53	-35
37	-2	-5	36	-41
35	-2	1	56	20
35	-2	-1	40	26
35	-2	3	43	-4
35	-2	5	50	-60
35	-2	-5	76	-60
35	-2	9	77	62
33	-2	1	62	51
33	-2	-1	47	-44
33	-2	3	45	52
33	-2	-3	74	-65
33	-2	-7	81	58
33	-2	11	40	12
33	-2	-11	54	-46
31	-2	1	65	34
31	-2	3	76	54
31	-2	-3	110	-100
31	-2	-5	29	2
31	-2	7	97	-104
31	-2	-7	125	128
31	-2	-9	47	-36
31	-2	11	78	76
31	-2	-11	98	-89
31	-2	13	52	-34
29	-2	1	72	-67
29	-2	-1	48	-51
29	-2	5	83	44
29	-2	-5	42	46
29	-2	9	36	-25
29	-2	-9	62	-42
29	-2	11	66	-50
29	-2	-11	76	56
29	-2	13	68	48
29	-2	-13	25	-17
27	-2	1	120	-104
27	-2	-1	133	-124
27	-2	3	100	90
27	-2	-3	123	117
27	-2	5	143	133
27	-2	-5	100	90
27	-2	7	164	-161
27	-2	-7	185	-177
27	-2	9	58	-67
27	-2	11	157	142
27	-2	-11	149	142
25	-2	1	229	-222
25	-2	-1	224	237
25	-2	3	132	-125
25	-2	-3	162	155
25	-2	5	175	178
25	-2	-5	186	-199
25	-2	7	34	-5
25	-2	-7	69	-52
25	-2	9	71	75
25	-2	-9	61	59
25	-2	11	39	-33
25	-2	-11	25	22
25	-2	13	45	-34
25	-2	-13	60	7
25	-2	15	40	56
25	-2	-15	68	-58
25	-2	17	234	-228
25	-2	-17	222	223
23	-2	1	182	-174
23	-2	-1	143	130
23	-2	3	143	154
23	-2	-3	137	-135
23	-2	5	33	42
23	-2	-5	35	-10
23	-2	7	60	41
23	-2	-7	39	41
23	-2	9	61	-33
23	-2	-9	72	59
23	-2	11	34	36
23	-2	-11	60	-55
21	-2	1	109	98
21	-2	-1	104	94
21	-2	3	55	-24
21	-2	-3	66	-57
21	-2	5	102	-95
21	-2	-5	120	-129
21	-2	7	48	-20
21	-2	9	102	108
21	-2	-9	100	111
21	-2	11	56	55
21	-2	-11	73	-75
21	-2	13	96	-83
21	-2	-13	41	-41
21	-2	15	85	69
21	-2	-15	45	13
21	-2	17	31	36
21	-2	-17	327	324
19	-2	1	252	242
19	-2	-1	234	-244
19	-2	3	221	-227
19	-2	-3	114	-103
19	-2	5	42	-5
19	-2	-5	89	112
19	-2	7	48	75
19	-2	-7	45	-17
19	-2	9	63	50
19	-2	-9	75	65
19	-2	11	32	-24
19	-2	-11	71	-66
19	-2	13	123	-111
19	-2	-13	129	-123
19	-2	15	79	67
19	-2	-15	76	63
19	-2	17	78	67
19	-2	-17	112	67
17	-2	1	63	-49
17	-2	-1	138	130
17	-2	3	219	-206
17	-2	-3	72	-40
17	-2	5	42	21
17	-2	-5	169	-192
17	-2	7	280	290
17	-2	-7	62	39
17	-2	9	47	-30
17	-2	-9	132	135
17	-2	11	179	-181
17	-2	-11	44	-19
17	-2	13	67	52
17	-2	-13	49	-24
17	-2	15	45	53
17	-2	-15	27	11
17	-2	17	44	-28
15	-2	1	452	446
15	-2	-1	497	-483
15	-2	3	402	380
15	-2	-3	299	-299
15	-2	5	353	-355
15	-2	-5	305	302
15	-2	7	76	-59
15	-2	9	214	227
15	-2	-9	175	-184
15	-2	11	31	-35
15	-2	13	33	-6
15	-2	-13	25	-29
15	-2	15	58	54
15	-2	-15	76	-81
15	-2	17	99	92
15	-2	-17	73	75
15	-2	21	50	-65
13	-2	1	169	146
13	-2	-1	208	176
13	-2	3	346	-342
13	-2	-3	374	-378
13	-2	5	251	273
13	-2	-5	252	256
13	-2	7	210	207
13	-2	-7	273	276
13	-2	9	395	-390
13	-2	-9	429	-447
13	-2	11	80	-87
13	-2	-11	129	-122
13	-2	13	219	221
13	-2	-13	267	268
13	-2	17	89	-82
13	-2	-17	110	-122
13	-2	19	52	36
13	-2	-21	25	34
11	-2	1	80	58
11	-2	-1	63	-62
11	-2	3	431	-421
11	-2	-3	423	-408
11	-2	5	252	243
11	-2	-5	366	369
11	-2	7	247	233
11	-2	-7	202	177
11	-2	9	388	-391
11	-2	-9	384	-393
11	-2	11	73	-41
11	-2	13	256	260
11	-2	-13	238	244
11	-2	17	76	-81
11	-2	-17	72	-73
9	-2	1	363	-355
9	-2	-1	269	249
9	-2	3	222	-223
9	-2	-3	220	229
9	-2	5	341	323
9	-2	-5	325	-315
9	-2	7	215	220
9	-2	-7	246	-255
9	-2	9	85	-73
9	-2	-9	103	105
9	-2	11	78	-77
9	-2	-11	130	129
9	-2	13	62	-51
9	-2	-13	52	36
9	-2	17	52	43
9	-2	-17	60	-38
9	-2	19	26	-21
9	-2	-19	44	18
9	-2	21	47	-40
9	-2	-21	43	57
7	-2	1	174	154
7	-2	-1	117	-104
7	-2	3	221	-207
7	-2	-3	354	364
7	-2	5	275	-271
7	-2	-5	201	185
7	-2	7	446	444
7	-2	-7	468	-457
7	-2	9	25	-4
7	-2	11	395	-415
7	-2	-11	316	318
7	-2	13	39	56
7	-2	-13	65	-64
7	-2	15	98	119
7	-2	-15	90	-88
7	-2	17	47	-58
7	-2	-17	27	34
5	-2	1	240	235
5	-2	-1	316	323
5	-2	3	545	-531
5	-2	-3	472	-463
5	-2	5	138	-135
5	-2	-5	60	-33
5	-2	7	205	169
5	-2	-7	285	270
5	-2	9	77	82
5	-2	-9	77	60
5	-2	11	128	144
5	-2	-11	161	167
5	-2	13	31	-29
5	-2	-13	62	-37
5	-2	15	129	-120
5	-2	-15	195	-192
5	-2	17	73	68
5	-2	-17	93	86
5	-2	19	55	59
5	-2	-19	87	92
5	-2	21	72	-63
5	-2	-21	108	-94
3	-2	1	58	-44
3	-2	-1	57	-53
3	-2	3	347	350
3	-2	-3	206	195
3	-2	5	157	-159
3	-2	-5	299	-298
3	-2	7	153	-201
3	-2	-7	179	-192
3	-2	9	425	425
3	-2	-9	365	366
3	-2	11	167	172
3	-2	-11	115	124
3	-2	13	300	-309
3	-2	-13	237	-226
3	-2	15	73	-71
3	-2	-15	44	-20
3	-2	17	124	136
3	-2	-17	95	104
3	-2	19	28	-15
3	-2	-19	40	-8
3	-2	21	59	-28
1	-2	-1	596	-578
1	-2	3	316	302
1	-2	-3	460	-458
1	-2	5	877	-877
1	-2	-5	925	941
1	-2	7	36	48
1	-2	9	170	158
1	-2	-9	297	-300
1	-2	11	94	-104
1	-2	-11	52	46
1	-2	13	116	114
1	-2	-13	124	-122
1	-2	15	62	55
1	-2	-15	42	-50
1	-2	17	92	-99
1	-2	-17	103	113
1	-2	21	88	81
1	-2	-21	54	-70
1	-2	-23	27	28
36	-3	0	192	192
36	-3	2	45	11
36	-3	-2	60	41
32	-3	2	258	261
32	-3	-2	238	-242
32	-3	4	94	77
32	-3	-4	109	-100
32	-3	6	188	-181
32	-3	-6	155	162
32	-3	8	116	-112
32	-3	-8	137	127
32	-3	10	81	86
32	-3	-10	72	-80
28	-3	0	320	-322
28	-3	2	66	-77
28	-3	-2	114	-106
28	-3	4	280	283
28	-3	-4	253	250
28	-3	6	184	185
28	-3	-6	200	197
28	-3	8	179	-183
28	-3	-8	158	-158
28	-3	10	181	-177
28	-3	-10	196	-200
28	-3	12	92	89
28	-3	-12	68	69
28	-3	14	135	137
24	-3	0	44	-25
24	-3	2	384	-386
24	-3	-2	380	376
24	-3	4	210	-215
24	-3	-4	254	254
24	-3	6	284	281
24	-3	-6	280	-269
24	-3	8	273	273
24	-3	-8	297	-302
24	-3	10	180	-182
24	-3	-10	167	166
24	-3	12	227	-236
24	-3	-12	245	252
24	-3	14	72	67
24	-3	-14	54	-56
24	-3	16	153	152
24	-3	-16	165	-166
20	-3	0	550	549
20	-3	2	129	123
20	-3	-2	166	163
20	-3	4	442	-442
20	-3	-4	467	-458
20	-3	6	295	-295
20	-3	-6	336	-339
20	-3	8	257	267
20	-3	-8	264	256
20	-3	10	325	319
20	-3	-10	327	323
20	-3	12	123	-126
20	-3	-12	109	-105
20	-3	14	265	-274
20	-3	-14	256	-258
20	-3	16	36	-6
20	-3	-16	43	-22
20	-3	18	147	148
20	-3	-18	153	154
16	-3	0	31	20
16	-3	2	688	692
16	-3	-2	727	-726
16	-3	4	190	204
16	-3	-4	247	-267
16	-3	6	464	-452
16	-3	-6	436	486
16	-3	8	355	-335
16	-3	-8	384	385
16	-3	10	196	204
16	-3	-10	161	-184
16	-3	12	365	363
16	-3	-12	344	-331
16	-3	-14	35	28
16	-3	16	266	-276
16	-3	-16	259	256

h	k	l	|Fo|	Fc
16	-3	18	72	-82
16	-3	-18	74	74
12	-3	0	[illegible]	-[illegible]
12	-3	2	61	-73
12	-3	-2	64	-70
12	-3	4	776	766
12	-3	-4	715	717
12	-3	6	259	242
12	-3	-6	340	349
12	-3	8	402	-394
12	-3	-8	356	-360
12	-3	10	407	-386
12	-3	-10	419	-416
12	-3	12	79	90
12	-3	-12	66	54
12	-3	14	356	364
12	-3	-14	356	330
12	-3	16	79	76
12	-3	-16	57	62
12	-3	18	231	-226
12	-3	-18	251	-236
12	-3	20	104	-96
12	-3	-20	117	-127
8	-3	0	55	28
8	-3	2	871	-880
8	-3	-2	868	895
8	-3	4	212	-229
8	-3	-4	230	242
8	-3	6	741	722
8	-3	-6	696	-702
8	-3	8	500	493
8	-3	-8	566	-565
8	-3	10	275	-285
8	-3	-10	228	213
8	-3	12	443	-441
8	-3	-12	459	456
8	-3	16	303	307
8	-3	-16	324	-325
8	-3	18	87	102
8	-3	-18	70	-71
8	-3	20	156	-147
8	-3	-20	161	163
4	-3	0	728	741
4	-3	2	97	108
4	-3	-2	53	56
4	-3	4	902	-895
4	-3	-4	881	-879
4	-3	6	516	-544
4	-3	-6	561	-575
4	-3	8	588	566
4	-3	-8	545	536
4	-3	10	569	554
4	-3	-10	625	636
4	-3	12	150	-162
4	-3	-12	131	-125
4	-3	14	375	-387
4	-3	-14	395	-408
4	-3	16	35	-40
4	-3	18	220	220
4	-3	-18	232	246
4	-3	20	126	120
4	-3	-20	121	100
0	-3	2	721	722
0	-3	4	354	374
0	-3	6	831	-807
0	-3	8	757	-776
0	-3	10	360	340
0	-3	12	530	539
0	-3	14	80	-92
0	-3	16	302	-314
0	-3	18	58	-60
0	-3	20	137	139
34	-3	0	119	-109
34	-3	2	43	-39
34	-3	4	75	68
34	-3	-4	93	86
30	-3	0	43	56
30	-3	2	30	-28
30	-3	4	144	-150
30	-3	-4	64	78
30	-3	6	49	51
30	-3	-6	40	23
30	-3	8	115	117
30	-3	-8	88	-107
30	-3	10	55	-61
30	-3	12	69	-63
30	-3	-12	100	94
26	-3	0	84	84
26	-3	2	95	94
26	-3	-2	35	48
26	-3	4	50	-36
26	-3	-4	53	-35
26	-3	6	111	-117
26	-3	-6	121	-118
26	-3	8	52	47
26	-3	10	92	87
26	-3	-10	104	112
26	-3	12	45	-49
26	-3	-12	44	-49
26	-3	14	79	-67
22	-3	0	89	-95
22	-3	-2	34	-66
22	-3	4	145	171
22	-3	-4	56	-56
22	-3	6	41	-7
22	-3	-6	152	-141
22	-3	8	111	114
22	-3	-8	49	26
22	-3	10	51	26
22	-3	-10	51	26
22	-3	12	151	164
22	-3	-12	124	-125
22	-3	14	37	15
22	-3	-14	70	-62
22	-3	16	94	95
18	-3	0	317	-324
18	-3	2	148	151
18	-3	-2	61	-67
18	-3	4	74	47
18	-3	-4	257	266
18	-3	6	156	-158
18	-3	-6	17	-19
18	-3	8	64	65
18	-3	-8	153	-150
18	-3	10	56	-47
18	-3	-10	51	37
18	-3	12	169	-161
18	-3	-12	134	125
18	-3	14	142	139
18	-3	-14	66	69
18	-3	16	66	-62
18	-3	-16	55	-48
14	-3	0	59	53
14	-3	2	78	-75
14	-3	-2	249	253
14	-3	4	53	49
14	-3	6	34	9
14	-3	-6	176	-172
14	-3	8	40	46
14	-3	-8	45	-42
14	-3	10	40	47
14	-3	-10	30	-14
14	-3	12	160	-152
14	-3	-12	69	71
14	-3	14	136	-125
14	-3	-14	87	77
14	-3	16	72	73
14	-3	-16	79	-79
14	-3	18	78	74
14	-3	-18	45	-36
14	-3	20	34	-14
14	-3	-20	93	89
10	-3	0	104	84
10	-3	2	65	63
10	-3	-2	54	-63
10	-3	4	70	-58
10	-3	-4	234	-220
10	-3	6	101	-118
10	-3	-6	97	97
10	-3	8	154	162
10	-3	-8	73	65
10	-3	10	130	137
10	-3	-10	80	97
10	-3	12	33	-43
10	-3	-12	40	-20
10	-3	14	159	-158
10	-3	-14	53	5
10	-3	16	50	27
10	-3	-16	101	102
10	-3	18	510	-508
10	-3	-18	267	-253
10	-3	20	403	400
6	-3	0	521	530
6	-3	2	103	-116
6	-3	-2	183	-202
6	-3	4	211	-206
6	-3	-4	352	-369
6	-3	6	366	384
6	-3	-6	218	212
6	-3	8	47	16
6	-3	-8	140	111
6	-3	10	314	-325
6	-3	-10	56	55
6	-3	12	76	65
6	-3	-12	130	133
6	-3	14	56	-51
6	-3	-14	85	-74
6	-3	16	63	-61
6	-3	-16	72	-67
2	-3	0	43	20
2	-3	2	153	-143
2	-3	-2	58	40
2	-3	4	39	26
2	-3	-4	34	59
2	-3	6	141	127
2	-3	-6	131	127
2	-3	8	40	-41
2	-3	-8	143	-161
2	-3	10	114	-99
2	-3	-10	166	-165
2	-3	12	87	-99
2	-3	-12	116	116
2	-3	14	98	91
2	-3	16	106	108
2	-3	-16	67	-45
2	-3	18	35	-27
2	-3	20	96	-94
35	-3	1	104	-83
35	-3	-1	115	98
35	-3	3	48	-43
35	-3	-3	107	102
35	-3	5	41	46
33	-3	-1	31	-13
33	-3	-3	44	-15
33	-3	5	64	-42
33	-3	-5	91	-57
33	-3	7	37	-3
33	-3	-7	25	-29
33	-3	9	110	96
33	-3	-9	97	91
31	-3	-1	37	74
31	-3	3	1	46
31	-3	5	47	-57
31	-3	-5	114	-152
31	-3	-7	45	-32
31	-3	9	74	76
31	-3	-9	127	122
29	-3	1	96	97
29	-3	-1	108	-114
29	-3	3	51	46
29	-3	-3	96	-126
29	-3	5	50	-49
29	-3	-5	51	63
29	-3	7	62	-46
29	-3	-7	91	79
29	-3	9	51	12
29	-3	-9	63	-42
29	-3	11	[illegible]	31
29	-3	-11	60	-60
29	-3	13	71	57
29	-3	-13	34	-15
27	-3	1	67	50
27	-3	-1	73	-44
27	-3	3	127	96
27	-3	-3	145	-132
27	-3	7	134	-113
27	-3	-7	170	178
27	-3	9	47	12
27	-3	11	116	107
27	-3	-11	118	-68
27	-3	13	34	6
25	-3	1	98	-120
25	-3	-1	125	-140
25	-3	3	78	72
25	-3	-3	62	59
25	-3	5	105	113
25	-3	-5	102	-86
25	-3	7	82	-58
25	-3	-7	96	99
25	-3	9	69	51
25	-3	-9	104	85
23	-3	1	94	-52
23	-3	-1	73	55
23	-3	3	86	94
23	-3	-3	153	163
23	-3	5	172	165
23	-3	-5	70	35
23	-3	7	66	50
23	-3	-7	156	-137
23	-3	9	135	-190
23	-3	-9	91	-55
23	-3	11	109	-113
23	-3	-11	120	116
23	-3	13	120	107
23	-3	-13	37	27
23	-3	15	104	-93
21	-3	1	253	-239
21	-3	-1	219	220
21	-3	3	165	-185
21	-3	-3	314	315
21	-3	5	95	78
21	-3	-5	73	-63
21	-3	7	83	26
21	-3	-7	98	-65
21	-3	9	62	-58
21	-3	-9	137	121
21	-3	11	42	-39
21	-3	-11	101	95
21	-3	13	95	-34
21	-3	17	84	46
21	-3	-17	79	-71
19	-3	1	267	-244
19	-3	-1	377	362
19	-3	3	237	-225
19	-3	-3	80	46
19	-3	5	396	391
19	-3	-5	364	-389
19	-3	7	221	218
19	-3	-7	164	-174
19	-3	9	74	-63
19	-3	-9	67	-52
19	-3	11	69	101
19	-3	17	66	56
19	-3	-17	84	-74
17	-3	1	283	300
17	-3	-1	239	210
17	-3	3	154	156
17	-3	-3	141	149
17	-3	5	214	-240
17	-3	-5	178	-191
17	-3	7	117	-116
17	-3	-7	196	-213
17	-3	9	149	150
17	-3	-9	139	141
17	-3	11	54	-36
17	-3	-11	42	-13
17	-3	13	146	-169
17	-3	-13	274	-277
17	-3	15	97	-68
17	-3	-15	57	46
17	-3	17	139	147
17	-3	-17	52	32
15	-3	1	373	-368
15	-3	-1	383	-351
15	-3	3	279	-249
15	-3	-3	219	-3 4
15	-3	5	74	65
15	-3	-5	88	98
15	-3	7	197	196
15	-3	-7	249	272
15	-3	9	152	145
15	-3	-9	16	154
15	-3	11	27	-31
15	-3	-11	57	-17
15	-3	13	126	127
15	-3	-13	53	72
15	-3	15	82	74
15	-3	-15	235	229
13	-3	1	262	-248
13	-3	-1	434	449
13	-3	3	465	-463
13	-3	-3	125	139
13	-3	5	222	-229
13	-3	-5	116	-126
13	-3	7	132	145
13	-3	-7	84	89
13	-3	9	102	98
13	-3	-9	192	-139
13	-3	11	81	-89
13	-3	-11	54	75
13	-3	13	109	-131
13	-3	-13	190	193
13	-3	15	95	-78
13	-3	-15	57	69
11	-3	1	176	171
11	-3	-1	165	-146
11	-3	3	104	76
11	-3	-3	145	-167
11	-3	5	378	-364
11	-3	-5	436	457
11	-3	7	523	-529
11	-3	-7	536	546
11	-3	9	137	-152
11	-3	-9	73	62
11	-3	11	71	78
11	-3	-11	97	-90
11	-3	-13	36	-4
11	-3	15	47	-31
11	-3	19	76	64
9	-3	1	513	-516
9	-3	-1	407	-413
9	-3	3	124	-116
9	-3	-3	111	-89
9	-3	5	404	392
9	-3	-5	295	300
9	-3	7	209	215
9	-3	-7	243	241
9	-3	9	93	-93
9	-3	-9	62	-51
9	-3	11	97	67
9	-3	-11	31	-12
9	-3	13	211	201
9	-3	-13	243	232
9	-3	15	103	94
9	-3	17	125	-120
9	-3	-17	156	-161
9	-3	19	90	-71
9	-3	-19	106	-96
9	-3	-21	40	38
7	-3	1	427	413
7	-3	-1	181	170
7	-3	3	41	23
7	-3	5	438	427
7	-3	-5	659	652
7	-3	7	336	350
7	-3	-7	164	150
7	-3	9	493	-493
7	-3	-9	534	-544
7	-3	11	279	-299
7	-3	-11	122	-132
7	-3	13	191	169
7	-3	-13	171	166
7	-3	15	75	-83
7	-3	-15	96	-72
7	-3	17	205	-211
7	-3	-17	135	-126
7	-3	19	62	-5
7	-3	-21	52	-10
5	-3	1	800	-792
5	-3	-1	621	607
5	-3	3	525	-468
5	-3	-3	765	793
5	-3	5	235	212
5	-3	-5	271	-269
5	-3	7	57	6
5	-3	-7	192	-174
5	-3	-9	129	126
5	-3	11	106	100
5	-3	-11	66	-95
5	-3	13	47	24
5	-3	-13	84	-76
5	-3	15	125	107
5	-3	-15	72	-61
5	-3	17	162	152
5	-3	-17	132	-124
5	-3	19	46	-19
5	-3	21	37	-83
5	-3	-21	100	97
3	-3	1	232	-219
3	-3	-1	358	362
3	-3	3	348	-375
3	-3	-3	252	240
3	-3	5	273	266
3	-3	-5	305	-314
3	-3	7	357	344
3	-3	-7	455	-441
3	-3	9	192	171
3	-3	-9	140	-155
3	-3	11	117	-99
3	-3	-11	72	63
3	-3	13	67	67
3	-3	-13	48	-15
3	-3	15	110	89
3	-3	-15	111	-116
3	-3	-17	57	-41
3	-3	19	66	-76
3	-3	21	92	-69
3	-3	-21	55	64
1	-3	1	234	249
1	-3	-1	464	452
1	-3	3	352	-334
1	-3	-3	313	-305
1	-3	5	379	-366
1	-3	-5	528	-502
1	-3	7	147	-172
1	-3	-7	75	-94
1	-3	9	90	95
1	-3	-9	136	114
1	-3	11	70	93
1	-3	-11	82	103
1	-3	13	151	-136
1	-3	-13	93	-61
1	-3	17	167	159
1	-3	-17	163	168
1	-3	19	97	94
1	-3	-19	122	105
1	-3	-21	51	-65
32	-4	0	150	159
32	-4	4	176	-177
32	-4	-4	156	-163
32	-4	6	69	-70
32	-4	-6	65	-76
28	-4	0	37	13
28	-4	2	232	231
28	-4	-2	213	-219
28	-4	6	249	-239
28	-4	-6	232	226
28	-4	8	141	-145
28	-4	-8	172	167
28	-4	10	82	79
28	-4	-10	55	-75
24	-4	0	152	-161
24	-4	-2	42	-50
24	-4	4	245	241
24	-4	-4	234	226
24	-4	6	199	216
24	-4	-6	222	222
24	-4	8	213	-210
24	-4	-8	207	-194
24	-4	10	279	-274
24	-4	-10	295	-292
24	-4	14	126	124
24	-4	-14	142	149
20	-4	0	51	-22
20	-4	2	300	-315
20	-4	-2	310	319
20	-4	4	105	-116
20	-4	-4	140	154
20	-4	6	341	330
20	-4	-6	347	-328
20	-4	8	295	301
20	-4	-8	309	-301
20	-4	10	145	-140
20	-4	-10	152	156
20	-4	12	249	-244
20	-4	-12	251	257
20	-4	14	37	6
20	-4	-14	47	7
20	-4	16	88	101
20	-4	-16	99	-136
16	-4	0	444	471
16	-4	2	89	92
16	-4	-2	116	116
16	-4	4	374	-381
16	-4	-4	381	-386
16	-4	6	241	-242
16	-4	-6	251	-246
16	-4	8	266	244
16	-4	-8	249	239
16	-4	10	364	352
16	-4	-10	349	329
16	-4	-12	51	-37
16	-4	14	241	-240
16	-4	-14	259	-253
16	-4	-16	72	-60
12	-4	0	44	6
12	-4	2	751	750
12	-4	-2	761	-780
12	-4	4	155	175
12	-4	-4	209	-211
12	-4	6	355	-373
12	-4	-6	361	365
12	-4	8	172	-168
12	-4	-8	173	163
12	-4	10	142	159
12	-4	-10	171	-172
12	-4	12	269	276
12	-4	-12	295	-280
12	-4	14	78	64
12	-4	-14	72	-61
12	-4	16	155	-156
12	-4	-16	207	213
12	-4	18	89	-73
12	-4	-18	96	103
8	-4	0	964	-983

h	k	l	|Fo|	Fc
8	-4	2	337	-349
8	-4	-2	341	-331
8	-4	4	479	467
8	-4	-4	448	453
8	-4	6	276	286
8	-4	-6	306	311
8	-4	8	240	-232
8	-4	-8	208	-196
8	-4	10	292	-268
8	-4	-10	297	-279
8	-4	12	126	112
8	-4	-12	128	123
8	-4	14	339	325
8	-4	-14	365	342
8	-4	16	95	87
8	-4	-16	94	91
8	-4	18	167	-162
8	-4	-18	177	-171
4	-4	0	40	14
4	-4	2	886	-869
4	-4	-2	867	867
4	-4	4	611	-626
4	-4	-4	631	640
4	-4	6	228	210
4	-4	-6	198	-179
4	-4	8	223	231
4	-4	-8	251	-255
4	-4	10	325	-313
4	-4	-10	332	308
4	-4	12	349	-339
4	-4	-12	370	367
4	-4	14	55	54
4	-4	-14	79	-69
4	-4	16	243	237
4	-4	-16	268	-262
4	-4	18	115	104
4	-4	-18	114	-98
4	-4	20	85	-82
4	-4	-20	85	76
0	-4	0	946	950
0	-4	2	635	644
0	-4	4	298	-266
0	-4	6	574	-589
0	-4	8	212	193
0	-4	10	361	365
0	-4	12	304	-291
0	-4	14	424	-415
0	-4	16	51	-26
0	-4	18	152	151
0	-4	20	69	69
30	-4	0	69	-49
30	-4	4	101	104
30	-4	-4	39	74
30	-4	6	80	78
30	-4	-8	95	-85
26	-4	0	50	29
26	-4	-2	79	-72
26	-4	4	153	-141
26	-4	-4	37	14
26	-4	6	92	104
26	-4	-6	49	-19
26	-4	8	228	230
26	-4	-8	134	-132
26	-4	-10	32	24
26	-4	12	79	-72
26	-4	-12	117	116
22	-4	0	58	54
22	-4	2	67	-84
22	-4	-2	60	16
22	-4	4	144	-151
22	-4	-4	108	-116
22	-4	6	133	-113
22	-4	-6	63	-39
22	-4	8	107	111
22	-4	-8	124	135
22	-4	10	81	71
22	-4	-10	94	99
22	-4	12	34	-41
22	-4	-12	34	-21
22	-4	14	54	-48
22	-4	-14	117	125
18	-4	2	82	-83
18	-4	-2	112	-119
18	-4	4	97	107
18	-4	-4	218	-219
18	-4	6	64	37
18	-4	-6	127	-123
18	-4	8	37	3
18	-4	-8	97	99
18	-4	10	50	-49
18	-4	-10	57	64
18	-4	12	72	-54
18	-4	-12	109	126
14	-4	0	240	-240
14	-4	2	193	191
14	-4	-2	43	-11
14	-4	4	224	230
14	-4	-4	321	312
14	-4	6	34	-18
14	-4	-6	60	40
14	-4	8	141	-140
14	-4	-8	63	-71
14	-4	10	79	69
14	-4	-10	215	-217
14	-4	12	70	52
14	-4	-12	99	104
14	-4	14	93	-70
14	-4	-14	89	-85
10	-4	0	163	152
10	-4	2	55	-63
10	-4	-2	50	19
10	-4	4	176	-146
10	-4	-4	140	159
10	-4	6	38	16
10	-4	-6	241	246
10	-4	8	93	-117
10	-4	-8	36	-4
10	-4	10	40	-35
10	-4	-10	92	-47
10	-4	12	47	59
10	-4	-12	92	-97
10	-4	14	41	10
10	-4	-14	174	-165
10	-4	16	50	48
6	-4	0	31	13
6	-4	2	176	190
6	-4	-2	64	-62
6	-4	4	54	-83
6	-4	-4	78	-77
6	-4	6	178	-173
6	-4	-6	163	-175
6	-4	8	85	86
6	-4	-8	40	8
6	-4	10	94	109
6	-4	-10	55	61
6	-4	12	34	16
6	-4	-12	151	-163
6	-4	-14	52	-68
6	-4	16	94	-96
6	-4	-16	109	125
6	-4	-18	108	108
2	-4	0	268	-266
2	-4	2	90	-81
2	-4	-2	59	61
2	-4	4	327	346
2	-4	-4	95	-72
2	-4	-6	101	-96
2	-4	8	212	-222
2	-4	-8	148	152
2	-4	10	101	102
2	-4	12	167	160
2	-4	-12	94	-89
2	-4	14	41	-21
2	-4	-14	159	157
2	-4	16	77	-52
2	-4	-16	174	166
2	-4	18	63	-68
2	-4	-18	55	-35
2	-4	20	61	-58
2	-4	-20	72	-86
33	-4	-1	71	60
33	-4	3	61	-58
33	-4	-3	56	53
31	-4	1	90	-86
31	-4	-1	84	82
31	-4	3	87	-73
31	-4	-3	111	115
31	-4	5	73	49
31	-4	-5	72	-59
31	-4	7	66	61
31	-4	-7	101	-91
29	-4	-1	53	46
29	-4	3	74	-18
29	-4	5	105	-90
29	-4	-5	87	-79
29	-4	7	56	-18
29	-4	9	114	69
29	-4	-9	87	85
27	-4	-1	89	84
27	-4	5	100	-86
27	-4	-5	188	-175
27	-4	7	71	-10
27	-4	9	126	114
27	-4	-9	165	153
25	-4	1	130	146
25	-4	3	60	50
25	-4	-3	176	-180
25	-4	-5	132	101
25	-4	7	89	-59
25	-4	-7	169	161
25	-4	9	58	-50
25	-4	-9	64	-77
25	-4	11	66	40
25	-4	-11	105	-100
23	-4	13	47	53
23	-4	1	67	43
23	-4	-1	129	-135
23	-4	3	148	165
23	-4	-3	102	-85
23	-4	5	94	-76
23	-4	-5	75	59
23	-4	7	207	-194
23	-4	-7	173	165
23	-4	9	66	63
23	-4	11	131	126
23	-4	-11	108	-115
23	-4	13	42	-11
23	-4	-13	53	-41
21	-4	1	99	-112
21	-4	-1	134	-139
21	-4	3	72	67
21	-4	-3	59	-1
21	-4	5	136	149
21	-4	-5	161	148
21	-4	7	38	29
21	-4	-7	34	-32
21	-4	9	111	-112
21	-4	-9	157	-157
21	-4	11	60	-49
21	-4	-11	77	-15
21	-4	13	66	71
21	-4	-13	119	121
21	-4	15	56	27
21	-4	-15	5	54
19	-4	1	122	-130
19	-4	-1	54	-65
19	-4	3	116	110
19	-4	-3	151	146
19	-4	5	191	197
19	-4	-5	175	164
19	-4	7	78	-55
19	-4	-7	34	13
19	-4	9	198	-178
19	-4	-9	195	-199
19	-4	11	45	-27
19	-4	-11	92	-86
19	-4	13	108	100
19	-4	-13	122	110
19	-4	15	44	40
17	-4	1	201	-183
17	-4	-1	156	165
17	-4	3	198	-218
17	-4	-3	220	209
17	-4	5	100	90
17	-4	-5	95	-69
17	-4	7	128	126
17	-4	-7	160	-166
17	-4	9	32	-11
17	-4	-9	59	31
17	-4	11	60	-45
17	-4	-11	174	181
17	-4	13	74	-33
17	-4	15	51	30
17	-4	-15	167	-119
17	-4	17	67	61
17	-4	-17	38	-38
15	-4	1	208	-201
15	-4	-1	298	280
15	-4	3	230	-228
15	-4	-3	136	153
15	-4	5	253	237
15	-4	-5	252	-255
15	-4	7	248	243
15	-4	-7	185	-208
15	-4	9	60	-48
15	-4	-9	50	-15
15	-4	11	108	-107
15	-4	-11	76	70
15	-4	13	46	-16
15	-4	-13	93	72
15	-4	15	75	60
15	-4	-15	56	-44
15	-4	17	78	44
15	-4	-17	82	-76
13	-4	1	328	339
13	-4	-1	106	105
13	-4	3	96	-89
13	-4	5	331	-337
13	-4	-5	117	-120
13	-4	7	59	26
13	-4	-7	77	-86
13	-4	9	186	184
13	-4	-9	142	152
13	-4	11	43	-49
13	-4	-11	106	93
13	-4	13	115	-109
13	-4	-13	205	-209
13	-4	15	126	-133
13	-4	-17	130	128
11	-4	1	85	41
11	-4	-1	246	253
11	-4	3	225	-231
11	-4	-3	184	-200
11	-4	5	174	-167
11	-4	-5	359	-382
11	-4	7	52	-23
11	-4	-7	105	114
11	-4	9	196	178
11	-4	-9	269	276
11	-4	11	131	125
11	-4	-11	45	7
11	-4	13	147	-136
11	-4	-13	105	-104
11	-4	15	87	-76
11	-4	-15	43	-28
11	-4	17	134	125
11	-4	-17	72	49
11	-4	19	70	59
9	-4	1	260	262
9	-4	-1	284	-295
9	-4	3	321	315
9	-4	-3	339	-364
9	-4	5	116	-87
9	-4	-5	95	90
9	-4	7	153	-149
9	-4	-7	206	219
9	-4	9	76	54
9	-4	-9	55	-39
9	-4	11	77	85
9	-4	-11	156	-155
9	-4	13	53	-5
9	-4	-13	54	-73
9	-4	15	136	134
9	-4	-15	74	-91
9	-4	17	85	78
9	-4	-17	263	264
7	-4	1	184	-188
7	-4	-1	237	238
7	-4	3	278	-296
7	-4	-3	148	-131
7	-4	5	198	209
7	-4	-5	299	-312
7	-4	7	301	311
7	-4	-7	61	-56
7	-4	9	66	-40
7	-4	-9	162	176
7	-4	11	145	-141
7	-4	-11	31	8
7	-4	13	31	-34
7	-4	-13	142	-138
7	-4	15	84	73
7	-4	-15	79	84
7	-4	17	62	59
5	-4	1	284	-294
5	-4	-1	315	-335
5	-4	3	76	54
5	-4	-3	145	152
5	-4	5	243	238
5	-4	-5	357	366
5	-4	7	34	45
5	-4	-7	190	-197
5	-4	9	177	-168
5	-4	-9	198	208
5	-4	13	171	157
5	-4	-13	67	52
5	-4	15	76	70
5	-4	-15	100	-82
5	-4	17	107	-111
5	-4	-17	46	-42
5	-4	19	106	-94
3	-4	1	164	-165
3	-4	-1	221	-228
3	-4	3	125	120
3	-4	-3	60	43
3	-4	5	356	357
3	-4	-5	320	316
3	-4	7	84	97
3	-4	-7	55	26
3	-4	9	247	-253
3	-4	-9	299	-293
3	-4	11	48	-60
3	-4	13	195	192
3	-4	-13	219	221
3	-4	15	50	34
3	-4	-15	28	42
3	-4	17	136	-140
3	-4	-17	98	-91
3	-4	19	89	-65
3	-4	-19	61	-33
1	-4	1	357	-346
1	-4	-1	230	226
1	-4	3	176	-148
1	-4	-3	573	585
1	-4	5	90	60
1	-4	-5	143	-141
1	-4	7	132	107
1	-4	-7	405	-403
1	-4	9	50	41
1	-4	-9	108	101
1	-4	11	144	-155
1	-4	-11	163	158
1	-4	13	85	-77
1	-4	-13	95	-86
1	-4	15	143	143
1	-4	-15	119	-107
1	-4	17	102	105
1	-4	-17	61	-48
1	-4	19	53	-28
28	-5	0	134	133
28	-5	-2	40	21
28	-5	4	128	-131
28	-5	-4	121	-133
24	-5	0	39	4
24	-5	2	195	189
24	-5	-2	185	-189
24	-5	4	67	54
24	-5	-4	72	-75
24	-5	6	173	-177
24	-5	-6	171	165
24	-5	8	115	-121
24	-5	-8	151	143
24	-5	10	72	79
24	-5	-10	73	-71
20	-5	0	156	-165
20	-5	2	60	-67
20	-5	-2	73	-62
20	-5	4	169	185
20	-5	-4	158	156
20	-5	6	179	186
20	-5	-6	176	176
20	-5	8	147	-146
20	-5	-8	140	-124
20	-5	10	205	-215
20	-5	-10	222	-225
20	-5	12	56	50
16	-5	0	42	-18
16	-5	2	319	-327
16	-5	-2	299	310
16	-5	4	119	-102
16	-5	-4	105	105
16	-5	6	230	239
16	-5	-6	224	-225
16	-5	8	176	181
16	-5	-8	160	-158
16	-5	10	102	-94
16	-5	-10	94	110
16	-5	12	159	-169
16	-5	-12	177	183
12	-5	0	382	367
12	-5	2	88	84
12	-5	-2	109	111
12	-5	4	284	-289
12	-5	-4	256	-265
12	-5	6	156	-191
12	-5	-6	147	-154
12	-5	8	157	152
12	-5	-8	167	164
12	-5	10	218	226
12	-5	-10	214	215
12	-5	-12	64	-35
12	-5	14	187	-179
12	-5	-14	206	-204
8	-5	0	49	31
8	-5	2	514	516
8	-5	-2	479	-466
8	-5	4	147	153
8	-5	-4	156	-172
8	-5	6	252	-259
8	-5	-6	266	256
8	-5	8	131	-148
8	-5	-8	124	127
8	-5	10	120	108
8	-5	-10	144	-156
8	-5	12	181	181
8	-5	-12	201	-203
8	-5	-14	56	-28
8	-5	16	144	-140
8	-5	-16	143	140
4	-5	0	447	-469
4	-5	2	185	-202
4	-5	-2	222	-230
4	-5	4	255	263
4	-5	-4	246	244
4	-5	6	272	261
4	-5	-6	275	276
4	-5	8	148	-155
4	-5	-8	182	-171
4	-5	10	262	-265
4	-5	-10	269	-269
4	-5	12	76	88
4	-5	-12	114	110
4	-5	14	239	235
4	-5	-14	247	252
4	-5	16	57	21
0	-5	2	454	-465
0	-5	4	283	-301
0	-5	6	211	207
0	-5	8	203	215
0	-5	10	185	-183
0	-5	12	231	-244
0	-5	16	155	157
26	-5	0	63	-59
26	-5	2	33	-16
26	-5	4	60	75
26	-5	-4	91	90
26	-5	6	85	83
26	-5	-6	60	48
26	-5	8	37	-26
26	-5	-8	90	-85
22	-5	0	49	39
22	-5	2	53	-59
22	-5	-2	40	24
22	-5	4	133	-128
22	-5	-4	51	14
22	-5	6	54	60
22	-5	-6	63	-55
22	-5	8	170	165
22	-5	-8	91	-87
22	-5	-10	60	44
18	-5	0	151	153
18	-5	2	48	10
18	-5	4	127	-128
18	-5	-4	127	-135
18	-5	6	113	-100
18	-5	-6	38	-13
18	-5	8	121	116
18	-5	10	74	70
18	-5	-10	43	38
18	-5	12	69	64
18	-5	-12	76	-63
18	-5	14	39	-45
18	-5	-14	66	-54
14	-5	0	36	-36
14	-5	2	178	177
14	-5	-2	130	-121
14	-5	4	147	148
14	-5	-4	34	14
14	-5	6	61	-52
14	-5	-6	73	71
14	-5	8	141	-142
14	-5	10	63	-54
14	-5	-10	77	-62
14	-5	12	49	62
14	-5	-12	59	-72
14	-5	14	37	32
10	-5	0	237	-234
10	-5	2	70	-63
10	-5	-2	29	-21
10	-5	4	151	146
10	-5	-4	153	157
10	-5	6	139	128
10	-5	-6	49	-15
10	-5	8	62	46
10	-5	-8	124	-122
10	-5	10	66	-45

h	k	l	|Fo|	Fc
10	-5	-10	34	2
10	-5	12	76	-70
10	-5	-12	108	130
10	-5	14	31	42
10	-5	-14	73	75
10	-5	16	59	73
6	-5	0	127	123
6	-5	2	111	-114
6	-5	-2	74	72
6	-5	4	267	-273
6	-5	-4	53	1
6	-5	-6	40	-26
6	-5	8	201	199
6	-5	-8	59	-40
6	-5	-10	81	72
6	-5	12	101	-94
6	-5	-12	90	98
6	-5	14	38	-6
6	-5	-14	72	-75
6	-5	16	69	49
6	-5	-16	136	-125
2	-5	0	155	155
2	-5	2	118	119
2	-5	4	52	-39
2	-5	-4	176	-178
2	-5	6	146	-142
2	-5	-6	41	-31
2	-5	8	79	-50
2	-5	-8	146	150
2	-5	10	98	91
2	-5	-10	40	22
2	-5	12	63	51
2	-5	-12	137	-135
2	-5	14	95	-77
2	-5	-14	69	-59
2	-5	16	85	-83
2	-5	-16	56	53
29	-5	1	77	-61
29	-5	-1	31	41
29	-5	3	60	-70
29	-5	-3	82	85
27	-5	1	89	-79
27	-5	-1	85	74
27	-5	3	94	-106
27	-5	-3	118	96
27	-5	5	43	52
27	-5	7	120	111
27	-5	-7	95	-80
25	-5	1	57	51
25	-5	-1	88	74
25	-5	-3	100	-64
25	-5	5	115	-105
25	-5	-5	126	-125
25	-5	7	52	-44
25	-5	-7	33	47
25	-5	9	86	82
25	-5	-9	123	123
23	-5	1	118	124
23	-5	-1	142	131
23	-5	3	47	-30
23	-5	-3	52	-1
23	-5	5	135	-130
23	-5	-5	147	-136
23	-5	9	138	129
23	-5	-9	137	132
21	-5	1	106	112
21	-5	-3	166	-144
21	-5	-5	105	112
21	-5	7	101	-95
21	-5	-7	243	234
21	-5	9	89	-80
21	-5	11	68	52
21	-5	-11	135	-130
19	-5	1	66	63
19	-5	-1	156	-141
19	-5	3	256	250
19	-5	-3	147	-141
19	-5	-5	72	-59
19	-5	7	180	-174
19	-5	-7	81	69
19	-5	9	72	69
19	-5	-9	62	19
19	-5	11	190	178
19	-5	-11	133	-135
19	-5	13	40	-5
19	-5	-13	40	-48
17	-5	1	101	-119
17	-5	-1	53	-21
17	-5	3	144	146
17	-5	-3	179	187
17	-5	5	194	197
17	-5	-5	140	119
17	-5	7	69	-79
17	-5	-7	72	-67
17	-5	9	168	-163
17	-5	-9	176	-184
17	-5	11	44	-45
17	-5	-11	102	-99
17	-5	-13	71	74
15	-5	1	260	-254
15	-5	-1	311	-318
15	-5	5	121	111
15	-5	-5	182	194
15	-5	9	111	-109
15	-5	-9	124	-121
15	-5	11	53	12
15	-5	13	160	160
15	-5	-13	149	145
15	-5	15	89	91

h	k	l	|Fo|	Fc
15	-5	-15	95	51
13	-5	1	118	-116
13	-5	-1	177	173
13	-5	3	135	-129
13	-5	-3	67	69
13	-5	5	220	224
13	-5	-5	209	-207
13	-5	7	222	217
13	-5	-7	234	-237
13	-5	-9	42	-32
13	-5	11	99	-88
13	-5	-11	159	171
13	-5	13	89	-86
13	-5	-13	101	91
13	-5	15	48	-17
13	-5	-15	73	-76
11	-5	1	249	-262
11	-5	-1	241	244
11	-5	3	283	-277
11	-5	-3	311	328
11	-5	5	56	17
11	-5	-5	37	-41
11	-5	7	56	58
11	-5	-7	51	-62
11	-5	9	103	-94
11	-5	-9	118	108
11	-5	11	188	-194
11	-5	-11	121	115
11	-5	13	56	-63
11	-5	-13	58	52
11	-5	15	126	128
11	-5	-15	69	-67
9	-5	1	181	176
9	-5	3	157	-159
9	-5	-3	245	-239
9	-5	5	254	-256
9	-5	-5	122	-131
9	-5	7	174	162
9	-5	-7	110	98
9	-5	9	292	293
9	-5	-9	232	227
9	-5	11	53	35
9	-5	-11	129	116
9	-5	13	86	-74
9	-5	-13	122	-119
9	-5	-15	101	-93
7	-5	1	279	275
7	-5	-1	443	454
7	-5	3	111	-119
7	-5	-3	63	-64
7	-5	5	85	-76
7	-5	-5	247	-252
7	-5	7	63	54
7	-5	-7	120	124
7	-5	9	108	95
7	-5	-9	185	170
7	-5	-11	79	-79
7	-5	13	195	-206
7	-5	-13	150	-149
7	-5	15	156	-154
7	-5	-15	56	-71
7	-5	17	66	64
7	-5	-17	34	17
5	-5	1	140	143
5	-5	-1	95	-82
5	-5	3	37	41
5	-5	-3	256	-261
5	-5	5	128	-111
5	-5	-5	148	149
5	-5	7	195	-200
5	-5	-7	344	346
5	-5	9	43	-30
5	-5	-9	71	-86
5	-5	11	213	225
5	-5	-11	270	-271
5	-5	13	155	141
5	-5	-15	81	88
5	-5	-17	43	27
3	-5	1	160	156
3	-5	-1	206	-208
3	-5	3	343	352
3	-5	-3	193	-184
3	-5	5	40	-34
3	-5	7	214	-222
3	-5	-7	114	107
3	-5	9	145	139
3	-5	-9	44	-34
3	-5	11	272	278
3	-5	-11	211	-214
3	-5	-13	119	-119
3	-5	15	116	-125
3	-5	-15	62	88
3	-5	17	79	-69
3	-5	-17	82	76
1	-5	1	157	-154
1	-5	-1	210	-216
1	-5	-3	76	77
1	-5	5	156	161
1	-5	-5	262	262
1	-5	7	68	-41
1	-5	-7	111	-105
1	-5	9	301	-301
1	-5	-9	286	-281
1	-5	11	75	-62
1	-5	13	189	201
1	-5	-13	201	169
1	-5	15	60	66
1	-5	-15	59	80
1	-5	-17	29	-41

h	k	l	|Fo|	Fc
20	-6	2	176	174
20	-6	-2	150	-155
20	-6	4	121	87
20	-6	-4	53	-60
20	-6	6	97	-94
20	-6	-6	71	72
16	-6	0	147	-145
16	-6	2	69	-58
16	-6	4	143	149
16	-6	-4	96	113
16	-6	6	134	139
16	-6	-6	126	118
16	-6	8	68	-85
16	-6	10	113	-115
16	-6	-10	129	-134
12	-6	0	53	-20
12	-6	2	191	-195
12	-6	-2	179	177
12	-6	4	74	-48
12	-6	6	179	177
12	-6	-6	183	-186
12	-6	8	140	145
12	-6	-8	112	-143
12	-6	-10	81	50
12	-6	12	95	-106
12	-6	-12	108	107
8	-6	0	95	104
8	-6	2	53	-50
8	-6	4	210	-214
8	-6	-4	225	-217
8	-6	6	135	-137
8	-6	-6	134	-129
8	-6	8	113	120
8	-6	-8	157	155
8	-6	10	191	200
8	-6	-10	200	199
8	-6	12	40	2
4	-6	0	49	29
4	-6	2	163	176
4	-6	-2	173	-177
4	-6	4	75	-45
4	-6	6	265	-270
4	-6	-6	303	301
4	-6	8	209	-205
4	-6	-8	200	205
4	-6	10	43	27
4	-6	-10	66	-54
4	-6	12	137	144
4	-6	-12	135	-134
0	-6	0	51	-55
0	-6	2	96	76
0	-6	4	242	247
0	-6	6	134	134
0	-6	8	159	-169
0	-6	10	244	-250
0	-6	12	72	-32
0	-6	14	111	110
22	-6	0	107	-107
22	-6	2	98	-108
22	-6	-4	55	66
18	-6	0	87	93
18	-6	2	71	-73
18	-6	-2	101	100
18	-6	4	143	-149
18	-6	-4	30	25
18	-6	-6	63	-62
18	-6	8	75	62
18	-6	-8	62	-57
14	-6	0	142	149
14	-6	2	135	128
14	-6	4	64	-47
14	-6	-4	108	-113
14	-6	6	95	-95
14	-6	-8	111	115
14	-6	10	65	52
14	-6	-10	82	70
10	-6	0	69	-68
10	-6	2	119	125
10	-6	-2	129	-138
10	-6	4	132	138
10	-6	6	31	1
10	-6	-6	137	139
10	-6	8	84	-88
10	-6	-8	38	10
10	-6	-10	107	-106
10	-6	12	79	83
10	-6	-12	90	-94
6	-6	0	149	-153
6	-6	2	76	-72
6	-6	-2	61	47
6	-6	4	79	77
6	-6	-4	155	163
6	-6	6	115	122
6	-6	-6	70	-59
6	-6	8	64	46
6	-6	-8	183	-187
6	-6	10	92	-87
6	-6	-10	66	-61
6	-6	12	72	-60
6	-6	-12	46	50
2	-6	0	70	74
2	-6	2	93	-100
2	-6	-2	113	103
2	-6	4	127	-140
2	-6	-4	89	-85
2	-6	6	38	26
2	-6	-6	172	-173
2	-6	8	159	166
2	-6	-8	38	-19

h	k	l	|Fo|	Fc
2	-6	10	80	71
2	-6	-10	131	124
2	-6	12	89	-77
2	-6	-12	86	92
2	-6	14	45	-53
23	-6	1	53	-62
23	-6	-1	64	63
21	-6	1	131	95
21	-6	-1	95	85
21	-6	3	35	-27
21	-6	-3	67	-55
21	-6	5	95	-86
21	-6	-5	146	-132
19	-6	1	134	135
19	-6	-1	156	153
19	-6	3	75	-44
19	-6	-3	27	-3
19	-6	5	140	-135
19	-6	-5	137	-121
17	-6	1	64	81
17	-6	-1	79	-101
17	-6	3	90	83
17	-6	-3	143	-139
17	-6	-5	55	70
17	-6	7	95	-91
17	-6	-7	172	166
17	-6	9	54	-31
15	-6	1	104	102
15	-6	-1	116	-113
15	-6	3	205	200
15	-6	-3	153	-153
15	-6	5	35	6
15	-6	-5	29	-19
15	-6	7	156	-143
15	-6	-7	96	82
15	-6	9	56	14
13	-6	1	200	-193
13	-6	-1	95	-73
13	-6	3	121	117
13	-6	-3	168	175
13	-6	5	205	194
13	-6	-5	111	100
13	-6	7	85	-87
13	-6	9	143	-144
13	-6	-9	111	-114
13	-6	11	50	-13
13	-6	-11	62	-62
11	-6	1	181	-182
11	-6	-1	273	-287
11	-6	3	133	124
11	-6	-3	87	90
11	-6	5	111	93
11	-6	-5	207	208
11	-6	7	66	-43
11	-6	-7	56	-69
11	-6	9	103	-85
11	-6	-9	110	-123
11	-6	11	32	-27
11	-6	-11	50	30
9	-6	1	115	-117
9	-6	-1	109	114
9	-6	3	143	-136
9	-6	-3	124	128
9	-6	5	97	98
9	-6	-5	95	-105
9	-6	7	190	183
9	-6	-7	195	-200
9	-6	9	55	30
9	-6	11	83	-100
9	-6	-11	159	162
9	-6	13	92	-75
9	-6	-13	89	56
7	-6	1	155	-155
7	-6	-1	184	186
7	-6	3	194	-199
7	-6	-3	212	211
7	-6	5	55	67
7	-6	-5	68	-63
7	-6	7	150	142
7	-6	-7	146	-131
7	-6	9	74	-40
7	-6	11	168	-160
7	-6	-11	114	98
7	-6	13	78	-57
7	-6	-13	44	67
5	-6	1	146	136
5	-6	-1	120	115
5	-6	3	117	-117
5	-6	-3	118	-118
5	-6	5	224	-227
5	-6	-5	169	-158
5	-6	7	40	31
5	-6	-7	86	64
5	-6	9	207	219
5	-6	-9	208	208
5	-6	11	71	60
5	-6	-11	51	41
5	-6	13	85	-78
5	-6	-13	98	-110
3	-6	1	183	183
3	-6	-1	201	204
3	-6	3	122	-116
3	-6	-3	134	-123
3	-6	5	143	-146
3	-6	-5	237	-228
3	-6	7	136	94
3	-6	9	176	172
3	-6	-9	182	186
3	-6	11	28	17

h	k	l	|Fo|	Fc
3	-6	-11	52	35
3	-6	13	109	-111
3	-6	-13	81	-88
1	-6	1	147	155
1	-6	-1	31	-27
1	-6	3	97	99
1	-6	-3	212	-214
1	-6	5	72	-31
1	-6	-5	73	69
1	-6	7	157	-155
1	-6	-7	271	271
1	-6	9	86	-99
1	-6	-9	73	-53
1	-6	11	141	147
1	-6	-11	232	-229
1	-6	13	[illegible]	103
12	-7	0	50	-74
8	-7	0	26	-9
8	-7	2	92	-77
8	-7	-2	120	105
8	-7	-4	72	47
8	-7	6	105	89
8	-7	-6	115	-123
4	-7	0	77	73
4	-7	-2	36	-8
4	-7	4	113	-117
4	-7	-4	153	-152
4	-7	-6	72	-88
0	-7	2	121	111
0	-7	6	134	-140
0	-7	8	111	-113
10	-7	0	71	72
10	-7	2	76	74
10	-7	-2	77	-76
10	-7	-4	119	-134
6	-7	0	51	-59
6	-7	2	70	67
6	-7	-2	139	-141
6	-7	4	36	35
6	-7	-4	61	58
6	-7	6	45	-28
6	-7	-6	163	169
2	-7	0	69	-83
2	-7	2	69	-79
2	-7	-2	66	80
2	-7	4	62	55
2	-7	-4	114	123
2	-7	6	95	101
13	-7	1	87	89
13	-7	-1	95	-99
11	-7	1	89	74
11	-7	-1	45	-72
11	-7	3	98	94
11	-7	-3	60	-78
9	-7	1	195	-195
9	-7	-1	151	-139
9	-7	3	71	49
9	-7	-3	62	78
9	-7	5	166	166
9	-7	-5	108	98
7	-7	1	60	-65
7	-7	-1	123	-116
7	-7	3	162	143
7	-7	-3	123	119
7	-7	5	129	127
7	-7	-5	189	183
5	-7	1	119	-116
5	-7	-1	95	82
5	-7	3	160	-156
5	-7	-3	160	155
5	-7	7	95	104
5	-7	-7	147	-141
3	-7	1	71	-75
3	-7	-1	112	108
3	-7	3	131	-129
3	-7	-3	131	117
3	-7	5	76	74
3	-7	7	190	184
3	-7	-7	149	-147
1	-7	1	148	139
1	-7	-1	124	119
1	-7	3	85	-86
1	-7	-3	88	-97
1	-7	5	183	-188
1	-7	-5	147	-140
1	-7	7	34	-29
1	-7	-7	37	28

THE 'ACCIDENTALLY ABSENT' REFLECTIONS

h	k	l	|Fo|	Fc
32	0	2		31
28	0	0		24
24	0	-6		-37
20	0			-16
16				23
38	0	-2		22
36	0	4		-15
34	0	4		-1
34	0	6		-16
34	0	-10		-17
30	0	-8		-31
26	0	4		23
22	0	-8		18
18	0	-14		25
14	0	-16		-21
14	0	-22		-6
10	0	20		7
6	0	6		1
6	0	22		23
6	0	-22		-25
2	0	16		-4
36	-1	2		-26
28	-1	16		-19
24	-1	18		-23
20	-1	6		-24
16	-1	18		27
12	-1	16		22
12	-1	-16		7
38	-1	0		-20
38	-1	6		13
34	-1	4		-29
34	-1	-8		29
30	-1	0		1
30	-1	-6		25
26	-1	-2		5
26	-1	-8		6
26	-1	-12		-38
22	-1	0		-5
22	-1	-6		-16
22	-1	16		15
14	-1	20		-27
10	-1	22		-29
2	-1	4		-34
2	-1	22		13
39	-1	1		5
39	-1	-1		-2
37	-1	1		32
37	-1	-3		-38
37	-1	5		32
37	-1	-7		23
35	-1	1		43
35	-1	-1		-9
35	-1	3		23
35	-1	9		8
35	-1	-9		-33
35	-1	11		-4
33	-1	5		34
33	-1	-5		22
33	-1	9		14
33	-1	-9		-44
33	-1	11		2
33	-1	-11		-15
31	-1	-11		-5
29	-1	13		21
29	-1	-13		11
29	-1	15		17
27	-1	-5		30
27	-1	9		31
27	-1	13		-14
27	-1	-13		2
27	-1	15		14
27	-1	-17		0
25	-1	-5		-9
25	-1	7		6
25	-1	-7		38
25	-1	9		-20
25	-1	-9		25
25	-1	11		-2
25	-1	13		2
25	-1	-13		24
25	-1	15		-18
25	-1	-15		-23
23	-1	3		-6
23	-1	5		-16
23	-1	-7		-12
23	-1	-9		-23
23	-1	17		53

h	k	l	|Fo|	Fc
23	-1	-19		13
21	-1	-3		9
21	-1	9		33
21	-1	-9		-19
21	-1	-11		6
21	-1	13		-23
21	-1	-13		-24
21	-1	17		-7
21	-1	19		-18
19	-1	-15		7
17	-1	-21		12
15	-1	17		16
15	-1	21		19
15	-1	-21		26
13	-1	19		-16
13	-1	21		7
9	-1	-17		27
9	-1	-19		-28
7	-1	21		14
7	-1	-21		-19
7	-1	23		36
5	-1	19		17
3	-1	-15		-4
3	-1	-17		9
3	-1	-21		3
3	-1	23		-12
1	-1	-17		-3
12	-2	0		-31
8	-2	16		-1
8	-2	-16		18
4	-2	18		-30
4	-2	-18		7
38	-2	2		10
38	-2	-2		-31
34	-2	0		9
34	-2	-6		-15
34	-2	-10		15
30	-2	4		-7
30	-2	-4		-41
30	-2	-8		6
26	-2	2		21
26	-2	6		16
22	-2	8		8
22	-2	-8		-10
22	-2	12		21
22	-2	-12		-25
22	-2	18		-9
22	-2	-18		-37
18	-2	-10		-1
14	-2	-16		-17
14	-2	-20		29
10	-2	-22		5
6	-2	22		-12
37	-2	1		-3
35	-2	-3		1
35	-2	7		-1
35	-2	-7		2
35	-2	-9		63
33	-2	5		-16
33	-2	-5		33
33	-2	7		-24
33	-2	9		3
33	-2	-9		-16
31	-2	-1		6
31	-2	5		4
31	-2	9		8
31	-2	-13		30
29	-2	3		15
29	-2	-3		30
29	-2	7		16
29	-2	-7		22
29	-2	11		-34
29	-2	-11		33
29	-2	13		45
27	-2	1		35
27	-2	-11		-35
27	-2	15		-8
27	-2	-15		1
25	-2	-7		-23
25	-2	13		-19
23	-2	9		-40
23	-2	11		-14
23	-2	15		31
23	-2	-15		-41
21	-2	7		-4
21	-2	11		21
21	-2	15		-23

h	k	l	|Fo|	Fc
21	-2	17		17
19	-2	9		-16
19	-2	-19		59
17	-2	19		-24
17	-2	-19		0
15	-2	-7		13
15	-2	-11		2
15	-2	-15		-13
15	-2	19		-14
15	-2	-19		-1
13	-2	15		-13
13	-2	-15		-15
13	-2	-19		16
13	-2	21		13
11	-2	-11		17
11	-2	15		5
11	-2	-15		-16
11	-2	19		4
11	-2	-19		5
11	-2	21		23
11	-2	-21		9
9	-2	15		-4
9	-2	-15		-8
7	-2	-9		38
7	-2	19		13
7	-2	-19		-2
7	-2	21		3
7	-2	-21		22
3	-2	21		-59
1	-2	-7		-2
1	-2	19		26
1	-2	-19		-23
1	-2	23		-17
32	-3	0		23
16	-3	14		-27
8	-3	14		21
8	-3	-14		-28
4	-3	-16		-16
34	-3	2		1
34	-3	6		13
34	-3	-6		29
30	-3	-2		-6
30	-3	-10		21
26	-3	-8		36
26	-3	12		-15
22	-3	2		30
22	-3	6		-3
22	-3	-14		-20
18	-3	-12		-25
18	-3	-14		7
14	-3	-4		-23
10	-3	6		16
10	-3	-14		-42
10	-3	18		-8
10	-3	-20		23
6	-3	14		-18
2	-3	14		-14
2	-3	16		20
2	-3	-20		-2
35	-3	-5		-52
33	-3	1		21
33	-3	3		19
31	-3	1		26
31	-3	-3		25
31	-3	7		-50
31	-3	11		-8
31	-3	-11		-5
27	-3	5		-1
27	-3	-5		33
27	-3	-9		19
27	-3	13		-24
25	-3	3		37
25	-3	7		-10
25	-3	-7		-17
25	-3	11		-54
25	-3	-11		-3
25	-3	13		52
23	-3	-1		-7
23	-3	15		32
21	-3	-13		-30
21	-3	15		2
21	-3	-15		-67
19	-3	11		29
19	-3	-11		0
19	-3	13		1
19	-3	15		1
19	-3	-15		-13

h	k	l	|Fo|	Fc
17	-3	15		-16
17	-3	19		9
15	-3	1		-9
15	-3	-1		-27
15	-3	13		3
15	-3	15		-20
15	-3	-19		4
13	-3	-9		-21
13	-3	19		-16
13	-3	-19		8
11	-3	13		-26
11	-3	-15		11
11	-3	17		34
11	-3	-17		42
11	-3	-19		-17
9	-3	15		22
9	-3	21		-13
7	-3	-3		41
7	-3	-19		-20
5	-3	9		-6
5	-3	-19		25
3	-3	17		-35
3	-3	-19		31
1	-3	15		-33
1	-3	-15		-34
1	-3	21		2
32	-4	2		-9
32	-4	-2		7
28	-4	4		30
28	-4	-4		-50
24	-4	2		-36
24	-4	12		48
24	-4	-12		34
16	-4	12		-32
16	-4	16		-20
30	-4	2		13
30	-4	-2		-14
30	-4	-6		40
30	-4	8		-31
26	-4	2		-19
26	-4	10		-11
22	-4	8		-5
18	-4	0		30
18	-4	4		6
18	-4	-4		52
18	-4	-14		1
14	-4	6		-22
14	-4	14		12
14	-4	-14		2
14	-4	-16		-1
10	-4	-4		2
10	-4	14		-43
10	-4	-18		-2
6	-4	14		-21
6	-4	18		-13
2	-4	6		5
2	-4	-10		0
33	-4	1		-36
29	-4	1		58
29	-4	-3		-49
29	-4	-7		21
27	-4	1		40
27	-4	3		-20
27	-4	-3		-25
27	-4	-7		-16
27	-4	11		20
27	-4	-11		12
25	-4	1		-62
25	-4	5		-44
25	-4	-13		6
23	-4	9		44
19	-4	-15		30
17	-4	-13		17
13	-4	3		-39
13	-4	15		-17
13	-4	17		33
11	-4	-19		49
9	-4	13		16
9	-4	19		2
9	-4	-19		-41
7	-4	17		-38
7	-4	-19		-17
5	-4	-7		11
5	-4	11		-1
5	-4	-11		6
3	-4	-11		-21
1	-4	-19		22

h	k	l	|Fo|	Fc
28	-5	2		44
20	-5	-12		32
16	-5	14		-4
16	-5	-14		28
12	-5	12		-35
12	-5	16		-22
12	-5	-16		-44
8	-5	14		25
4	-5	-16		32
0	-5	14		26
26	-5	-2		-4
22	-5	10		-1
18	-5	-2		18
18	-5	8		-21
14	-5	-8		9
14	-5	-14		26
10	-5	-16		-10
6	-5	6		16
6	-5	10		7
2	-5	-2		-18
27	-5	-5		-27
25	-5	3		-36
23	-5	7		26
23	-5	-7		-19
23	-5	11		-2
23	-5	-11		-6
21	-5	-1		-37
21	-5	3		32
21	-5	5		-49
21	-5	-9		-20
19	-5	5		12
17	-5	13		31
15	-5	3		52
15	-5	-3		30
15	-5	7		-34
15	-5	-7		-25
15	-5	-11		50
13	-5	9		-16
9	-5	-1		16
9	-5	15		-31
7	-5	11		-3
5	-5	-13		-31
5	-5	15		-52
5	-5	17		-37
3	-5	-5		21
3	-5	13		20
1	-5	3		32
1	-5	-11		31
1	-5	17		-40
20	-6	0		-1
16	-6	-2		40
16	-6	-8		-59
12	-6	-4		45
12	-6	10		-52
8	-6	-2		-6
8	-6	-12		9
4	-6	-4		23
22	-6	-2		1
22	-6	4		18
18	-6	6		5
14	-6	-2		-24
14	-6	-6		-3
14	-6	8		4
10	-6	-4		44
10	-6	10		-16
2	-6	-14		-9
19	-6	7		6
19	-6	-7		-3
17	-6	5		-43
17	-6	-9		3
15	-6	-9		4
13	-6	-7		-53
9	-6	-9		-4
7	-6	-9		3
3	-6	-7		37
1	-6	-13		-29
12	-7	2		-28
12	-7	-2		-14
8	-7	4		-19
4	-7	2		-32
4	-7	6		-66
0	-7	4		-5
10	-7	4		-34
2	-7	-6		-35
5	-7	5		-19
5	-7	-5		-25
3	-7	-5		-41

THE 'EXTINCTION REFLECTIONS' REMOVED FROM THE DATA USED IN STRUCTURE REFINEMENT

h	k	l	|Fo|	Fc
16	0	0	1358	1456
16	0	4	1144	-1199
16	0	-4	1116	-1151
12	0	4	1773	1842
12	0	-4	1836	-1973
12	0	8	1386	-1441
12	0	-8	1393	1455
8	0	0	2263	-2879

h	k	l	|Fo|	Fc
8	0	2	1510	-1561
8	0	-2	1619	-1682
8	0	6	1166	1199
8	0	-6	1141	1160
4	0	2	2116	-2831
4	0	-2	2074	2868
4	0	4	1902	-2219
4	0	-4	1846	2155

h	k	l	|Fo|	Fc
0	0	4	2329	-3211
20	-1	0	1335	-1374
8	-1	4	1398	1437
8	-1	-4	1374	-1444
8	-1	8	1407	-1457
8	-1	-8	1381	1428
4	-1	0	2660	-3666
4	-1	4	2081	2344

h	k	l	|Fo|	Fc
4	-1	-4	2070	2343
0	-1	2	2124	-2592
7	-1	3	1411	1368
7	-1	-3	1399	1429
5	-1	-5	1170	1177
8	-2	4	1296	-1322
8	-2	-4	1295	-1317

h	k	l	|Fo|	Fc
4	-2	6	1516	-1551
4	-2	-6	1497	1522
4	-2	8	1138	-1175
4	-2	-8	1166	1191
0	-2	2	1133	1135
0	-2	4	1953	2115
1	-2	1	1183	1211

APPENDIX 5

A diagram of the structure

The accompanying diagram shows the positions of the atoms of the asymmetric unit, as determined at the end of refinement, in an (010) projection. The volume $\underline{a}/2 \times \underline{b} \times \underline{c}/2$ is shown. This includes two asymmetric units. The symmetry related atoms are primed. Alongside each atom is given its fractional y-coordinate.

The above volume is the shaded portion in fig. 3.4.1.. The latter shows the symmetry elements which relate the two asymmetric units in this volume, and which relate these to the remainder of the unit cell.

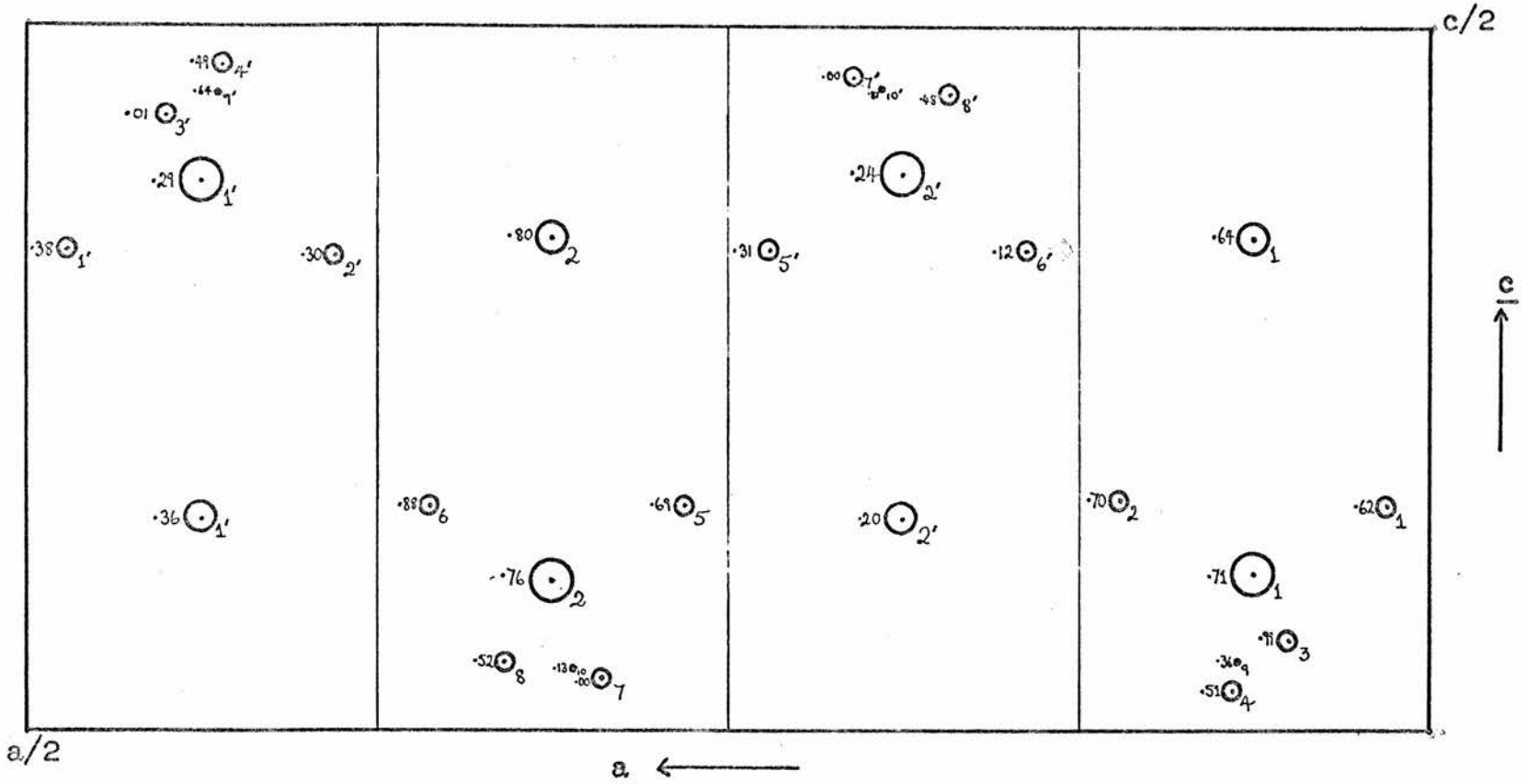

◯ denotes a sulphur atom, o an oxygen atom, ◯ a nitrogen atom, and • a hydrogen atom
The dots show the final refined positions of the atoms (table 7.3.1.) ; they are accurately placed, but the scales along a and c are not quite the same -- there is a relative small expansion of the structure along a.

APPENDIX 6

Published work

The following paper presents work unrelated to that reported in this thesis.

REFERENCES

Abrahams, S.C., Alexander, L.E., Furnas, T.C., Hamilton, W.C., Ladell, J., Okaya, Y., Young, R.A. and Zalkin, A., Acta Cryst. 22, 1.

Alexander, L.E. and Smith, G.S., 1962, Acta Cryst. 15, 983.

Arndt, U.W. and Willis, B.T.M., 1966, Single Crystal Diffractometry. Cambridge: University Press.

Bacon, G.E., 1962, Neutron Diffraction. Oxford: Clarendon Press.

Bacon, G.E. and Pease, R.S., 1955, Proc. Roy. Soc. A230, 359.

Bazhulin, P.A., Myasnikova, T.P. and Rakov, A.V., 1963, Sov. Phys. Sol. State 5, 1299.

Bengtssen, E., 1941, Ark. Kemi Min. Geol. 15B(7), 8.

Bhuiya, A.K. and Stanley, E., 1963, Acta Cryst. 16, 981.

Boutin, H., Frazer, B.C. and Jona, F., 1963, J. Phys. Chem. Solids 24, 1341.

Bunce, L.J. and Wheeler, D.A., 1965, A.E.R.E. Harwell Report.

Burns, G., 1961, Phys. Rev. 123, 64.

Busch, G. and Scherrer, P., 1935, Naturwiss. 23, 737.

Buyers, W.J.L., Cowley, R.A., Paul, G.L. and Cochran, W., 1968, Symposium on Neutron Inelastic Scattering. Copenhagen: International Atomic Energy Agency. SM104/48.

Chandrasekhar, S., Ramaseshan, S. and Singh, A.K., 1969, Acta Cryst. A25, 140.

Chidambaram, R. and Sikka, S.K., 1968, Chem. Phys. Lett. 2, 162.

Chynoweth, A.G., 1959, Phys. Rev. 113, 159.

Cochran, W., 1948, Acta Cryst. 1, 138.

Cochran, W., 1951, Acta Cryst. 4, 408.

Cochran, W., 1952, Acta Cryst. 5, 65.

Cochran, W., 1960, Phil. Mag. Suppl. 9, 387.

Cochran, W., 1969, Acta Cryst. A25, 95.

Cochran, W. and Cowley, R.A., 1962, J. Phys. Chem. Solids 23, 447.

Cochran, W. and Zia, A., 1968, Phys. Stat. Solidi 25, 273.

Cook, W.R. and Jaffe, H., 1952, Phys. Rev. 88, 1426.

Coppens, P., 1968, Acta Cryst. A24, 253.

Couture, L. and Riche, N., 1949, J. de Physique et le Radium 10, 151.

Cromer, D.T. and Mann, J.B., 1968, Acta Cryst. A24, 321.

Crowfoot, D., Bunn, C.W., Rogers-Low, B.W. and Turner-Jones, A., 1949, Chemistry of Penicillin. Princeton: University Press.

Cruickshank, D.W.J., 1961, J. Chem. Soc., 5486.

Cruickshank, D.W.J., 1965, Computing Methods in Crystallography. Ed. Rollett. London: Pergamon Press.

Cruickshank, D.W.J. and Pilling, D.E., 1961, Computing Methods and the Phase Problem in X-ray Crystal Analysis. London: Pergamon Press.

Davis, M.F. and Whitaker, A., 1966, Acta Cryst. 21, 822.

Dawson, B., 1960, Acta Cryst. 13, 403.

Devonshire, A.F., 1954, Advances in Physics 3, 10.

Doyle, P.A. and Turner, P.S., 1968, Acta Cryst. A24, 390.

Durning, A.J. and Vand, V., 1969, Acta Cryst. A25, 489.

Elcombe, M.M. and Taylor, J.C., 1968, Acta Cryst. A24, 410.

Evans, H.T., 1952, Philips Lab., Inc. Research Lab. Tech. Report No. 54.

Evans, H.T., 1961, Acta Cryst. 14, 1019.

Fatuzzo, E., Harbeke, G., Merz, W.J., Nitsche, R., Roetschi, H. and Ruppel, W., 1962, Phys. Rev. 127, 2036.

Frazer, B.C., 1962, J. Phys. Soc. Japan 17, Suppl. B-II, 376.

Freeman, A.J., 1959, Acta Cryst. 12, 261.

Geller, S., 1961, Acta Cryst. 14, 1026.

Groenewegen, P.P.M. and Feil, D., 1969, Acta Cryst. A25, 444.

Hamilton, W.C., 1962, Ann. Rev. Phys. Chem. 13, 19.

Hamilton, W.C., 1969, Acta Cryst. A25, 194.

Hamilton, W.C. and La Placa, S.J., 1968, Acta Cryst. B24, 1147.

Holden, A.N., Matthias, B.T., Merz, W.J. and Remeika, J.P., 1955, Phys. Rev. 98, 546.

Hughes, E.W., 1941, J. Amer. Chem. Soc. 63, 1737.

International Tables for X-ray Crystallography, 1962, Birmingham: Kynoch Press.

Jensen, L.H. and Sundaralingam, M., 1964, Science 145, 1185.

Jona, F. and Shirane, G., 1962, Ferroelectric Crystals. London: Pergamon Press.

Kaminow, I.P. and Damen, T.C., 1968, Phys. Rev. Lett. 20, 1105.

Ladell, J. and Spielberg, N., 1966, Acta Cryst. 21, 103.

Liminga, R., 1968, Arkiv för Kemi 28, 471.

Lipson, H. and Cochran, W., 1966, The Determination of Crystal Structures. 3rd Ed. London: Bell.

Lyddane, R.H., Sachs, R.G. and Teller, E., 1941, Phys. Rev. 59, 673.

Mason, R. and Robertson, G.B., 1965, Advances in Structure Research by Diffraction Methods. Vol. II. Ed. Brill. New York and London: Berlin Interscience Publishers.

Mathieson, A. McL., 1969, Acta Cryst. A25, 264.

Matthias, B.T., Miller, C.E. and Remeika, J.P., 1956, Phys. Rev. 104, 849.

Matthias, B.T. and Remeika, J.P., 1956, Phys. Rev. 103, 262.

Megaw, H.D., 1957, Ferroelectricity in Crystals. London: Methuen.

Merz, W.J., 1962, Progress in Dielectrics 4, 103.

Miller, S.R., Blinc, R., Brenman, M. and Waugh, J.S., 1962, Phys. Rev. 126, 528.

Myasnikova, T.P., 1962, Materialy Chetvertoi Nauchn. Konf. Aspirantov (Rostov-on-Don: Rostov Sk. Univ.) Sb, 61.

Myasnikova, T.P. and Arefev, I.M., 1964, Optika i Spektroskopiya XVI (3), 540.

Myasnikova, T.P. and Yatsenko, A.F., 1962, Sov. Phys. Sol. State 4, 475.

Nahringbauer, I., 1968, Acta Chem. Scand. 22, 1141.

N.D.C., 1969, Acta Cryst. A25, 391.

Oden, L.L., 1966, Dissertation Abstracts XXVI (7), 3654.

O'Reilly, D.E. and Tsang, T., 1967, J. Chem. Phys. 46, 1291.

Pepinsky, R., Jona, F. and Shirane, G., 1956, Phys. Rev. 102, 1181.

Pepinsky, R., Vedam, K., Hoshino, S. and Okaya, Y., 1958, Phys. Rev. 111, 1508.

Pepinsky, R. and Vedam, K., 1960, Phys. Rev. 117, 1502.

Pippard, A.B., 1964, The Elements of Classical Thermodynamics. Cambridge: University Press.

Polandov, I.N., Mylov, V.P. and Strukov, B.A., 1969, Sov. Phys. Sol. State 10, 1754.

Post, B., 1969, Acta Cryst. A25, 94.

Powell, M.J.D., 1966, A.E.R.E. Harwell Report.

Pringle, G.E. and Broadbent, T.A., 1965, Acta Cryst. 19, 426.

Qurashi, M.M., 1963, Acta Cryst. 16, 307.

Rush, J.J. and Taylor, T.I., 1965, Inelastic Scattering of Neutrons, Vol. II. International Atomic Energy Agency, Vienna. p. 333.

Sato, S., 1968, J. Phys. Soc. Japan 25, 185.

Schlemper, E.O. and Hamilton, W.C., 1966, J. Chem. Phys. 44, 4498.

Slater, J.C., 1941, J. Chem. Phys. 9, 16.

Srivastava, R.C. and Lingafelter, E.C., 1966, Acta Cryst. 20, 918.

Stewart, R.F., Davidson, E.R. and Simpson, W.T., 1965, J. Chem. Phys. 42, 3175.

Strukov, B.A. and Danilycheva, M.N., 1963, Sov. Phys. Sol. State 5, 1253.

Strukov, B.A., Koptsik, V.A. and Ligasova, V.D., 1962, Sov. Phys. Sol. State 4, 977.

Strukov, B.A., Minaeva, K.A. and Rodicheva, E.N., 1964, Sov. Phys. Sol. State 6, 59.

Templeton, D.H., 1962, International Tables for X-ray Crystallography. Birmingham: Kynoch Press. Vol. III, p. 213.

Valasek, J., 1921, Phys. Rev. 17, 475.

von Groth, G.P., 1908, Chemische Krystallographie. Liepzig: W. Engelmann. Vol. 2, p. 314.

von Hippel, A., Breckenridge, R.G., Chesley, F.G. and Tisza, L., 1946, Ind. Eng. Chem. 38, 1097.

Webb, M.W., 1965, Acta Cryst. 18, 298.

Whittaker, E.T. and Robinson, G., 1944, The Calculus of Observations, London: Blackie and Son.

Wiebenga, E.H. and Smits, D.W., 1950, Acta Cryst. 3, 265.

Willis, B.T.M., 1969, Acta Cryst, A25, 277.

Willis and Arndt, 1966. See Arndt and Willis, 1966.

Wilson, A.J.C., 1942, Nature, 150, 152.

Woolfson, M.M., 1961, Direct Methods in Crystallography. Oxford: University Press.

Wul, B. and Goldman, I.M., 1945, Compt. rend. Acad. sci. U.R.S.S. 46, 139.

Zachariasen, W.H., 1967, Acta Cryst. 23, 558.

Zachariasen, W.H., 1968, Acta Cryst. A24, 421.

Zachariasen, W.H., 1968a, Acta Cryst. A24, 212.

Zachariasen, W.H., 1968b, Acta Cryst. A24, 324.

Zachariasen, W.H., 1968c, Acta Cryst. A24, 425.

Zachariasen, W.H., 1969, Acta Cryst. A25, 102.